STRUCTURE-ACTIVITY-RESISTANCE RELATIONSHIPS OF NOVEL NUCLEOSIDE AND NUCLEOTIDE HIV-1 REVERSE TRANSCRIPTASE INHIBITORS

by

Brian David Herman

BS, Allegheny College, 2005

Submitted to the Graduate Faculty of

the School of Medicine Molecular Virology and Microbiology Graduate Program

in partial fulfillment of the requirements for the degree of

Doctor of Philosophy

University of Pittsburgh

2012

UNIVERSITY OF PITTSBURGH

SCHOOL OF MEDICINE

This dissertation was presented

by

Brian David Herman

It was defended on

July, 9, 2012

and approved by

Nicolas Sluis-Cremer, Ph.D.
Associate Professor, Dissertation Director
Department of Medicine
School Medicine, University of Pittsburgh

John W. Mellors, M.D.
Professor, Committee Member
Department of Medicine
School Medicine, University of Pittsburgh

Zandrea Ambrose, Ph.D.
Assistant Professor, Committee Member
Department of Medicine
School Medicine, University of Pittsburgh

Saleem A. Khan, Ph.D.
Professor, Committee Member
Department of Microbiology and Molecular Genetics
School Medicine, University of Pittsburgh

Michael Trakselis, Ph.D.
Assistant Professor, Committee Member
Department of Chemistry
School of Arts and Sciences, University of Pittsburgh

STRUCTURE-ACTIVITY-RESISTANCE RELATIONSHIPS OF NOVEL NUCLEOSIDE AND NUCLEOTIDE HIV-1 REVERSE TRANSCRIPTASE INHIBITORS

Brian David Herman, PhD

University of Pittsburgh, 2012

Nicolas Sluis-Cremer, Ph.D.

STRUCTURE-ACTIVITY-RESISTANCE RELATIONSHIPS OF NOVEL NUCLEOSIDE AND NUCLEOTIDE HIV-1 REVERSE TRANSCRIPTASE INHIBITORS

Brian David Herman, Ph.D.

University of Pittsburgh, 2012

ABSTRACT

Nucleos(t)ide reverse transcriptase inhibitors (N(t)RTI) are essential components of combination antiretroviral therapy for treatment of human immunodeficiency virus type-1 (HIV-1) infection. N(t)RTI are analogs of natural 2'-deoxyribonucleos(t)ides that lack a 3'-hydroxyl. Once metabolized by host kinases to the active form, their incorporation into viral DNA by HIV-1 reverse transcriptase (RT) results in chain termination of DNA synthesis. N(t)RTI efficacy is undermined primarily by rapid selection of resistant/cross-resistant HIV-1 variants. Consequently, the development of novel N(t)RTI with activity against a broad range of N(t)RTI-resistant HIV-1 is of critical importance. Rational design of novel N(t)RTI with knowledge of analog structure-activity-resistance relationships with the RT target enzyme is the most promising approach. We hypothesized that uncovering knowledge of how N(t)RTI base, sugar, and phosphate structures influence activity and resistance phenotypes would aid in the rational design of new N(t)RTI with improved activity and resistance profiles. Therefore, a combination of biochemical, antiviral, molecular modeling, and cellular pharmacology analyses provided a

detailed characterization of structure-activity-resistance relationships for inhibition of wild-type and NRTI-resistant HIV-1 by novel N(t)RTI. First, we studied two novel nucleoside phosphonate NtRTI, (*R*)-6-[2-phosphonylmethoxy]propoxy]-2,4-diaminopyrimidine (PMEO-DAPym) and (5-(6-amino-purin-9-yl)-4-fluoro-2,5-dihydro-furan-2-yloxymethyl)phosphonate (GS-9148). We showed the diphosphate (-DP) form, PMEO-DAPym-DP acts as a purine mimetic that is recognized by RT as an adenosine analog and unambiguously incorporated across from thymine (DNA) or uracil (RNA). Studies indicated that PMEO-DAPym-DP and GS-9148-DP were superior to tenofovir-DP against both discrimination and excision RT resistance mechanisms. Next, we examined structure-activity-resistance relationships of 6-modified, 3'-azido-2',3'-dideoxyguanosine (3'-azido-ddG) NRTI analogs. In RT-mediated DNA synthesis assays the triphosphate (-TP) form of each analog behaved as an adenosine mimetic for incorporation by HIV-1 RT. Importantly, the structure-activity relationships for incorporation and ATP-mediated excision were different, suggesting that new analogs can be designed that are efficiently incorporated but poorly excised by RT. RS-788, a 5'-monophosphate prodrug of 3'-azido-2',3'-dideoxy-2,6-diaminopurine (3'-azido-2,6-DA-P), displayed potent activity against multi-NRTI-resistant HIV-1 and unique cellular metabolism. RS-788 was metabolized ~1:1 to both 3'-azido-2,6-DA-P and 3'-azido-ddG, thus delivering two distinct metabolites, each of which are potent RT chain-terminators that are incorporated opposite different bases, thymine and cytosine, respectively. Combinations of 3'-azido-2,6-DA-P+3'-azido-ddG synergistically inhibited multi-NRTI-resistant RT DNA synthesis.

TABLE OF CONTENTS

LIST OF TABLES

LIST OF FIGURES

ACKNOWLEDGEMENTS

First and foremost, I thank my dissertation advisor, Dr. Nicolas Sluis-Cremer. He believed in me from beginning and has been an excellent mentor and teacher throughout the past five years. He allowed me to work on a multidisciplinary research project and to collaborate with researchers from multiple institutions. Dr. Sluis-Cremer gave me the academic freedom to pursue independent lines of research but was always available to provide guidance whenever I found a roadblock. He encouraged me to attend and present my work at several international research conferences. Dr. Sluis-Cremer also gave me the opportunities to publish first-author, peer-reviewed manuscripts in well respected academic journals, as well as a first-author book chapter. My experience working with Dr. Sluis-Cremer has broadened and enhanced my academic, research, interpersonal, and communication skills. His mentorship has guided me to become the scientist I am today, for that I am truly grateful.

I also thank my committee members Dr. John Mellors, Dr. Zandrea Ambrose, Dr. Saleem Khan, and Dr. Michael Trakselis. They provided excellent guidance to enable me to achieve my research goals. I would like to thank Drs. Mellors and Ambrose, in particular, for stimulating conversations about virology and always pushing me to achieve more. I also owe my gratitude to Dr. Saleem Khan for being an outstanding advocate for all graduate students and being a friend

and mentor outside of my research career. I thank Dr. Trakselis for providing additional insight about enzyme kinetics and biochemistry.

I am eternally grateful to past and present members of the Sluis-Cremer laboratory and other members of our HIV research group. They have given advice and assistance with experiments countless times and produced a laboratory environment that is relaxed yet productive. I especially thank Jeff Meteer, Dr. Jessica Brehm, and Dianna Koontz for guidance with cell culture and virology. I owe my heartfelt gratitude to Dr. Jessica Radzio for being one of the best co-workers and friends a person could have.

I also thank my fellow MVM, MMG, and interdisciplinary biomedical graduate students that provided excellent conversations and perspectives from many disciplines. I am grateful to many professors and teachers throughout my academic career that have provided a strong scientific education and outstanding mentorship, especially Dr. JoAnne Flynn, Dr. Brandi Baros, Dr. Anthony LoBello, Carol Wack, and Bill Wesley.

Finally, I want to thank my friends, especially Greg Schwartz, and the brothers of Delta Tau Delta Alpha Chapter, especially Dr. John Krempecki, who were always there for moral support. I thank my fiancé Meredith Ponczak for being with me every day through this long journey. I especially thank her for her love and emotional support when times were tough. Most of all, I want to thank my parents David and Teddi Herman and my brother Brad Herman for their ever-present love, encouragement, and confidence in me throughout my pursuit of higher education.

1.0 INTRODUCTION

In 1983, the human immunodeficiency virus (HIV) was independently discovered by research groups led by Robert Gallo and Luc Montagnier as the etiologic agent of acquired immunodeficiency syndrome (AIDS) (1, 2). Only two years later, Samuel Broder and colleagues showed that the nucleoside analog 3'-azido-thymidine (AZT, zidovudine) had inhibitory activity against HIV replication targeting the viral enzyme reverse transcriptase (RT) (3-5). This seminal discovery demonstrated that HIV replication could be suppressed by small molecule chemotherapeutic agents, and provided the basis for the field of antiviral therapeutics. However, the rapid development of viral resistance to antiviral medications remains a significant challenge to successful antiviral therapy. Therefore, there is a continued need to develop novel drugs. This introductory chapter will discuss key aspects of HIV virology, RT structure and function, antiretroviral therapeutics focusing on nucleoside/nucleotide inhibitors of HIV-1 reverse transcriptase (NRTI), and antiviral drug resistance.

1.1 HIV CLASSIFICATION

HIV is a Lentivirus from the family Retroviridae that originated in West and Central sub-Saharan Africa from closely related non-human primate simian immunodeficiency viruses (SIV) (2, 6, 7). HIV is classified into two groups, type 1 (HIV-1) and type 2 (HIV-2). HIV-1 is most closely

related to SIV endemic in chimpanzees (SIVcpz) and is believed to have entered the human population through multiple primate to human zoonotic transmissions (7, 8). HIV-2 likely originated from viruses carried by the sooty mangabey (SIVsmm) (9, 10).

The more virulent HIV-1 is responsible for worldwide human infections while HIV-2 is largely confined to sub-Saharan Africa (11). HIV-1 is divided into three groups M (major), O (outlier), and N (non-major/non-outlier) based on the viral envelope (*env*) gene (12, 13). Group M HIV-1 is the most prevalent worldwide and is genetically subdivided into nine clades (clades A-K) which are largely geographically distinct (13).

1.2 EPIDEMIOLOGY

HIV-1 infection has grown to a worldwide pandemic. As of 2010, the WHO estimates 34 million people are living with HIV-1 (11). Of those, 16 million are women and 2.5 million are children under the age of 15. Approximately 2.6 million people were newly infected with HIV in 2010 and more than 30 million people have died from HIV/AIDS-related disease since the beginning of the pandemic.

Sub-Saharan Africa is the most heavily affected region, accounting for more 68% of HIV-1 infections and 66% of AIDS-related deaths (11). Approximately 5% of the population in sub-Saharan Africa was living with HIV-1 in 2009. The second most afflicted region is south and south-east Asia with approximately 12% of worldwide infections. India alone accounts for more than 2.4 million cases. The most heavily impacted regions occur in the developing world where low income countries have limited access to antiviral medications. In 2003, it was estimated that

> 7% of HIV-1 infected individuals in sub-Saharan Africa had access to antiretroviral drugs. Initiatives by the World Health Organization, UNAIDS, and PEPFAR have increase access to 37% of those in need by 2010 (11).

The lowest prevalence of HIV infection is in west and central Europe with about 0.2% of the population infected. In the United States and Canada, approximately 1.5 million people are infected with HIV-1, representing ~ 0.5% of the adult population. In 2009, there were ~ 70,000 people newly infected with HIV-1 in the United States and Canada and about 26,000 AIDS-related deaths (11).

1.3 HIV-1/AIDS TRANSMISSION AND PATHOGENESIS

HIV-1 is transmitted through direct contact with blood, semen, vaginal fluid, or breast milk of infected persons (14, 15). The most common route of infection is through sexual contact with an infected person (15). Infections also result from intravenous drug use, blood transfusions, and mother-to-child-transmission (intrapartum, peripartum, or via breast feeding). Instances of these infections have decreased substantially due to greater awareness, blood bank screening, and improved prenatal treatment, respectively (11).

Following exposure, HIV-1 infects host lymphocytic cells harboring the cell surface protein CD4. HIV-1 infection proceeds through three clinical stages of disease (**Figure 1.1**): acute infection, secondary infection (clinical latency), and AIDS (15, 16). Acute HIV-1 infection (also referred to as primary infection) lasts approximately 2-4 weeks post-transmission and is characterized by influenza-like illness. Common symptoms include fever, lymphadenopathy,

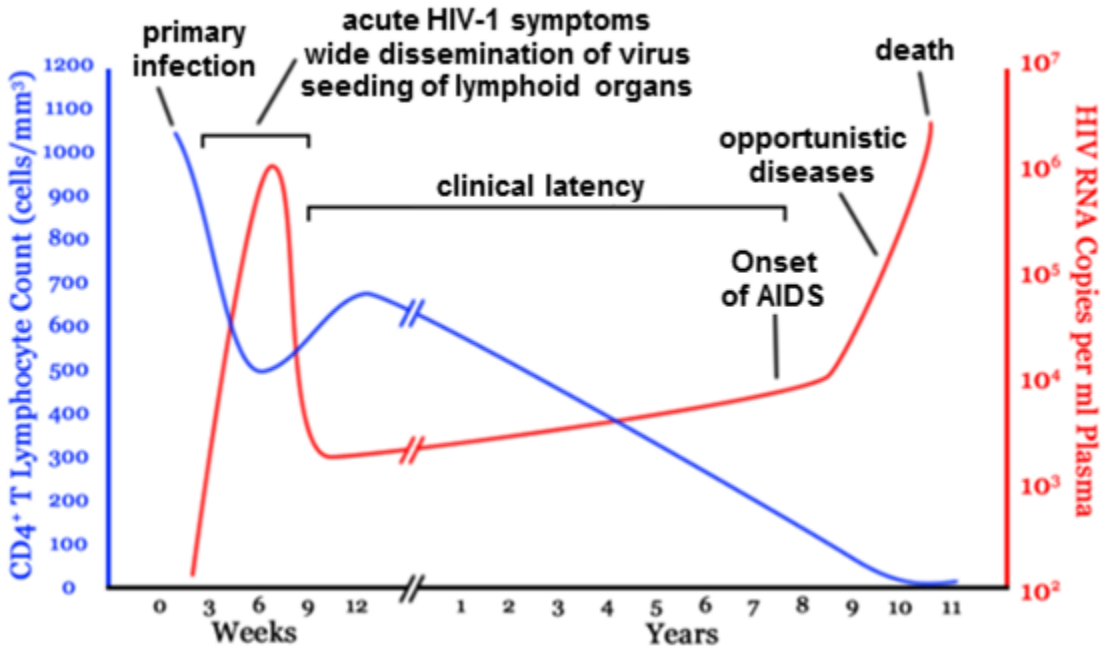

Figure 1.1 A generalized graph of HIV-1 disease progression showing the relationship of CD4+ T lymphocyte decay and plasma viral load over time.
The CD4+ T lymphocyte count is indicated in blue of the left axis, while the number of HIV-1 RNA copies per milliliter of plasma is indicated in red on the right axis. The landmarks of clinical disease progression are indicated in black. This figure was adapted from references (15, 16).

pharyngitis, rash, myalgia, and malaise. Acute infection is associated with a sharp spike in viral load (up to > 1 million HIV-1 RNA copies / ml of plasma) with a concurrent drop in target CD4+ T cells (14, 15). Acute symptoms wane as the host immune system elicits a cytotoxic T cell response, resulting in viral load reduction and partial recovery of CD4+ T cell counts. Recent studies suggest that it is during the initial acute phase of infection that viral reservoirs of latently infected cells are established (17, 18). The specific cell types or tissue compartments that harbor latent HIV-1 are not fully recognized and there is currently substantial debate about how these reservoirs contribute to persistent viremia. HIV-1 replication continues during asymptomatic infection, resulting in a steady decrease in CD4+ T cells over a period of 1 to 10 years (15).

Without intervention, the clinical development of AIDS occurs once CD4+ T cell counts drop below 200 cells per mL. The severe impairment of the immune system renders the individual highly susceptible to opportunistic infections or cancer. Following the onset of AIDS, patients succumb to opportunistic infections which commonly include pneumocystis pneumonia, tuberculosis, and candidiasis or cancers such as Kaposi's sarcoma and lymphoma (15, 19).

1.4 HIV-1 STRUCTURE AND VIRAL LIFE CYCLE

The roughly spherical 110 nM HIV-1 virions are composed of a conical capsid core surrounded by a host cell membrane-derived lipid envelope (**Figure 1.2**) (20). The capsid core is composed of approximately 1500 molecules of the viral p24 capsid (CA) protein (21). The HIV-1 capsid core encloses two copies of the positive-sense single-stranded RNA genome that are 5'-methyl-GDP capped and 3'-polyadenylated (20). The RNA genomes are tightly bound and stabilized by the nucleocapsid (NC) protein. The virion also contains cellular components, the essential viral enzymes protease (PR), reverse transcriptase (RT), and integrase (IN), and the accessory proteins Vif, Vpr, Nef, and Vpu. The matrix (MA) protein coats the interior of the viral envelope, which is studded with envelope glycoproteins composed of trimers of the gp120 surface protein (SU) and gp41 transmembrane protein (TM) complex.

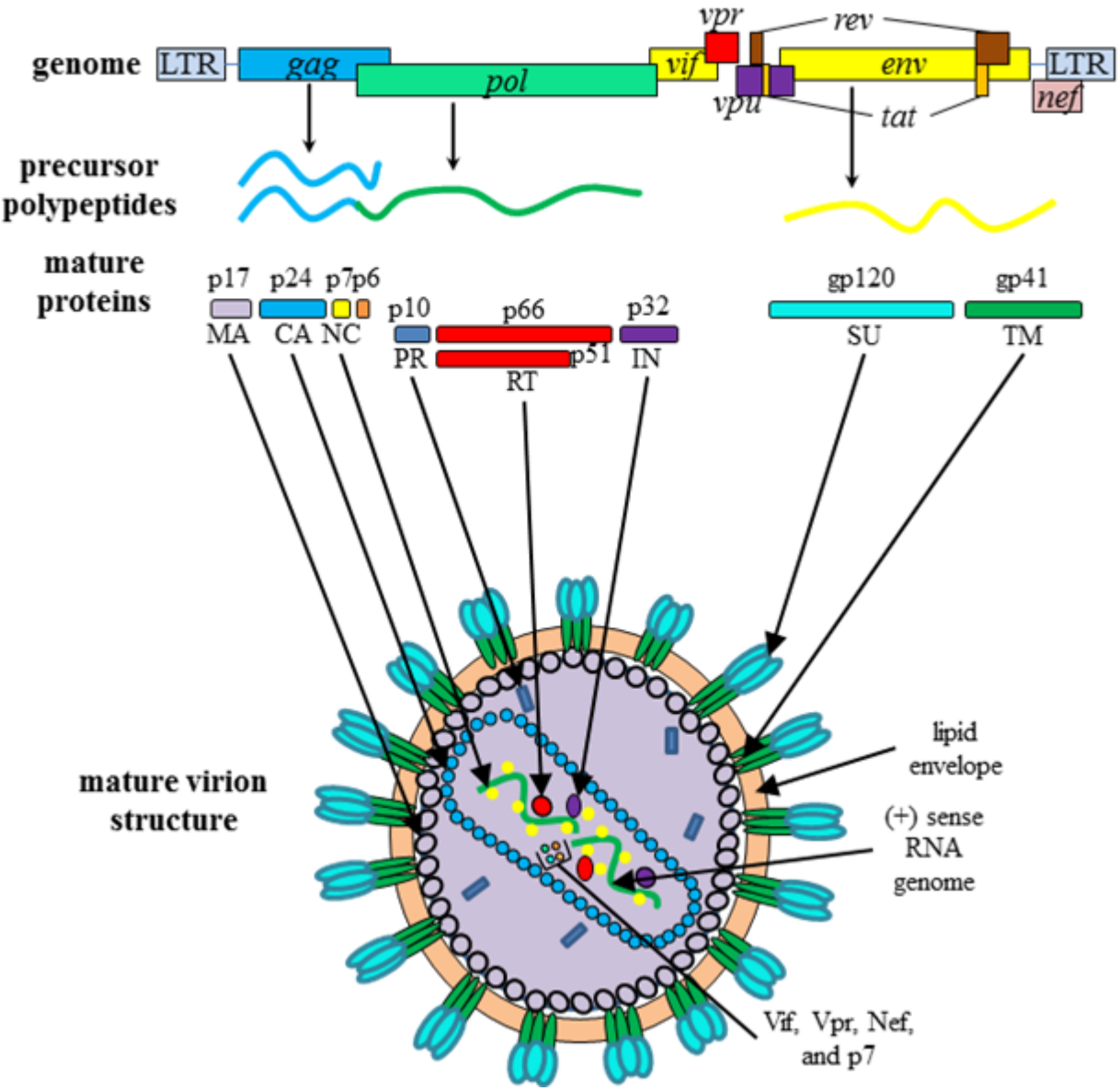

Figure 1.2 HIV-1 genome organization, viral proteins, and mature virion structure. The genome structure and protein products were adapted from reference (20). The virion structure was adapted from reference (18).

The 9.2 kb HIV-1 RNA genome encodes three primary genes *gag*, *pol*, and *env*, as well as six accessory genes *tat*, *rev*, *vif*, *vpr*, *vpu*, and *nef* (**Figure 1.2**) (20). In the proviral form, the HIV-1 genome, like all retroviruses, contains two copies of the long terminal repeat (LTR) at the 5'- and 3'- ends of the genome. The LTRs are composed of the segments U3 (derived from a unique sequence at the 3' end), R (repeated sequence at both ends), and U5 (derived from a unique sequence at the 5' end) (20).

The HIV-1 replication cycle begins when the virion gp120 envelope glycoprotein recognizes and binds the cell surface protein CD4 on host lymphocytes (22, 23). Viral entry requires additional binding to one co-receptor molecules (24). The seven-transmembrane, G-protein-coupled, receptors CCR5 and CXCR4 are most commonly used as HIV-1 entry coreceptors, however others such as CCR8 have also been identified (25-27). Early in HIV-1 infection, viruses predominantly infect CD4+ cells expressing the co-receptor CCR5. During the course of infection, viruses often switch cell entry tropism to infect cells expressing the co-receptor CXCR4 (26, 27). Tight binding of gp120 to CD4 and a co-receptor triggers a conformational change exposing the gp41 viral fusion protein which inserts into the host cell membrane. The resulting fusion of the virus and host membranes releases the viral core into the host cell cytoplasm (24-27).

Although evidence suggests reverse transcription may begin within the virion, the availability of host cytoplasmic dNTP pools facilitates the completion of reverse transcription. (described in detail below) (28). The full-length double-stranded DNA product of reverse transcription together with viral integrase, MA and Vpr and various cellular proteins form the pre-integration complex (PIC) (29). The PIC is transported into the cell nucleus where the viral DNA is inserted into a host chromosome through the action of viral integrase and several host factors (30).

Viral genes are expressed from the integrated proviral DNA by the host transcription machinery including RNA polymerase II (31). Proviral transcription is initiated at the U3 region of the 5' LTR that contains numerous binding sites for viral regulators such as Tat (trans-activator of transcription), Rev (regulator of viral gene expression), and Nef (negative factor) as well as host transcription factors, including Sp1, NFκB, AP-1, and NFAT. Following transcription initiation, Tat binds the stem-loop TAR element at the 5' end of the nascent mRNA and promotes transcription elongation (31). Proviral transcription results in the production of a genome length mRNA which can serve as the message for viral polyprotein translation or can be modified to serve as a new RNA genome to be incorporated into a virion (31). The full length mRNA transcript contains multiple splice sites to allow for the generation of over 40 unique viral transcripts for the expression of the nine viral genes. The full length (unspliced) mRNA serves as the message for translation of the Gag and Gag- Pol precursor polyproteins by host ribosomes. During Gag translation, a -1 ribosomal frameshifting mechanism allows for the production of the Gag- Pol polyprotein (31, 32). This mechanism produces approximately one Gag- Pol polyprotein for every 10-20 Gag polyproteins.

The Env polyprotein undergoes multiple glycosylation events in the endoplasmic reticulum and is then trafficked to and inserted into the cellular membrane (33). Full-length RNA genomes interact with the Gag polyprotein through packaging sequences to be transported to the assembling virion at the cell membrane (33, 34). The Gag- Pol polyprotein is also transported via interactions with Gag (33). Virion budding is promoted when RNA/Gag complexes bind the cytoplasmic tail of membrane associated Env proteins. Assembled immature viral particles are released from the cell membrane and the action of the HIV-1 protease begins the maturation process (33). The viral protease first auto-cleaves from the Gag- Pol precursor polyprotein. Further proteolysis of the Gag- Pol precursor liberates the mature RT and IN enzymes. Proteolytic cleavage of the Gag precursor polyprotein yields the mature structural proteins CA, MA, and NC, while cleavage of the Env polyproteins produces the gp41 and gp120 envelope proteins (20, 33). The proteolytic liberation of the mature HIV-1 structural proteins promotes the condensation of the core into its characteristic bullet shape, thus producing mature, infectious viral progeny.

1.5 ANTIRETROVIRAL THERAPY

At the beginning of the AIDS epidemic in the early 1980s, HIV-1 infection meant near certain mortality within 1 year from the onset of AIDS. The grave need to curtail this rapidly progressing epidemic led to the development of the RT inhibitor 3’-azido-3’-deoxythymidine (zidovudine, AZT) in 1985 (3-5). This was only two years after the identification of HIV-1 as the etiologic agent of AIDS. AZT, the first drug for the treatment of any viral infection, became clinically available as a monotherapy in 1987 (35). Since then 24 additional antiretroviral drugs

have been approved by the United States FDA, rendering HIV-1 a chronic manageable infection, in which patients receiving therapy can now live many healthy years before the onset of AIDS (19, 35).

1.5.1 Antiretroviral drug targets and classes

The FDA-approved antiretrovirals are divided into 6 classes that target 4 key steps in the HIV-1 life cycle: viral entry, reverse transcription, integration, and protein processing/maturation (35, 36).

The first steps in the HIV-1 life cycle, viral attachment and membrane fusion are targeted by two classes of drugs known collectively as entry inhibitors. The first class of entry inhibitors are CCR5 antagonists, represented by one FDA approved antiretroviral, maraviroc. Maraviroc binds the viral chemokine co-receptor CCR5, thus preventing gp120 mediated viral attachment (37). Maraviroc, however, has no efficacy against CXCR4-tropic viruses and susceptible viruses can easily become resistant via point mutations in gp120. The viral envelope fusion inhibitor enfuvirtide (T-20) represents the second class of entry inhibitors. Enfuvirtide acts as a peptidomimetic of the HIV-1 gp41 fusion peptide to prevent fusion of the viral and cell membranes (36, 38). Enfuvirtide is reserved for treatment experienced patients because proteolysis of the drug in the gastrointestinal tract requires administration by twice daily intravenous injections.

Reverse transcription is inhibited by 12 FDA approved drugs from two classes (36, 39): nucleoside/nucleotide reverse transcriptase inhibitors (NRTI) and non-nucleoside reverse transcriptase inhibitors (NNRTI). The FDA approved NRTI (**Figure 1.3**) include one monophosphate nucleotide, tenofovir (TFV; [FDA approved as the prodrug tenofovir disoproxil

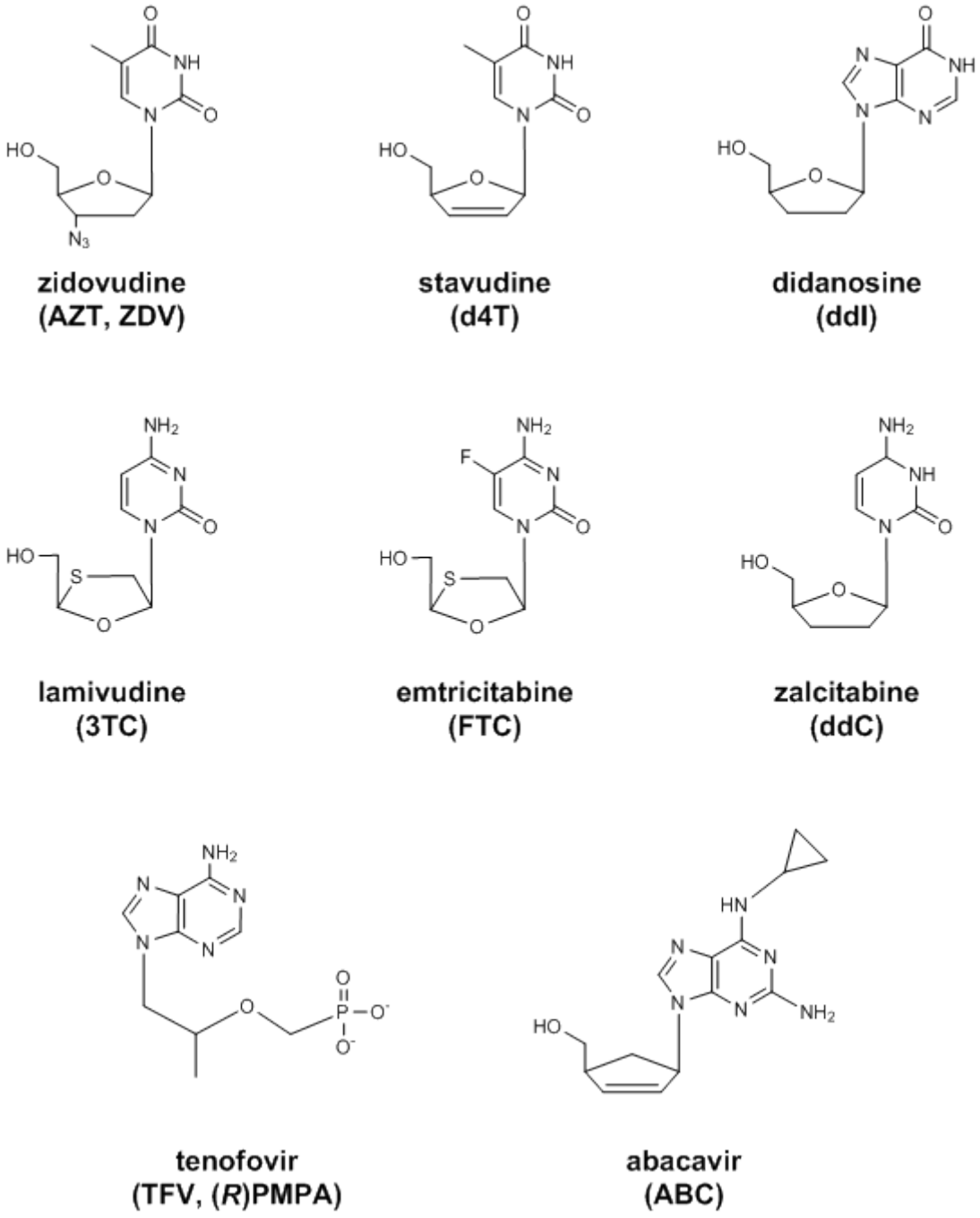

Figure 1.3 Structures of the FDA approved NRTI.

fumarate, TDF]), and 7 nucleosides; zidovudine (AZT), stavudine (d4T), lamivudine (3TC), emtricitabine (FTC), zalcitabine (ddC), didanosine (ddI), and abacavir (ABC). For the remainder of this work the abbreviation "NRTI" will refer to both nucleoside and nucleotide analogs while the abbreviation "NtRTI" will be used when specifically referring to nucleotide analogs. NRTI are analogs of natural 2'-deoxribonucleotides that must be metabolized by host cell enzymes to their active triphosphate forms. NRTI-triphosphates (NRTI-TP) compete with cellular dNTPs for incorporation by RT into HIV-1 DNA. Once incorporated into DNA, NRTI result in chain-termination of viral DNA synthesis due to the lack of a 3'-OH group (39). NRTI mechanisms of action and resistance will be described in detail below.

The five NNRTI, efavirenz (EFV), etravirine (ETV), nevirapine (NVP), delavirdine (DLV), and rilpivirine (RPV) are allosteric, non-competitive inhibitors that bind RT in a specific hydrophobic pocket near the polymerase active site (40, 41). NNRTI binding perturbs active site residues, resulting in decreased nucleotide incorporation (41). Single amino acid substitutions in RT can induce resistance and broad cross-resistance to each member of this drug class (42).

Following reverse transcription, the viral cDNA must be integrated into the host chromosome. Integration is blocked by inhibitors of the HIV-1 encoded integrase enzyme. The integrase inhibitor raltegravir was FDA approved in 2007 for treatment-experienced patients and has been subsequently approved for treatment-naïve patients (36, 43). Raltegravir competitively inhibits the strand transfer step of integration by binding the divalent metal cations in the integrase active site. Integrase inhibitors result in decreased HIV-1 DNA integration. The discovery of novel integrase inhibitors with improved efficacy is an active area of investigation.

The final step in producing infectious HIV-1 particles is viral maturation through the proteolytic processing of precursor polypeptides by the virally encoded protease. Protease

inhibitors (PI) mimic natural protease substrates and block the action of HIV-1 protease (35, 36, 44). Protease inhibition thus prevents the maturation of infectious virions. FDA approved protease inhibitors include indinavir, saquinavir, fosamprenavir, ritonavir, darunavir, atazanavir, tipranovir, lopinavir, and nelfinavir. Most protease inhibitors cause adverse side effects and have poor bioavailability (36, 44). The PI ritonavir also inhibits the cytochrome P-450 CYP3A4 enzyme which is responsible for metabolism of most PI (45). Thus, current FDA guidelines suggest the co-administration of ritonavir with other PIs to minimize metabolism and improve bioavailability and half-life.

1.5.2 Combination antiretroviral therapy

The initial use of AZT as monotherapy quickly led to the development of viral populations with decreased drug susceptibility (46, 47). Multiple studies have shown that treatment regimens including two NRTIs with an NNRTI or a PI suppress HIV-1 replication without the emergence of drug resistance (36, 48, 49). Thus, the use of three or more antiretrovirals from different drug classes in combination, termed highly active antiretroviral therapy (HAART) became the treatment standard in 1996. HAART decreased resistance development, reduced patient morbidity, and improved survival (36, 39). To this day, standard antiretroviral treatment regimens include two NRTIs with at least one NNRTI, PI, or integrase inhibitor.

The requirement of multiple drug combination therapy provides a heavy pill burden on HIV-1 patients that often require multiple daily doses at various intervals. To ease patient pill burden and increase regimen adherence several fixed-dose combination pill formulations have been developed (36). These include Combivir (AZT+3TC), Trizivir (ABC+3TC+AZT), Truvada (TDF+FTC), Epzicom (ABC+3TC), and Kaletra (lopinavir boosted with ritonavir). The three

drug combination Atripla (TDF+FTC+EFV) was the first once daily antiretroviral pill including 2 NRTIs and an NNRTI that can fully suppress HIV-1 replication in some patients. Atripla was followed by the approval in 2011 of the multi-class triple combination Complera (TDF+FTC+RPV). The recently developed 4-drug combination Quad pill containing the novel integrase inhibitor elvitegravir, the novel pharmacoenhancer cobicistat (a CYP3A4 inhibitor that boosts levels of other drugs but has no antiviral activity itself), tenofovir, and emtricitabine represents the first once daily dual-target combination pill (50). The Quad pill is expected to be approved by the FDA in the summer of 2012.

1.6 HIV-1 REVERSE TRANSCRIPTASE

Successful retrovirus replication requires the conversion of the positive sense, single-stranded RNA genome to double stranded cDNA that is competent for incorporation into the host chromosome (51). The RNA-directed DNA synthesis or reverse transcription activity necessary for this process is not required for the growth of eukaryotic cells. Therefore, this step provides a unique viral characteristic that can be targeted for inhibition of viral replication. Reverse transcription was first observed in Rous sarcoma virus by Baltimore and Temin in 1970 (52, 53). In order to complete the complex reverse transcription process, the HIV-encoded reverse transcriptase enzyme is capable of both RNA- directed and DNA-directed DNA synthesis, ribonuclease H cleavage (RNase H, ‘H’ for hybrid), and strand transfer activity.

1.6.1 Steps of HIV-1 reverse transcription

The multi-step process of HIV-1 reverse transcription will be described in detail here (**Figure 1.4**):

1) Reverse transcription begins with minus strand DNA synthesis by RNA-dependent DNA polymerase (RDDP) activity of RT (54). A host $tRNA^{Lys3}$ hybridized to the RNA genome at a primer binding site (PBS) near the 5' end serves as the initial primer (55).

RT elongates the minus strand to the 5' end of the genome, producing a product termed minus strand strong stop DNA (-ssDNA). The RNA template of the subsequent RNA/DNA heteroduplex is simultaneously removed by the RNase H activity of RT.

2) RNase H removal of template RNA and subsequent dissociation of -ssDNA is essential for minus strand DNA transfer and annealing to a homologous repeat region near the 3' end of the genomic RNA template (56, 57). This strand transfer may occur intra- or inter-molecularly (58). Intermolecular strand transfer provides a source of recombination and genetic diversity during reverse transcription (59).

3) Minus strand elongation with concurrent RNase H cleavage results in a complete cDNA. RNase H cleavages during cDNA synthesis leave 3' and central polypurine tract (PPT) sequences uncleaved which serve as primers for plus strand DNA initiation (60). Highly specific RNase H cleavages occur at the 3' and 5' ends of the PPT through specific RNase H primer grip contacts with mismatched and unpaired residues in the PPT (61-66) . Correct cleavage of the 3' PPT is essential to properly produce the integrase recognition site for proviral integration (65).

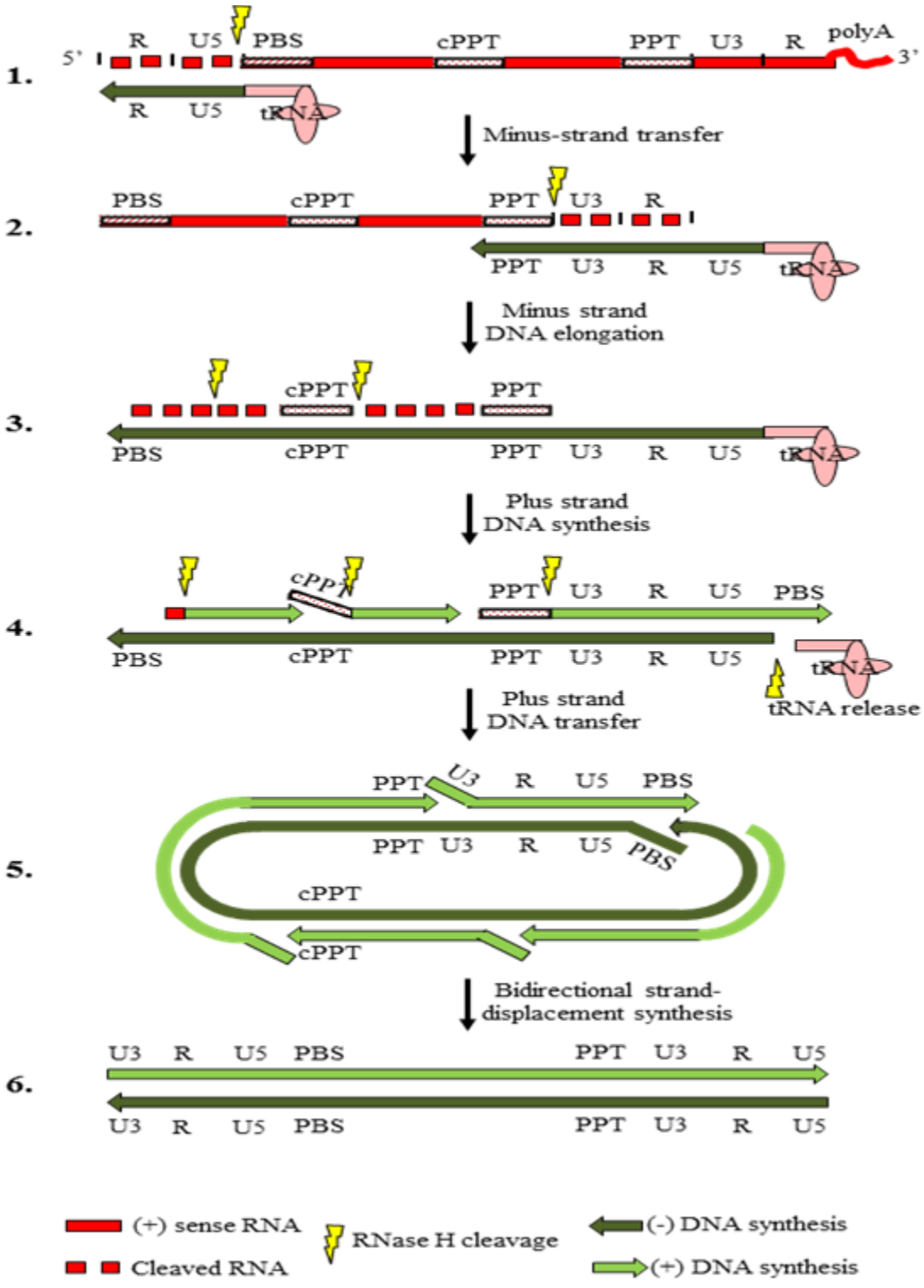

Figure 1.4 Mechanism of HIV-1 reverse transcription.
The steps required to produce the full length integration competent HIV-1 double-stranded viral DNA are described in detail in Section 1.6.1. This figure was adapted from (51).

4) Initiation of plus strand DNA synthesis proceeds from the PPT (65-67). After incorporation of exactly 12 nucleotides, the PPT RNA:DNA junction resides in the RNase H primer grip, which promotes RT pausing and dissociation (67, 68). RT then rebinds the substrate in polymerase-independent manner (described below) to specifically cleave the PPT RNA:DNA junction. The enzyme can then dissociate once again and re-associate in a polymerase-dependent confirmation to continue plus strand elongation to the to the 5' cDNA template end and the attached $tRNA^{Lys3}$ primer. The first 18 ribonucleotides of the $tRNA^{Lys3}$ primer serve as the template for the plus strand PBS sequence (67). RT pausing at a modified $tRNA^{Lys3}$ ribonucleotide at position 19 allows specific RNase H cleavage at the DNA/$tRNA^{Lys3}$ interface to release $tRNA^{Lys3}$ (68, 69).

5) The complementary PBS sequences at the ends of the plus and minus strands facilitate a second strand transfer event (69, 70). If this transfer occurs in an intramolecular fashion the complex becomes circularized.

6) Bidirectional DNA synthesis elongates the plus strand ultimately resulting in a complete double stranded genome with identical LTR sequences on each end (51). Due to the presence of internally primed DNA fragments (such as from the central PPT), plus strand elongation occurs in a discontinuous fashion (67-69). A combination of RT mediated strand displacement synthesis and gap repair/ligation by cellular enzymes results in the full length, double stranded, integration-competent DNA genome (51).

1.6.2 RT Structure

The requirement of reverse transcription for HIV-1 replication and the lack of reverse transcriptase activity in host cells make RT an ideal drug target. The structure and function of

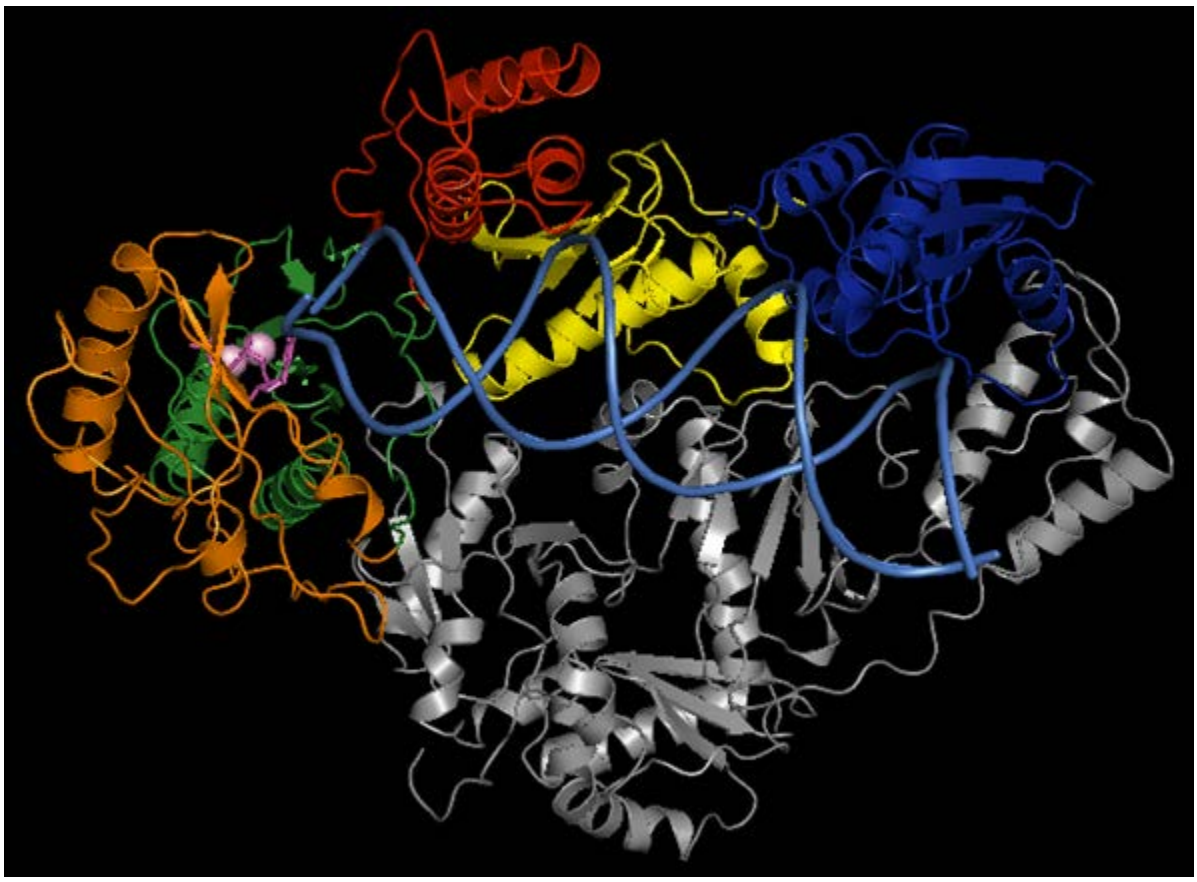

Figure 1.5 Structure of HIV-1 in complex with a DNA/DNA template/primer substrate. The fingers (orange), palm (green), and thumb (red) subdomains make up the polymerase domain of the p66 subunit of RT. The p66 connection and RNase H domains are colored in yellow and blue, respectively. The RT p51 subunit is lacking the C-terminal RNase H domain and is colored in grey. The structure was drawn using PyMol based on the PDB Coordinates 1RTD from Huang et al. 1998 (77).

HIV-1 RT has been intensely studied to inform antiretroviral drug discovery. RT is expressed as part of the Gag- Pol precursor polyprotein and is cleaved by HIV-1 protease to release the polymerase (31, 33). HIV-1 RT is a large multidomain heterodimer of 66 kDa (p66) and 51 kDa (p51) subunits comprised of 560 and 440 amino acids, respectively (**Figure 1.5)** (71-74). Early studies revealed that the 51 kDa subunit is a C-terminal proteolytic truncation of the p66 subunit (73, 75, 76).

RT was first crystallized in 1992 by the laboratory of Thomas Steitz, shedding light on the structure and function of each subunit (76). This study revealed that p51 is structurally distinct from p66 and that it may serve primarily as a structural scaffold for the catalytic domains of p66. Furthermore, the crystal structure identified spatially distinct polymerase (residues 1-318) and RNase H (residues 427-560) domains of p66 linked by a connection domain (residues 319-426). The RT polymerase domain is structurally homologous to other polymerases, including the previously crystallized *E. coli* DNA Pol I Klenow fragment (71, 76). This structure is described as a "right hand" containing "palm, finger, and thumb" subdomains, which form a nucleic acid binding cleft at the polymerase active site. The RNase H domain, resembles the *E. coli* RNase HI enzyme (71, 76). The polymerase and RNase H catalytic active sites are approximately 60 Å apart, spanning 18 nucleotides of a bound nucleic acid substrate (63, 71). Numerous additional studies of the three dimensional structure of HIV-1 RT co-crystallized with various nucleic acid substrates and inhibitors have helped to elucidate RTs catalytic mechanisms of action (63, 71, 76-85).

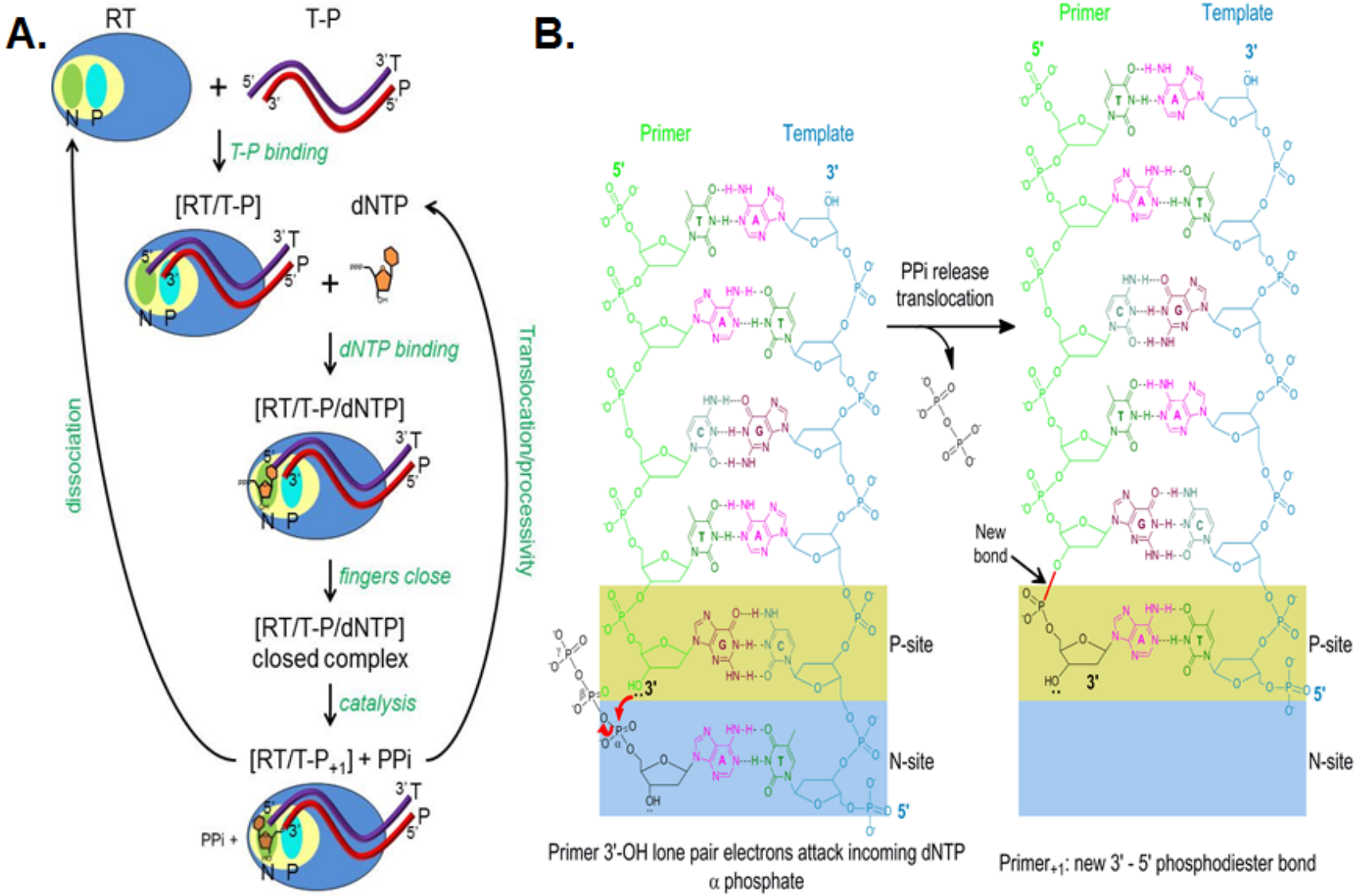

Figure 1.6 Steps required for nucleotide addition (A) and the molecular mechanism of nucleotide incorporation (B).

1.6.3 Nucleic acid substrate binding

In order for polymerase or RNase H catalysis to occur, RT must first bind its RNA/DNA or DNA/DNA nucleic acid substrate (**Figure 1.6A**). Upon substrate binding, the thumb subdomain rotates outward to an open conformation (71, 83). RT preferentially binds most nucleic acid substrates in a conformation (polymerase competent) in which the primer 3'-OH is situated adjacent to the polymerase active site, termed the priming site (P-site). Specific contacts between the polymerase domain and the primer and template strands are essential for proper substrate positioning during catalysis (71). The p66 palm subdomain forms a "primer grip" region composed of residues 227-235 that form the β12 and β13 sheets (62, 71, 83, 86). The p51 subunit also makes contact with the primer near the base of the palm in p66. The template strand is stabilized through contacts in the fingers and palm subdomains (71, 83). The bound nucleic acid substrate spans the polymerase and RNase H domains therefore important contacts are also made by the connection and RNase H domains of p66 as wells as by p51 (87). An "RNase H primer grip" region makes multiple contacts with an RNA/DNA hybrid substrate to allow cleavage of the RNA template (87).

To facilitate the variety of RNase H cleavage activities required during reverse transcription, RT is capable of binding nucleic acid substrates in multiple conformations (88, 89). As described above, the polymerase competent (or polymerase dependent) binding mode has the primer 3'-OH situated in the polymerase P-site with the RNase active site 18 nucleotides downstream. This binding mode allows for polymerase dependent RNase H activity during processive DNA synthesis (83, 88). Alternatively, RT can bind an RNA/DNA hybrid with the RNA template 5' end in the polymerase active site thus positioning the RNase H active site 13-

19 nucleotides from the 5' end (89-91). This binding mode, called RNase H competent (or polymerase independent) binding is responsible for the highly specific RNase cleavages at both ends of the PPT during reverse transcription. RT can also bind the nucleic acid substrate irrespective of the primer 3'- or template 5'-termini (92). Template/primer binding in this manner results in random internal cleavage of the RNA template. Certain HIV-1 sequences and RNA secondary structures lead to directed cleavage events when RT is bound in this mode (92).

Multiple biochemical and kinetic studies have examined the binding affinity of RT for nucleic acid substrates (57, 83, 86-89, 91, 93). Binding affinity was dependent on several factors including hybrid structure (DNA/DNA or RNA/DNA), substrate length, and template sequence. Generally, the kinetic binding constants (K_d) for RT binding to RNA/DNA and DNA/DNA substrates were approximately 5-20 nM (93, 94).

1.6.4 Mechanism of nucleotide binding and incorporation

RT binding to a template/primer substrate (in the polymerase competent mode) situates the primer 3'-OH terminus in the P-site and exposes the binding site for an incoming dNTP, called the N-site, or nucleotide site. (**Figures 1.6 and 1.7**). Multiple structural studies of [RT-template/primer/dNTP or NRTI] complexes have elucidated the molecular mechanisms of dNTP binding and incorporation (76, 77, 83-85). The RT polymerase active site in the palm subdomain contains the catalytic triad residues D110, D185, and D186 (**Figure 1.7**). Residues D185 and D186 are part of the YXDD motif conserved among all retroviruses, with X being methionine for HIV-1 (83). The catalytic triad aspartate residues coordinate two divalent metal cations (likely

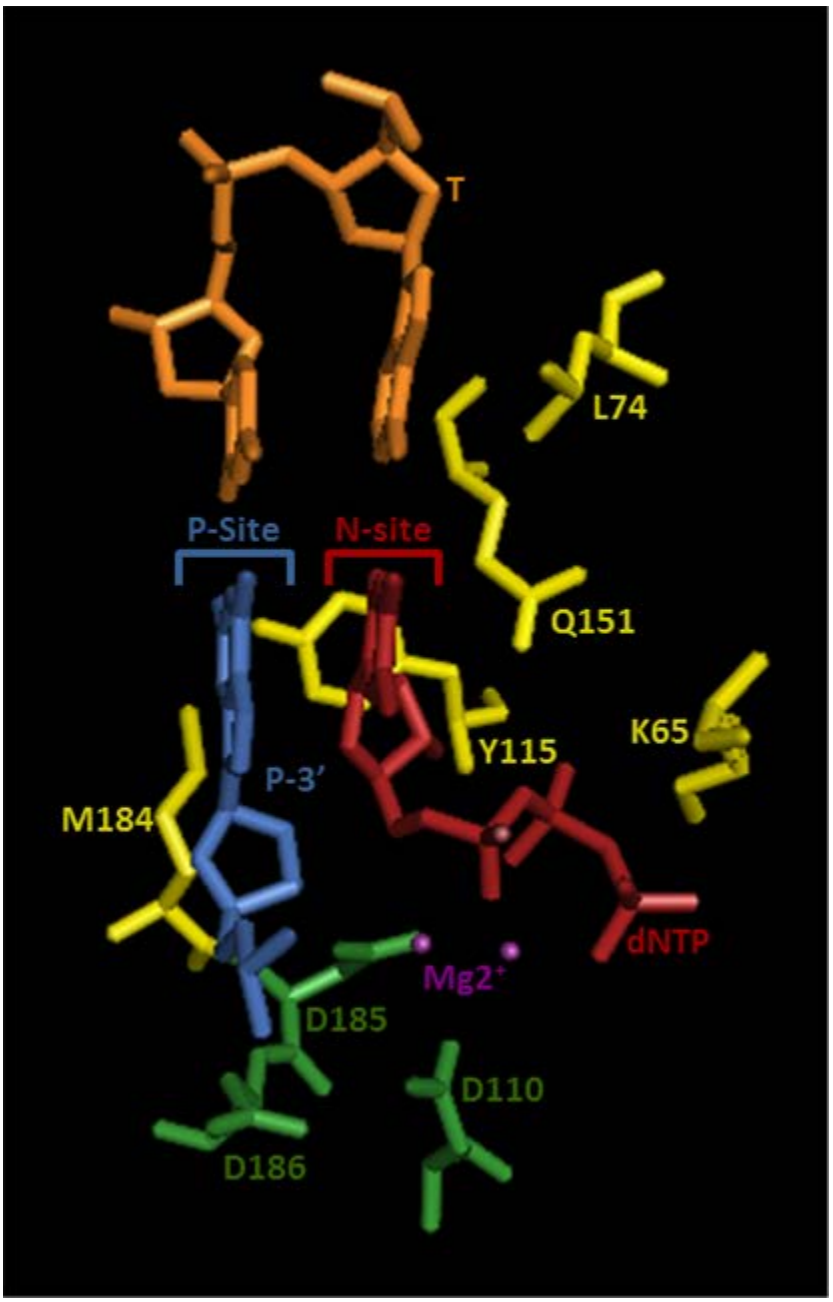

Figure 1.7 Molecular model of the RT active site showing the pre-incorporation complex of a bound dNTP substrate (red).
The positions of the priming site (P-site) with the primer 3'-residue (P-3', blue) and the nucleotide binding site (N-site) with a bound dNTP (red) are indicated. The catalytic triad residues D110, D185, and D186 (green) coordinate the two magnesium ions shown in purple. Residues K65 L74, Y115, Q151, and M184, shown in yellow, contact the incoming dNTP and are often mutated to confer resistance through the discrimination mechanism. The template residues (T) that are base paired with the primer 3'-residue and the incoming dNTP are shown in orange. The structure was drawn using PyMol based on the PDB Coordinates 1RTD from Huang et al. 1998 (77).

Mg^{2+} *in vivo*) supporting the proposed two metal ion model for the phosphoryl transfer reaction by RT and other polymerases (77, 79). Residues K65, R72, L74, Y115, Q151 and M184 form the N-site for dNTP binding and base pairing with the corresponding template base. Residues K65 and R72 interact with the incoming dNTP β and γ phosphates, respectively, while residue Q151 contacts the 3'-OH of the incoming dNTP. The 2'-position of the dNTP is in particularly close proximity to residue Y115, which is believed to confer specificity for dNTP over rNTP (95, 96).

Structural and kinetic studies support an induced fit model where dNTP binding at the N-site and appropriate template base pairing causes a conformational change where the fingers subdomain clamps down on the template/primer and dNTP (77, 97-99). The resulting "closed" polymerase complex has the dNTP α phosphate aligned for nucleophilic attack by the primer 3'-hydroxyl (**Figure 1.6B**). This reaction forms the phosphodiester bond between the primer and dNTP while producing pyrophosphate. The opening of the fingers subdomain allows pyrophosphate release, template/primer translocation for processive polymerization, or RT dissociation (77, 83). Incorporation fidelity has been attributed to the conformational change dependence on correct dNTP binding and base pairing (96, 98, 100).

1.6.5 Pre-steady state kinetics of nucleotide incorporation

Steady state kinetic assays demonstrate that RT dissociation and template/primer rebinding is rate limiting during DNA synthesis (83). However, pre-steady state or transient kinetic studies, where RT is pre-bound with the template/primer substrate, allow for the measurement of the kinetic binding constant (K_d) and incorporation rate (k_{pol}) of *single* nucleotide addition (98, 100). These studies demonstrate that the rate limiting step of single nucleotide incorporation is the conformational change to a closed ternary complex rather than dNTP binding or catalysis.

The binding constants of dNTP vary with respect to base. However, in general dNTPs bind with K_d values in the low micromolar range. Studies have shown that dNTPs may bind more efficiently with DNA/DNA substrates than with RNA/DNA substrates (98, 100). However, the incorporation rates of bound dNTP are approximately 2-fold higher for incorporation in RNA/DNA hybrids compared to DNA/DNA hybrids. Pre-steady state analyses of NRTI-TP incorporation compared to the analogous dNTP are used to evaluate the relative ability of NRTI-TP to compete for binding and incorporation by RT.

1.7 NRTI PHOSPHORYLATION AND MECHANISM OF RT INHIBITON

In order to be orally bioavailable and readily transported across cell membranes, NRTI are administered as prodrugs in the form of nucleosides (lacking phosphates) or chemically shielded monophosphate nucleotides in the case of NtRTI. NRTI and NtRTI must undergo successive phosphorylation by host enzymes to produce the NRTI-TP substrate required for incorporation by RT (36, 39, 101). Some NRTI prodrugs (e.g. ddI and ABC) also require additional modification by other cellular enzymes to produce the nucleotide form active against RT (discussed with respect to each NRTI below). Therefore, NRTI antiviral activity is not only dependent on activity against HIV-1 RT but also on their ability to serve as substrates for host phosphorylating enzymes.

1.7.1 NRTI Phosphorylation

The general phosphorylation scheme required to produce the NRTI-TP RT substrate is presented in **Figure 1.8**. NRTI-MP is usually produced through the action of the constitutively active deoxynucleoside kinases responsible for endogenous nucleotide salvage or through phosphotransfer from 5'-nucleotidase (101-106). Addition of the second phosphate to produce NRTI-DP is carried out by the nucleotide monophosphate kinases: thymidylate kinase, uridylate-cytidylate kinase, adenylate kinases 1–5 and guanylate kinase (107). Production of NRTI-TP from NRTI-DP is readily catalyzed by many cellular enzymes but most commonly by nucleotide diphosphate kinase, phosphoglycerate kinase, pyruvate kinase and creatine kinase (108, 109). Conversely, many cellular dephosphorylating enzymes also act on mono-, di-, and tri-phosphate forms of NRTI (36). Therefore, the equilibrium of phosphorylation and dephosphorylation greatly influences intracellular NRTI-TP pools and subsequent antiviral activity.

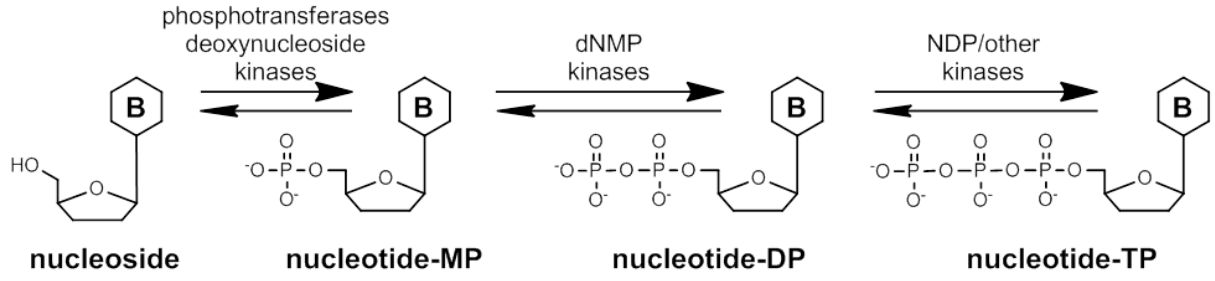

Figure 1.8 General scheme of NRTI phosphorylation to the NRTI-MP, NRTI-DP, and NRTI-TP forms.
The NRTI-TP form acts as a competitive substrate with respect to the analogous dNTP for incorporation by HIV-1 RT. A generic NRTI base (B) is depicted.

1.7.2 Mechanism of NRTI Inhibition

Once metabolized by host cell enzymes to their triphosphate forms, NRTI-TP inhibit RT-catalyzed proviral DNA synthesis by two mechanisms (83). First, they are competitive inhibitors for binding and/or catalytic incorporation with respect to the analogous dNTP substrate. Second, they terminate further viral DNA synthesis due to the lack of a 3'-OH group. Obligate chain termination is the principal mechanism of NRTI antiviral action. NRTI-TP binding affinity and incorporation rate are generally similar to their analogous dNTP counterparts (83). Notable exceptions will be discussed with regard to the specific NRTI.

In theory, NRTI-TPs should be ideal antivirals. Each HIV virion carries only two copies of genomic RNA. There are about 20,000 nucleotide incorporation events catalyzed by RT during the synthesis of complete viral DNA, thus providing approximately 5000 chances for chain-termination by any given NRTI (20). Since HIV-1 RT lacks a formal proof-reading activity (51, 110), a single NRTI incorporation event should effectively terminate reverse transcription. In reality, however, NRTIs are less potent than might be expected. The two primary reasons responsible for this are: (i) HIV-1 RT can effectively discriminate between the natural dNTP and NRTI-TP, and the extent of this discrimination can be increased dramatically by nucleic acid sequence; and (ii) HIV-1 RT can excise the chain-terminating NRTI-MP by using either pyrophosphate (pyrophosphorolysis) or ATP as a substrate (83). These two RT characteristics can be selectively enhanced by single amino acid substitutions thus providing the mechanisms for NRTI resistance (111).

1.8 NRTI RESISTANCE SELECTION AND MECHANISMS

Populations of HIV-1 circulating within individual patients are highly diverse. Genetic diversity is driven by both replication errors resulting in mutation and genome recombination during reverse transcription (58, 59, 110). Mutations are easily generated in HIV-1 genomes for two key reasons; the high rate of viral replication and the lack of a formal proofreading activity in RT. Approximately 10.3×10^9 virions per day are produced in a typical patient and estimates of RT error rate are as high as 5-10 misincorporations per genome per replication cycle (111-113). Under selective pressure, such as from antiretroviral drugs, mutated species that provide a replication advantage quickly become dominant viral populations. Antiviral resistance is conferred by mutations that decrease the effectiveness of a drug to inhibit viral replication. Mutations in RT confer resistance to NRTI through two distinct molecular mechanisms: nucleotide discrimination (**Figure 1.9**) and the phosphorolytic removal (excision; **Figure 1.10**) of a chain-terminating NRTI-MP (111).

1.8.1 Nucleotide discrimination

The nucleotide discrimination mechanism of NRTI resistance involves the preferential incorporation of natural dNTP substrates over NRTI-TP substrates **(Figure 1.9).** NRTI-resistant viruses maintain the ability to complete reverse transcription in the presence of drug by excluding NRTI-TP substrates while retaining the ability to incorporate natural dNTP substrates

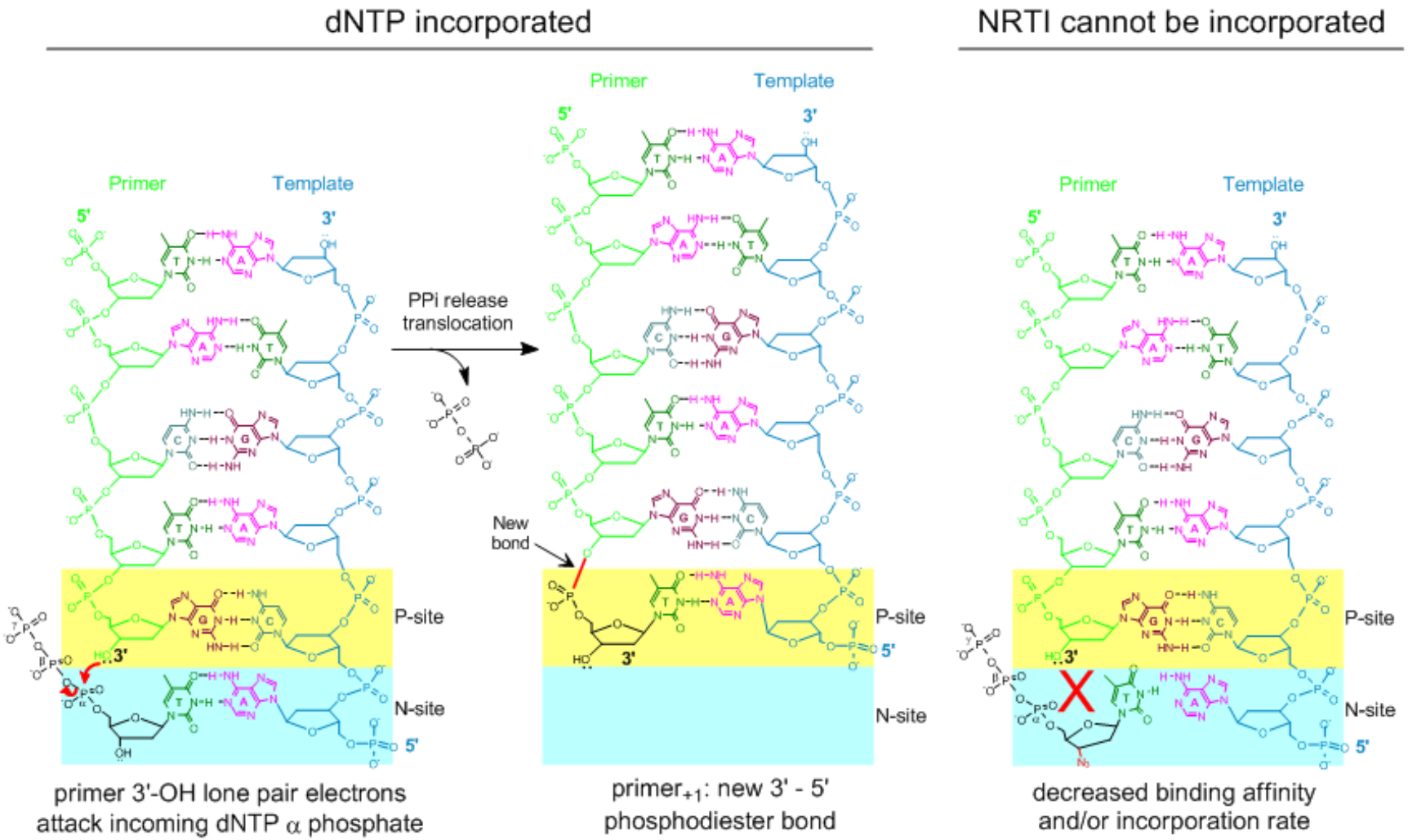

Figure 1.9 Molecular mechanism of NRTI discrimination by HIV-1 RT.
Mutations that confer resistance to NRTI by the discrimination mechanism maintain the ability to incorporate natural dNTP while selectively excluding NRTI-TP. NRTI-TP exclusion occurs by decreased NRTI-TP binding affinity (K_d) for the RT active site or decreased rate of NRTI incorporation (k_{pol}).

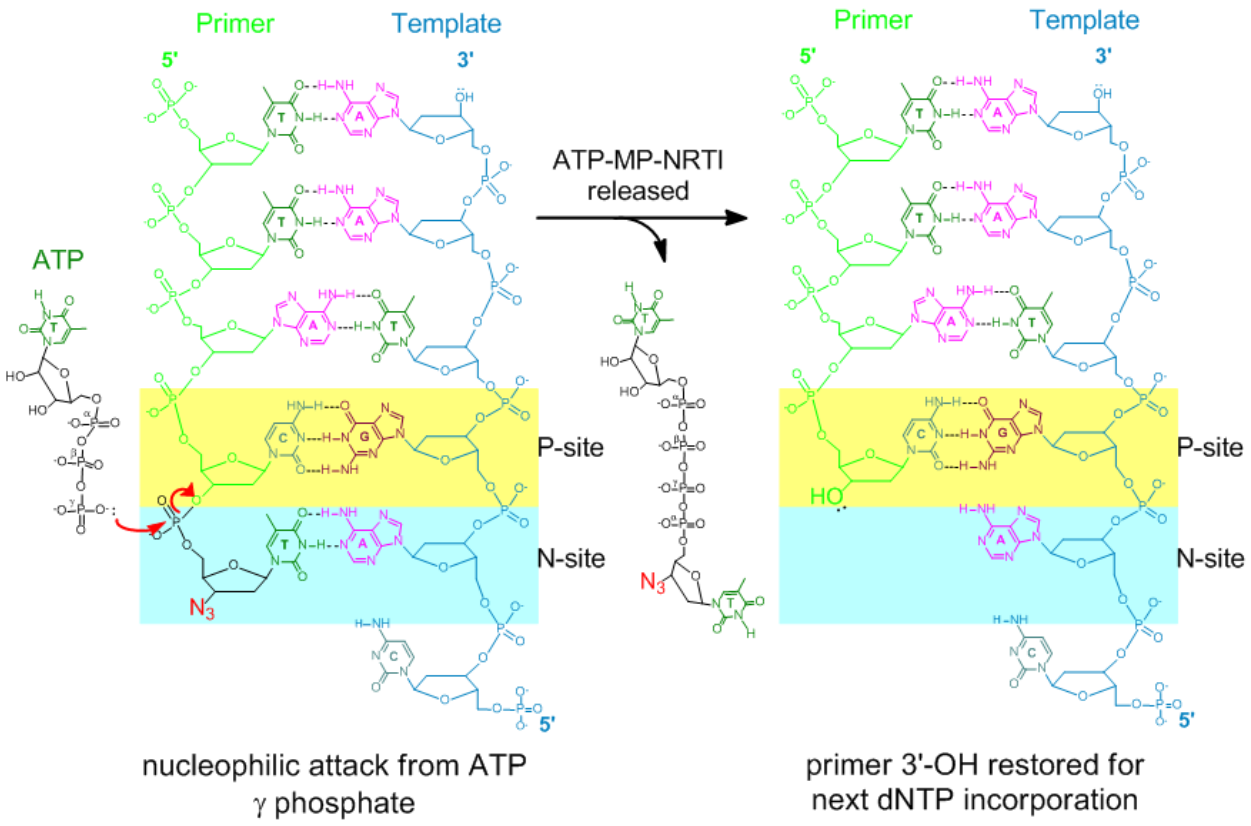

Figure 1.10 Molecular mechanisms of HIV-1 RT primer unblocking by ATP-mediated NRTI-MP excision.
Nucleophilic attack of the chain-terminating NRTI-MP from an ATP pyrophosphate donor results in the release of an adenosine-NRTI dinucleoside tetraphosphate and restores the primer 3'-OH for subsequent nucleotide incorporation.

with reasonable efficiency (39, 83, 111). Mutations conferring enhanced NRTI-TP discrimination selectively decrease NRTI binding efficiency or rate of catalysis while preserving binding and incorporation of the analogous dNTP. NRTI discrimination mutations occur at residues in the fingers or palm of the polymerase active site including L74V, K65R, Q151M (in complex with other mutations) and M184V/I, some of which form the dNTP binding pocket (80, 114-127). These mutations affect NRTI and dNTP binding and incorporation through direct interaction or via conformational distortions of the active site. These mutations and their discrimination phenotypes and mechanism toward specific NRTI will be discussed below.

1.8.2 NRTI-MP excision

Although RT does not possess a distinct exonucleolytic proofreading mechanism, RT does have an innate ability to catalyze the reverse reaction to nucleotide incorporation, the pyrophosphorolytic removal of an incorporated nucleotide monophosphate (**Figure 1.10**), typically referred to as excision (128-132). When a newly incorporated nucleotide-monophosphate sits in the N-site prior to RT translocation, it is susceptible to nucleophilic attack by an incoming pyrophosphate donor molecule such as inorganic pyrophosphate (PPi) or ATP (129, 130). This reaction results in the removal of incorporated nucleotide monophosphate from the primer. When PPi or ATP act as the pyrophosphate donor, a dNTP or a dinucleotide-tetraphosphate product is released, respectively. Nucleotide monophosphate removal, however, is greatly disfavored for wild-type RT during normal DNA synthesis due to the low binding affinity of PPi or ATP and the slow rate of pyrophosphorolysis compared to nucleotide incorporation (83, 128). Mutations in the RT polymerase domain primarily selected by AZT and d4T can enhance the ATP-mediated excision phenotype (46, 47, 133, 134). These mutations are

termed thymidine analog mutations (TAMs), or alternatively excision enhancing mutations, and will be discussed in detail below with regard to AZT and d4T resistance. TAMs selectively increase the ATP-mediated NRTI-MP excision from a chain-terminated primer (82-84, 135). Although slight discrimination has been observed in some cases, mutant RTs containing TAMs generally incorporate NRTI with similar efficiency as dNTP (136). The primary mechanism by which TAMs confer resistance is through increased NRTI-MP removal from chain-terminated primers. In absence of the next complimentary dNTP, most NRTI can be excised from the chain-terminated primer (137). The mechanism of excision enhancement has been under considerable debate, but is now believed to be primarily due to increased binding affinity of the ATP pyrophosphate donor for most TAMs (82, 135, 138). The T215F/Y mutation in particular increases ATP binding because the F or Y side chains facilitate Pi-Pi stacking with the ATP adenine ring.

Excision can only occur prior to RT translocation, while the incorporated NRTI-MP remains in the N-site. Cellular concentrations of dNTP can promote RT translocation such that the terminating NRTI-MP moves to the P-site, thus freeing the N-site (83, 137, 139, 140). Binding of the next correct dNTP to the N-site results in a stable closed conformation dead-end complex (**Figure 1.11**): the lack of a 3'-hydroxyl prevents incorporation of the incoming dNTP, the terminating NRTI-MP cannot be excised from the primer, and the dNTP bound at the N-site prevents retrograde translocation. The dead-end complex model may explain why cellular concentrations of the next complementary dNTP inhibit the excision of most terminating NRTI-MP except AZT. It has been suggested that the bulky 3'-azido group of AZT protrudes into the N-site preventing dNTP binding (82). Some studies have also suggested that primers terminated

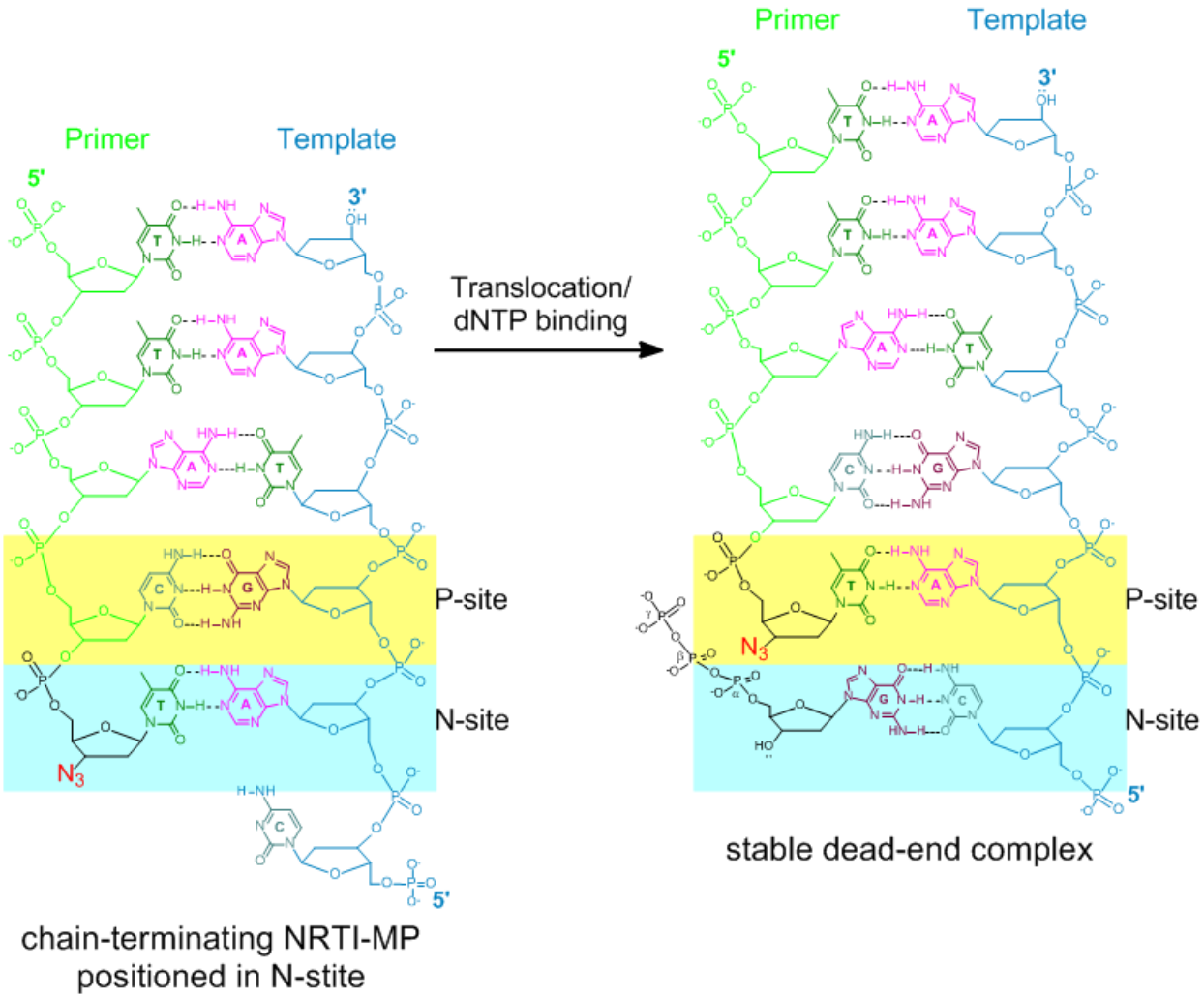

Figure 1.11 Formation of a stable, dead-end RT/T-P-NRTI-MP/dNTP complex.
Following NRTI-MP incorporation, translocation and binding of the next correct dNTP results in a stable dead-end complex, in which further nucleotide incorporation and NRTI-MP excision are not possible.

with AZT-MP preferentially bind in the N-site (137). These explanations are not complete, however, because not all 3'-azido containing analogs are readily excised, suggesting that NRTI base and sugar moieties must also influence excision capacity (141-143). The selection of multiple amino acid insertions following position 69 as well as several dipeptide insertions in the fingers subdomain in addition to TAMs (described in detail below) also destabilizes the dead-end ternary complex, thus allowing for improved excision of most chain-terminating NRTI-MP in the presence of the next dNTP (144-146).

1.8.3 Antagonism between the discrimination and excision mechanisms

The use of two NRTI together with an antiretroviral drug from another class is recommended for combination antiretroviral therapy because several studies have shown synergy between NRTI combinations, such as AZT/ddI and AZT/3TC (147-152). The observed antiviral synergy of these combinations has been attributed to antagonism between the discrimination mutations K65R, L74V, and M184V and TAMs (81, 120, 153-160). K65R, K70E, L74V, or M184V when present in combination with TAMs reverse the AZT resistance observed with TAMs alone. The rate of primer unblocking by ATP-mediated excision is decreased by the addition of K65R, K70E, L74V, and M184V in the background of TAMs (156, 158, 160, 161). Multiple hypotheses have been proposed to explain how these residues diminish excision activity. K65R and M184V may reposition or limit the flexibility of the chain-terminated primer in the active site (81, 155). L74V may alter the base pairing interaction of the NRTI with the template (77, 81). Additionally, TAMs also negatively affect the ability of K65R to discriminate between NRTI-TP and dNTP by partially restoring the rate of incorporation (160).

The poor excision and discrimination phenotypes observed with viruses carrying both TAMs and discrimination mutations can be partially restored by the accumulation of additional mutations (152, 162-166). These mutations, some of which are in the connection and RNase H domains, include E44A/D, T69D, V75M/T, V118I, H208Y, R211K, K219R, N348I, and G333D.

1.9 FDA-APPROVED NRTI

NRTI remain an invaluable component of combination antiviral therapy that suppresses viral replication to undetectable levels, thus dramatically improving patient survival and quality of life. However, the rapid selection of NRTI resistance mutations that often confer cross-resistance to multiple NRTI remains the greatest challenge to their success. Much research effort has focused on understanding NRTI activity and resistance. This section will: i) provide a detailed review of the properties of the FDA-approved NRTI, including cellular phosphorylation and metabolism, inhibition of RT, and resistance mutations/mechanisms; and ii) discuss the limitations of the current NRTI to highlight the need for novel NRTI development.

1.9.1 Zidovudine (AZT) and Stavudine (d4T)

Zidovudine (3'-azido-2',3'-dideoxythymidine, AZT) and stavudine (2',3'-didehydro-3'-deoxythymidine, d4T) were first synthesized in the 1960s as potential anticancer drugs, but were abandoned due to toxicity concerns (167). However, both were found to have potent and selective anti-HIV-1 activity at much lower concentrations (3-5). AZT was approved by the FDA for clinical use in 1987, thus becoming the first available antiviral drug. FDA approval of d4T

followed in 1994. AZT and d4T are both thymidine analogs that lack a 3'-hydroxyl group. The ribose ring 3'-hydroxyl of AZT has been replaced with an azido (-N3) group, whereas d4T contains an unsaturated 2',3'-didehyro ribose ring. AZT and d4T are both activated by sequential phosphorylation by thymidine kinase, dTMP kinase, and nucleotide diphosphate kinase to produce the nucleotide mono-, di-, and triphosphate forms (168). AZT is also subject to metabolism in the liver, kidney, and intestinal mucosa to produce the 5'-glucuronide and 3'-amino-thymidine which is highly toxic (169, 170). AZT-TP and d4T-TP also act as substrates for incorporation by mitochondrial polymerase γ resulting in a reduction of mitochondrial DNA and subsequent mitochondrial poisoning (171).

AZT-TP and d4T-TP are incorporated by RT into viral DNA across from adenosine bases, resulting in chain-termination with submicromolar 50 % inhibitory concentrations (IC_{50}) (141). Pre-steady state studies show that AZT-TP and d4T-TP are good substrates for incorporation by RT (136). The binding affinities of AZT-TP and d4T-TP are similar to that of TTP with K_d values of 2.0 μM, 2.7 μM, and 2.2 μM, respectively (172). The k_{pol} values for TTP, AZT-TP, and d4T-TP are 9.2 sec^{-1}, 8.8 sec^{-1}, and 4.3 sec^{-1}, respectively.

Soon after its introduction, AZT monotherapy was shown to lead to rapid resistance development and subsequent therapeutic failure. (46, 47, 133, 134). Decreased AZT susceptibility was associated with the selection of the K70R mutation, which was followed by D67N and K219E/Q. Clinical isolates from patients failing AZT or d4T therapy were found to contain similar TAMs (173, 174). TAMs are typically selected in two patterns i) M41L, D67N, L210W, T215Y, and K219E/Q; and ii) M41L, D67N, K70R, T215F, and K219E/Q (174). These patterns are not exclusive, however, and the reasons they are selected together are not clear. The presence of each TAM in either pattern is not required for substantial resistance, but additional

TAMs usually results in increased resistance (83). The selection of TAMs is associated with very high levels of viral resistance resulting in up to a three log reduction in AZT or d4T susceptibility. TAMs also confer cross-resistance to all other NRTI (46). The selection of TAMs is often followed by the selection of additional mutations (E44D, A62V, V118I, H208Y, R211K, L214F, multiple insertions following T69, and multiple dipeptide insertions in the fingers subdomain) that further increase resistance and cross-resistance (144, 145, 162, 175). As described above, TAMs confer resistance by selectively increasing the excision of NRTI-MP from chain-terminated primers. RT containing TAMs are significantly more efficient at unblocking AZT-MP- and d4T-MP-terminated primers than WT RT (130-132, 141). The efficiency with which TAM-containing RTs excise incorporated AZT-MP or d4T-MP varies with the number of TAMs present and the template sequence (39, 83).

1.9.2 Didanosine (ddI)

Didanosine (ddI, 2',3'-dideoxyinosine) is a prodrug that is converted to ddATP, the active metabolite recognized by RT. Initially, 2',3'-dideoxyadenosine (ddA) was evaluated as a clinical candidate but was ultimately discovered to cause nephrotoxicity (176, 177). Interestingly, ddA was shown to be metabolized to ddI by adenosine deaminase and that the ddI metabolite is responsible for much of the antiviral activity of ddA. Therefore, the administration of ddI avoids the ddA associated nephrotoxicity (176, 178). Didanosine is phosphorylated to didanosine-MP by cytosolic 5'-nucleotidase, which uses either inosine monophosphate (IMP) or guanosine monophosphate (GMP) as phosphate donors (179). Didanosine-MP is then converted to ddAMP by adenylosuccinate synthetase and 5' adenosine monophosphate-activated protein (AMP) kinase (178). The enzymes involved in phosphorylation of ddAMP to ddADP and ddATP have not been

identified, although AMP kinase and NDP kinase have been proposed to play a role. Didanosine can be hydrolyzed by purine nucleoside phosphorylase (PNP) to release the hypoxanthine base (180).

After metabolism and activation, ddATP can be incorporated by HIV-1 RT into the nascent viral DNA causing chain-termination. In cell culture assays, the concentrations of ddI required to inhibit HIV-1 replication by 50 % (EC_{50}) were between 0.1 μM and 4 μM depending on the assay system and cell type (178). ddATP binds RT with similar affinity as dATP however, the rate of incorporation is > 5-fold slower for ddATP compared to dATP (126).

Clinical isolates from patients that received didanosine monotherapy for 1-2 years harbored the mutations L74V, K65R, M184V, as well as some TAMs with L74V being most prevalent (116). The L74V mutation confers at least 5-fold resistance to ddI compared to WT HIV-1 (116, 151). Pre-steady state incorporation assays with L74V RT indicate that the incorporation rate for ddATP is severely decreased (10-fold) compared to WT RT, indicating a discrimination phenotype (126, 181). The L74V mutation also causes reduced viral fitness due to decreased ability to incorporate natural dNTPs (126, 181).

Additionally, AZT+ddI combination treatment can select a cluster of mutations with Q151M appearing first followed by A62V, V75I, F77L, and F116Y (182). Together these mutations are referred to as the Q151M complex ($Q151M_c$). This complex results in high level resistance to most NRTI (tenofovir is the exception) by the discrimination mechanism (183, 184). The rate of incorporation of each NRTI was significantly decreased compared to that of its counterpart dNTP. It is believed that a loss of interaction between Q151 and the 3'-OH of the incoming dNTP or NRTI is responsible for this mechanism (183).

1.9.3 Abacavir (ABC)

Abacavir (1S,4R)-4-[2-amino-6-(cyclopropylamino)-9H-purin-9-yl]cyclopent-2-en-1-yl]methanol) is a prodrug of carbovir (2-Amino-1,9-dihydro-9-[(1R,4S)-4-(hydroxymethyl)-2-cyclopenten-1-yl]-6H-purin-6-one), a deoxyguanosine analog (185). Abacavir is phosphorylated to abacavir-MP by adenosine phosphotransferase (186). A yet unidentified cytosolic deaminase then converts abacavir-MP to carbovir-MP. Phosphorylation to the diphosphate derivative occurs via guanidinylate monophosphate kinase. The final phosphorylation step can be catalyzed by a number of cellular enzymes including 5'-nucleotide diphosphate kinase, pyruvate kinase, and creatine kinase (186). Abacavir is extensively catabolized in the liver and only 1.2% is excreted as unchanged abacavir in urine (187). Abacavir oxidation by alcohol dehyrogenases produces a 5'-carboxylic acid derivative and UDP glucuronosyltransferase yields the 5'-O-glucronide (187).

Abacavir demonstrated equivalent activity to AZT against HIV-1 clinical isolates in peripheral blood lymphocytes with EC_{50} values of 0.26 μM and 0.23 μM, respectively (185). CBV-TP potently and selectively inhibited HIV-1 RT with a Ki value of 21 nM.

Both cell culture selection experiments and clinical isolates from patients treated with ABC identified the similar resistance mutations as those selected by ddI (188). The most frequent mutations selected by ABC were M184V and the combination of L74V+M184V. Both of these mutations alone conferred low-level resistance (2- to 4-fold over WT) to ABC. In combination, L74V+M184V conferred 11-fold ABC resistance over WT (188). Like L74V, M184V confers resistance to ABC and other NRTI through the discrimination mechanism(189-191). Discrimination by M184V has been more thoroughly characterized for 3TC and FTC so the molecular mechanism by which M184V discriminates NRTI will be discussed further below.

1.9.4 Zalcitabine (ddC), lamivudine (3TC), and emtricitabine (FTC)

Zalcitabine (2',3'-dideoxycytidine; ddC), lamivudine ((-)-3'-thia-2',3'-dideoxycytidine; 3TC) and emtricitabine ((-)-3'-thia-5-flouro-2',3'-dideoxycytidine; FTC) are the three cytidine analog NRTI and were FDA approved in 1992, 1994, and 1995, respectively (192). Zalcitabine never saw widespread application due to delayed peripheral neuropathy that progressed with cumulative dose and did not resolve with stoppage of use (193). Neuropathic cytotoxicity was later associated with potent inhibition of mitochondrial polymerase γ (194). ddC was subsequently removed from the market in 2006 (153).

Like ddC, 3TC and FTC are cytidine analogs. However, both contain the unnatural L-enantiomer ribose with a sulfur atom replacing the C3' position. Emtricitabine has an additional 5-flouro modification to the cytosine ring. The modified sugar ring results in decreased affinity of 3TC-TP and FTC-TP compared to ddCTP for polymerase γ (171). Lamivudine and emtricitabine are both metabolized to their respective 5'-mono- and di- and triphosphate derivatives by deoxycytidine kinase, deoxycytidine monophosphate kinase, and 5'-nucleoside diphosphate kinase, respectively (195-198).

3TC and FTC demonstrate antiviral activity against HIV-1 in cell culture and their 5'-triphosphate forms are potent chain-terminators of DNA synthesis upon incorporation by HIV-1 RT (199-201). Cell culture selection as well as sequencing of patient isolates identified the mutations M184V or I to confer decreased susceptibility to 3TC and FTC (202-205). M184I is selected within two weeks in patients receiving 3TC which is replaced with M184V within two months (205). M184V conferred greater than 1400-fold resistance to 3TC and FTC and cross-resistance to ddI and ABC (203).

The mechanism of M184V resistance has been extensively characterized with structural and kinetic studies. Multiple kinetic studies have demonstrated a severely reduced catalytic efficiency of incorporation of 3TC-TP and FTC-TP by HIV-1 RT containing the M184V mutation (189-191). 3TC-TP and FTC-TP demonstrated drastically impaired binding to M184V RT (K_d values increased 76- and 19- fold, respectively) compared to WT enzyme with relatively unchanged incorporation rates. The catalytic efficiencies of dCTP binding and incorporation for M184V and WT RT were similar, indicating that M184V can effectively discriminate between dCTP and 3TC-TP or FTC-TP (189-191). A crystal structure of RT containing the M184I mutation revealed that branched side chains at position 184 (i.e. I and V) cause a steric clash with the L-enantiomer ribose of 3TC-TP or FTC-TP but not with the natural D- ribose of dCTP (80). This explains why 3TC-TP and FTC-TP binding is diminished while dCTP binding is maintained. Together, these findings describe the molecular mechanism of discrimination by which the M184V/I mutations confer resistance to 3TC and FTC.

1.9.5 Tenofovir (TFV)

The acyclic nucleoside phosphonate tenofovir (R-9-(2-phosphonylmethoxypropyl)-adenine; (*R*)PMPA) has no sugar ring structure but contains an acyclic methoxypropyl linker between the base N9 atom and a non-hydrolyzable C-P phosphonate bond (206). Thus TFV represents the only currently approved NtRTI. Tenofovir is poorly absorbed by the oral route and is therefore administered as a lipophilic orally bioavailable prodrug, tenofovir disoproxil fumarate (TDF), a fumaric acid salt of the bis-isopropoxycarbonyloxymethyl ester of tenofovir (206). Degradation of TDF to its monoester and, subsequently, to tenofovir occurs readily in the intestinal mucosa by the action of carboxylesterases and phosphodiesterases, respectively (207). Tenofovir is

rapidly converted intracellularly to tenofovir-monophosphate (TFV-MP) and the active tenofovir-diphosphate (TFV-DP) forms by adenylate monophosphate kinase and 5'-nucleoside diphosphate kinase, respectively (208).

Cell culture selection experiments identified K65R as the predominant resistance mutation which conferred 3- to 4- fold resistance to TFV compared to WT HIV-1 (209). It has been reported that the K70E mutation is also selected in HIV-1 patients receiving tenofovir in combination with other NRTI (210). However, the K65R and K70E mutations are antagonistic to one another and are not believed to exist on the same genome (211).

The K65R mutation provides some level of cross-resistance to all approved NRTI except AZT (212). Both K65R and K70E mutations confer resistance to tenofovir via the discrimination mechanism (122, 160, 161, 212, 213). Unlike the discrimination of 3TC-TP and FTC-TP by M184V, the discrimination phenotype conferred by K65R and K70E toward TFV-DP is driven by decreased k_{pol}, and not by significantly altered binding (122, 160, 161, 212, 213).

1.9.6 Limitations of the currently approved NRTI

Despite their important contribution to the success of combination antiretroviral therapy, the currently approved NRTI have significant limitations that include adverse events associated with drug toxicity, pharmacokinetic limitations (e.g. short intracellular half-life) or interactions with other antiretroviral drugs, and the selection of drug-resistant variants that are cross-resistant to other NRTI (36). The development of novel NRTI with considerations for these shortcomings is necessary for the continued success of the NRTI drug class.

Treatment with NRTI is associated with both short- and long-term toxicities resulting in occasionally life-threatening adverse events (214). Toxicity associated adverse events often

result in lower drug regimen adherence by patients, thus reducing their anti-HIV-1 efficacy. Examples of acute toxicity from NRTI include: fatigue, dizziness and dyspepsia common with treatment of most NRTI, hypersensitivity reaction from ABC, nausea and vomiting with ddI and ZDV, anemia and neutropenia observed with ZDV treatment, pancreatitis and lactic acidosis in patients treated with ddI or d4T, acute renal failure and drug induced hepatitis are rare but have been observed with treatment of most NRTI (214-219). Long term NRTI adverse events include: cardiovascular disease with ABC and ddI, peripheral and central neuropathy with d4T, ddI, ddC, ZDV, diabetes with ZDV, d4T, and DDI, Dyslipidemia with ZDV, d4T, and ABC, various hepatic pathologies with most NRTI, lipodystrophy with d4T and ZDV (214, 218-222). It has been suggested that mitochondrial toxicity from inhibition of mitochondrial DNA polymerase γ represents a common mechanism responsible for many NRTI associated toxicities (223). Mitochondrial toxicity has been directly linked to myopathy and cardiomyopathy resulting from treatment with AZT (224, 225). Indeed, polymerase γ is potently inhibited by the active triphosphate forms of ddC, ddI (metabolized to ddATP), and d4T, however, the active forms of AZT, ABC, and TFV were found to be poor substrates for incorporation by polymerase γ (226). Recent evidence suggests that mitochondrial toxicity may also be due to inhibition of the thymidine phosphorylating enzymes causing indirect inhibition of mitochondrial DNA replication through reduction in mitochondrial TTP pools (227). Mitochondrial toxicity via polymerase γ inhibition or other mechanisms does not explain adverse events from treatment of NRTI such as by ABC and TDF that do not deplete mitochondrial DNA (228). Other mechanisms of NRTI toxicity include the involvement of the major histocompatability complex class 1 human leukocyte antigen 57.1 haplotype in ABC hypersensitivity and TFV accumulation in renal proximal tubules due to influx transport via the human organic anion transporter 1 in

TDF-associated renal toxicity. (215, 222). The previously identified mechanisms of NRTI toxicity do not explain all NRTI-related adverse events (214). As such, there is much to be learned about the mechanisms of NRTI-induced toxicity in order to inform the development of novel NRTI with improved safety. However, all novel NRTI under current development should be thoroughly evaluated with respect to their propensity to cause cellular and tissue toxicity via known mechanisms such as mitochondrial toxicity and bone marrow depletion.

Antiretroviral combination therapy regimens often require patients to take 3 or more drugs daily, which often require multiple pills and multiple doses per day (229). This high therapeutic burden can lead to low patient adherence to antiretroviral regimens thus decreasing the antiretroviral effectiveness. As such, simplifying antiretroviral regimens through fixed-dose combinations that limit pill count and the development of drugs with pharmacokinetic properties amenable to once daily dosing (i.e. long half-life) is an important concern. The requirement of NRTI for intracellular phosphorylation to the active NRTI-TP form suggests that the intracellular concentration of NRTI-TP is more important for antiviral effectiveness than plasma half-life (230, 231). It has been demonstrated that intracellular concentrations of the active triphosphate metabolites of 3TC, FTC, and d4T, rather than levels of unchanged drugs in plasma, correlated with virologic response in HIV-infected patients (230, 232). The intracellular kinetics of activation and half-life of any NRTI-TP is subject to many cellular factors such as: cell activation state; cellular kinase expression levels, activation, and efficiency of NRTI substrate phosphorylation; cell cycle; activity of cellular dephosphorylating enzymes; and intracellular ratios of NRTI/deoxynucleoside, NRTI-MP/dNMP, NRTI-DP/dNDP, and NRTI-TP/dNTP (229) (233). For example, ZDV and d4T are phosphorylated to a greater extent and yield higher

ZDV-TP/dTTP and d4T/dTTP ratios in activated lymphocytes, thus exerting more potent antiretroviral activity in activated cells than in resting cells (234, 235). Conversely, ddI, ddC, and 3TC produce higher NRTI-TP/dNTP ratios and exert more potent antiretroviral activity in resting cells (234, 235). Thus, characterization of the NRTI activation by cellular phosphorylating enzymes and other factors that influence NRTI-TP intracellular half-life must be considered in the development of novel NRTI. To facilitate once or twice daily dosing, novel NRTI should maintain the minimally antiviral effective intracellular NRTI-TP concentration over a period a 12-24 hours.

Another factor that restricts patient antiretroviral regimen options and effectiveness is intra- and inter-antiretroviral class drug-drug interactions. The shared and overlapping phosphorylation pathways for activation of many NRTI leads to intra-NRTI drug class pharmacokinetic interactions by competition for phosphorylating enzymes when some NRTI are co-administered (233). For example, AZT and d4T are both phosphorylated to their –MP and –DP forms by thimidine kinase 1 and thymidylate kinase, respectively, however, AZT-and AZT-MP have stronger affinities for these enzymes (105). This pharmacokinetic interaction results in reduced cellular d4T-TP levels when AZT and d4T are co-administered in cell culture and antagonistic anti-HIV-1 activity in patients receiving AZT and d4T co-therapy (105, 236). A similar interaction has been observed for 3TC and ddC due to their common phosphorylation by deoxycitidine kinase (237). However, not all pharmacokinetic interactions between NRTI are detrimental. Despite competition between TFV and ddA for the same phosphorylating enzymes, co-administration of TDF and ddI leads to higher intracellular and plasma levels, and a longer half-life of the active ddI metabolite ddATP (238). This is due to TFV-mediated inhibition of ddI/ddA catabolism by purine nucleoside phosphorylase. NRTI are also subject to

pharmacokinetic interactions with drugs from other antiretroviral classes. For example, when ABC is co-administered with some PIs (e.g. atazanavir and lopinavir), ABC exposure is decreased up to 32 % via increased glucuronidation of ABC by uridine diphosphate glucuronyltransferase and subsequence ABC clearance (239, 240). Similarly, co-administration of TDF with some PIs (notably fosamprenavir and atazanavir) cause changes in TFV plasma and cellular levels, however the mechanism of this interaction is currently under debate (241). These studies illustrate the complex pharmacokinetic interactions of NRTI that must be given careful consideration when choosing which combination of NRTI to include in antiretroviral regimens.

Possibly the most important factor affecting the efficacy of the currently approved NRTI is the rapid selection of drug-resistance mutations that can lead to regimen failure. The mechanisms of HIV-1 resistance to NRTI and the specific mutations conferring resistance have been described in detail in the previous sections. Here, I will describe why NRTI resistance posses a significant hurdle to the continued success of the NRTI drug class that must be overcome when developing novel NRTI.

The increased access of NRTI-containing antiretroviral regimens along with the successful extension of life span of HIV-1 infected individuals has led to the increasing prevalence of resistance development to some NRTI within infected individuals as well as transmitted NRTI resistance (242). For example, in developing countries, where regimens containing 3TC, FTC, and ABC have become increasing available, the M184V mutation has been observed in 40 % to 85 % of patients failing antiretroviral therapy (243-245). Transmitted drug resistance was evident in recent drug resistance surveys of antiretroviral naïve HIV-1 infected patients in America and Europe, where antiretroviral therapy is widely available. These studies identified HIV-1 drug resistance mutations (including resistance to NRTI) in 8 % to 20 %

of the untreated population (246-249). In antiretroviral experienced patients complex combinations of mutations have been identified that confer broad spectrum resistance across multiple drug classes including NRTI, NNRTI, and PI (242, 250-252). Furthermore, patient non-adherence to therapy regimens (often due to adverse events and the high therapy burden discussed above) leads to sub-inhibitory drug levels that promote the selection and survival of drug-resistant variants. In order to stay ahead of the complex and constantly changing antiviral resistance problem, novel NRTI development efforts must focus on analogs that have a low potential for cross-resistance from the current circulating resistant viruses.

1.10 NOVEL NRTI DEVELOPMENT

Despite substantial investment and research, there is no vaccine for the prevention of HIV-1 infection (253). Efforts to prevent HIV-1 transmission using pre-exposure chemoprophylaxis, as well as research into strategies to cure HIV-1 infected individuals, are in their infancy (254, 255). Thus, combination antiretroviral therapy remains the best means to curtail the HIV-1 epidemic and improve patient quality of life. Potent combination antiretroviral therapy containing at least two NRTI has drastically decreased death rates and HIV-1 associated morbidities among infected individuals, and has contributed to decreased transmission rates by suppressing viral replication within infected persons (11, 250, 256). The limitations of current NRTI described in the previous section demonstrate the critical need to develop new NRTI that have excellent activity and safety profiles and exhibit little or no cross-resistance with existing drugs. This section will: i) illustrate

how a comprehensive mechanistic understanding of the molecular interactions of NRTI with RT can guide efforts to identify novel NRTI that are potent against NRTI-resistant HIV-1 and ii) introduce two recent NRTI discovery efforts that will provide the background for the work in this dissertation.

1.10.1 Novel NRTI design through structure-activity-resistance relationships

The rational design of new drugs with considerations for target enzyme structural and specificity determinants has been a productive approach to drug discovery (257, 258). This approach has been employed in the development of novel HIV-1 protease inhibitors, however, a rational drug design approach has not been extensively applied to the development of novel NRTI (259, 260). The world-wide multidisciplinary research effort in the 27 years of the HIV-1 epidemic has provided a detailed molecular understanding of the mechanisms of HIV-1 reverse transcription, RT inhibition, and NRTI activity, resistance, and pharmacology (83). This extraordinary wealth of knowledge provides a distinct advantage for the development of novel NRTI using a rational design approach.

The primary focus of this work is understanding NRTI structure-activity-resistance relationships in order to inform the development of novel NRTI that demonstrate low-cross resistance and potent activity against NRTI-resistant HIV-1. In order to develop new NRTI with little or no cross-resistance with existing NRTI, novel drug candidates must have potent activity against viruses carrying mutations that confer resistance via both the discrimination and excision mechanisms. Previous NRTI discovery efforts have largely relied on an empirical approach in which novel analogs are synthesized and evaluated for antiviral activity and toxicity, with, initially, little regard for activity against drug-resistant HIV-1. This approach provides

unpredictable results in terms of the activity of an investigational NRTI against drug-resistant HIV-1. A rational design approach in which novel analogs are synthesized based on an understanding of NRTI structural components that influence activity towards drug-resistant virus may prove more successful.

In 2005, Sluis-Cremer et al. and Parikh et al. described two of the first studies comparing the activity of structurally diverse NRTI against drug-resistant HIV-1 viral replication or RT DNA synthesis (141, 212). These studies provided the novel insight that identified the 3'-azido-2',3'-dideoxypurine nucleosides as a lead class of novel NRTI with potent activity against drug-resistant HIV-1 and will be discussed in detail below. Structure-activity-resistance characterizations such as these may allow the optimization of lead investigational NRTI to overcome one or both of the RT resistance mechanisms. The following two sections provide the background for the work in this dissertation by introducing two classes of novel investigational NRTI and describe why their specific structure-activity-resistance profiles should be characterized.

1.10.2 Second generation phosphonate NtRTIs: PMEO-DAPY derivatives and GS-9148.

Nucleoside phosphonate analogs are a structurally distinct class of antiviral compounds that were first developed by De Clercq and colleagues in 1986 (206). Analogs such as the NtRTI tenofovir (TFV) that was discussed above and adefovir (PMEA; 9-(2-phosphonylmethoxyethyl)adenine), an antiviral approved for the treatment of hepatitis B virus, contain no sugar ring and are considered 'acyclic' nucleoside phosphonates (ANP) (206).

A group of novel 'second generation' acyclic nucleoside phosphonates, the 6-[2-(phosphonomethoxy)alkoxy]-2,4-diaminopyrimidines (PMEO-DAPy) was recently described by

Balzarini and colleagues (261, 262). These analogs differ from their parent compounds TFV and PMEA in that they contain a pyrimidine base with the phosphonate moiety linked via the C-6 position, whereas TFV and PMEA have a phosphonate linkage at the N-9 position of an adenine base. Several 5-substituted PMEO-DAPy derivatives were characterized and reported to inhibit a broad range of HIV-1 clinical isolates. These compounds also demonstrated greater activity against drug-resistant clinical isolates than the parent compounds TFV and PMEA. One compound a 5-Me-substituted PMEO-DAPy (PMEO-DAPym) analog demonstrated the most potent inhibition of replication of all the clinical isolates tested (EC_{50} against WT = 0.062 µg/mL) (262). Clinical isolates containing the K65R mutation demonstrated some resistance to PMEO-DAPym but to a lesser extent than for tenofovir. Additionally, PMEO-DAPym was more effective against HIV-1 isolates containing TAMs than TFV and PMEA (262). These encouraging activity and resistance phenotypes warrant a detailed characterization of the molecular mechanisms of RT inhibition and resistance of PMEO-DAPym-DP. The structure-activity-resistance information obtained from these studies may allow further optimization of the promising qualities of this lead compound.

Recently, the novel phosphonate NtRTI, (5-(6-amino-purin-9-yl)-4-fluoro-2,5-dihydro-furan-2-yloxymethyl)phosphonic acid (GS-9148), was described by Cihlar and colleagues (263-265). GS-9148 differs structurally from the acyclic analogs TFV, PMEA, and PMEO-DAPym in that it contains a fluoro-modified-didehydro-ribose sugar ring, as well as an alternative phosphonate linkage. TFV and PMEA, and GS-1948 share a common adenine base. The phosphonoamidate prodrug of GS-9148, called GS-9131, demonstrated potent antiviral activity against a broad group of clinical HIV-1 isolates in cell culture (mean EC_{50} = 37 nM) (263, 266). GS-9148, also had potent activity against purified WT RT (steady state inhibitory constant, K_i =

0.8 µM) (263). GS-9148 displayed a favorable resistance profile against NRTI-resistant HIV-1 strains. Notably, K65R, K70E, and M184V, individually and in every combination had no effect on the activity of GS-9148 compared to WT and TAMs conferred modest resistance to GS-9148 (263). Cell culture selection experiments yielded resistant variants with the novel combination of resistance mutations K70E/D123N/T165I that are not selected by other NRTI and are infrequently observed in treatment-naïve and treatment-experience patients (267, 268). The low cross-resistance with existing NRTI and the selection of a unique resistance pattern warrant a mechanistic understanding of GS-9148-DP activity against WT and drug-resistant RT. Transient kinetic analyses will be used in this dissertation to examine the mechanisms of inhibition of GS-9148-DP against WT RT and RT containing the novel resistant mutations K70E/D123N/T165I.

1.10.3 The 3'-azido-2',3'-dideoxypurine analogs

Two studies published in 2005 provide the rationale for pursuing 3'-azdio-2',3'-dideoxypurines as a lead class of novel NRTI with potent activity against viruses carrying discrimination mutations and those carrying excision enhancing mutations (i.e. TAMs) (141, 212). Parikh et al. examined the antiviral activity of a structurally diverse panel of approved and investigational NRTIs that differed by enantiomer, sugar/pseudosugar, and base against HIV-1 carrying the K65R mutation to determine how NRTI structure affects activity (212). The results indicated that NRTI sugar/pseudosugar structure and base identity but not enantiomer influenced antiviral activity against K65R HIV-1. Importantly, NRTIs containing 3'-azido-modified sugars remained active against K65R HIV-1 while NRTI with other sugar/pseudosugar structures demonstrated

up to 77-fold decreased susceptibility to K65R compared to WT HIV-1. The 3'-azido-2',3'-dideoxynucleosides with thymine and adenine bases had similar activity against K65R HIV-1 as WT HIV-1 in MT-2 cells. The 3'-azido-2',3'-dideoxynucleosides with guanine and cytosine bases had 2.0-fold and 2.5-fold reduced activity against K65R HIV-1 in MT-2 cells, respectively, but these reductions compared to WT were not significant (p-value = 0.09 for 3'-azido-2',3'-dideoxyguanosine) or borderline significant (p-value = 0.05 for 3'-azido-2',3'-dideoxycytidine). This study demonstrates that NRTI base and sugar structure influence antiviral activity against drug-resistant HIV-1. Furthermore, these results suggest that novel NRTI with 3'-azido-sugars may also demonstrate superior activity against viruses carrying the multi-NRTI discrimination mutation K65R.

In the second study, Sluis-Cremer et al. examined the 3'-azido-2',3'-dideoxynucleosides containing the four DNA nucleobases for activity against AZT-resistant HIV-1 viral replication and RT DNA synthesis (141). In antiviral activity assays in MT-2 cells, 3'-azido-2',3'-dideoxycytidine and AZT demonstrated 10.7-fold and 11.7-fold reduced activity, respectively, against HIV-1 containing TAMs (D67N/K70R/T215F/K219Q) compared to WT HIV-1. However, 3'-azido-2',3'-dideoxyadenosine and 3'-azido-2',3'-dideoxyguanosine demonstrated only 1.2-fold and 1.3-fold reduced activity, respectively, against HIV-1 containing TAMs compared to WT HIV-1. Furthermore, RT DNA synthesis assays showed that TAMs increase the ATP-mediated pyrophosphorylytic excision of the monophosphate forms of AZT and 3'-azido-2',3'-dideoxycytidine but not the excision of the monophosphate forms of 3'-azido-2',3'-dideoxyadenosine and 3'-azido-2',3'-dideoxyguanosine. These results clearly demonstrate that TAMs confer resistance to 3'-azido-2',3'-dideoxypyrimidine nucleosides (i.e. thymine and cytosine bases) but not to 3'-azido-2',3'-dideoxypurine nucleosides (i.e. adenine and guanine

bases). Contrary to the accepted dogma at the time, this study demonstrated that the 3'-azido group is not the sole determinant of the RT excision phenotype, but the NRTI base also influences activity against RT containing TAMs.

Together these two structure-activity-resistance studies identified 3'-azido-2',3'-dideoxypurine analogs a novel lead class of NRTI with potent activity against HIV-1 containing the discrimination mutation K65R and HIV-1 containing multiple TAMs. A later study by Sluis-Cremer et al. further demonstrated that 3′-azido-2′,3′-dideoxyguanosine (3′-azido-ddG) exhibits potent activity against HIV-1 variants that contain the discrimination mutations K65R, L74V or M184V and against HIV-1 that contains multiple thymidine analog mutations (TAMs) that enhance nucleotide excision (172). Furthermore, 3′-azido-ddG does not exhibit cytotoxicity in primary lymphocytes or epithelial and T-cell lines, and does not decrease the mitochondrial DNA content of HepG2 cells.

With the exception of FTC that contains a 5–fluoro modification, the active metabolites of all FDA approved NRTI contain natural DNA nucleobases. Given that natural base identity can influence NRTI activity towards drug-resistant RT, it is expected that base modification will also impact NRTI activity. However, the molecular interactions of base-modified analogs with WT or NRTI-resistant HIV-1 RT have not been extensively studied. Accordingly, we synthesized a series of novel base modified 3′-azido-2′,3′-dideoxypurine analogs (143). In this dissertation, the structure-activity-resistance relationships of these analogs was characterized in order to identify base modifications that may further improve 3′-azido-2′,3′-dideoxypurine activity against NRTI-resistant HIV-1.

2.0 HYPOTHESIS AND SPECIFIC AIMS

Hypothesis

Nucleoside/nucleotide reverse transcriptase inhibitors (NRTI/NtRTI) remain an indispensible component of combination antiretroviral therapy. However, NRTI efficacy can be undermined by toxicity and the selection of resistance mutations, which often confer cross-resistance to other NRTI. Consequently, the development of novel NRTI with improved safety and resistance qualities is of critical importance. The rational design of novel therapeutics with considerations for target enzyme structural and specificity determinants has been the most productive approach to drug discovery. **Uncovering specific knowledge of how NRTI base, sugar, and phosphate structure influence activity, resistance, and toxicity will inform the rational design and development of new analogs that demonstrate favorable resistance and pharmacologic properties.** This information will be obtained through the following specific aims:

Specific Aims

1. Use steady-state and transient kinetic analyses to examine the mechanism(s) of action and resistance of two second-generation phosphonate NtRTI-diphosphates against WT and drug-resistant HIV-1 RT.

2. Identify structure-activity-resistance relationships of novel base modified 3'-azido-2',3'-dideoxypurine nucleosides using a combination of biochemical and antiviral assays.

3.0 CHAPTER ONE. THE ACYCLIC 2,4-DIAMINOPYRIMIDINE NUCLEOSIDE PHOSPHONATE ACTS AS A PURINE MIMETIC IN HIV-1 REVERSE TRANSCRIPTASE DNA POLYMERIZATION

Brian D. Herman[1], Ivan Votruba[2], Antonin Holý[2], Jeffrey Meteer[1], Nicolas Sluis-Cremer[1], and Jan Balzarini[3]

[1]Department of Medicine, Division of Infectious Diseases, University of Pittsburgh, Pittsburgh, PA, 15261, USA; [2]Institute of Organic Chemistry and Biochemistry, Academy of Sciences of the Czech Republic, CZ-16610 Prague, Czech Republic; and [3]Rega Institute for Medical Research, K.U. Leuven, B-3000 Leuven, Belgium

3.1 PREFACE

This chapter is adapted in part from a manuscript originally published in *the Journal of Biological Chemistry*; Herman, B. D., Votruba, I., Holý, A., Sluis-Cremer, N., and J. Balzarini. (2010). The Acyclic 2,4-Diaminopyrimidine Nucleoside Phosphonate Acts as a Purine Mimetic in HIV-1 Reverse Transcriptase DNA Polymerization. *J Biol Chem* 285(16): pp. 12101–12108.

Furthermore, this work was presented in part as a poster at *The 9th Annual Symposium on Antiviral Drug Resistance: Targets and Mechanisms, November 16-19, 2008 Richmond, VA. USA.* Herman, B. D., Meteer, J., Balzarini, J., and N. Sluis-Cremer. Mechanism of action and resistance to PMEO-5-methyl-DAPy, a novel pyrimidine nucleotide reverse transcriptase inhibitor.

The work presented in this chapter is in partial fulfillment of dissertation Aim 1. Brian Herman performed all work with the exception of the steady-state kinetic analyses on homopolymeric template/primers, which were performed by Ivan Votruba.

3.2 ABSTRACT

The acyclic pyrimidine nucleoside phosphonate (ANP) phosphonylmethoxyethoxy-diamino-pyrimidine (PMEO-DAPym) differs from other ANPs in that the aliphatic alkyloxy linker is bound to the C-6 of the 2,4-diaminopyrimidine base through an ether bond, instead of the traditional alkyl linkage to the N-1 or N-9 of the pyrimidine or purine base. In this study, we have analyzed the molecular interactions between PMEO-DAPym-diphosphate (PMEO-

DAPym-DP) and the active sites of WT and drug-resistant HIV-1 RT. Pre-steady-state kinetic analyses revealed that PMEO-DAPym-DP is a good substrate for WT HIV-1 RT: its catalytic efficiency of incorporation (k_{pol}/K_d) is only 2- to 3-fold less than that of the corresponding prototype purine nucleotide analogs PMEA-DP or TFV-DP. HIV-1 RT recognizes PMEO-DAPym-DP as a purine base instead of a pyrimidine base and incorporates it opposite to thymine (in DNA) or uracil (in RNA). Molecular modeling demonstrates that PMEO-DAPym-DP fits into the active site of HIV-1 RT without significant perturbation of key amino acid residues and mimics an open incomplete purine ring that allows the canonical Watson-Crick base pairing to be maintained. PMEO-DAPym-DP is incorporated more efficiently than TFV-DP by mutant K65R HIV-1 RT and is not as efficiently excised as TFV by HIV-1 RT containing TAMs. Overall, the data revealed that PMEO-DAPym represents the prototype compound of a novel class of pyrimidine acyclic nucleoside phosphonates that are recognized as a purine nucleotide and should form the rational basis for the design and development of novel purine nucleo(s)(t)ide mimetics as potential antiviral or antimetabolic agents.

3.3 INTRODUCTION

Acyclic nucleoside phosphonates (ANPs) are nucleotide analogs that are characterized by the presence of a phosphonate group linked to a pyrimidine or purine base through an aliphatic linker (269). ANPs can be functionally divided into different structural subclasses (**Figure 3.1**) that include: (i) the phosphonylmethoxyethyl (PME) derivatives (e.g. PMEA (adefovir)); (ii) the phosphonylmethoxypropyl (PMP) derivatives (e.g. TFV ((*R*)PMPA) and (*S*)FPMPA); and (iii) the hydroxyphosphonylmethoxypropyl (HPMP) derivatives (e.g. (*S*)HPMPA and (*S*)HPMPC

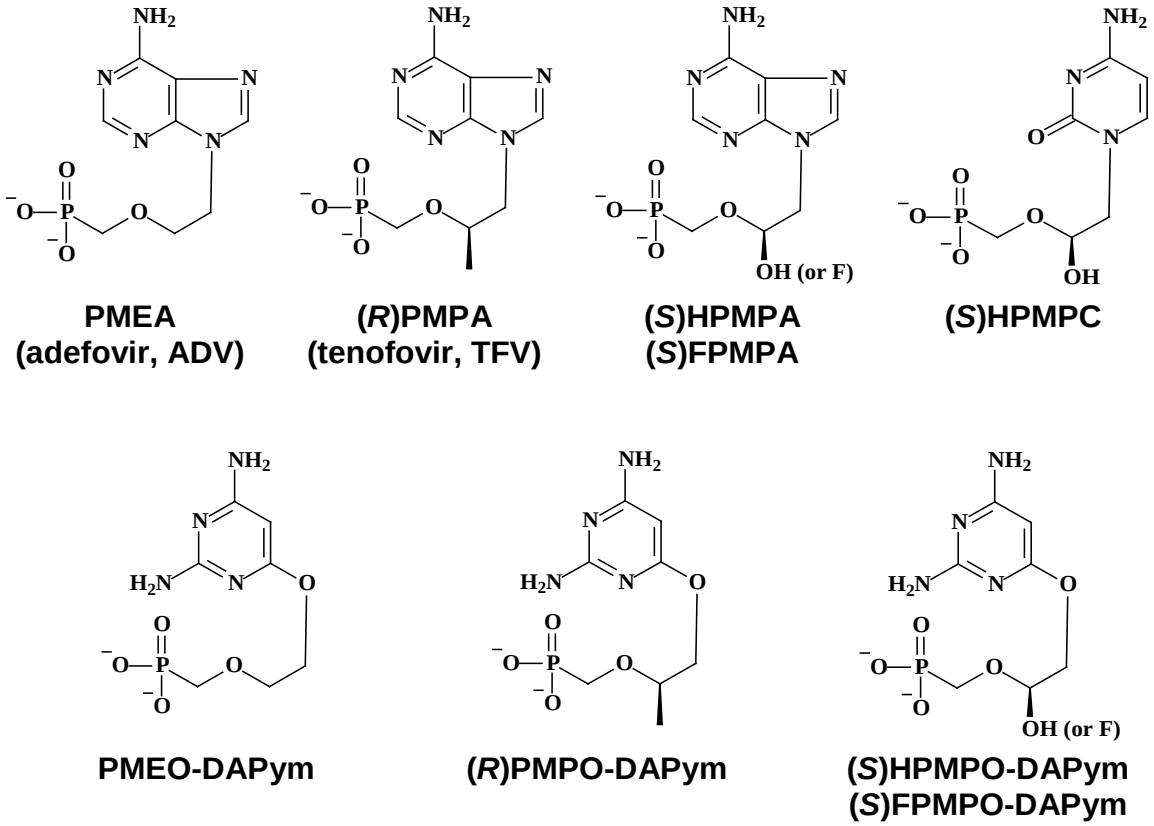

Figure 3.1 Structures of select acyclic nucleoside phosphonate derivatives.
The structures of PME (PMEA), PMP ((*R*)PMPA), and HPMP ((*S*)HPMPA, (*S*)FPMPA and (*S*)HPMPC) ANP derivatives and the corresponding PMEO-, (*R*)PMPO-, (S)HPMPO-, and (*S*)FPMPO-diamino pyrimidines (DAPym) are shown.

(cidofovir)) ((269-273). Analogs of each subclass are endowed with a characteristic and specific antiviral activity spectrum (274). For example, the PME-purine derivatives are active against several DNA viruses (i.e. herpesviruses, poxviruses and hepatitis B virus (HBV)) and retroviruses (e.g.HIV-1), whereas the PMP-purine derivatives display antiviral activity against retroviruses and HBV only. The HPMP-purine derivatives are active against a broad variety of DNA viruses (i.e. herpesviruses, poxviruses, and adenoviruses), whereas the cytosine derivative (*S*)HPMPC represents the sole HPMP-pyrimidine derivative that shows selective activity against cytomegalovirus and poxviruses. Interestingly, the PME- and PMP-pyrimidine derivatives do not exhibit antiviral activity. Thus, minor structural modifications in the side chain and also the identity of the base have a marked impact on the ANP antiviral activity spectrum. All of the ANPs described above are metabolized to a diphosphate form in the cell and act as competitive inhibitors (alternative substrates) of the virus-encoded DNA polymerase (270, 275-279). The ANP-diphosphate binds to the active site of the viral polymerase and competes with the corresponding natural nucleotide (i.e. dATP for (*S*)HPMPA, PMEA, (*S*)FPMPA and TFV and dCTP for (*S*)HPMPC) for subsequent incorporation into the growing DNA chain.

Recently, a new structural subclass of ANP, the acyclic phosphonylmethoxyethoxy- and phosphonylmethoxypropoxy-diaminopyrimidines (designated PMEO- and PMPO-DAPym) derivatives, was identified (262, 280-282). These ANPs differ from the other subclasses by the presence of an aliphatic alkyloxy linker bound to the C-6 of a 2,4-diaminopyrimidine base through an ether bond instead of the traditional alkyl linker bond to the N-1 of a pyrimidine or the N-9 of a purine (**Figures 3.1, 3.2**). Interestingly, and in contrast to the PME- and PMP-pyrimidines, the PMEO- and PMPO-pyrimidine ANP derivatives exhibit pronounced activity against both retroviruses and HBV (283). Of further interest, these analogs display an antiviral

Figure 3.2 Structural similarity between the PME-diaminopurine (DAP) derivative and PMEO-DAPym.

activity spectrum that is similar to the PME- and PMP-purines. Therefore, it was speculated that there was structural similarity between the 2,6-diaminopurine (DAP) PME-derivative (PMEDAP) and the PMEO-DAPym derivatives (280). This was supported by molecular modeling and superimposition of their optimized three-dimensional structures which demonstrated that the 2,4-diamino-substituted pyrimidine could be regarded as an open-ring analog of the purine system in the 2,6-diaminopurine ANPs (**Figure 3.2**) (283).

In this study, we have analyzed the molecular interactions between PMEO-DAPym-DP and the active site of HIV-1 reverse transcriptase (RT) using both steady-state and pre-steady-state kinetic analyses. The *in vitro* activity of PMEO-DAPym-DP against WT and drug-resistant recombinant purified HIV-1 RT was also compared to the PME-purine (i.e. PMEA-DP) and PMP-purine (i.e. TFV-DP) analogs. Importantly, we show for the first time that the acyclic pyrimidine nucleoside phosphonate derivative PMEO-DAPym-DP is incorporated into the growing DNA chain by HIV-1 RT as a purine nucleotide analog but not as a pyrimidine nucleotide analog. Therefore, PMEO-pyrimidine derivatives successfully mislead the viral DNA polymerase and act as purine nucleotide mimetics. Also, we obtained kinetic evidence that PMEO-DAPym may have a therapeutic edge over TFV in terms of its level of phenotypic drug

resistance. Additionally, we examined the ability of PMEO-DAPym-DP, PMEA-DP, and TFV-DP to directly inhibit steady-state DNA polymerization *in vitro* by recombinant, purified human DNA polymerases alpha (Pol α), beta (Pol β), and gamma (Pol γ). Interestingly, PMEO-DAPym-DP was recognized and incorporated by Pol α, resulting in chain-termination, but was not incorporated by Pol β or Pol γ. The identification of modified pyrimidine analogs opens new perspectives for developing novel types of such ambiguous pyrimidine nucleo(s)(t)ides with antiviral or antimetabolic potential.

3.4 MATERIALS AND METHODS

3.4.1 Reagents

The WT HIV-1 RT EC 2.7.7.49 used in the steady-state kinetic experiments that utilized homopolymeric template/primers (T/Ps) was derived from an HIV-1 (SF2 strain) pol gene fragment coding for the RT (Pro156-Leu715). The stock solution was 0.36 mg/ml. The WT, K65R, K70E, M184V, M41L/L210W/T215Y (TAM41), and D67N/K70R/T215F/K219Q (TAM67) HIV-1 RTs used in the steady-state and pre-steady-state kinetic experiments that utilized heteropolymeric T/Ps were purified as described previously (284, 285). The protein concentration of these enzymes was determined spectrophotometrically at 280 nm using an extinction coefficient (ε280) of 260450 M−1 cm−1, and by Bradford protein assays (Sigma-Aldrich, St. Louis, MO). The RNA- and DNA-dependent DNA polymerase activities of the purified WT and mutant enzymes were essentially identical (data not shown). Purified human DNA polymerases α. B, and γ were purchased from CHIMERx (Milwaukee, WI). TFV

diphosphate (TFV-DP) and PMEA diphosphate (PMEA-DP) were purchased from Moravek Biochemicals (Brea, CA). PMEO-DAPym-DP was synthesized and provided by A. Holý (Prague, Czech Republic). ATP, dNTPs, and ddNTPs were purchased from GE Healthcare (Piscataway, NJ), and [γ-32P]ATP was acquired from PerkinElmer Life Sciences (Boston, MA). RNA and DNA heteropolymeric oligonucleotides were synthesized by IDT (Coralville, IA). The templates poly(rC), poly(rA), poly(rI) and poly(rU) as well as the primers oligo(dG)12-18, oligo(dT)12-18, oligo(dC)12-18, and oligo(dA)12-18 were from Pharmacia (Uppsala, Sweden). The homopolymeric T/P substrates poly(rC)/oligo(dG), poly(rA)/oligo(dT), poly(rI)/oligo(dC) and poly(rU)/oligo(dA) were prepared by mixing 0.15 mM of template with an equal volume of 0.0375 mM primer.

3.4.2 Steady-state assays using homopolymeric T/Ps

Reactions (50 µl in volume) were carried out in a 50 mM Tris-HC1 (pH 7.8) buffer that contained 5 mM dithiothreitol, 300 mM glutathione, 0.5 mM EDTA, 150 mM KC1, 5 mM $MgC1_2$ or 5 mM $MnCl_2$, 1.25 µg of BSA, 0.06% Triton X-100, an appropriate concentration of [^{3}H]-dTTP, [^{3}H]-dGTP, [^{3}H]-dCTP or [^{3}H]-dATP (2 µCi/assay), varying concentrations of ANP analog, and a fixed concentration of poly(rA)/oligo(dT) (0.015 mM), poly(rC)/oligo(dG) (0.1 mM), poly(rI)/oligo(dC) (0.015 mM) or poly(rU)/oligo(dA) (0.015 mM). Reactions were initiated by the addition of 1 µl of RT and were incubated for 15 min at 37°C. Reactions were then terminated by the addition of 100 µl of 150 µg/ml calf thymus DNA, 2 ml of 0.1 M $Na_4P_2O_7$ (in 1 M HCl), and 2 ml of 10% (v/v) trichloroacetic acid. The solutions were kept on ice for 30 min after which the acid-insoluble material was washed and analyzed for radioactivity. For IC_{50} determinations, fixed concentrations of 1.25 µM [^{3}H]dTTP, 2.5 µM [^{3}H]dGTP, 1.75 µM

[^{3}H]dATP, or 2.5 µM [^{3}H]dCTP were used. For the Ki determinations with respect to the natural substrates, a fixed concentration of T/P was used (as indicated above). For the Ki determinations with respect to T/P, varying concentrations of the T/P were used in the presence of a fixed concentration of 1.25 µM [^{3}H]dTTP, 2.5 µM [^{3}H]dGTP, 1.75 µM [^{3}H]dATP or 2.5 µM [^{3}H]dCTP. The steady state kinetic constants Ki and Km were calculated using the Michaelis-Menten equation derived from double reciprocal (Lineweaver-Burke) plots.

3.4.3 Steady-state assays using heteropolymeric T/P

The ability of PMEO-DAPym-DP to inhibit HIV-1 RT DNA synthesis was also evaluated using heteropolymeric DNA/DNA and RNA/DNA T/Ps. Briefly, reactions were carried out in 50 mM Tris (pH 7.5), 50 mM KCl, 10 mM $MgCl_2$ containing 20 nM T/P, 0.5 µM each dNTP and various concentrations of PMEO-DAPym-DP (0 to 40 µM). The sequences of the T/P substrates are provided in **Figure 3.4**, and the DNA primers were 5′-radiolabeled with [γ-^{32}P]ATP as described previously (141). Reactions were initiated by the addition of 200 nM WT RT, incubated for 10 min at 37 °C and then quenched using 20 µL of gel loading buffer (98 % deionized formamide containing 1 mg/mL each of bromophenol blue and xylene cyanol). Control reactions included the addition of either TFV-DP or PMEA-DP. Samples were then denatured at 95 °C for 10 min and polymerization products were separated from substrates by denaturing gel electrophoresis using 14 % acrylamide containing 7 M urea. Gels were analyzed using phosphorimaging with a GS525 Molecular Imager and Quantity One Software (Biorad Laboratories, Inc., Hercules, CA). The concentrations required to inhibit the formation of final product by 50 % were calculated using non-linear regression from three independent experiments.

3.4.4 Pre-steady-state assays

A rapid quench instrument (Kintek RQF-3 instrument, Kintek Corporation, Clarence, PA) was used for pre-steady-state experiments with reaction times ranging from 20 ms to 60 s. The typical experiment was performed at 37 °C in 50 mM Tris-HCl (pH 7.5) containing 50 mM KCl, 10 mM $MgCl_2$ and varying concentrations of nucleotide. All concentrations reported refer to the final concentrations after mixing. HIV-1 RT (200 nM) was pre-incubated with 20 nM T/P substrate, prior to rapid mixing with nucleotide and divalent metal ions to initiate the reaction that was quenched with 50 mM EDTA. The sequences of the template and 5'-radiolabeled primer were 5'-

CTCAGACCCTTTTAGTCAGAATGGAAATTCTCTAGCAGTGGCGCCCGAACAGGGACA -3' and 5'-TCGGGCG CCACTGCTAGAGA-3', respectively. The quenched samples were then mixed with an equal volume of gel loading buffer and products were separated from substrates as described above. The disappearance of substrate (20mer) and the formation of product (21mer) were quantified using a Bio-Rad GS525 Molecular Imager (Bio-Rad Laboratories, Inc., Hercules, CA). Data were fitted by nonlinear regression with Sigma Plot software (Systat Software, Inc., San Jose, CA) using the appropriate equations (286). The apparent burst rate constant (k_{obs}) for each particular concentration of dNTP was determined by fitting the time courses for the formation of product (21mer) using the following equation: [21mer] = A[1-exp(-$k_{obs}t$)], where A represents the burst amplitude. The turnover number (k_{pol}) and apparent dissociation constant for dNTP (K_d) were then obtained by plotting the apparent catalytic rates (k_{obs}) against dNTP concentrations and fitting the data with the following hyperbolic equation: $k_{obs} = (k_{pol}[dNTP])/([dNTP] + K_d)$. Catalytic efficiency was calculated as the ratio of turnover number over dissociation constant ($[k_{pol}/K_d]$). Selectivity for natural dNTP versus ANP was

calculated as the ratio of catalytic efficiency of dNTP over that of ANP ($[(k_{pol}/K_d)^{dNTP}/(k_{pol}/K_d)^{ANP}]$). Resistance was calculated as the ratio of selectivity of the mutant over that of WT ($[(\text{selectivity})^{Mutant}/(\text{selectivity})^{WT}]$).

3.4.5 Excision assays

A 26 nucleotide DNA primer (P; 5′-CCTGTTCGGGCGCCACTGCTAGAGAT-3′) was 5′-radiolabeled with [γ-^{32}P]ATP and chain-terminated with either PMEO-DAPym-DP, TFV-DP or PMEA-DP as reported previously (141).

This chain-terminated primer was then annealed to a DNA template (5'-CTCAGACCCTTTTAGTCAGAATGGAAATTCTCTAGCAGTGGCGCCCGAACAGGGACA-3'). ATP-mediated excision assays were carried out by first incubating 20 nM T/P with 3 mM ATP, 10 mM $MgCl_2$, 1 μM dATP, and 10 μM ddGTP in a buffer containing 50 mM Tris-HCl (pH 7.5) and 50 mM KCl. Reactions were initiated by the addition of 200 nM WT or mutant RT. Aliquots were removed at defined times, quenched with sample loading buffer, denatured at 95 °C for 10 min, and then the product was resolved from substrate by denaturing polyacrylamide gel electrophoresis and analyzed, as described above. Dead-end complex formation was evaluated using the same assay set-up described above. However, the concentration of the next correct dNTP (i.e. dATP) was varied from 0-100 μM and reactions were quenched after 60 min.

3.4.6 Molecular modeling

Molecular models were constructed using the X-ray crystallographic coordinates for the RT/T/P/TFV-DP ternary complex (PDB, 1T05) (85). PMEO-DAPym-DP was docked into the

DNA polymerization active site and energy minimization experiments were carried out using Molecular Operating Environment (Chemical Computing Group, Montreal, Quebec, Canada). Charges were calculated using the Gasteiger method, and iterative minimizations were carried out using the AMBER 99 force field until the energy difference between iterations was less than 0.0001 kcal/mol per Å.

3.4.7 Steady state DNA synthesis by human DNA polymerases α, β, and γ

The ability of PMEO-DAPym-DP to inhibit DNA synthesis by human polymerases α, β, and γ was evaluated using the heteropolymeric DNA/DNA T/Ps indicated in **Figure 3.7**. The DNA primers were 5′-radiolabeled with [γ-^{32}P]ATP and annealed to the template as described previously (141). Preliminary experiments were performed to identify the T/P substrate and reaction conditions that provided the best activity from each human polymerase (data not shown). DNA synthesis reactions for Pol α were carried out in a reaction buffer containing 60 mM Tris (pH 8.0), 5 mM Mg Acetate, 1mM DTT, 0.1 mM spermine, and 0.3 mg/mL BSA. DNA synthesis reactions for Pol β and Pol γ were carried out in the same reaction buffer but in the absence of spermine and with 10 mM $MgCl_2$ instead of 5 mM Mg Acetate. A solution of the appropriate reaction buffer containing 20 nM T/P, 10 μM each dNTP and various concentrations of PMEO-DAPym-DP (0 to 60 μM) was mixed with 3 units of Pol α, 2 units of Pol β, or 2 units of Pol γ to initiate the reaction. One unit is defined as the amount of enzyme required to incorporate 1 nmol (Pol α and Pol β) or 1 pmol (Pol γ) total nucleotide into the acid-insoluble form in 60 min at 37 °C. Control reactions included the addition of either TFV-DP or PMEA-DP. Reactions were incubated for 60 min at 37 °C and then quenched using 20 μL of gel loading buffer (98 % deionized formamide containing 1 mg/mL each of bromophenol blue and xylene

cyanol). Samples were then denatured at 95 °C for 10 min and polymerization products were separated from substrates by denaturing gel electrophoresis using 14 % acrylamide containing 7 M urea. Gels were analyzed using phosphorimaging with a GS525 Molecular Imager and Quantity One Software (Biorad Laboratories, Inc., Hercules, CA). The concentrations required to inhibit the formation of final product by 50 % were calculated using non-linear regression from three independent experiments.

3.5 RESULTS

3.5.1 Inhibition of HIV-1 RT-mediated DNA synthesis by PMEO-DAPym-DP in the presence of homopolymeric T/Ps

The ability of PMEO-DAPym-DP to inhibit HIV-1 RT mediated DNA synthesis was first evaluated using four different homopolymeric T/Ps (**Table 3.1**). PMEA-DP and the 2',3'-dideoxynucleotide derivatives ddATP, ddTTP and AZT-TP were included as controls in these experiments. Reactions were carried out using either $MgCl_2$ or $MnCl_2$ as the divalent metal ion. In general, $MgCl_2$-mediated DNA polymerization reactions proceeded 10- to 100-fold more efficiently than $MnCl_2$-mediated reactions when poly(rC)/oligo(dG), poly(rA)/oligo(dT) or poly(rI)/oligo(dC) were used as the T/P substrate. By contrast, efficient DNA synthesis on the poly(rU)/oligo(dA) T/P was only observed when $MnCl_2$ was used as the divalent metal ion (data not shown). PMEO-DAPym-DP showed pronounced submicromolar inhibitory activity (IC_{50} = 0.26 µM), that was similar to PMEA-DP (IC_{50} = 0.12 µM) or ddATP (IC_{50} = 0.23 µM), when poly(rU)/oligo(dA) and $MnCl_2$-dATP were used as substrates. By contrast, AZT-TP and ddTTP

Table 3.1 Inhibition of HIV-1 RT mediated DNA synthesis by PMEO-DAPym-DP and other nucleoside analogs using hompolymeric T/Ps.

	IC_{50} (μM) [a]							
	Poly(rC)/oligo(dG) [^{3}H]dGTP		Poly(rU)/oligo(dA) [^{3}H]dATP		Poly(rA)/oligo(dT) [^{3}H]dTTP		Poly(rI)/oligo(dC) [^{3}H]dCTP	
	$MgCl_2$	$MnCl_2$	$MgCl_2$	$MnCl_2$	$MgCl_2$	$MnCl_2$	$MgCl_2$	$MnCl_2$
PMEO-DAPym-DP	> 200	16 ± 3.3	N.D.[b]	0.26 ± 0.10	> 200	> 200	> 200	> 200
PMEA-DP	> 100	75 ± 21	N.D.[b]	0.12 ± 0.06	> 100	> 100	> 100	> 100
ddATP	> 100	72 ± 13	N.D.[b]	0.23 ± 0.17	> 100	> 100	> 100	> 100
ddTTP	> 100	> 100	N.D.[b]	> 100	0.053 ± 0.011	0.072 ± 0.001	> 100	> 100
AZT-TP	> 100	> 100	N.D.[b]	67 ± 7	0.024 ± 0.020	0.006 ± 0.004	> 100	59 ± 7

[a] Concentration (μM) required to inhibit the RT reaction by 50%. The concentration of $MgCl_2$ or $MnCl_2$ in the reaction mixture was 5 mM. Data are the means ± standard deviations of 2 to 3 independent experiments.
[b] N.D., not detectable.

were required at 257- and > 385-fold higher concentrations, respectively, to inhibit these reactions in the presence of this T/P (**Table 3.1**). Interestingly, whereas PMEO-DAPym-DP did not inhibit reactions on the poly(rA)/oligo(dT) or poly(rI)/oligo(dC) T/P substrates at 200 µM, the compound was found to exert a 62-fold weaker inhibition (IC_{50} = 16 µM) when poly(rC)/oligo(dG) and $MnCl_2$-dGTP were used as substrates than when poly(rU)/oligo(dA) T/P was used. No inhibition was noticed at 100 µM when $MnCl_2$ was replaced by $MgCl_2$. PMEA-DP and ddATP did not show pronounced inhibitory activity (IC_{50} = 72-75 µM) under similar assay conditions (**Table 3.1**). Additional studies demonstrated that PMEO-DAPym-DP acted as a competitive inhibitor of $MnCl_2$-[^{3}H]dATP or $MnCl_2$-[^{3}H]dGTP binding, and as a linear mixed-type inhibitor of poly(rU)/oligo(dA) or poly(rC)/oligo(dG) binding (**Figure 3.3**). The steady state Michaelis-Menten binding (K_m) and inhibitory (K_i) constants determined from these experiments are provided in **Table 3.2**. Taken together, these data demonstrate that HIV-1 RT recognizes and incorporates PMEO-DAPym-DP as an adenine nucleotide derivative. The fact that PMEO-DAPym-DP was also weakly incorporated by HIV-1 RT into the poly(rC)/oligo(dG) T/P substrates when $MnCl_2$ was used as the divalent metal ion suggests that this nucleotide might also base pair with cytosine. Alternatively, it is well known that nucleotide misincorporation is more readily facilitated by $MnCl_2$ in comparison with $MgCl_2$, because $MnCl_2$ can partially compensate for the rate-limiting chemistry step that governs misincorporation reactions (287). Also, homopolymeric T/P substrates represent more artificial reaction conditions than heteropolymeric T/P substrates, making the latter more relevant to the physiological situation.

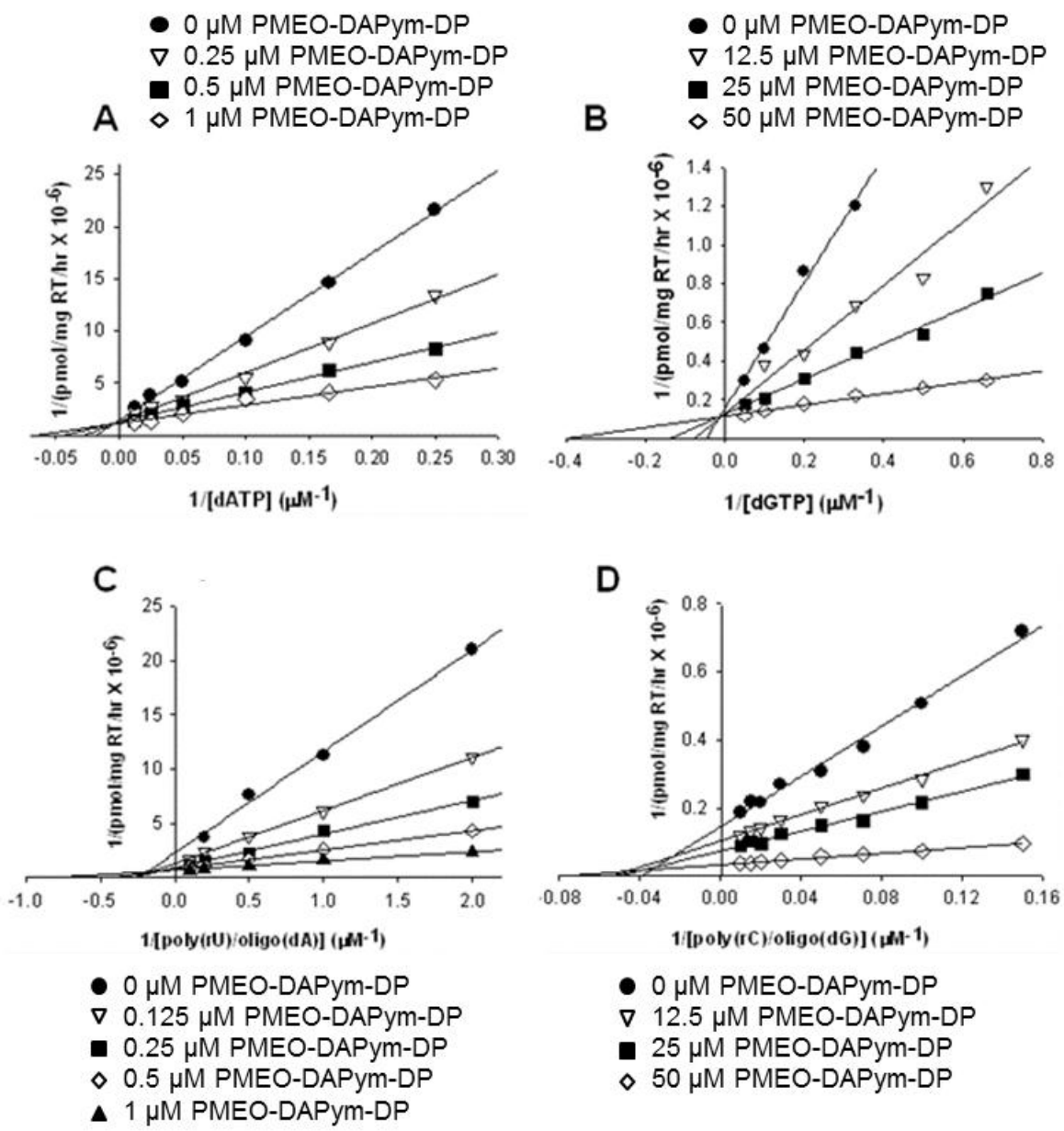

Figure 3.3 Double reciprocal plots for HIV-1 RT inhibition by PMEO-DAPym-DP using poly(rU)/oligo(dA) and MnCl2-dATP or poly(rC)/oligo(dG) and MnCl2-dGTP as substrates.

The assay conditions are described in the Materials and Methods. PMEO-DAPym-DP was determined to be a competitive inhibitor of dATP (A) and dGTP (B) binding and a linear mixed-type inhibitor of poly(rU)/oligo(dA) (C) or poly(rC)/oligo(dG) (D) binding. The K_i values determined from these experiments are provided in **Table 3.2**.

Table 3.2 Km and Ki values for PMEO-DAPym-DP and PMEA-DP against HIV-1 RT on homopolymeric T/Ps.

Inhibitor	Competing entity				Competing entity			
	Poly(rU)/oligo(dA)		dATP		Poly(rC)/oligo(dG)		dGTP	
	K_m (μM) [a]	K_i (μM) [a]	K_m (μM)	K_i (μM)	K_m (μM)	K_i (μM)	K_m (μM)	K_i (μM)
PMEO-DAPym-DP	1.2 ± 0.1 [b]	0.41 ± 0.10	16 ± 5	0.29 ± 0.22	17 ± 10	12 ± 2.2	2.7 ± 0.5	5.8 ± 1.2
PMEA-DP	1.2 ± 0.4	0.12 ± 0.05	10 ± 2	0.10 ± 0.06	17 ± 10	46 ± 1.0	3.0 ± 0.7	39 ± 5.7

[a] K_m and K_i values were calculated from the kinetic data in **Figure 3.3** using linear regression analysis.
[b] Data are the means ± standard deviations of 2 to 3 independent experiments.

3.5.2 Inhibition of HIV-1 RT-mediated DNA synthesis by PMEO-DAPym-DP in the presence of heteropolymeric T/Ps

In order to determine the incorporation profile of PMEO-DAPym-DP, we next examined inhibition HIV-1 RT-mediated DNA polymerization on heteropolymeric DNA/DNA and RNA/DNA T/Ps with $MgCl_2$ as the divalent metal cation (**Figure 3.4**). In these experiments, TFV-DP and PMEA-DP were included as controls. Consistent with the studies described above, we found that HIV-1 RT recognized PMEO-DAPym-DP as a purine but not a pyrimidine nucleotide analog and incorporated it opposite to thymine in the DNA template or uracil in the RNA template. As expected, its incorporation resulted in chain-termination of DNA synthesis. The concentration of PMEO-DAPym-DP required to inhibit HIV-1 RT-catalyzed DNA synthesis by 50 % (IC_{50}) was calculated to be 3.5 μM and 15 μM on the DNA/DNA and RNA/DNA template/primer substrates, respectively. By comparison, the IC_{50} values for TFV-DP and PMEA-DP were calculated to be 0.79 μM and 0.78 μM for the DNA/DNA, and 1.83 μM and 1.21 μM for the RNA/DNA T/P substrates, respectively. In these assays, PMEO-DAPym-DP was not incorporated opposite to the alternative pyrimidine cytosine, even when $MnCl_2$ was used as the divalent metal ion (data not shown).

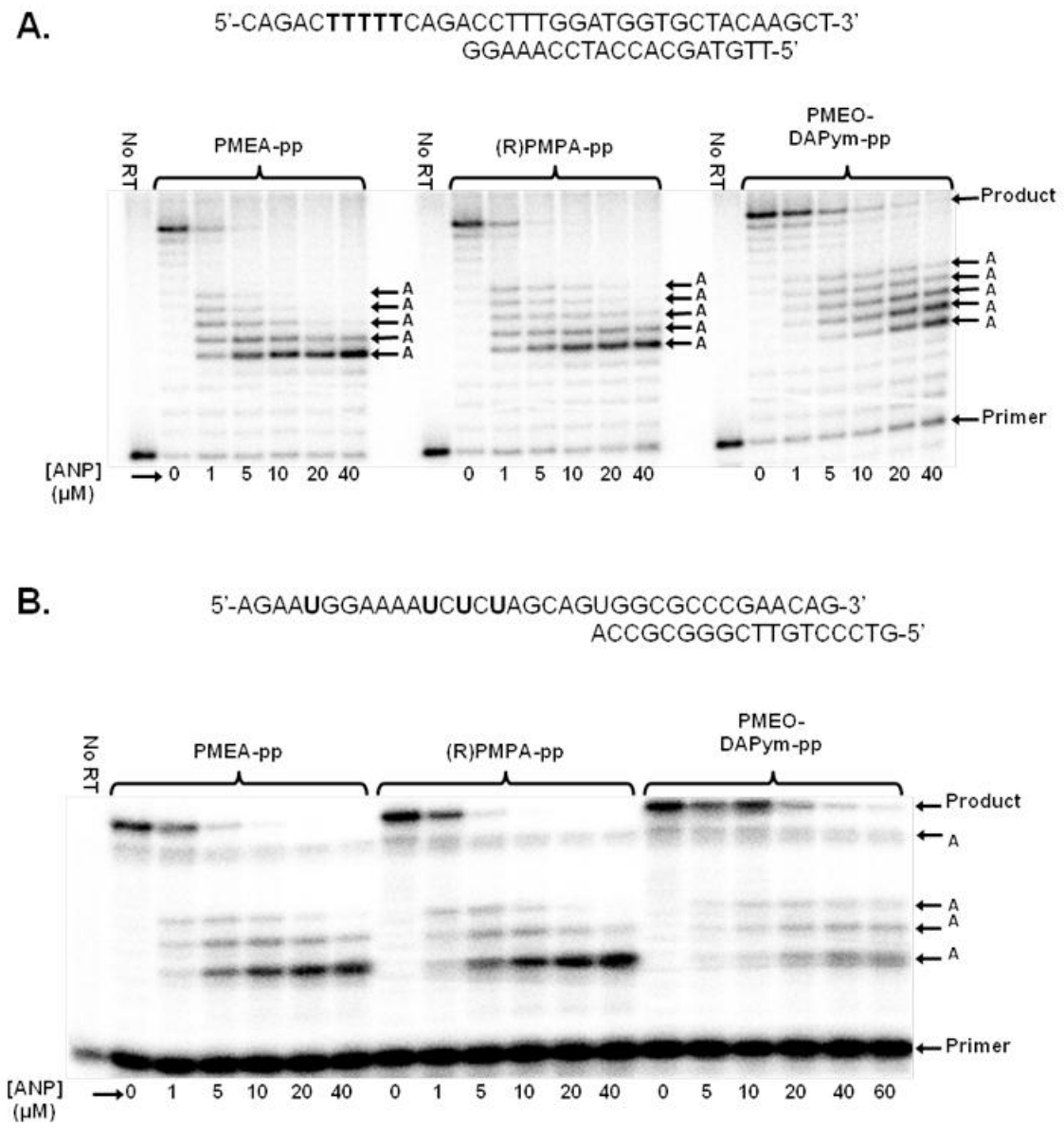

Figure 3.4 Incorporation of PMEO-DAPym-DP as an adenosine analog by WT HIV-1 RT in DNA/DNA (panel A) or RNA/DNA (panel B) T/P.
The sequences of the DNA/DNA and RNA/DNA T/P are indicated above each autoradiogram.

3.5.3 Pre-steady-state incorporation of PMEO-DAPym-DP by WT, K65R, K70E, and M184V HIV-1 RT

Pre-steady-state kinetic analyses were carried out to elucidate, in detail, the interactions between PMEO-DAPym-DP and the polymerase active site of HIV-1 RT (**Table 3.3**). Because PMEO-DAPym-DP behaves as an adenine nucleotide analog, we again included TFV-DP and PMEA-DP as controls. In addition, we examined the activity of PMEO-DAPym-DP against RTs containing the K65R and K70E mutations that are associated with TFV and PMEA resistance, respectively (288, 289). The M184V mutation, which may confer hypersusceptibility to TFV, was also examined. The results (**Table 3.3**) show that the catalytic efficiency of incorporation (k_{pol}/K_d) of PMEO-DAPym-DP for WT HIV-1 RT is approximately 2- to 3-fold less than the k_{pol}/K_d values determined for PMEA-DP or TFV-DP. This decrease in the k_{pol}/K_d value for PMEO-DAPym-DP (relative to PMEA-DP and TFV-DP) is driven predominantly by a slower rate of nucleotide analog incorporation (k_{pol}) and not by a diminished binding affinity (K_d) for the DNA polymerase active site of RT. As reported previously, the catalytic efficiency of incorporation of TFV-DP is decreased 12.4- and 2.5-fold by the K65R and K70E mutations in RT (122, 161). Consistent with previously published cross-resistance data (288, 289), both the K65R and K70E mutations in HIV-1 RT also conferred resistance to PMEA-DP. Similar to TFV-DP, this resistance was driven primarily by a selective decrease in the rate of PMEA-DP incorporation (k_{pol}) and not by a decrease in the nucleotide binding affinity (K_d).

Table 3.3 Pre-steady state kinetic incorporation values of PMEO-DAPym-DP for WT and drug-resistant HIV-1 RT.

	dATP			ANP				
	k_{pol} (s^{-1})	K_d (μM)	k_{pol}/K_d (μM^{-1} s^{-1})	k_{pol} (s^{-1})	K_d (μM)	k_{pol}/K_d (μM^{-1} s^{-1})	Selectivity [b]	Resistance [c]
				PMEO-DAPym-DP				
WT	24.4 ± 3.9 [a]	3.2 ± 1.2	7.6	1.1 ± 0.3	2.3 ± 1.1	0.49	15.5	--
K65R	12.6 ± 1.9	3.2 ± 0.7	4.0	0.21 ± 0.04	3.5 ± 2.1	0.06	65.8	4.2
K70E	18.0 ± 2.8	3.3 ± 0.9	5.5	0.18 ± 0.01	2.3 ± 0.6	0.08	69.3	4.5
M184V	14.8 ± 6.4	2.5 ± 0.8	5.9	1.2 ± 0.08	4.3 ± 0.2	0.27	21.7	1.4
				TFV-DP				
WT	24.4 ± 3.9	3. 2 ± 1.2	7.6	6.16 ± 1.0	4.3 ± 1.0	1.44	5.3	--
K65R	12.6 ± 1.9	3.2 ± 0.7	4.0	0.45 ± 0.06	7.3 ± 2.7	0.06	65.8	12.4
K70E	18.0 ± 2.8	3.3 ± 0.9	5.5	2.1 ± 0.1	5.1 ± 1.5	0.41	13.5	2.5
M184V	14.8 ± 6.4	2.5 ± 0.8	5.9	2.0 ± 0.9	2.6 ± 0.3	0.76	7.8	1.5
				PMEA-DP				
WT	24.4 ± 3.9	3. 2 ± 1.2	7.6	5.1 ± 1.3	4.0 ± 1.5	1.26	6.0	--
K65R	12.6 ± 1.9	3.2 ± 0.7	4.0	0.52 ± 0.28	4.2 ± 1.8	0.12	32.9	5.5
K70E	18.0 ± 2.8	3.3 ± 0.9	5.5	2.5 ± 0.5	4.3 ± 1.4	0.59	9.39	1.6
M184V	14.8 ± 6.4	2.5 ± 0.8	5.9	1.95 ± 0.6	3.4 ± 1.3	0.57	10.3	1.7

[a] Values represent the means ± standard deviations of three independent experiments.
[b] Selectivity is $(k_{pol}/K_d)^{dNTP}/(k_{pol}/K_d)^{ANP}$.
[c] Resistance (*n*-fold) is $selectivity^{mutant}/selectivity^{WT}$.

Both the K65R and K70E mutations in RT also conferred resistance to PMEO-DAPym-DP via a similar mechanism (i.e. selective decrease in k_{pol}). However, PMEO-DAPym-DP displayed better incorporation activity against K65R RT than TFV-DP. In this regard, a previous study reported that PMEO-DAPym exhibited better antiviral activity (lower levels of phenotypic drug resistance) against a panel of clinical virus isolates that contained multiple drug resistance mutations, including K65R, than did either PMEA or TFV (262). Furthermore, these data highlight that subtle changes in the side chains and identity of the base have a marked impact on the ANP anti-HIV-1 activity spectrum.

3.5.4 ATP-mediated excision of PMEO-DAPym by WT and mutant HIV-1 RT

HIV-1 RT has the intrinsic ability to rescue DNA synthesis from a blocked primer by ATP-mediated phosphorolytic excision of the DNA chain-terminating nucleotide (130). This ATP-mediated excision activity of HIV-1 RT is selectively increased by TAMs (131, 132), but can be diminished by other mutations, including K65R and K70E (122, 161). Accordingly, we next investigated the ability of WT, K65R, K70E and TAM-containing RT to excise PMEO-DAPym from a DNA chain-terminated template/primer. Two RT enzymes that contained different patterns of TAMs (i.e. M41L/L210W/T215Y (TAM41) and D67N/K70R/T215F/K219Q (TAM67)) were included in this study. In addition, TFV- and PMEA-chain terminated DNAs were included as controls. The results (**Figure 3.5, Table 3.4**) demonstrate that, in comparison

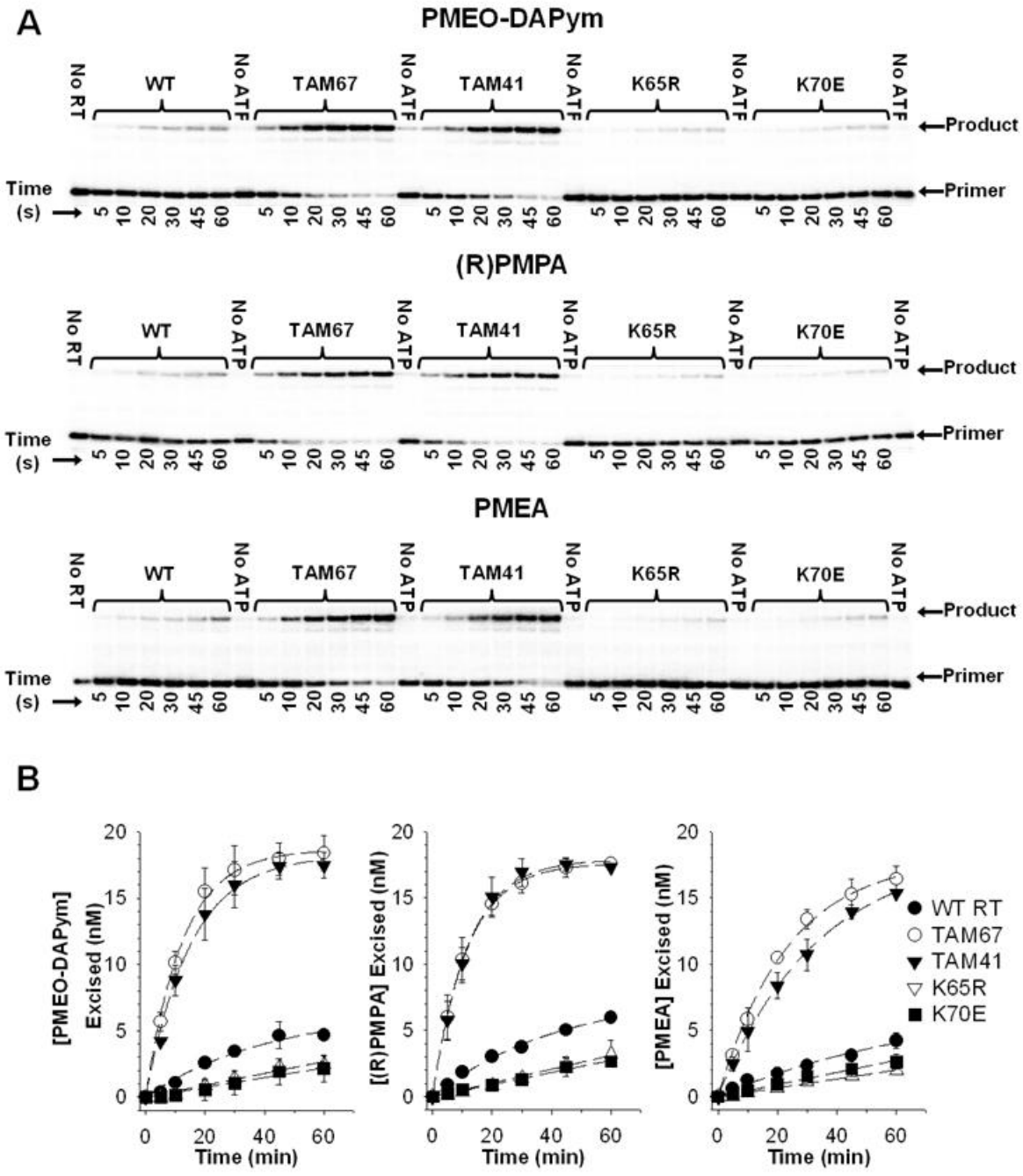

Figure 3.5 Autoradiograms (panel A) and rates (panel B) for ATP-mediated excision of PMEO-DAPym, TFV, and PMEA by WT and mutant HIV-1 RT.
For panel B, data represent the means ± standard deviations of two independent experiments.

Table 3.4 Excision rates and dead-end complex formation by WT and mutant RT.

RT	Excision Rate[a] (min^{-1})			IC_{50} for DEC formation[b] (μM)		
	TFV	PMEA	PMEO -DAPym	TFV	PMEA	PMEO -DAPym
WT	0.024 ± 0.00	0.014 ± 0.00	0.025 ± 0.01	30.1 ± 6.5	14.7 ± 2.7	14.6 ± 1.8
TAM67[c]	0.088 ± 0.02 (3.7)[e]	0.043 ± 0.01 (3.1)	0.080 ± 0.01 (3.2)	79.0 ± 4.5	65.9 ± 1.6	67.4 ± 4.6
TAM41[d]	0.086 ± 0.02 (3.6)	0.030 ± 0.01 (2.1)	0.065 ± 0.01 (2.6)	78.3 ± 5.4	50.0 ± 9.0	55.6 ± 7.5

[a] Values represent the means ± standard deviations from two independent experiments.
[b] Values represent means ± standard deviations from three independent experiments.
[c] TAM67: D67N/K70R/T215F/K219Q
[d] TAM41: M41L/L210W/T215Y
[e] Values in parentheses indicate fold change compared to WT RT.

with the WT enzyme, both TAM41 and TAM67 HIV-1 RT exhibited increased capacities to excise all three ANPs. However, the excision of PMEA and PMEO-DAPym by TAM41 RT occurred less efficiently than that of TFV. In contrast to the RTs containing TAMs, the mutant K70E and K65R RT enzymes exhibited poor excision activity that was independent of the DNA chain-terminating nucleotide analog. Previous studies have shown that the next complementary nucleotide can inhibit ATP-mediated chain terminator removal (81). To determine the magnitude and nature of this inhibition against PMEO-DAPym, PMEA, and TFV, we determined the IC_{50} of the next complementary nucleotide for the ATP-dependent removal of each of the acyclic nucleoside phosphonate analogs. The results (**Table 3.4**) show that the inhibitory concentrations of the next complementary dNTP were found to be somewhat higher for TFV compared with either PMEA or PMEO-DAPym. Taken together, these data suggest that PMEO-DAPym is a less efficient substrate for ATP-mediated excision than TFV. These findings may suggest that PMEO-DAPym may eventually be superior to TFV as an antiretroviral drug in respect of phenotypic drug resistance levels.

3.5.5 Molecular modeling

A molecular model of PMEO-DAPym-DP bound at the DNA polymerase active site of HIV-1 RT was generated by docking this compound into the RT-T/P-TFV-DP structure (PDB co-ordinates 1T05) (85). The model (**Figure 3.6A**) shows that PMEO-DAPym-DP can reside in the DNA polymerase active site of RT without significant perturbation of its key residues (i.e. K65, R72, D110, Y115, D185, D186 and Q151). In fact, overlay of the RT-T/P-TFV-DP structure with our model suggests that the active site architecture is essentially unchanged including the YMDD motif that is essential for catalysis (**Figure 3.6B**). In addition, the model shows that the

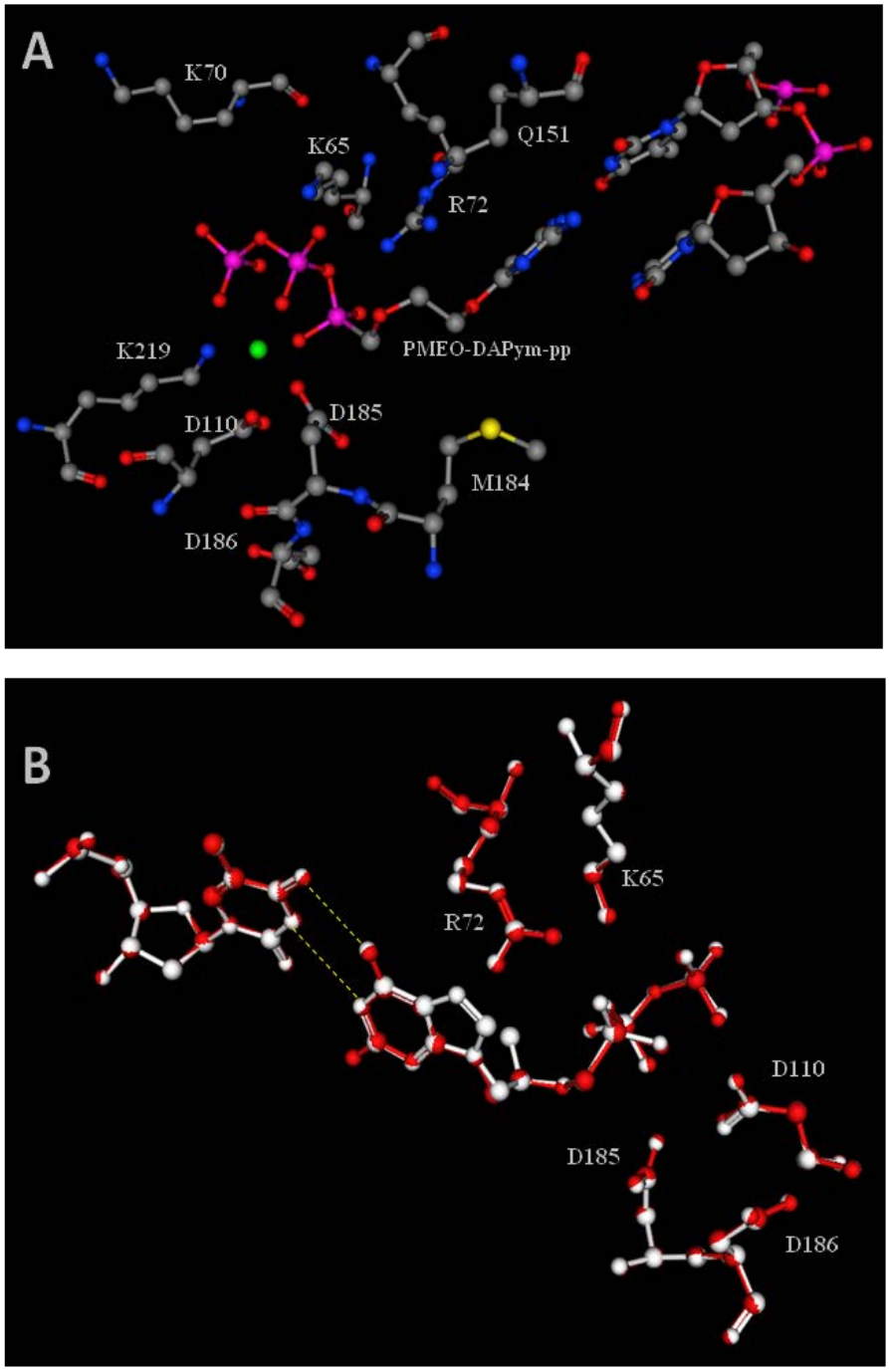

Figure 3.6 A model of PMEO-DAPym-DP bound at the DNA polymerase active site of HIV-1 RT.
PMEO-DAPym-DP was docked into the RT-T/P-TFV-DP ternary structure (PDB co-ordinates 1T05; A). No significant disruption of the active site residues was observed. An overlay of the RT-T/P-PMEO-DAPym-DP model with the RT-T/P-TFV-DP structure (B) demonstrates that PMEO-DAPym-DP mimics an incomplete purine ring and allows canonical Watson-Crick base pairing.

C-6 phosphonate linkage allows the pyrimidine ring in PMEO-DAPym to mimic an open incomplete purine ring that allows the canonical Watson-Crick base pairing to be maintained.

3.5.6 Inhibition of human DNA polymerase α-, β-, and γ-mediated DNA synthesis by PMEO-DAPym-DP

We also examined the potential for PMEO-DAPym-DP to inhibit steady state DNA synthesis by the human DNA polymerases α, β, and γ (**Figure 3.7**). PMEO-DAPym-DP was recognized and incorporated as an A-analog by DNA Pol α, resulting in chain termination. DNA synthesis by Pol α was also inhibited by PMEA-DP but not by TFV-DP. Human Pol β DNA synthesis was inhibited by TFV-DP (IC_{50} = 20.3 μM) and PMEA-DP (IC_{50} = 28.8 μM) but was not inhibited by PMEO-DAPym-DP. PMEO-DAPym-DP, TFV-DP, PMEA-DP were not substrates for incorporation by DNA Pol γ.

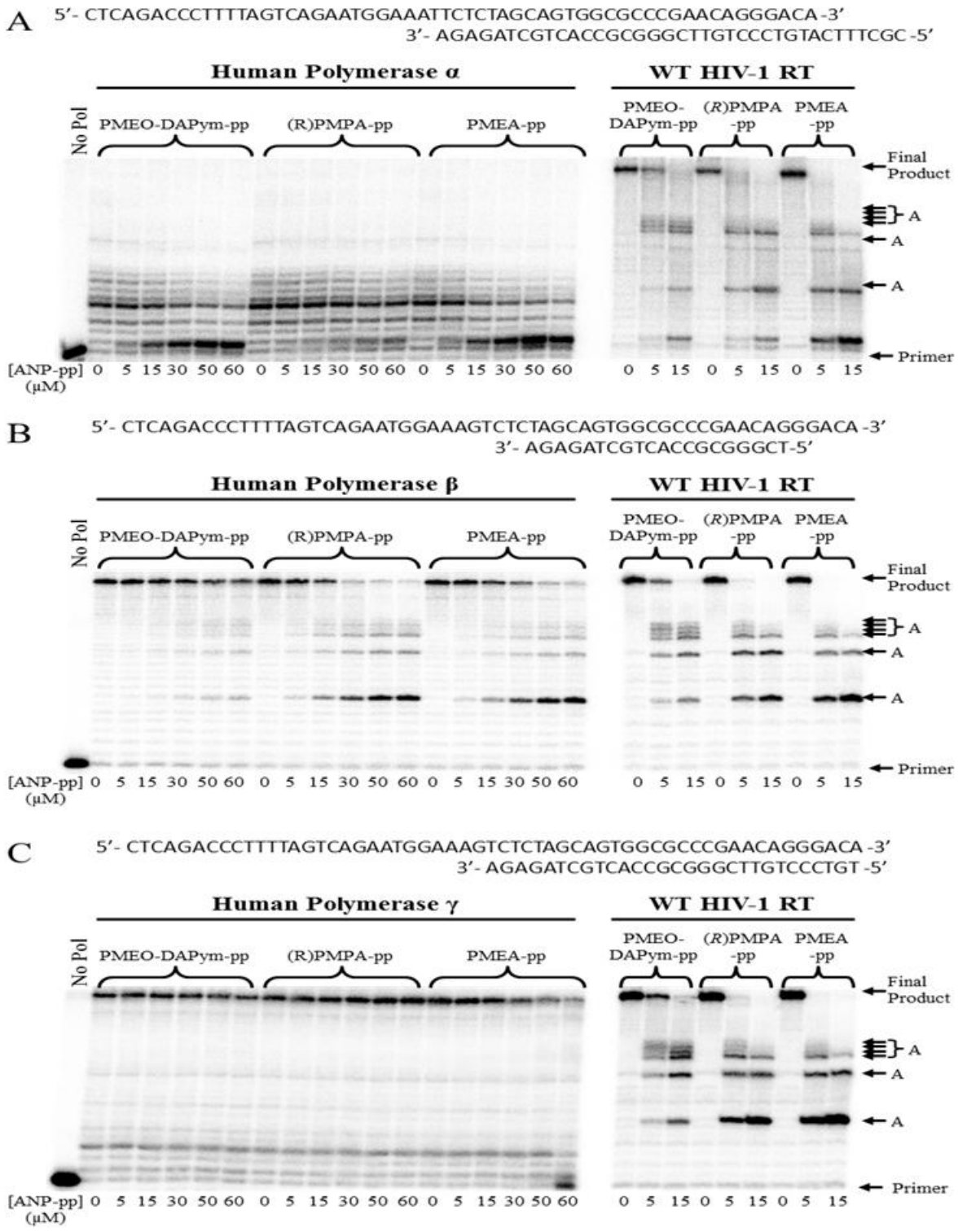

Figure 3.7 Inhibition of human polymerase α (A), β (B), and γ (C) steady state DNA synthesis by PMEO-DAPym-DP.
The DNA/DNA T/P used is indicated in each panel and the reaction conditions are provided in the Materials and Methods section.

3.6 DISCUSSION

In the present study, we demonstrate that HIV-1 RT efficiently recognizes PMEO-DAPym-DP as a purine (i.e. adenine) nucleotide derivative but not as a pyrimidine nucleotide derivative. Our modeling and docking studies in HIV-1 RT confirm the similarities between PMEO-DAPym-DP and TFV-DP in terms of a mimetic of an incomplete purine ring (DAPym) and are in full agreement with the obtained kinetic data. This is a striking observation and the first demonstration that a pyrimidine nucleotide analog can be unambiguously recognized as an adenine nucleotide derivative for both binding and incorporation into the growing DNA chain by HIV-1 RT. Moreover, such a wrongly-incorporated nucleotide derivative shows a less efficient increase of excision from the terminated DNA chain by mutant RTs than TFV. Such drugs may make it more difficult for the virus to escape drug pressure and may eventually exert lower phenotypic drug resistance levels, as has been experimentally shown in cell culture when PMEO-DAPym is compared to TFV (262). PMEO-DAPym-DP was also recognized as adenosine by human pol α for incorporation across from thymine, suggesting that the molecular mimicry phenotype extends beyond HIV-1 RT.

4.0 CHAPTER TWO. MECHANISM OF DISCRIMINATION OF GS-9148-DP BY K70E/D123N/T165I RT

Brian D. Herman[1], Kirsten White[2], Michael Miller[2], and Nicolas Sluis-Cremer[1]

[1]Department of Medicine, Division of Infectious Diseases, University of Pittsburgh, Pittsburgh, PA, 15261, USA; [2]Gilead Sciences, Inc., Foster City, CA, 94404 USA

4.1 PREFACE

The work presented in this chapter is in partial fulfillment of dissertation Aim 1 and was conducted as part of a research contract with Gilead Sciences, Inc., Foster City, CA, USA. Brian Herman performed all experiments described in this chapter.

4.2 ABSTRACT

GS-9148 is a novel adenosine analog phosphonate NtRTI that demonstrates potent antiviral activity and favorable toxicity and resistance profiles. In cell culture selection experiments, viruses with decreased susceptibility to GS-9148 harbored a novel set of resistance mutations. The RT mutation K70N was initially selected, which was later replaced with K70E followed by the addition of D123N and T165I. The K70E/D123N/T165I combination represents a novel set of resistance mutations that are not selected by other NRTI and are infrequently observed in treatment-naïve and treatment-experience patients. We have used pre-steady state assays to determine the single nucleotide kinetic binding and incorporation parameters of GS-9148-DP by WT RT and RT containing the mutations K70N, K70E, D123N/T165I, and K70E/D123N/T165I. The results indicated that K70E/D123N/T165I RT has a decreased catalytic efficiency (k_{pol}/K_d) of GS-9148-DP incorporation compared to WT RT. This decreased catalytic efficiency was driven by substantially weaker GS-9148-DP binding to the active site of K70E/D123N/T165I RT relative to WT RT (2.3-fold difference in K_d) with no effect on incorporation rate. This is different from the mechanisms of decreased catalytic efficiency toward TFV-DP; i) we observed changes in both TFV-DP binding and incorporation for K70E/D123N/T165I RT compared to

WT, ii) the previously characterized K65R and K70E mutations display predominantly decreased TFV-DP incorporation rates with little effect on binding. Our data indicate that the novel set of resistance mutations selected by GS-9148 confer decreased susceptibility to the drug by an alternative mechanism. Furthermore, these data reaffirm the importance of nucleotide base as a resistance determinant.

4.3 INTRODUCTION

GS-9148 [(5-(6-amino-purin-9-yl)-4-fluoro-2,5-dihydro-furan-2-yloxymethyl)phosphonic acid] is a novel adenosine analog phosphonate NtRTI with a 2',3'-dihydrofuran ring structure that also contains a 2'-fluoro group modification (**Figure 4.1**) (263). GS-9148 demonstrated potent activity against HIV-1 replication in multiple cell types and the active form GS-9148-diphosphate (GS-9148-DP) was a competitive inhibitor of RT with respect to dATP (K_i = 0.8 μM) resulting chain-termination of DNA synthesis. GS-9148-DP had poor activity against human DNA polymerases α, β, and γ with selectivity indices with respect to activity against RT (calculated as IC_{50} $^{\text{human polymerase}}$ / IC_{50} $^{\text{HIV-1 RT}}$) of 19, > 76, and > 130, respectively (263, 266). GS-9148 demonstrated a favorable resistance profile against multiple NRTI-resistant HIV-1 strains. The RT mutations K65R, L74V, and M184V individually or in combination did not reduce the antiretroviral activity of GS-9148. Additionally, viruses with multiple TAMs resulted in a smaller decrease in susceptibility to GS-9148 compared to most other NRTI. Furthermore, GS-9148 demonstrated encouraging biological properties, including a low potential for mitochondrial toxicity, minimal cytotoxicity in multiple cell types and synergistic antiviral activity in combination with other antiretrovirals (263, 264, 266, 290).

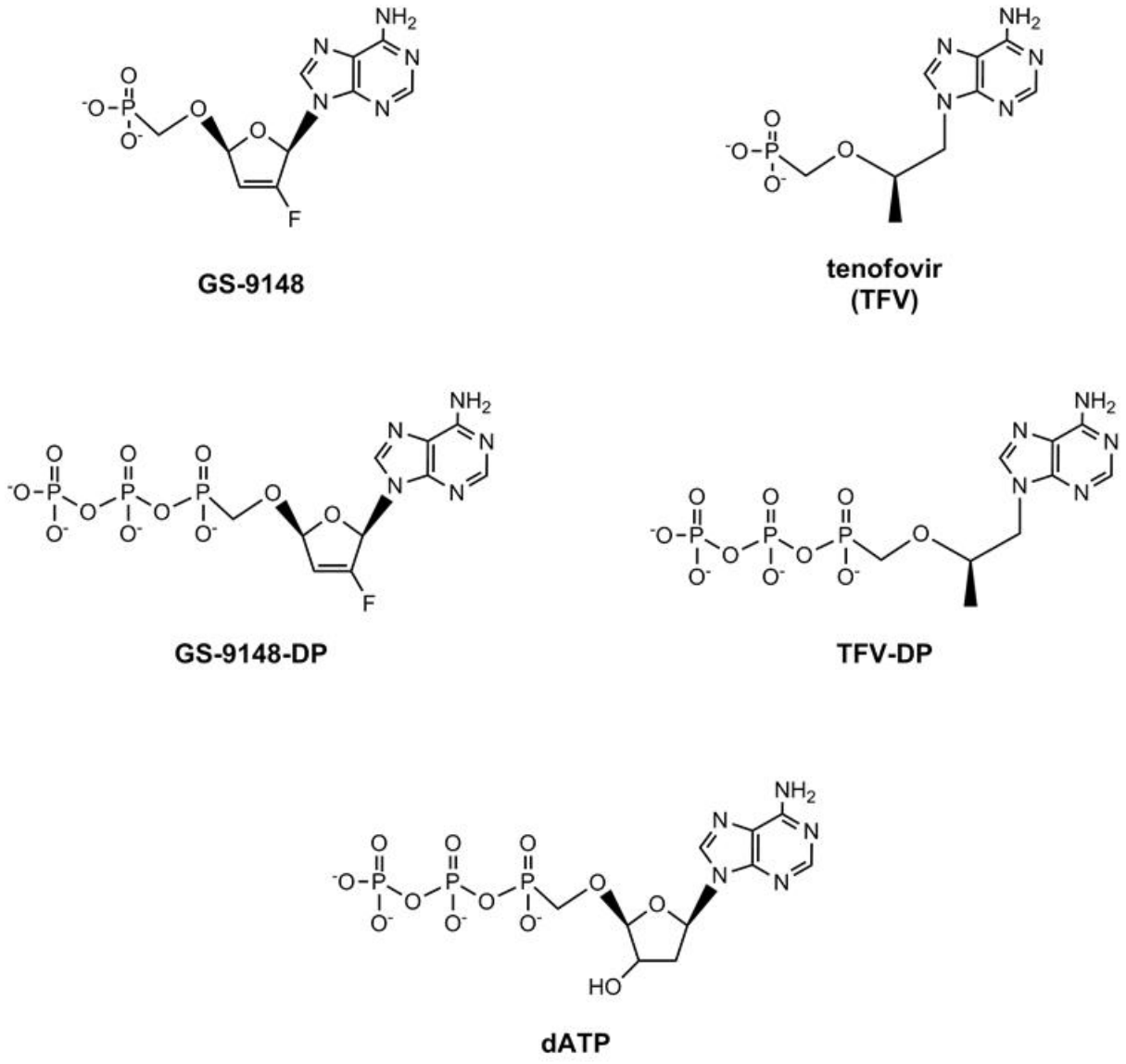

Figure 4.1 Structures of GS-9148, tenofovir (TFV), GS-9148-diphosphate (GS9148-DP), tenofovir-diphosphate (TFV-DP), and dATP.

Cell culture selection experiments with GS-9148 resulted in the emergence of two different resistance pathways: Q151L or the combination of K70E/D123N/T165I (267, 268, 291). The Q151L mutation resulted in high-level resistance to GS-9148, but it was present infrequently due to a replication deficiency (291). In the alternative pathway, K70N was selected first which was later replaced with K70E and the additional mutations D123N and T165I (267, 268). By the end of the selection 100 % of the sequenced clones contained the K70E mutation with 80 % and 90 % also containing D123N and T165I, respectively. The K70N and K70E mutations are present in NRTI-experienced patients with frequencies of 0.2 % and 0.3%, respectively (267, 268). D123N and T165I are polymorphisms that occur in approximately 9% and 5% of NRTI-experienced patients. However, the combination of K70E/D123N/T165I that was selected by GS-9148 has not been observed in treatment-naïve or treatment experienced patients. This suggests that GS-9148 selects a unique pathway to viral resistance that is selected by other NRTI and is not found in patient-derived clinical isolates.

The K70N and K70E mutations alone did not confer decreased HIV-1 susceptibility to GS-1948, however the combination K70E/D123N/T165I resulted in 3.3-fold resistance compared to WT HIV-1 (267). This combination also showed low-level cross-resistance (2- 3-fold compared to WT) to TFV, ddI, ABC, and D4T. Interestingly, the K70E/D123N/T165I mutations conferred 6.7-fold resistance to FTC but hypersusceptibility to AZT (0.4- fold) compared to WT HIV-1 (267). Steady-state kinetic analyses demonstrated that K70E, K70N, and K70E/D123N/T165I decreased the catalytic efficiency (K_i/K_m) of GS-9148-DP incorporation by RT 2.4-, 2.6-, and 4.0-fold, relative to WT, respectively (267). These results suggest that these mutations, like K65R, confer resistance via a discrimination mechanism by decreased binding/incorporation of GS-9148-DP compared to WT. Also like K65R, the K70E, K70N, and

K70E/D123N/T165I mutations decreased the excision of NRTI-MP from chain-terminated primers. As described previously, the K65R mutation confers a discrimination phenotype toward TFV-DP and other NRTI-TP, primarily due to a decreased k_{pol} with minimal changes in nucleotide binding (122, 160, 212).

While K70E/D123N/T165I displayed a similar discrimination phenotype as K65R in steady-state assays, the specific contributions of incorporation rate or nucleotide binding affinity for this novel mutant combination is not known. Furthermore, it is unknown what role the previously unidentified mutations D123N and T165I might play. Accordingly, this chapter will describe the pre-steady state assays used to determine the single nucleotide kinetic binding and incorporation parameters of GS-9148-DP compared to TFV-DP by RT containing the mutations K70N, K70E, D123N/T165I, and K70E/D123N/T165I.

4.4 MATERIALS AND METHODS

4.4.1 Reagents

The wild-type (WT), K70N, K70E, D123N/T165I, and K70E/D123N/T165I HIV-1 RTs were constructed, over-expressed in *E. coli*, and purified as described previously (284, 285). The protein concentration of these enzymes was determined spectrophotometrically at 280 nm using an extinction coefficient (ε280) of 260450 M−1 cm−1, and by Bradford protein assays (Sigma-Aldrich, St. Louis, MO). The RNA- and DNA-dependent DNA polymerase activities of the purified WT and mutant enzymes were essentially identical (data not shown). Tenofovir diphosphate (TFV-DP) and GS-9148 diphosphate (GS-9148-DP) were provided by Gilead

Sciences, Inc. (Foster City, CA). dATP was purchased from GE Healthcare (Piscataway, NJ), and [γ-32P]ATP was acquired from PerkinElmer Life Sciences (Boston, MA). DNA oligonucleotides were synthesized by IDT (Coralville, IA).

The sequences of the DNA template and primer were 5'-CTCAGACCCTTTTAGTCAGAATGGAAATTCTCTAGCAGTGGCGCCCGAACAGGGACA-3' and 5'-TCGGGCG CCACTGCTAGAGA-3', respectively. The DNA primer was 5′-radiolabeled with [γ-^{32}P]ATP and annealed to the template as described previously (141).

4.4.2 Pre-steady-state assays

A rapid quench instrument (Kintek RQF-3 instrument, Kintek Corporation, Clarence, PA) was used for pre-steady-state experiments with reaction times ranging from 50 ms to 60 s. Experiments were performed and data were analyzed in the same manner described in CHAPTER ONE under the section '3.4.4 Pre-steady-state assays' except using GS-9148-DP and TFV-DP substrates and WT, K70N, K70E, D123N/T165I, and K70E/D123N/T165I HIV-1 RT.

4.5 RESULTS

Pre-steady-state kinetic analyses were carried out to elucidate, in detail, the interactions of GS-9148-DP with the polymerase active site of HIV-1 RT. The natural nucleotide dATP and TFV-DP were included as controls. The results (**Table 4.1**) show that the catalytic efficiency of incorporation (k_{pol}/K_d) of GS-9148-DP for WT HIV-1 RT is ~32-fold less than the k_{pol}/K_d value determined for dATP (selectivity with respect to dATP). The decrease in the k_{pol}/K_d value for

Table 4.1 Pre-steady state kinetic values for GS-9148-DP incorporation by WT and drug-resistant HIV-1 RT.

	dATP			Nucleotide analog				
	K_{pol} (s^{-1})	K_d (μM)	K_{pol}/K_d (μM^{-1} s^{-1})	K_{pol} (s^{-1})	K_d (μM)	K_{pol}/K_d (μM^{-1} s^{-1})	selectivity [b]	resistance [c]
dATP/TFV-DP								
WT	29.6 ± 3.1 [a]	3.01 ± 0.9	9.84	6.11 ± 1.0	1.40 ± 0.3	4.36	2.26	---
K70E	25.7 ± 2.0	3.08 ± 0.5	8.35	2.87 ± 0.3	1.26 ± 0.2	2.28	3.66	1.6
K70N	39.0 ± 3.1	2.60 ± 0.4	15.0	8.50 ± 0.6	3.14 ± 0.3	2.70	5.56	2.5
D123N/T165I	16.5 ± 2.8	3.85 ± 0.2	4.29	3.53 ± 0.5	1.07 ± 0.2	3.31	1.30	0.6
K70E/D123N/T165I	20.3 ± 2.3	3.02 ± 0.7	6.70	2.43 ± 0.4	2.31 ± 0.2	1.05	6.38	2.8
dATP/GS-9148-DP								
WT	29.6 ± 6.1	3.01 ± 0.9	9.84	3.90 ± 0.3	12.5 ± 0.7	0.312	31.5	---
K70E	25.7 ± 3.4	3.08 ± 0.5	8.35	2.84 ± 0.6	14.5 ± 1.9	0.196	42.6	1.4
K70N	39.0 ± 6.3	2.60 ± 0.4	15.0	4.07 ± 0.8	13.1 ± 0.3	0.310	48.4	1.5
D123N/T165I	16.5 ± 4.8	3.85 ± 0.2	4.29	3.41 ± 0.5	13.2 ± 0.5	0.259	16.6	0.5
K70E/D123N/T165I	20.3 ± 4.6	3.02 ± 0.7	6.70	3.82 ± 0.5	29.3 ± 1.9	0.131	51.1	1.6

[a] Values represent mean ± SEM of at least 3 independent experiments.
[b] Selectivity is $(K_{pol}/K_d)_{dNTP}/(K_{pol}/K_d)_{NRTI\text{-}TP}$
[c] Resistance (*n*-fold) is $selectivity_{mutant}/selectivity_{WT}$

GS-9148-DP (relative to dATP) is driven by both a slower rate of nucleotide analog incorporation (k_{pol}) and by a diminished binding affinity (K_d) for the DNA polymerase active site of RT. This is contrary to TFV-DP in that the decreased k_{pol}/K_d value (compared to dATP) is driven primarily by slower incorporation. In fact, TFV-DP (K_d = 1.4 μM) demonstrated 2.2-fold stronger binding to the WT HIV-1 active site than dATP (K_d = 3.0 μM). The K70N RT showed no deficit in catalytic efficiency of incorporation (k_{pol}/K_d) of GS-9148-DP compared to WT RT. The catalytic efficiency of TFV-DP incorporation by K70N RT, however was decreased 2-fold compared to WT. The D123N/T165I RT showed only a 1.2-fold decrease in the k_{pol}/K_d value compared to WT RT. Importantly, the catalytic efficiencies of GS-9148-DP incorporation by K70E RT (k_{pol}/K_d = 0.196) and K70E/D123N/T165I RT (k_{pol}/K_d = 0.131) were 1.6-fold and 2.4-fold lower, respectively, compared to WT RT (k_{pol}/K_d = 0.312). The decreased catalytic efficiency of GS-9148-DP incorporation by K70E RT (compared to WT RT) is due to small changes in both incorporation rate and binding affinity. However, the decreased catalytic efficiency of GS-9148-DP incorporation by K70E/D123N/T165I RT relative to WT RT is driven strongly by decreased nucleotide binding affinity (K_d values of 12.5 μM and 29.3 μM for WT RT and K70E/D123N/T165I RT, respectively). Also of note, the K70E/D123N/T165I RT incorporated dATP 1.5-fold less efficiently than WT RT, primarily due to a slower rate of incorporation. This decrease in dATP incorporation rate was more pronounced with RT containing D123N/T165I alone, which also showed a slightly weaker dATP binding affinity relative to WT RT.

4.6 DISCUSSION

Overall, the pre-steady state kinetic assays we performed in this study indicate low levels of resistance to GS-9148 by progressively increasing discrimination phenotypes towards GS-9148-DP by K70N, K70E, and K70E/D123N/T165I RT, respectively. These results are consistent with the previously determined steady state kinetic data (267). Moreover, our results indicate that GS-9148-DP discrimination by K70E/D123N/T165I RT is driven by a 2.4-fold decrease in nucleotide binding affinity (K_d), compared to WT RT, with little effect on incorporation rate (**Table 4.1**). This is contrary to the previously described mechanisms of discrimination toward TFV-DP by RT containing the K65R or K70E mutations, which is due primarily to decreased incorporation rate with little effect on nucleotide binding to the active site (122, 161, 213). We found that K70E/D123N/T165I RT also showed a decreased rate of TFV-DP incorporation but this was accompanied by a decrease in TFV-DP binding affinity for the active site. Together, these factors resulted in a K70E/D123N/T165I RT discrimination phenotype toward TFV-DP that was not observed in the prior steady state kinetic assays (267). Taken together, these data show that the novel combination of mutations selected by GS-9148, K70E/D123N/T165I, confer resistance to GS-9148 and TFV by different mechanisms. Moreover, the fact that GS-9148 and TFV both contain an adenine base but differ only in their “ribose sugar” (TFV contains an acyclic “pseudo-sugar”) structure, reaffirms that nucleotide sugar an important determinant for NtRTI resistance development.

5.0 CHAPTER THREE. SUBSTRATE MIMICRY: HIV-1 REVERSE TRANSCRIPTASE RECOGNIZES 6-MODIFIED-3'-AZIDO-2',3'-DIDEOXYGUANOSINE-5'-TRIPHOSPHATES AS ADENOSINE ANALOGS

Brian D. Herman[1], Raymond F. Schinazi[2], Hong-wang Zhang[2], James H. Nettles[2], Richard Stanton[2], Mervi Detorio[2], Aleksandr Obikhod[2], Ugo Pradère[2], Steven J. Coats[3], John W. Mellors[1] and Nicolas Sluis-Cremer[1]

[1]Department of Medicine, Division of Infectious Diseases, University of Pittsburgh, Pittsburgh, PA 15261; [2]Center for AIDS Research, Department of Pediatrics, Emory University School of Medicine, and Veterans Affairs Medical Center, Decatur, Georgia 30033; [3]RFS Pharma, LLC, Tucker, Georgia 30084.

5.1 PREFACE

This chapter is adapted in part from a manuscript originally published in *Nucleic Acids Research*; Herman, B. D., Schinazi, R. F., Zhang. H-W., Nettles, J. H., Stanton, R., Detorio, M., Obikhod, A., Pradère, U., Coats, S. J., Mellors, J.W. and N. Sluis-Cremer. (2012). Substrate mimicry: HIV-1 reverse transcriptase recognizes 6-modified-3'-azido-2',3'-dideoxyguanosine-5'-triphosphates as adenosine analogs. *Nucleic Acids Res*. 40(1): pp. 381-90.

Additionally this work was presented in part as a poster at *The XVIII International HIV Drug Resistance Workshop June 9-13, 2009 Fort Myers, Fl, USA*. Abstract # 144. Herman, B. D., Obikhod, A., Detorio, M., Zhang, H-W., Nettles, J., Coats, S.J., Schinazi, R. F., Mellors, J. W. and N. Sluis-Cremer. Structure-activity-resistance relationships of 6-modified 3'-azido-2',3'-dideoxyguanosine nucleotides as inhibitors of HIV-1 reverse transcriptase. *Antiviral Therapy 2009; 14 Suppl 1:A144*; and in part at *The 17th Conference on Retroviruses and Opportunistic Infections February 16-19, 2010, San Francisco, CA USA*. Abstract # 489. Herman, B. D., Obikhod, A., Asif, G., Zhang, H-W., Coats, S. J., Schinazi, R. F., Mellors, J. W. and N. Sluis-Cremer. RS-788, a Prodrug of β-D-3'-Azido-2,6-diamino-2',3'-dideoxypurine, Exhibits Potent Activity Against NRTI-Resistant HIV-1.

The work presented in this chapter is in partial fulfillment of dissertation Aim 2. Brian Herman performed all work with the exception of synthesis of the triphosphate (TP) forms of the 6-modified-3'-azido-ddG analogs and the molecular modeling studies. Synthesis of the 6-modified-3'-azido-ddG analogs and their triphosphate forms was performed by Steven J. Coats, Hong-Wang Zhang, Aleksandr Obikhod, and Ugo Pradère. The molecular modeling studies were performed by James H. Nettles and Richard Stanton.

5.2 ABSTRACT

β-D-3'-Azido-2',3'-dideoxyguanosine (3'-azido-ddG) is a potent inhibitor of HIV-1 replication with a superior resistance profile to zidovudine. Recently, we identified five novel 6-modified-3'-azido-ddG analogs that exhibit similar or superior anti-HIV-1 activity compared to 3'-azido-ddG in primary cells. To gain insight into their structure-activity-resistance relationships, we synthesized their triphosphate (TP) forms and assessed their ability to inhibit HIV-1 RT. Steady-state and pre-steady-state kinetic experiments show that the 6-modified-3'-azido-ddGTP analogs act as adenosine rather than guanosine mimetics in DNA synthesis reactions, and are incorporated by HIV-1 RT opposite thymine (in DNA) or uracil (in RNA). The order of potency of the TP analogs was: 3'-azido-2,6-diaminopurine > 3'-azido-6-chloropurine; 3'-azido-6-*N*-allylaminopurine > 2-amino-6-*N*,*N*-dimethylaminopurine; 2-amino-6-methoxypurine. Molecular modeling studies reveal unique hydrogen bonding interactions between the nucleotide analogs and the template thymine base in the active site of RT. Surprisingly, the structure-activity relationship of the analogs differed in HIV-1 RT ATP-mediated excision assays of their monophosphate forms, suggesting that it may be possible to rationally design a modified base analog that is efficiently incorporated by RT but serves as a poor substrate for ATP-mediated excision reactions. Overall, these studies identify a promising strategy to design novel nucleoside analogs that exert profound antiviral activity against both WT and drug-resistant HIV-1.

5.3 INTRODUCTION

Most combination therapies used to treat antiretroviral-naïve and -experienced HIV-1 infected individuals include at least two NRTIs. NRTIs are analogs of 2'-deoxyribonucleosides that lack a 3'-OH group on the ribose sugar/pseudosugar. Once metabolized by host cell kinases to their active -TP forms, they inhibit viral reverse transcription by acting as chain-terminators of HIV-1 RT DNA synthesis (292). Although combination therapies that contain two or more NRTIs have substantially reduced mortality from HIV-1 associated disease, the approved NRTIs have significant limitations that include acute and chronic toxicity, and the selection of drug-resistant variants of HIV-1 that exhibit cross-resistance to other NRTIs. Accordingly, there is a need to develop potent and safe NRTIs that demonstrate activity against a broad-range of drug-resistant HIV-1.

To date, most NRTIs were discovered by an empirical approach in which novel sugar-modified nucleoside analogs were synthesized without *a priori* knowledge of their activity against WT or drug-resistant HIV-1. To specifically identify NRTIs that retain activity against a broad spectrum of drug-resistant HIV-1, our group adopted a rational discovery approach that utilized structure-activity-resistance relationships to identify NRTI base and sugar moieties that retain potent activity against drug-resistant HIV-1 (141, 212). Importantly, this approach identified 3'-azido-2',3'-dideoxyguanosine (3'-azido-ddG) as a lead compound that exhibits potent activity against HIV-1 variants that contain the discrimination mutations K65R, L74V or M184V and against HIV-1 that contains multiple TAMs that enhance nucleotide excision (172). Furthermore, 3'-azido-ddG does not exhibit cytotoxicity in primary lymphocytes or epithelial and T-cell lines, and does not decrease the mitochondrial DNA content of HepG2 cells (172).

To further improve the antiviral activity of 3'-azido-ddG, we recently synthesized and characterized a series of novel base modified 3'-azido-2',3'-dideoxypurine analogs (143). Of the 26 analogs studied, five (namely, 3'-azido-2',3'-dideoxy-2,6-diaminopurine (3'-azido-2,6-DA-P), 3'-azido-2',3'-dideoxy-2-amino-6-chloropurine (3'-azido-6-Cl-P), 3'-azido-2',3'-dideoxy -2-amino-6- *N*,*N*-dimethylaminopurine (3'-azido-6-DM-P), 3'-azido-2',3'-dideoxy-2-amino-6-methoxypurine (3'-azido-6-MX-P) and 3'-azido-2',3'-dideoxy-2-amino-6-*N*-allylaminopurine (3'-azido-6-AA-P)) exhibited superior or equivalent activity to 3'-azido-ddG in primary lymphocytes (**Figure 5.1**). To gain additional insight into the structure-activity-resistance relationships of these compounds, we synthesized their TP forms and assessed their ability to inhibit DNA synthesis by recombinant purified HIV-1 RT. Importantly, we show for the first time that HIV-1 RT recognizes and incorporates these 6-modified-3'-azido-ddGTP nucleotides as adenosine analogs. These findings reveal new avenues for developing novel, ambiguous nucleoside analogs that could be used to treat HIV-1 infection.

5.4 MATERIALS AND METHODS

5.4.1 Reagents

WT, K65R, L74V, M184V, A62V/V75I/F77L/F116Y/Q151M (Q151M complex, $Q151M_c$), M41L/L210W/T215Y (TAM41) and D67N/K70R/T215F/K219Q (TAM67) HIV-1 RTs were purified as described previously (284, 285). The protein concentration of the purified enzymes was determined spectrophotometrically at 280 nm using an extinction coefficient (ε_{280}) of 260450 M^{-1} cm^{-1}, and by Bradford protein assays (Sigma-Aldrich, St. Louis, MO). The RNA-

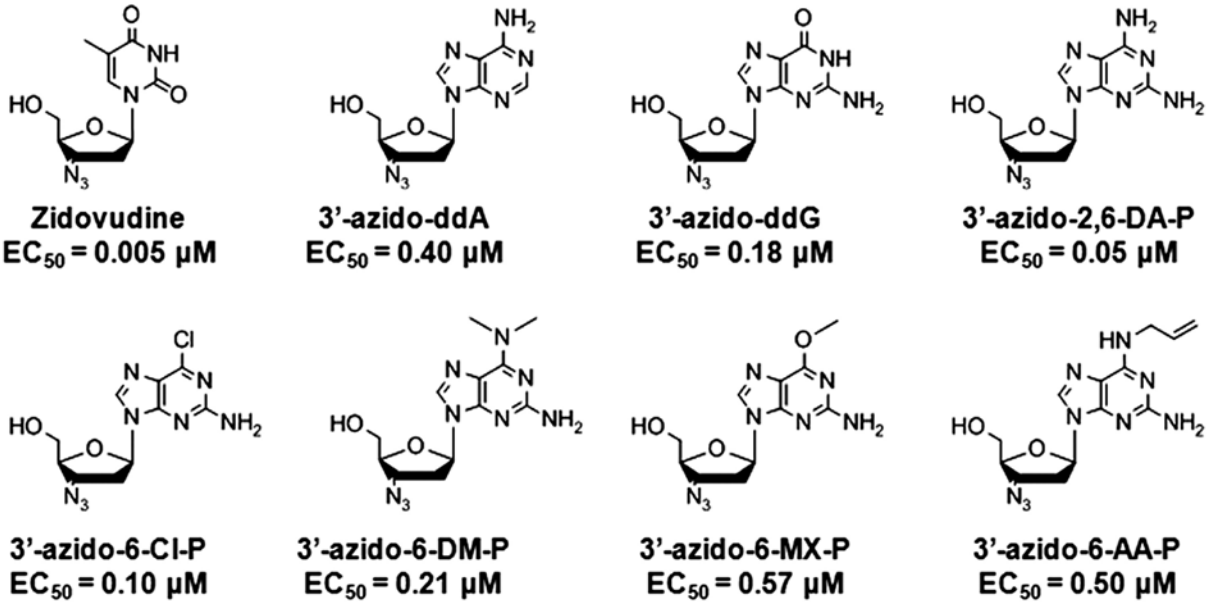

Figure 5.1 Structures of 6-modified-3'-azido-dideoxyguanosine analogs.
The molecular structures of zidovudine (ZDV), 3'-azido-2',3'-dideoxyadenosine (3'-azido-ddA), 3'-azido-2',3'-dideoxyguanosine (3'-azido-ddG), 3'-azido-2',3'-dideoxy-2,6-diaminopurine (3'-azido-2,6-DA-P), 3'-azido-2',3'-dideoxy-2-amino-6-chloropurine (3'-azido-6-Cl-P), 3'-azido-2',3'-dideoxy-2-amino-6-N,N-dimethylaminopurine (3'-azido-6-DM-P), 3'-azido-2',3'-dideoxy-2-amino-6-methoxypurine (3'-azido-6-MX-P) and 3'-azido-2',3'-dideoxy-2-amino-6-N-allylaminopurine (3'-azido-6-AA-P) are shown. The EC_{50} values, determined for WT HIV-1 in peripheral blood mononuclear (PBM) cells, were adapted from reference (143).

and DNA-dependent DNA polymerase activities of the purified WT and mutant enzymes were similar (data not shown). The triphosphate (TP) forms of each of the 6-modified-3'-azido-ddG analogs were synthesized and purified using the methods of Ludwig and Eckstein (250). 3'-Azido-ddGTP, 3'-azido-ddATP, 3'-azido-ddCTP and zidovudine-TP (ZDV-TP) were purchased from TriLink Biotechnologies, Inc. (San Diego, CA). [γ-^{32}P]ATP was obtained from PerkinElmer Life Sciences (Boston, MA). All DNA oligonucleotides were synthesized by Integrated DNA Technologies (Coralville, IA).

5.4.2 Inhibition of HIV-1 RT DNA synthesis under steady-state conditions by the 6-modified-3'-azido-ddGTP analogs

The ability of the 6-modified-3'-azido-ddGTP analogs to inhibit HIV-1 RT DNA- or RNA-dependent DNA synthesis was determined using two different template/primer (T/P) substrates, as described below:

(i) RT DNA synthesis was evaluated using a 214 nucleotide RNA or DNA template that corresponds to the HIV-1 sequence used for (–) strong stop DNA synthesis. The RNA and DNA templates were prepared as described previously (141). Both the RNA- and DNA-dependent DNA synthesis reactions were primed with the same 5'-end-^{32}P-labeled 18 nucleotide DNA primer (5'- GTCCCTGTTCGGGCGCCA-3') that corresponds to the HIV-1 primer binding site. DNA synthesis reactions (20 µL) were carried out in a 50 mM Tris-HCl (pH 7.5) buffer that contained 50 mM KCl, 10 mM $MgCl_2$, 20 nM T/P, 0.5 µM of each dNTP and varying concentrations of the 6-modified-3'-azido-ddGTP analogs. Reactions were initiated by the addition of 200 nM WT HIV-1 RT, incubated at 37 °C for 30 min (DNA-dependent DNA synthesis) or 60 min (RNA-dependent DNA synthesis) and then quenched by addition of 20 µL

of gel loading buffer (98 % deionized formamide containing 1 mg/mL each of bromophenol blue and xylene cyanol). Samples were then denatured at 95 °C for 10 min and polymerization products were separated from substrates by denaturing gel electrophoresis using 14 % acrylamide gels containing 7 M urea. DNA synthesis was analyzed by phosphorimaging using a GS-525 Molecular Imager and Quantity One Software (Bio-Rad Laboratories, Inc., Hercules, CA).

(ii) Inhibition of HIV-1 RT DNA synthesis was also evaluated to determine IC_{50} values using a 5'-end-^{32}P-labeled 19 nucleotide DNA primer (5'-TTGTAGCACCATCCAAAGG-3') that was annealed to one of three 36 nucleotide DNA templates that contained five consecutive thymine, cytosine, or adenosine bases. In this regard, inhibition of HIV-1 RT DNA synthesis by analogs with adenine, guanine, or thymine bases were evaluated using the templates (T1**,** 5'-CAGACTTTTTCAGACCTTTGGATGGTGCTACAAGCT-3'), (T2**,** 5'-CAGAGCCCCCGAGACCTTTGGATGGTGCTACAAGCT-3'), or (T3**,** 5'-CTGCTAAAAACTGCCCTTTGGATGGTGCTACAAGCT-3'), respectively. The T1 template was used for inhibition of WT and mutant HIV-1 RT DNA synthesis by each of the 6-modified-3'-azido-ddGTP analogs. Reaction conditions and gel electrophoresis were identical to those described above except 100 nM of WT or mutant HIV-1 RT was used to initiate the reaction. Reactions were quenched following incubation at 37 °C for 10 min. The amount of final product on the denaturing PAGE gels was quantified by densiometric analysis using Quantity One Software. The concentration of each 6-modified-3'-azido-ddGTP analog required to inhibit the formation of final product by 50 % was calculated using non-linear regression analyses (SigmaPlot Software Version 11, Systat Software, Inc., San Jose, CA) from at least

three independent experiments. Two-tailed homoscedastic T-tests were used to calculate the reported p-values.

5.4.3 Pre-steady-state incorporation of 6-modified-3’-azido-ddGTP analogs

A rapid quench instrument (Kintek RQF-3 instrument, Kintek Corporation, Clarence, PA) was used for pre-steady-state experiments. Experiments were performed and data were analyzed in the same manner described in CHAPTER ONE under the section 3.4.4 Pre-steady-state assays. A 5’-radiolabeled primer (5’-TCGGGCGCCACTGCTAGAGA-3’) was annealed to one of two different templates. The sequence of the template used to evaluate the 6-modified-3’-azido-ddGTP nucleotides as ‘A’ analogs was

3’-

ACAGGGACAAGCCCGCGGTGACGATCTCTTAAAGGTAAGACTGATTTTCCCAGACTC

-5’.

The sequence of the template used to evaluate the 6-modified-3’-azido-ddGTP nucleotides as ‘G’ analogs was

3’-

ACAGGGACAAGCCCGCGGTGACGATCTCTCAAAGGTAAGACTGATTTTCCCAGACT

C-5’.

5.4.4 Excision of the 6-modified-3'-azido-ddG monophosphate (MP) analogs by WT or TAM-containing HIV-1 RTs

The ability of WT or TAM-containing HIV-1 RT to facilitate ATP-mediated excision of the 6-modified-3'-azido-ddG-MP analogs from a DNA/DNA chain-terminated T/P was assessed as described previously (141). Briefly, a 23-nucleotide DNA primer was 5'-radiolabeled with [γ-^{32}P]ATP, annealed to the appropriate 36-nucleotide DNA template, and then chain-terminated with the appropriate nucleotide analog. For excision of 3'-azido-ddGMP the T/P pair was T2/pr23G (pr23G**:** 5'-TTGTAGCACCATCCAAAGGTCTC-3') whereas for the excision of 3'-azido-ddAMP and each 6-modified-3'-azido-ddGMP analog the T/P pair was T1/pr23A (pr23A: 5'-TTGTAGCACCATCCAAAGGTCTG-3'). Reactions were carried out in a 50 mM Tris-HCl (pH 7.5) buffer that contained 50 mM KCl, 10 mM $MgCl_2$, 3 mM ATP and 1 μM dGTP/10 μM ddCTP (for the excision of 3'-azido-ddGMP) or1 μM dATP/10 μM ddGTP (for excision of 3'-azido-ddAMP and each 6-modified-3'-azido-ddGMP analog). Reactions were initiated by the addition of 200 nM WT or mutant RT. Aliquots (5 μL) were removed at defined times, quenched with gel loading buffer, denatured at 95 °C for 10 min, and product was then resolved from substrate by denaturing polyacrylamide gel electrophoresis and analyzed, as described above.

5.4.5 Molecular modeling

Molecular models of incorporation were constructed using the X-ray crystallographic coordinates (PDB entry 1 RTD) for the RT-T/P-TTP ternary complex (77). The 3'-OH of the primer strand as well as the 6-modified-3'-azido-2',3'-ddGTP analogs and complementary bases in the template strand were built into the model to generate a pre-initiation complex, as described

previously (84). Tautomerization and protonation potential of the entire system was calculated using the Generalized Born/Volume Integral (GB/VI) electrostatics method of Labute (293). Energy gradient minimization was carried out using MMFF94x force field in the Molecular Operating Environment (MOE 2008.02; Chemical Computing Group, Montreal, Quebec, Canada). Ligand interactions were quantified and images generated using the LigX interaction function in MOE. Structural models comparing incorporation and excision of specific nucleotide analogs used the PDB co-ordinates 3KLF and 3KLE that contain the excision product AZT adenosine dinucleoside tetraphosphate (AZTppppA) in complex with HIV-1 RT containing multiple TAMs (82). To eliminate the potential force field bias from alignment of bases, empirically derived angle relations were used for all analogs tested. 3KLF and 3KLE were fit to the p66 subunit of 1RTD using the Matchmaker function in Chimera version 1.51 (UCSF Chimera, Resource for Biocomputing, Visualization, and Informatics at the University of California, San Francisco). Aligned structures were opened in MOE and dihedral angles were measured from bases relative to the ribose ring O and C1 of both template and bound nucleotides for each complex. MOE's builder function was used to modify each template/bound nucleotide base pair retaining the experimental dihedrals. Hydrogen bonding potential between the aligned base pairs was quantified using the "FindHBond" function in Chimera with default settings. Parts of the modeling workflow were automated using Pipeline Pilot 7.5 (Accelrys Corporation, San Diego, California).

5.5 RESULTS

5.5.1 Steady-state incorporation of 6-modified 3'-azido-ddGTP nucleotides by HIV-1 RT

To characterize the ability of WT HIV-1 RT to incorporate the 6-modified-3'-azido-ddGTP analogs, we first conducted steady-state DNA synthesis reactions using heteropolymeric DNA/DNA and RNA/DNA T/P substrates (**Figure 5.2**). The sequences of the RNA and DNA templates correspond to the HIV-1 sequence used for (–) strong stop DNA synthesis, and both reactions were primed with the same 18 nucleotide DNA primer that was complementary to the HIV-1 primer binding site (141). 3'-Azido-ddGTP, 3'-azido-ddATP, 3'-azido-ddCTP and ZDV-TP were included as controls in these experiments. Unexpectedly, we found that HIV-1 RT recognized all of the 6-modified-3'-azido-ddGTP nucleotides as adenosine analogs and incorporated them opposite thymine in DNA (**Figure 5.2A**) or uracil in RNA (**Figure 5.2B**). As anticipated, their incorporation resulted in chain-termination of DNA synthesis. Under the assay conditions described in **Figure 5.2**, the 6-modified-3'-azido-ddGTP nucleotides were not incorporated into the nascent DNA opposite cytosine. However, if the dNTP concentration was lowered to 0.1 μM, chain-termination opposite cytosine was observed (data not shown). We also determined the concentration of 6-modified-3'-azido-ddGTP analog required to inhibit DNA synthesis (i.e. IC_{50}) using a different heteropolymeric DNA/DNA T/P substrate, as described in the Materials and Methods (**Table 5.1**). Their order of potency against WT RT was determined to be: 3'-azido-ddATP, 3'-azido-ddGTP > 3'-azido-2,6-DA-P-TP > 3'-azido-6-Cl-P-TP, 3'-azido-6-AA-P-TP > 3'-azido-6-DM-P-TP, 3'-azido-6-MX-P-TP.

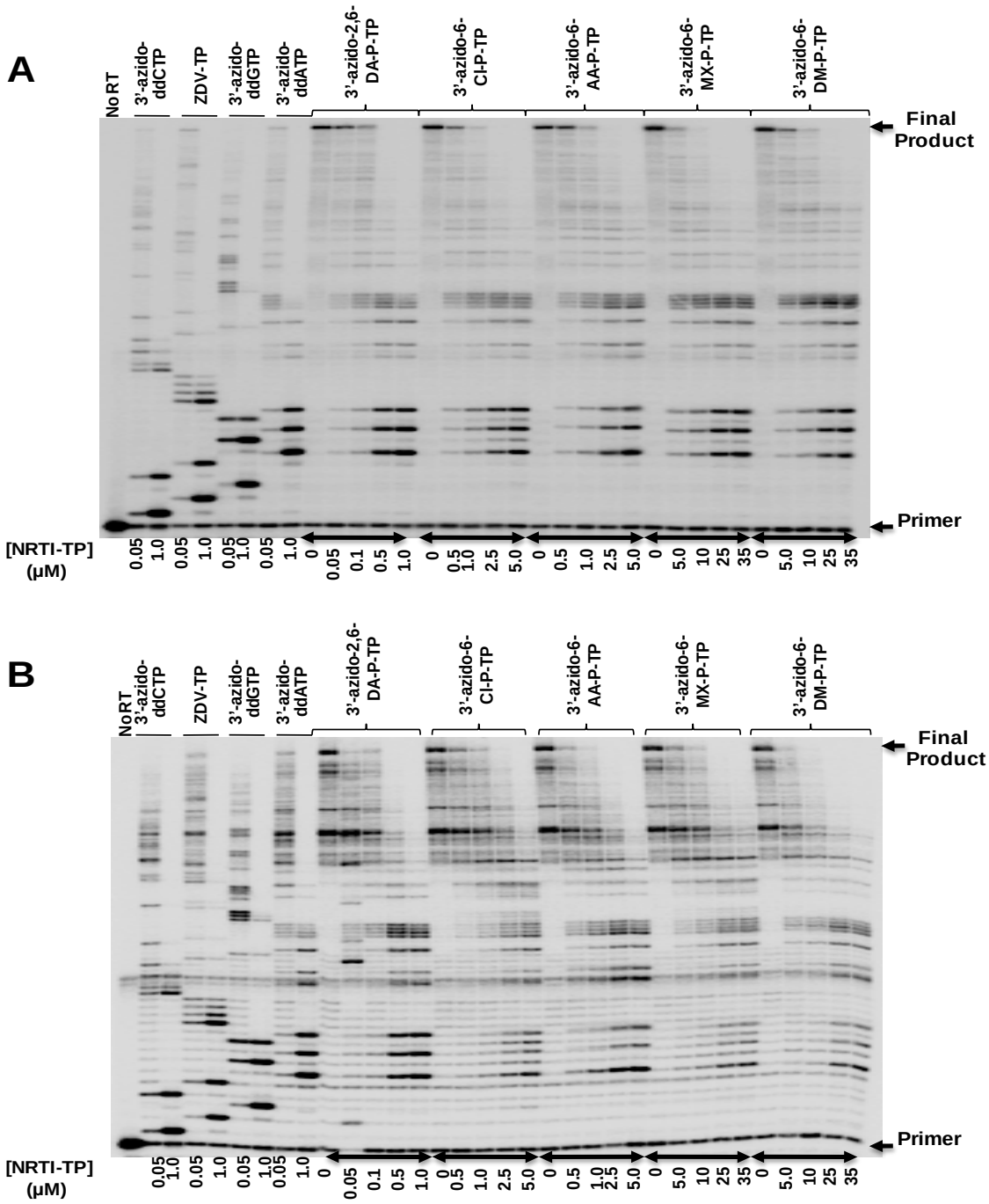

Figure 5.2 The 6-Modified-3'-azido-ddGTP analogs are recognized and incorporated by WT HIV-1 as adenosine analogs.
(A) Representative denaturing polyacrylamide gel showing chain-termination of HIV-1 RT DNA synthesis by each of the 3'-azido-ddGTPs on a heteropolymeric DNA/DNA T/P under steady-state assay conditions. (B) Representative denaturing polyacrylamide gel showing chain termination of WT HIV-1 RT DNA synthesis by each of the 3'-azido-ddGTPs on a heteropolymeric RNA/DNA T/P under steady-state assay conditions. Reaction conditions are described in the Materials and Methods section.

Table 5.1 Inhibition of steady-state WT and mutant HIV-1 RT DNA synthesis by 6-modified-3'-azido-ddGTP analogs.

Nucleotide analog	HIV-1 RT				
	WT	**K65R**	**L74V**	**M184V**	**Q151M** [a]
ZDV-TP					
IC_{50} (μM) [b]	0.13 ± 0.04	0.66 ± 0.20	0.18 ± 0.10	0.12 ± 0.03	2.7 ± 1.0
Fold-R [c]	-	5.2	1.4	0.9	21.0
3'-azido-ddGTP					
IC_{50} (μM)	0.15 ± 0.01	0.36 ± 0.02	0.25 ± 0.10	0.06 ± 0.02	0.30 ± 0.20
Fold-R	-	2.5	1.7	0.4	2.1
3'-azido-ddATP					
IC_{50} (μM)	0.16 ± 0.10	0.70 ± 0.10	0.42 ± 0.10	0.19 ± 0.10	1.44 ± 1.00
Fold-R	-	4.3	2.5	1.2	8.8
3'-azido-2,6-DA-P-TP					
IC_{50} (μM)	0.80 ± 0.10	2.5 ± 1.6	1.3 ± 0.4	0.34 ± 0.10	4.2 ± 3.6
Fold-R	-	3.1	1.6	0.4	5.3
p-value [d]	-	0.36	0.08	0.02	0.45
3'-azido-6-Cl-P-TP					
IC_{50} (μM)	3.2 ± 0.8	9.1 ± 3.8	11.8 ± 3.9	2.5 ± 1.0	30.8 ± 6.1
Fold-R	-	2.9	3.7	0.8	9.7
p-value	-	0.12	0.15	0.22	0.81
3'-azido-6-AA-P -TP					
IC_{50} (μM)	4.10 ± 0.8	8.8 ± 0.8	10.3 ± 1.9	4.8 ± 0.6	21.8 ± 12.0
Fold-R	-	2.2	2.5	1.2	5.3
p-value	-	0.0006	0.97	0.94	0.43
3'-azido-6-DM-P-TP					
IC_{50} (μM)	23.4 ± 13.0	>50	>50	n.d. [e]	>50
Fold-R	-	>2.0	>2.0		>2.0
p-value	-	-	-	-	-
3'-azido-6-MX-P-TP					
IC_{50} (μM)	24.4 ± 7.0	80.1 ± 6.1	>100	32.9 ± 23.0	78.0 ± 34.0
Fold-R	-	3.3	>4.0	1.3	3.2
p-value	-	0.10	-	0.71	0.31

[a] The Q151M RT contains the A62V, V75I, F77L, F116Y and Q151M mutations.
[b] IC_{50} values are the concentration of drug required to inhibit 50% of DNA synthesis under steady-state assay conditions. Data are shown as the means ± standard deviations of at least three independent experiments.
[c] Fold-resistance (Fold-R) values are calculated by $IC_{50}^{\text{mutant RT}}/IC_{50}^{\text{WT RT}}$.
[d] P-value compares the Fold-R values determined for the 6-modified 3'-azido-ddGTP analogs to the Fold-R value determined for 3'-azido-ddATP.
[e] n.d. Not determined

5.5.2 Pre-steady-state incorporation of 6-modified 3'-azido-ddGTP nucleotide analogs by HIV-1 RT

Pre-steady-state kinetic analyses were carried out to elucidate, in detail, the interactions between the 6-modified-3'-azido-ddGTP analogs and the polymerase active site of WT HIV-1 RT (**Table 5.2**). Because the 6-modified-3'-azido-ddGTP analogs behave as adenine nucleotide analogs, we included 3'-azido-ddATP as a control. The results (**Table 5.2**) show that the catalytic efficiency of incorporation (k_{pol}/K_d) of 3'-azido-2,6-DA-P-TP was similar to that of dATP and 3'-azido-ddATP. Consistent with the steady-state kinetic experiments, 3'-azido-6-Cl-P-TP, 3'-azido-6-AA-P-TP, and 3'-azido-6-MX-P-TP were all less efficiently incorporated by WT HIV-1 compared to dATP. The observed decreases in catalytic efficiency for each of these substrates was driven by both a decrease in the rate of nucleotide incorporation (i.e. k_{pol}) and a decrease in the affinity of the nucleotide for the polymerase active site (i.e. K_d). Due to limited quantities of the 3'-azido-6-DM-P-TP, we were unable to obtain pre-steady-state kinetic data for this analog. We also assessed the ability of the 6-modified-3'-azido-ddGTP analogs to be incorporated opposite cytosine (**Table 5.2**). The data show that, in comparison to dGTP, the 6-modified-3'-azido-ddGTP analogs were inefficiently incorporated by HIV-1 RT. The only compound with reasonable activity as a G-analog was 3'-azido-6-Cl-P-TP; however its selectivity value versus dGTP (SI = 254) was ~ 7-fold less than its selectivity value versus dATP (SI = 35).

Table 5.2 Pre-steady-state kinetic values for incorporation of 6-modified-3'-azido-ddGTP analogs by WT HIV-1 RT.

Incorporation as an "A" analog				
Nucleotide Analog	k_{pol} (sec^{-1})	K_d (μM)	k_{pol} / K_d (μM^{-1} sec^{-1})	Selectivity[a] vs dATP
dATP	17.0 ± 2.1[b]	0.33 ± 0.05	52	-
3'-azido-ddATP	14.0 ± 5.6	0.32 ± 0.13	44	1.2
3'-azido-2,6-DA-P-TP	14.0 ± 4.9	0.29 ± 0.05	48	1.1
3'-azido-6-Cl-P-TP	2.7 ± 0.5	1.8 ± 1.0	1.5	35
3'-azido-6-AA-P-TP	2.1 ± 0.2	4.8 ± 2.3	0.44	118
3'-azido-6-MX-P-TP	2.8 ± 0.2	12.0 ± 1.2	0.23	226
Incorporation as a "G" analog				
Nucleotide Analog	k_{pol} (sec^{-1})	K_d (μM)	k_{pol} / K_d (μM^{-1} sec^{-1})	Selectivity vs dGTP
dGTP	17.3 ± 1.4	0.17 ± 0.05	102	-
3'-azido-2,6-DA-P-TP	0.16 ± 0.02	34 ± 14	0.005	20400
3'-azido-6-Cl-P-TP	0.37 ± 0.04	0.92 ± 0.02	0.402	254
3'-azido-6-AA-P-TP	n.m.[c]	> 50	n.m.	n.m.
3'-azido-6-MX-P-TP	0.22 ± 0.09	16.3 ± 4.3	0.013	7846

[a] Selectivity is $(kpol/Kd)^{dNTP}/(kpol/Kd)^{3'\text{-azido-ddNTP}}$.
[b] Values represent the means ± standard deviations of three to four independent experiments.
[c] n.m. Not measurable. The rate of incorporation was so inefficient that accurate kinetic parameters could not be determined.

5.5.3 Activity of the 6-modified-3'-azido-ddGTP analogs against HIV-1 RT containing NRTI discrimination mutations

The amino acid substitutions K65R, L74V, Q151M (in complex with A62V, V75I, F77L and F116Y) or M184V in HIV-1 RT improve the enzyme's ability to discriminate between the natural dNTP substrate and an NRTI-TP. These substitutions are typically referred to as NRTI discrimination mutations. To determine whether NRTI discrimination mutations impacted the ability of RT to recognize and incorporate the 6-modified-ddGTP analogs, we determined the concentration of nucleotide analog required to inhibit 50% of the DNA polymerase activity (i.e. IC_{50}) under steady-state assay conditions using the heteropolymeric DNA/DNA T/P substrates as described in the Materials and Methods (**Table 5.1**). 3'-Azido-ddATP, 3'-azido-ddGTP and ZDV-TP were again included as controls. The 6-modified-3'-azido-ddGTP analogs were also incorporated as adenosine analogs by the mutant HIV-1 RTs (data not shown). In general, the mutant HIV-1 RTs exhibited fold-resistance values to each of the 6-modified-3'-azido-ddGTP analogs that were similar (i.e. less than 2-fold) to the fold-change in resistance values determined for 3'-azido-ddATP. The only statistically significant exceptions ($p < 0.05$) included 3'-azido-6-AA-P-TP and 3'-azido-2,6-DA-P-TP which exhibited better activity against K65R HIV-1 RT and M184V HIV-1 RT, respectively. Of interest, all of the 3'-azido-dideoxypurines exhibited greater activity than ZDV-TP against multi-NRTI resistant HIV-1 RT containing A62V/V75I/F77L/Y116F/Q151M.

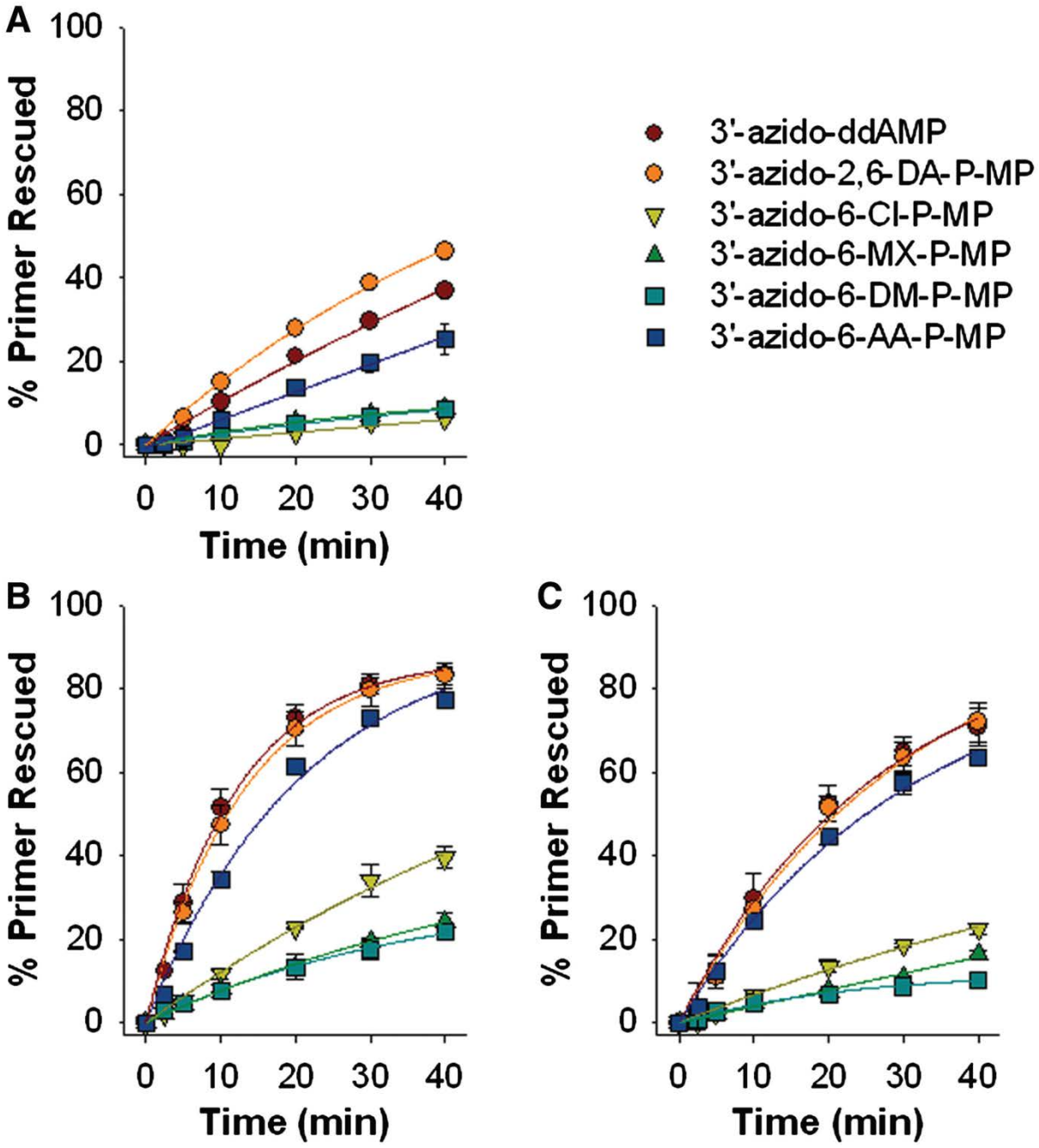

Figure 5.3 ATP-mediated excision of 6-modified-3'-azido-ddGMP analogs by WT (A), TAM67 (B), or TAM41 (C) HIV-1 RT.
Data are the means ± standard deviations from at least three independent experiments. Reaction conditions are described in the Materials and Methods section.

5.5.4 Excision of 6-modified-3’-azido-ddG-5’-MP analogs by WT and TAM containing HIV-1 RT

HIV-1 RT has the intrinsic ability to rescue DNA synthesis from an NRTI-MP blocked primer, using ATP as a phosphate donor (130). This ATP-mediated excision activity of HIV-1 RT is selectively increased by TAMs (131). Accordingly, we investigated the ability of WT and TAM-containing RT to excise the 6-modified-3’-azido-ddGMP analogs from a DNA chain-terminated T/P (**Figure 5.3**). Two RT enzymes that contained different patterns of TAMs (i.e. D67N/K70R/T215F/K219Q (TAM67) and M41L/L210W/T215Y (TAM41)) were studied. Our results showed that the WT, TAM67, and TAM41 RTs could unblock T/Ps chain-terminated with 3’-azido-ddAMP, 3’-azido-2,6-DA-P-MP and 3’-azido-6-AA-P-MP, although TAM41 RT and TAM67 RT were more efficient in this regard than was the WT enzyme. By contrast, both the WT and TAM-containing RTs could not efficiently unblock T/P substrates chain-terminated with 3’-azido-ddGMP, 3’-azido-6-MX-P-MP, 3’-azido-6-Cl-P-MP or 3’-azido-6-DM-P-MP.

5.5.5 Molecular models of 3'-azido-2,6-DA-P-TP and 3'-azido-6-Cl-P-TP in the active site of HIV-1 RT

We used molecular modeling to gain structural insight into the binding interaction between the 6-modified-3'-azido-ddGTP analogs and the thymine base in the DNA template in the active site of HIV-1 RT. Specifically, we modeled 3'-azido-2,6-DA-P-TP and 3'-azido-6-Cl-P-TP into the active site of HIV-1 RT using the co-ordinates (1RTD) from the RT-T/P-TTP complex (77). Both 3'-azido-2,6-DA-P-TP and 3'-azido-6-Cl-P-TP, were found to fit comfortably into the active site of HIV-1 RT and formed hydrogen bond interactions with the thymine base in the DNA template (**Figure 5.4**). However, the base hydrogen bonding characteristics differed for each analog. The base of 3'-azido-6-Cl-P-TP forms two hydrogen bond interactions through the nitrogen (NH) at position 1 and the amine (NH_2) at position 2 with the template thymine (**Figure 5.4B**). In addition to these two hydrogen bonding interactions, 3'-azido-2,6-DA-P-TP can form an additional hydrogen bond via the amino group (NH_2) at the 6-position of the purine base (**Figure 5.4D**). Therefore, the 2,6-diaminopurine:thymine base pairing interaction mimics the canonical Watson-Crick guanine:cytidine interaction.

5.5.6 Molecular models for ATP-mediated excision of the 6-modified-3'-azido-ddG-5'-MP analogs

To gain structural insight into why the 6-modified-3'-azido-ddG analogs are differentially excised by HIV-1 RT containing TAMs, we modeled their excision products (6-modified-3'-azido-ddG adenosine dinucleoside tetraphosphate) in the enzyme's active site. These models reveal a hydrogen bonding network that is different from those observed for the TP forms.

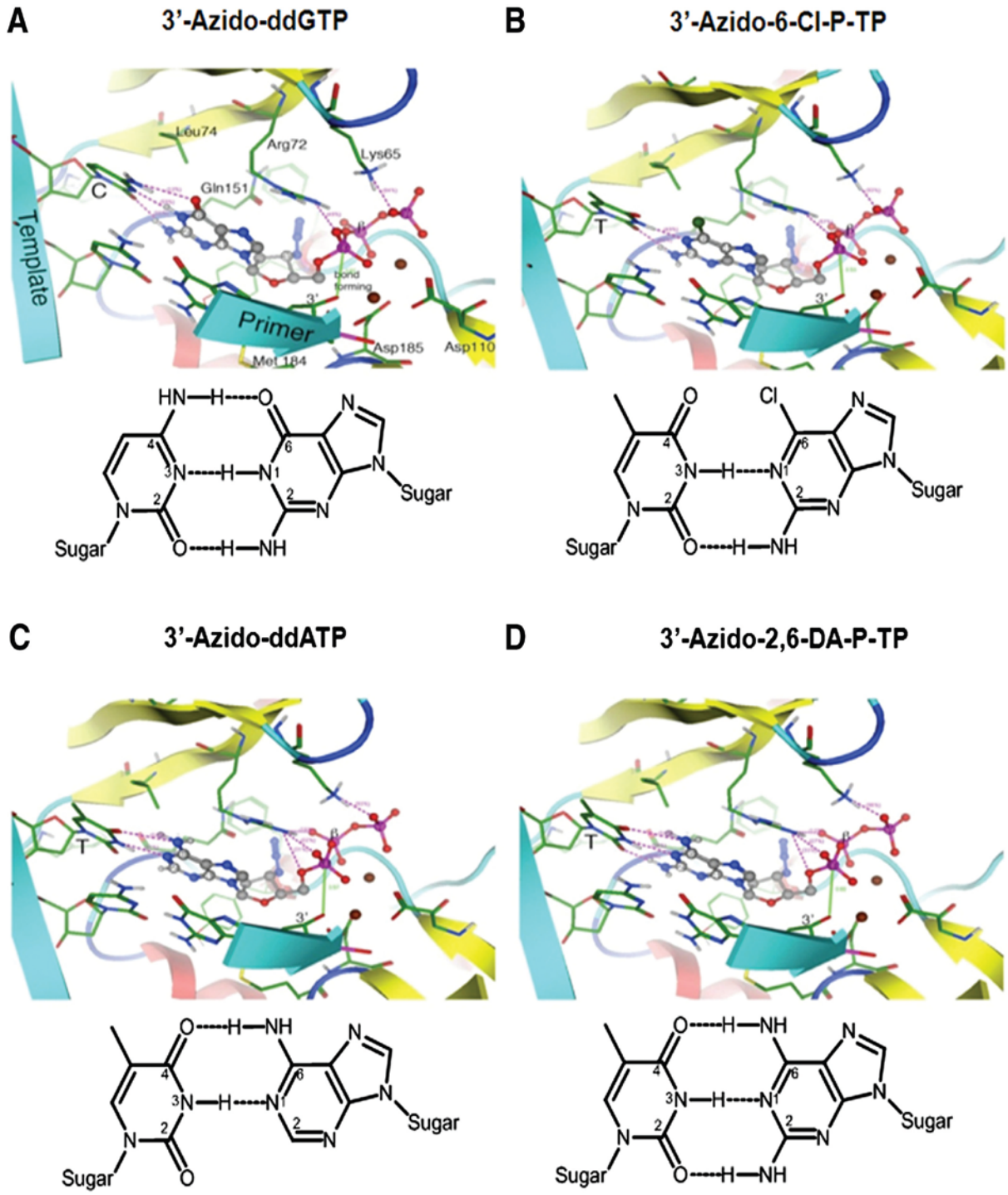

Figure 5.4 Molecular models of 3'-azido-ddGTP (A), 3'-azido-6-Cl-P-TP (B), 3'-azido-ddATP (C), and 3'-azido-2,6-DA-P-TP (D) in the DNA polymerase active site of WT HIV-1 RT.

Each of the analogs was modeled into the ternary RT-T/P-TTP complex (pdb co-ordinates 1RTD). A schematic representation of the hydrogen-bonding patterns between the incoming nucleotide analog and the template base is depicted below each model.

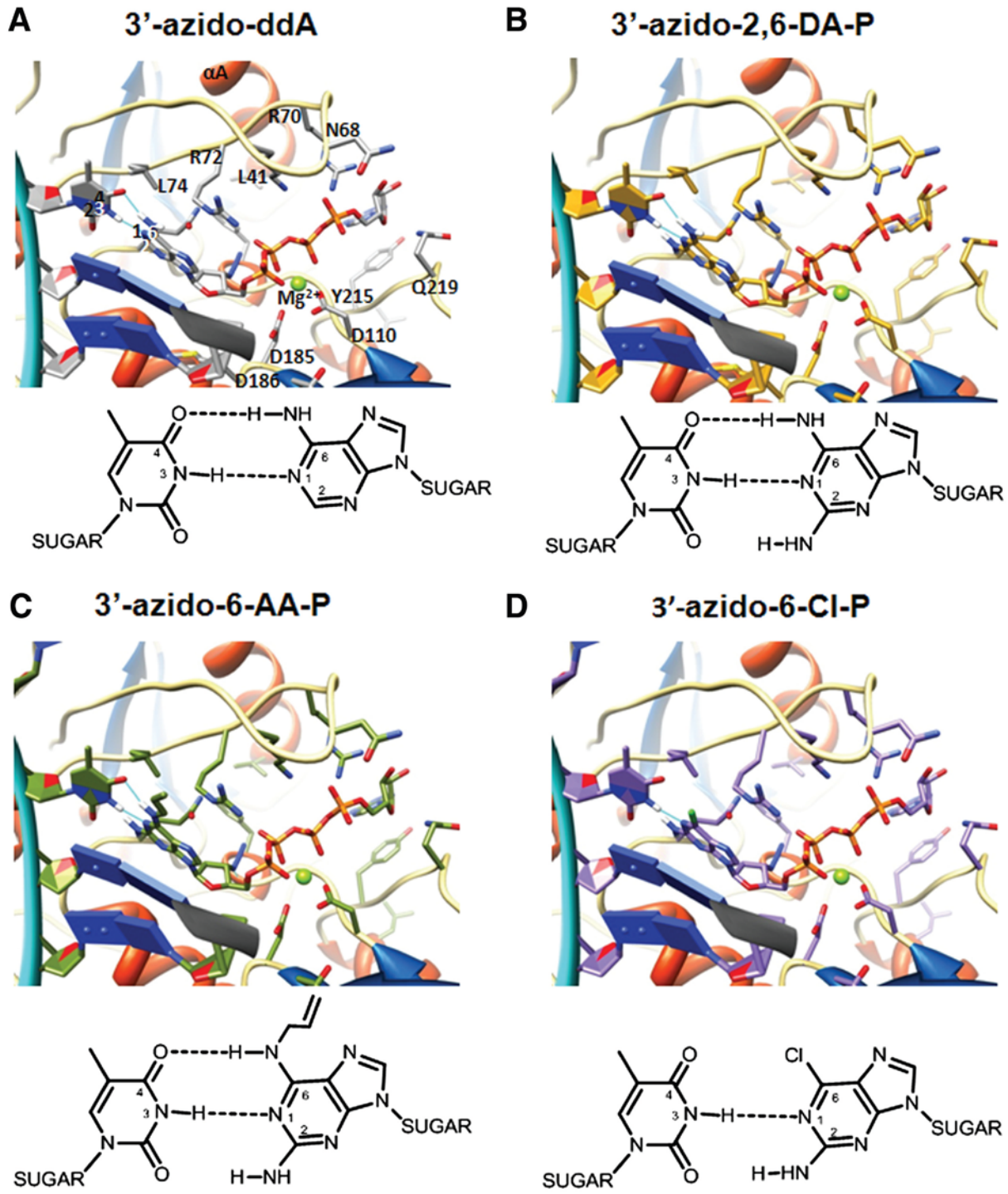

Figure 5.5 Molecular models of the excision products of 3'-azido-ddA (A), 3'-azido-2,6-DA-P (B), 3'-azido-6-AA-P (C), and 3'-azido-6-Cl-P (D) in the DNA polymerase active site of HIV-1 RT containing TAMs.

Each of the analogs was modeled into the ternary RT-T/P-AZTppppA complex (pdb co-ordinates 3KLE). A schematic representation of the hydrogen-bonding patterns between the excised nucleotide analog and the template base is depicted below each model.

3’-azido-ddA forms hydrogen bonds from the 1 and 6 atoms to the 3 and 4 atoms of the complementary thymine template in both the incorporation (**Figure 5.4C**) and excision (**Figure 5.5A**) models. By contrast, the hydrogen bond observed between the 2-amino substitution and the 2-carbonyl of the thymine template observed for the nucleotide triphosphate analogs (**Figure 5.4B, 5.4D**) is lost in all related excision complexes (**Figure 5.5B, 5.5C, 5.5D**). 3’-azido-2,6-DA-P (**Figure 5.5B**) and 3’-azido-6-AA-P (**Figure 5.5C**) retain an H-bond from the 6 atom position of the purine ring and the 4 atom position on the template thymine, whereas this interaction is not maintained for 3’-azido-6-Cl-P (**Figure 5.5D**), 3’-azido-6-DM-P and 3’-azido-6-MX-P (data not shown). Taken together, these different hydrogen bonding patterns may explain why 3’-azido-2,6-DA-P and 3’-azido-6-AA-P are more efficiently excised by HIV-1 RT than are 3’-azido-6-Cl-P, 3’-azido-6-DM-P and 3’-azido-6-MX-P.

5.6 DISCUSSION

In this study, we demonstrated that 6-modified-3’-azido-ddGTP nucleotides act as adenosine mimetics for DNA synthesis carried out by HIV-1 RT. Of the five analogs studied, 3’-azido-2,6-DA-P-TP, which has a 2,6-diaminopurine base, was found to be the most efficient substrate for incorporation by HIV-1 RT. In pre-steady-state kinetic experiments, 3’-azido-2,6-DA-P-TP was recognized and incorporated by WT HIV-1 RT as efficiently as dATP and 3’-azido-ddATP. The analogs that contain the 2-amino-6-*N*,*N*-dimethylaminopurine (3’-azido-6-DM-P-TP) or 2-amino-6-methoxypurine (3’-azido-6-MX-P-TP) bases, however, were poor substrates for incorporation by HIV-1 RT. Our molecular modeling studies suggest that 6-modifications with a branched side-chain (e.g. 3’-azido-6-DM-P-TP) or one with electronic incompatibility (e.g. 3’-

azido-6-MX-P-TP) may alter the alignment of the bases and move their α–phosphate away from the primer 3'-OH thus impairing nucleotide incorporation. In contrast, 3'-azido-2,6-DA-P-TP, 3'-azido-6-CL-P-TP, and 3'-azido-6-AA-P-TP form relatively planar base pairing interactions with the template thymine that enhance their α-phosphate interaction with the 3'-OH of the primer. Compared to the canonical A:T base pair, the additional hydrogen bond achieved by the 3'-azido-2,6-DA-P:thymine base pair may further stabilize the α-phosphate, facilitating the favorable catalytic efficiency observed in pre-steady-state assays. In contrast, the 6-modified-3'-azido-ddGTP nucleotide analogs are inefficiently incorporated by HIV-1 RT opposite cytosine bases. Taken together, these findings are consistent with those of Cheong *et al.*, who reported that oligodeoxyribonucleotide duplexes containing 2,6-diaminopurine formed more stable base pairs opposite thymine than cytosine (294).

The mutations K65R, L74V, Q151M (in complex with A62V, V75I, F77L and F116Y) or M184V in HIV-1 RT allow the enzyme to discriminate between the natural dNTP substrate and modified nucleotide analogs. In **Table 5.2**, we show that the K65R, L74V and Q151M mutations confer low levels of resistance to both 3'-azido-ddATP and 3'-azido-ddGTP at the enzyme level. Modification at the 6-position of the purine base does not appear to enhance this discrimination phenotype: the K65R, L74V or A62V/V75I/F77L/F116Y/Q151M HIV-1 RTs all exhibited fold-resistance changes to each of the 6-modified-3'-azido-ddGTP analogs that were largely similar (i.e. less than 2-fold) to the fold-change in resistance values determined for 3'-azido-ddATP. Interestingly, the structure-activity relationship for the ATP-mediated excision of the 6-modified-3'-azido-ddGMP analogs by WT or TAM-containing HIV-1 RT differed from the structure-activity relationship for their incorporation. For example, whereas 3'-azido-6-Cl-P-TP is a relatively good substrate for incorporation, it is not efficiently excised by either WT or

TAM-containing HIV-1 RT. In this regard, our excision complex modeling data show that the hydrogen bonding pattern observed for 3'-azido-6-Cl-P-TP differs from that of 3'-azido-2,6-DA-P and 3'-azido-6-AA-P (**Figure 5.5**). As such, it is possible that the change in transition state geometry needed for excision is not sufficiently stabilized by the 6-Cl substituted guanine analog base paired with thymine. Taken together, these data suggest that the optimal conformation of the HIV-1 RT active site differs for incorporation and excision and further suggests that 6-position modifications differentially effect these two reactions. This finding provides "proof of concept" that modified base analogs can be identified that are efficiently incorporated by HIV-1 RT but serve as a poor substrate for HIV-1 ATP-mediated excision reactions. Further optimization of these divergent but favorable properties of purine analogs is in progress to develop novel, ambiguous NRTI that exert profound antiviral activity against WT and drug-resistant HIV-1.

6.0 CHAPTER FOUR. RS-788, A PRODRUG OF 3'-AZIDO-2,6-DIAMINO-2',3'-DIDEOXYPURINE: UNIQUE METABOLISM, EXCELLENT RESISTANCE PROFILE, AND SYNERGISTIC INHIBITION OF HIV-1 RT

Brian D. Herman[1], Hong-wang Zhang[2], Aleksandr Obikhod[2], Ghazia Asif[2], Steven J. Coats[3], Raymond F. Schinazi[2], John W. Mellors[1] and Nicolas Sluis-Cremer[1]

[1]Department of Medicine, Division of Infectious Diseases, University of Pittsburgh, Pittsburgh, PA 15261; [2]Center for AIDS Research, Department of Pediatrics, Emory University School of Medicine, and Veterans Affairs Medical Center, Decatur, Georgia 30033; [3]RFS Pharma, LLC, Tucker, Georgia 30084.

6.1 PREFACE

The data described in this chapter were presented in part as a poster at *The 17th Conference on Retroviruses and Opportunistic Infections February 16-19, 2010, San Francisco, CA USA.* Abstract # 489. Herman, B. D., Obikhod, A., Asif, G., Zhang, H-W., Coats, S. J., Schinazi, R. F., Mellors, J. W. and N. Sluis-Cremer. RS-788, a Prodrug of β-D-3'-Azido-2,6-diamino-2',3'-dideoxypurine, Exhibits Potent Activity Against NRTI-Resistant HIV-1; and in part at *The 18th Conference on Retroviruses and Opportunistic Infections February 27- March 2, 2011, Boston, MA USA.* Abstract # 519. Herman, B. D., Zhang, H-W., Coats, S., Schinazi, R,, Mellors, J. and N. Sluis-Cremer. The 5'-triphosphates of 3'-azido-2',3'-dideoxyguanosine and 3'-azido-2,6-diamino-2',3'-dideoxypurine act synergistically to inhibit wild-type and NRTI-resistant HIV-1 reverse transcriptase.

The work presented in this chapter is in partial fulfillment of dissertation Aim 2. Brian Herman performed all the experiments presented in this chapter. The detection of NRTI-TP metabolites in P4/R5 cells was performed by Brian Herman, along with Aleksandr Obikhod, and Ghazia Asif.

6.2 ABSTRACT

Although 3'-azido-2,6-DA-P-TP potently inhibited DNA synthesis by NRTI-resistant RT through incorporation and chain-termination as an adenosine analog in biochemical assays, 3'-azido-2,6-DA-P is extensively metabolized to 3'-azido-ddG in cells. To further improve 3'-azido-2,6-DA-P antiviral activity by increasing the intracellular delivery of its triphosphate form,

we synthesized RS-788, a novel phosphoramidate prodrug of 3'-azido-2,6-DA-P. RS-788 has potent anti-HIV-1 activity and is metabolized ~1:1 to both 3'-azido-2,6-DA-P-TP and 3'-azido-ddG-TP in peripheral blood mononuclear (PBM) cells. Thus, RS-788 delivers two chemically distinct metabolites, each of which are potent HIV-1 RT chain terminators that are incorporated opposite different complementary bases; thymine for 3'-azido-2,6-DA-P-TP and cytosine for 3'-azido-ddG-TP. In the current study, we further characterized the activity of this unique prodrug by examining the intracellular metabolism and antiviral cross-resistance profiles of RS-788, and its parent analogs, 3'-azido-2,6-DA-P and 3'-azido-ddG. We found that RS-778 exhibits a superior phenotypic cross-resistance profile against a broad range of NRTI-resistant viruses compared to 3'-azido-2,6-DA-P or 3'-azido-ddG. For example, against HIV-1 with the multi-NRTI resistance mutation Q151M (in complex with A62V/F77L/V75I/F116Y; Q151M complex) the potency of RS-788 was decreased only 2.3-fold compared to WT, whereas that of 3'-azido-2,6-DA-P and 3'-azido-ddG were decreased 23- and 26-fold, respectively. Therefore, the potent inhibition of multi-drug resistant HIV-1 by RS-788 may be due to incorporation and chain termination at both thymine and cytosine positions by 3'-azido-2,6-DA-P-TP and 3'-azido-ddG-TP, respectively. To evaluate this hypothesis, we examined the inhibitory activity of combinations of the active metabolites 3'-azido-2,6-DA-P-TP+3'-azido-ddG-TP against WT and multi-NRTI-resistant HIV-1 RT DNA synthesis. Drug synergy analyses by both the median-effect and normalized isobologram methods indicated synergistic inhibition of multi-NRTI resistant HIV-1 RT DNA synthesis by combinations of 3'-azido-2,6-DA-P-TP+3'-azido-ddG-TP at the intracellular molar ratios detected in P4/R5 and PBM cells. Furthermore, the excision mechanism conferred by TAMs did not diminish the observed synergy. Taken together, our data

demonstrate that the combined intracellular delivery of 3'-azido-2,6-DA-P-TP and 3'-azido-ddG-TP by RS-788 provides synergistic inhibition of reverse transcription by NRTI-resistant RT.

6.3 INTRODUCTION

The rational design of a series of novel 3'-azido-2',3'-dideoxypurine analogs led to the identification of 3'-azido-2',3'-dideoxy-2,6-diaminopurine (3'-azido-2,6-DA-P) as a potent and selective inhibitor of HIV-1 replication in primary lymphocytes (**Figure 5.1**) (143). 3'-azido-2,6-DA-P showed superior activity against WT and NRTI resistant HIV-1 replication compared to its parent analog 3'-azido-2',3'-dideoxygaunosine (3'-azido-ddG) . The kinetic and molecular modeling studies described in the previous chapter indicated that the triphosphate form, 3'-azido-2,6-DA-P-TP, was specifically recognized by HIV-1 RT as an adenosine analog and efficiently incorporated across from thymine in DNA or uracil in RNA, resulting in chain termination (**Table 5.1, Figure 5.2, and Figure 5.4**). Intracellular pharmacology analyses, however, revealed that 3'-azido-2,6-DA-P was extensively metabolized to 3'-azido-ddG in PBM cells, resulting in the production of 382-fold more 3'-azido-ddG-TP than 3'-azido-2,6-DA-P-TP (**Figure 6.1**) (295, 296). Incubation with purified adenosine deaminase *in vitro* led to the efficient conversion of 3'-azido-2,6-DA-P to 3'-azido-ddG (143). Therefore, the potent anti-HIV-1 activity of 3'-azido-2,6-DA-P is primarily attributed to RT inhibition by 3'-azido-ddG-TP and not due to incorporation of 3'-azido-2,6-DA-P-TP as an adenosine analog. In order to further improve 3'-azido-2,6-DA-P antiviral activity by increasing the intracellular delivery of its triphosphate form, we synthesized a series of 5'-monophosphate prodrugs.

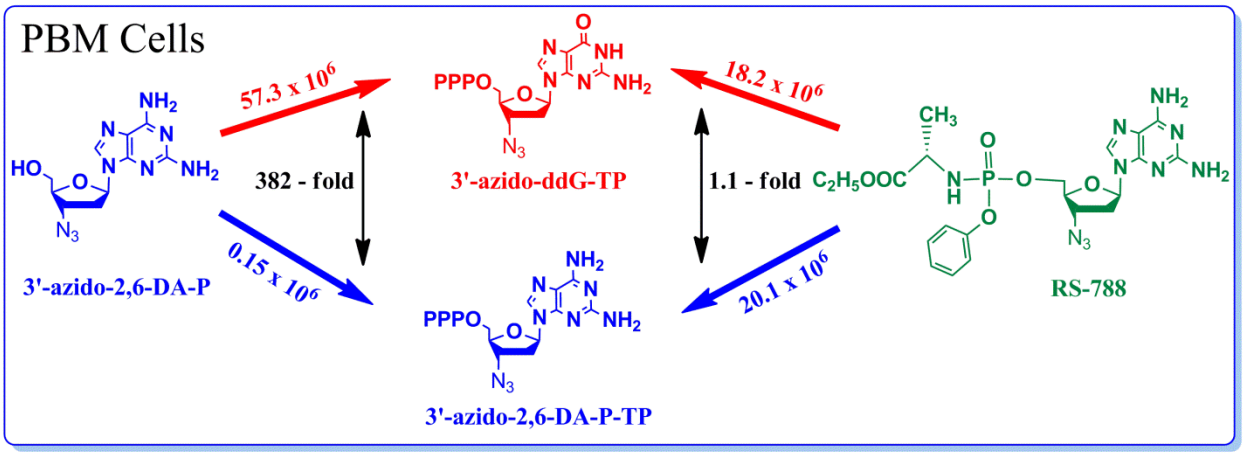

Figure 6.1 Structures and intracellular pharmacology in PBM cells of 3'-azido-2,6-DA-P and RS-788.
PBM cells were incubated with 50 µM 3'-azido-2,6-DA-P or RS-788 for 4 hours and the resulting nucleotide-TP metabolites were detected using LC-MS/MS. Values are in pmol/million cells and are from references (295, 296).

One such prodrug, RS-788, is a chemically shielded 5'-phosphoramidate prodrug of 3'-azido-2,6-DA-P. In PBM cells, RS-788 was metabolized approximately 1:1 to both 3'-azido-2,6-DA-P-TP and 3'-azido-ddG-TP, whereas the parent molecules 3'-azido-2,6-DA-P and 3'-azido-ddG were both converted to 3'-azido-ddG-TP as the major active metabolite (**Figure 6.1**). Consequently, RS-788 delivers two chemically distinct metabolites, each of which are potent HIV-1 RT chain terminators that are incorporated opposite different complementary bases: thymine for 3'-azido-2,6-DA-P-TP and cytosine for 3'-azido-ddG-TP. Intracellular delivery of two different chain terminating nucleotides from one parent prodrug has not been previously reported.

RS-788 showed 60- and 17-fold more potent anti-HIV-1 activity in PBM cells than its parent molecules 3'-azido-ddG and 3'-azido-2,6-DA-P, respectively (**Table 6.1**) (295, 296). Importantly, RS-788 also showed a good cytotoxicity profile in PBM, CEM, and Vero cells. The selectivity index (SI; calculated as CC_{50}/EC_{50}) of RS-788 (CC_{50} = 17.6 µM) in PBM cells was

Table 6.1 Activity, cytotoxicity, and selectivity index of 3'-azido-ddG, 3'-azido-2,6-DA-P and RS-788 in peripheral blood mononuclear (PBM) cells.

NRTI [a]	EC_{50} (μM) [b]	CC_{50} (μM) [c]	Selectivity Index [d]
3'-azido-ddG	0.18	100	555.6
3'-azido-2,6-DA-P	0.05	54.0	1080
RS-788	0.003	17.6	5867

[a] Data are from references (295, 296).
[b] EC_{50} is the concentration required to inhibit 50 % wild-type (WT) HIV-1 replication.
[c] CC_{50} is the concentration required to inhibit 50% cell growth.
[d] Selectivity index is calculated as CC_{50}/EC_{50}.

10.6-fold and 5.4-fold better than 3'-azido-ddG (CC_{50} = 100 μM) and 3'-azido-2,6-DA-P (CC_{50} = 54 μM), respectively. Unlike the tenofovir prodrug (TDF) that delivers significantly higher concentrations of TFV-DP to cells than tenofovir alone, the increased potency of RS-788 was not due to increased delivery of active metabolite (206, 207). The total intracellular concentrations of 3'-azido-ddG-TP/3'-azido-2,6-DA-P-TP in PBM cells treated with 50 μM of drug were 57.5 x 10^6 and 38.3 x 10^6 pmol/million cells for 3'-azido-2,6-DA-P and RS-788, respectively (**Figure 6.1**).

The unique cellular pharmacology of RS-788 and the improved anti-HIV-1 activity over its parent analogs warranted further investigation of its activity and mechanisms of inhibition against WT and NRTI-resistant RT. Accordingly, this chapter describes the metabolism and antiviral cross-resistance profiles of RS-788, 3'-azido-2,6-DA-P, and 3'-azido-ddG in HIV-1 reporter cell line P4/R5. We found that RS-778 exhibits a superior phenotypic cross-resistance profile against a broad range of NRTI-resistant viruses compared to 3'-azido-2,6-DA-P or 3'-azido-ddG. The activity of RS-788 against HIV-1 with the multi-NRTI resistance mutation Q151M (in complex with A62V/F77L/V75I/F116Y; Q151M complex) and the 69-insertion mutations (T69S-SS in the background of TAMs M41L/L210W/T215Y; T69SSS) was

particularly compelling. To gain mechanistic insight into the potent activity of RS-788 against multi-NRTI resistant HIV-1, we also evaluated the inhibitory activity of the active metabolites 3'-azido-2,6-DA-P-TP and 3'-azido-ddG-TP and combinations of 3'-azido-2,6-DA-P-TP+3'-azido-ddG-TP against WT and NRTI-resistant HIV-1 RT.

6.4 MATERIALS AND METHODS

6.4.1 Cells, viruses, and NRTI for intracellular metabolism and drug susceptibility studies

The human T-cell leukemia MT-2 cell line (AIDS Research and Reference Reagent Program) was cultured in RPMI 1640 with 2 mM L-glutamine (Lonza, Walkersville, MD) supplemented with 10% fetal bovine serum (HyClone Laboratories, Inc., Logan, UT), 10 mM HEPES buffer (Gibco, Grand Island, NY), and 50 IU/ml of penicillin and 50 µg/ml of streptomycin (Gibco). The HeLa cell derived P4/R5 reporter cell line (provided by Nathaniel Landau, Salk Institute), which expresses the β-galactosidase gene under the control of the HIV-1 LTR that is transactivated by HIV-1 Tat, was maintained in phenol red-free Dulbecco's modified Eagle medium (Gibco) supplemented with 10% fetal bovine serum, 50 IU/ml of penicillin, 50 µg/ml of streptomycin, and 0.5 µg/ml of puromycin (Clontech, Palo Alto, CA).

The L74V, M184V, K65R, D67N/K70R/T215F/K219Q (AZT2), M41L/L210W/T215Y (AZT3), M41L/D67N/K70R/T215F/K219Q (AZT7), and M41L/D67N/K70R/L210W/T215Y/K219Q (AZT9) NRTI-resistant HIV-1_{LAI} full-length proviral clones were kindly provided by Dianna Koontz (University of Pittsburgh). RT clones

containing the mutations A62V/F77L/V75I/F116Y/Q151M (Q151M complex, $Q151M_c$) and M41L/T69S-SS/L210W/T215Y (T69SSS) were generated by site-directed mutagenesis (QuikChange II site-directed mutagenesis kit; Stratagene, La Jolla, CA) using the p6HRT-MO plasmid. This plasmid contains the entire RT and protease coding sequence and four silent restriction sites (XmaI, MluI, XbaI, and NgoMIV from the 5' to 3'ends of RT at codons 14, 358, 490, and 554, respectively) (297). After site-directed mutagenesis, the mutated RT was ligated into pxxHIV-1_{LAI} -MO, which contains the entire genome of HIV-1_{LAI} and the same silent restriction sites in RT as p6HRT-MO plasmid provided by Jessica Brehm (University of Pittsburgh). All mutations in recombinant viruses were confirmed by sequencing. Stock viruses were prepared in MT-2 cells as described previously (212). Briefly, 5 -10 µg of plasmid DNA was electroporated into 1.3×10^7 MT-2 cells. Cell-free supernatants were collected 5 to 7 days post-transfection at peak cytopathic effect (CPE) and stored at -80°C. The infectivity of the virus stocks were determined by 3-fold end point dilution in P4/R5 cells, and the 50% tissue culture infectivity dose was calculated using the Reed and Muench equation (298).

Zidovudine (AZT) was obtained from Sigma Chemical Corporation (St. Louis, MO) and 3'-azido-ddG was obtained from Berry & Associates, Inc. (Ann Arbor, MI). 3'-azido-2,6-DA-P and RS-788 were synthesized as described previously and kindly provided by Raymond Schinazi (Emory University) (143). All NRTIs were prepared as 40 mM stock solutions in dimethyl sulfoxide and stored at -20°C.

6.4.2 Quantification of the intracellular metabolites of 3'-azido-2,6-DA-P, 3'-azido-ddG, and RS-788 in P4/R5 cells

MT-2 cells (5×10^6) were incubated with 50 µM 3'-azido-2,6-DA-P, 3'-azido-ddG, or RS-788 for 4 hours. The cells were then centrifuged for 10 min at 350 × g at 4 °C, and the pellet was resuspended and washed three times with cold phosphate-buffered saline (PBS). Nucleoside triphosphates were extracted by incubation overnight at -20 °C with 1 ml 60% methanol in water. The supernatant was collected and centrifuged at 16,000 × g for 5 min. After decanting the supernatant, an additional 200 µL of 60% methanol in water was added to the pellets, which were then incubated on ice for 1 hour followed by centrifugation at 16,000 × g for 5 min. The extracts were dried under a gentle filtered airflow and stored at -20°C. The dried residues were resuspended in 100 µL of water prior to liquid chromatography (LC)-tandem mass spectrometry analysis.

The LC system was an UltiMate 3000 modular system (Dionex, Sunnyvale, CA) consisting of a quaternary pump, vacuum degasser, temperature-controlled autosampler (4 °C), and temperature-controlled column compartment (28 °C). An API5000 mass spectrometer (AB/SCIEX, Foster City, CA) was used as the detector. LC Analyst software version 1.4.2 was used to control both the LC and the mass spectrometer as well as for the data analysis and quantification. Phosphorylated nucleosides were quantified by ion exchange, with the separation performed on a 5µm particle-size Biobasic C_{18} (50-mm by 1.0-mm) column (Thermo Electron, Bellefonte, PA) using a gradient. The mobile phase consisted of A (10 mM ammonium acetate), B (ammonia buffer [pH 9.6]), and C, acetonitrile. Sample volumes of 5 µL were injected onto the column.

The flow was diverted to waste for the initial 1 min of the analysis. Initial composition of the mobile phase was 70 % A and 30 % C with a gradient at 3.5 min to 70 % B and 30 % C for 5 min. The mass spectrometer was operated in positive ionization mode with a spray voltage of 5 kV, gas 1 at 15 (arbitrary units), gas 2 at 20 (arbitrary units), and source temperature of 230 °C. A standard curve was prepared by spiking standards of synthesized 3'-azido-2,6-DA-P, 3'-azido-ddG, or RS-788 in the range of 1 nM to 500 nM in control cell lysates.

6.4.3 Drug susceptibility assays for WT and NRTI-resistant HIV-1

The susceptibilities of WT and NRTI-resistant HIV-1 to 3'-azido-2,6-DA-P, 3'-azido-ddG, RS-788, and AZT (as a control) were determined in P4/R5 cells as described previously (212). Briefly, 3-fold dilutions of inhibitor were added to P4/R5 cells in triplicate, and the cells were infected with an amount of virus that produced 100 relative light units (RLU) in control wells without drug. After 48 h, the cells were lysed (Gal-Screen; Tropix/Applied Biosystems, Foster City, CA) and the RLU were measured using a ThermoLab Systems luminometer (Waltham, MA). The concentration of drug required to inhibit viral replication by 50% (EC_{50}) was calculated by linear regression from data points in the linear dose-response range. Data are reported as the mean EC_{50} ± standard deviations from 3-4 independent experiments. Fold resistance was calculated as the ratio $EC_{50}^{mutant}/EC_{50}^{WT}$.

6.4.4 Reagents for Steady RT DNA synthesis assays

WT, T69SSS, and Q151M$_c$ HIV-1 RTs were purified as described previously (284, 285). The protein concentration of the purified enzymes was determined spectrophotometrically at 280 nm using an extinction coefficient (ε_{280}) of 260450 M^{-1} cm^{-1}, and by Bradford protein assays (Sigma-Aldrich, St. Louis, MO). The RNA- and DNA-dependent DNA polymerase activities of the purified WT and mutant enzymes were similar (data not shown). The triphosphate forms of 3'-azido-2,6-DA-P and 3'-azido-ddG were synthesized and purified using the methods of Ludwig and Eckstein (299). The dNTPs, ATP, [α-^{32}P]dATP, and [α-^{32}P]dGTP and Whatman® DE81 anion exchange paper were obtained from GE Healthcare (Piscataway, NJ). Activated calf thymus DNA was purchased from Sigma-Aldrich (St. Louis, MO).

6.4.5 Steady-state RT DNA synthesis assays with 3'-azido-2,6-DA-P-TP, 3'-azido-ddG-TP, and their fixed-ratio combinations

Steady State DNA synthesis reactions with WT, T69SSS, or Q151M$_c$ HIV-1 RT were carried out in a reaction buffer containing 50 mM Tris-HCl (pH 7.5), 50 mM KCl, and 10 mM $MgCl_2$. All concentrations refer to the final concentration after mixing unless noted otherwise. Reactions were initiated by mixing solutions A and B, which were preincubated at 37 °C. Solution A contained 0.5 μM dATP and dGTP, 0.5 μCi/μL [α-^{32}P]dATP or [α-^{32}P]dGTP, 10 nM RT, and various concentrations of 3'-azido-2,6-DA-P-TP, 3'-azido-ddG-TP, or their fixed-ratio combinations in reaction buffer. Solution B contained 100 ng/μL activated calf thymus DNA, 50 μM dTTP, and 50 μM dCTP in reaction buffer. Reactions were incubated at 37 °C for 4 min and then 5 μL aliquots were spotted onto DE81 anion exchange paper. After successive washes with

Na_2PO_4 buffer (50 g/L, 3 × 5 min washes), dH_20 (5 min), and EtOH (5 min) the paper was air dried, sealed in saran wrap, and then exposed to a phosphorimaging screen. Products were analyzed using BioRad Quantity One Software.

3'-azido-2,6-DA-P-TP+3'-azido-ddG-TP combinations were evaluated using a series of assays with increasing total drug concentrations at three fixed ratios. The 3'-azido-2,6-DA-P-TP: 3'-azido-ddG-TP ratios of 2.4:1 and 1.1:1 were chosen because these are the intracellular molar ratios of 3'-azido-2,6-DA-P-TP: 3'-azido-ddG-TP detected in PBM and P4/R5 cells, respectively. The third series of assays used the experimental ratio of 1:3 3'-azido-2,6-DA-P-TP: 3'-azido-ddG-TP. Assays using each of three 3'-azido-2,6-DA-P-TP: 3'-azido-ddG-TP ratios were performed using [α-^{32}P]dATP as the reporter nucleotide and using [α-^{32}P]dGTP as the reporter nucleotide. Experimental control combinations of 1:1 3'-azido-2,6-DA-P-TP:3'-azido-2,6-DA-P-TP and 3'-azido-ddG-TP: 3'-azido-ddG-TP were also performed and, as expected, these combinations were always additive, regardless of whether [α-^{32}P]dATP or [α-^{32}P]dGTP was used as the reporter nucleotide (data not shown). Lastly, assays using all three combination ratios and both reporter nucleosides were also performed with the addition of 3 mM ATP in order to examine steady state DNA synthesis in the presence of a functional excision mechanism. All assays were performed at least 3 times.

6.4.6 Synergy analysis using the median-effect principle

The degree of synergy or antagonism for inhibition of HIV-1 RT DNA synthesis by fixed-ratio combinations of 3'-azido-2,6-DA-P-TP and 3'-azido-ddG-TP was evaluated based on the median-effect principal of Chou and Talalay (300). Using CompuSyn Software (ComboSyn, Inc, Paramus, NJ) the log (f_a/f_u) was plotted versus the log ([drug]), where f_a is the fractional

inhibition of drug relative to no drug control and $f_u = (1-f_a)$. The IC_{50} values were calculated from the antilog of the x-intercept. The combination index (CI) was calculated in a mutually exclusive model by the equation: $CI = [(f_a/f_u)_1 / (f_a/f_u)_{1,2}] + [(f_a/f_u)_2 / (f_a/f_u)_{1,2}]$; where 1 and 2 represent drugs 1 and 2 individually, while 1,2 represents their combined activity. The CI values of < 1, = 1, and > 1 indicate synergy, additive effect, and antagonism, respectively. The degree of synergy is further categorized based on CI values as: very strong synergy (< 0.1), strong synergy (0.1 to 0.3), synergy (0.3 to 0.7), moderate synergy (0.7 to 0.85), additive effect (0.85 to 1.20), moderate antagonism (1.20 to 1.45), antagonism (1.45 to 3.3), strong antagonism (3.3 to 10), and very strong antagonism (> 10).

For each experiment, a set of CI values was determined at the 50 %, 75 %, 90 %, and 95 % inhibition levels (i.e. IC_{50}, IC_{75}, IC_{90}, and IC_{95}, respectively). As recommended in the software manual, we report the average CI calculated from those at each of the four inhibition levels. On some occasions when the effect did not reach the 95 % inhibition level, the IC_{95} CI value was not included in the average CI calculation. Additionally, data points that were > 99 % inhibition were also excluded from analysis.

6.4.7 Synergy analysis using normalized isobolograms

In order to eliminate bias based on the analysis method, we also evaluated the data set by plotting normalized (equipotent) isobolograms (301, 302). These were constructed by plotting $drug_1$ as $[IC_{50}]_{1,2}/[IC_{50}]_1$ and $drug_2$ as $[IC_{50}]_{1,2}/[IC_{50}]_2$ on the x- and y- axes, respectively. The terms $[IC_{50}]_1$ and $[IC_{50}]_2$ represent the IC_{50} of each drug individually and $[IC_{50}]_{1,2}$ represents the IC_{50} of the combination. The diagonal line between coordinates (1,0) and (0,1) represents additivity. Data points that are above the additivity line represent antagonism between the compounds,

whereas data points below the additivity line represent synergy between the compounds. The relative strength of synergy or antagonism can be specified by average deviation from additivity (ADA), which indicates the statistical distance from dose-wise additivity line (302). ADA is calculated by the equation $([\Sigma(IC_{50a},IC_{50b})]-N)/N$ where N is the population size. ADA significance (p-value < 0.05) was measured by a one-tailed homoscedastic t-test. If the ADA value is statistically significant, then negative values represent synergy. Values of -0.5 and lower indicate strong synergy.

6.5 RESULTS

6.5.1 Intracellular pharmacology of 3'-azido-2,6-DA-P, 3'-azido-ddG, and RS-788 in P4/R5 cells

We quantified the levels of nucleotide triphosphate that accumulated in P4/R5 cells treated with 50 µM 3'-azido-2,6-DA-P, 3'-azido-ddG, or RS-788 for 4 hours (**Figure 6.2, Table 6.2,**). As expected, 3'-azido-ddG-TP (20.8×10^6 pmol/million cells) was the only NRTI-TP species found in P4/R5 cells treated with 3'-azido-ddG. Consistent with data from PBM cells, almost all of the NRTI-TP quantified from 3'-azido-2,6-DA-P-treated P4/R5 cells was 3'-azido-ddG-TP (295, 296). Cells treated with 3'-azido-2,6-DA-P contained 470-fold more 3'-azido-ddG-TP (23×10^6 pmol/million cells) than 3'-azido-2,6-DA-P-TP (0.05×10^6 pmol/million cells). Conversely, cells treated with RS-788 accumulated 2.4-fold more 3'-azido-2,6-DA-P-TP (27×10^6 pmol/million cells) than 3'-azido-ddG-TP (11.4×10^6 pmol/million cells). Also of note, incubation with RS-788, but not 3'-azido-ddG or 3'-azido-2,6-DA-P, reduced the intracellular levels of natural

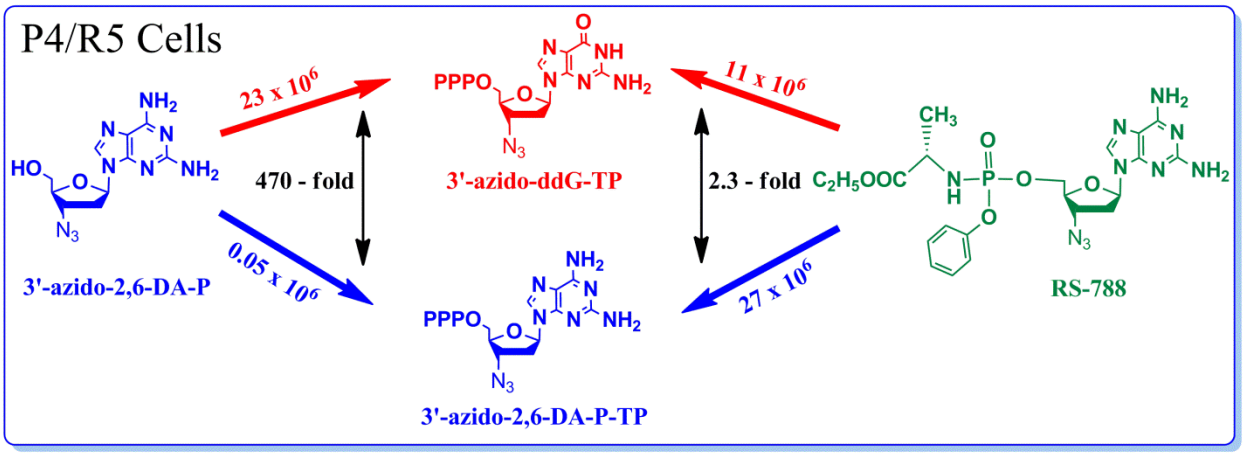

Figure 6.2 Intracellular pharmacology of 3'-azido-2,6-DA-P and RS-788 in P4/R5 cells. P4/R5 cells were incubated with 50 µM 3'-azido-2,6-DA-P or RS-788 for 4 hours and the resulting nucleotide-TP metabolites were detected using LC-MS/MS as described in the Materials and Methods. Values are in pmol/million cells.

Table 6.2 Levels of NRTI-TP and dNTP detected in P4/R5 cells incubated with 50 µM 3'-azido-ddG, 3'-azido-2,6-DA-P, or RS-788 for 4 hours.

	nucleotide triphosphates detected (×10^6 pmol/million cells) [a]					
drug incubated	3'-azido-ddG-TP	3'-azido-2,6-DA-P-TP	dGTP	dATP	dCTP	dTTP
None	---	---	33.4 ± 1.9	38.6 ± 1.5	29.4 ± 1.8	78.6 ± 1.3
3'-azido-ddG	20.8 ± 2.8	no peak	35.3 ± 5.9	40.0 ± 3.3	31.5 ± 4.2	76.3 ± 8.0
3'-azido-2,6-DA-P	23.3 ± 5.9 [b]	0.05 ± 0.03	28.2 ± 1.2	36.0 ± 0.5	27.4 ± 1.0	71.6 ± 2.9
RS-788	11.4 ± 2.2 [b]	27.0 ± 18	23.8 ± 0.8	18.4 ± 0.7	16.1 ± 0.5	70.9 ± 4.3

[a] Values are means ± standard deviations from triplicate experiments performed as described in the Materials and Methods.
[b] The actual concentration of 3'-azido-ddG-TP in cells treated with either 3'-azido-2,6-DA-P or RS-788 could be lower than reported due to interfering signal from 3'-azido-2,6-DA-P-TP in the LC-MS/MS analyses.

dGTP, dATP, and dCTP (but not dTTP) nucleotide pools. This is presumably due to competition for host nucleoside/nucleotide phosphorylating enzymes. These data show that RS-788 is efficiently metabolized in P4/R5 cells to both 3'-azido-2,6-DA-P-TP and 3'-azido-ddG-TP, two structurally distinct active NRTI-TP metabolites that are recognized by HIV-1 RT as adenosine- and guanosine-analogs, respectively.

6.5.2 Antiviral activity of 3'-azido-2,6-DA-P, 3'-azido-ddG, and RS-788 against WT and NRTI-resistant HIV-1

The activities of 3'-azido-2,6-DA-P, 3'-azido-ddG, and the 3'-azido-2,6-DA-P-prodrug RS-788 against WT HIV-1 replication were determined in P4/R5 cells **(Table 6.3)**. The anti-HIV-1 activity of AZT was also examined as a control. RS-788 potently inhibited WT HIV-1 replication with an EC_{50} value of 0.12 µM. RS-788 had similar potency as AZT (EC_{50} against WT = 0.13 µM) against WT HIV-1 and was approximately 10-fold more potent than 3'-azido-ddG and 3'-azido-2,6-DA-P that showed EC_{50} values of 1.1 µM and 1.2 µM, respectively. The phenotypic cross-resistance of a broad panel of NRTI-resistant HIV-1 to 3'-azido-2,6-DA-P, 3'-azido-ddG, and RS-788 was also examined in P4/R5 cells **(Table 6.3, Figure 6.3)**.

As described above, 3'-azido-2,6-DA-P was almost entirely converted to 3'-azido-ddG-TP in P4/R5 cells. Therefore, it was expected that 3'-azido-2,6-DA-P and 3'-azido-ddG would demonstrate similar activity against each virus. The data confirm that there was no statistically significant difference between the activities of 3'-azido-2,6-DA-P and 3'-azido-ddG against any virus examined. RS-788 potently inhibited the replication of every virus examined with EC_{50} values between 0.05 µM and 0.28 µM **(Table 6.3)**.

Table 6.3 Antiviral activity of RS-788, 3'-azido-2,6-DA-P, and 3'-azido-ddG against WT and NRTI-resistant HIV-1 in P4/R5 cells.

Virus	NRTI			
	RS-788	3'-azido-2,6-DA-P	3'-azido-ddG	AZT
WT				
EC50 (μM)	0.12 ± 0.06 [a]	1.2 ± 0.3	1.1 ± 0.5	0.13 ± 0.06
M184V				
EC50 (μM)	0.05 ± 0.03	0.8 ± 0.6	0.87 ± 0.3	0.10 ± 0.06
Fold-R [b]	0.4 b	0.7	0.8	0.8
L74V				
EC50 (μM)	0.07 ± 0.02	1.4 ± 0.4	1.6 ± 0.7	0.16 ± 0.06
Fold-R	0.6	1.2	1.5	1.2
K65R				
EC50 (μM)	0.11 ± 0.07	2.2 ± 0.7	2.3 ± 0.8	0.16 ± 0.06
Fold-R	0.9	1.8	2.1	1.3
AZT3				
41L/210W/215Y				
EC50 (μM)	0.19 ± 0.02	2.7 ± 0.5	3.0 ± 0.9	2.9 ± 0.06
Fold-R	1.6	2.3	2.8	23
AZT2				
67N/70R/215F/219Q				
EC50 (μM)	0.27 ± 0.07	3.7 ± 0.7	3.1 ± 1.1	11.1 ± 0.06
Fold-R	2.3	3.2	3.0	88
AZT7				
41L/67N/70R/215F/219Q				
EC50 (μM)	0.27 ± 0.05	6.0 ± 0.8	4.2 ± 0.1	>90
Fold-R	2.3	5.1	4.0	>714
AZT9				
41L/67N/70R/210W/215Y/219Q				
EC50 (μM)	0.25 ± 0.09	3.9 ± 1.3	3.8 ± 0.4	>90
Fold-R	2.1	3.3	3.6	>714
69SSS				
41L/69SSS/210W/215Y				
EC50 (μM)	0.44 ± 0.15	11.2 ± 5.2	8.7 ± 3.8	>90
Fold-R	3.7	9.5	8.3	>714
$Q151M_c$				
62V/75I/77L/116Y/151M				
EC50 (μM)	0.28 ± 0.07	26.6 ± 10	27.3 ± 7.3	>90
Fold-R	2.3	22.6	26	>714

[a] Values represent the EC_{50} means ± standard deviations determined from 3-4 independent experiments.
[b] Values represent fold-change (Fold-R) compared to WT HIV-1.

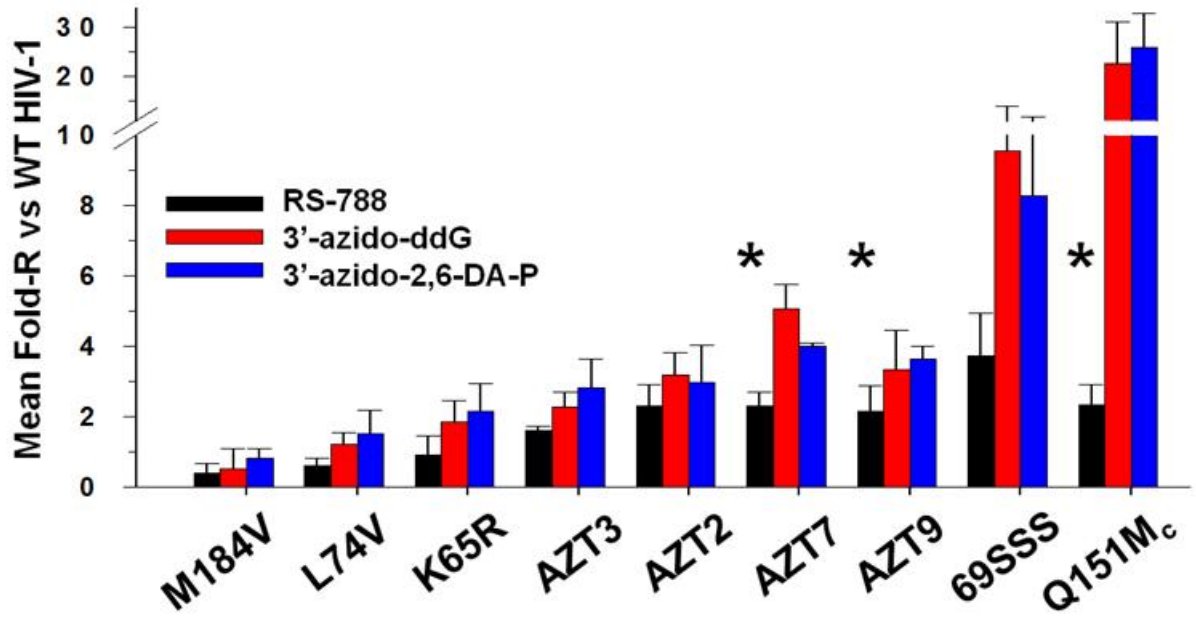

Figure 6.3 Fold-change in the susceptibility of NRTI-resistant HIV-1 to RS-788, 3'-azido-2,6-DA-P, and 3'-azido-ddG compared to WT HIV-1.
Bars represent the mean fold-resistance values ± standard deviations of drug-resistant HIV-1 compared to WT HIV-1 calculated from EC_{50} values determined from 3-4 independent experiments. Asterisks indicate p-value <0.05 compared to 3'-azido-ddG.

HIV-1 containing the NRTI discrimination mutation M184V was slightly more susceptible to inhibition by 3'-azido-2,6-DA-P and 3'-azido-ddG than WT virus and the L74V and K65R mutations conferred only low level resistance (up to 2.1-fold over WT) to 3'-azido-2,6-DA-P and 3'-azido-ddG **(Figure 6.3)**. Similarly, the M184V and L74V mutations conferred hypersusceptibility to RS-788 with fold-resistance values of 0.4 and 0.6, respectively, compared to WT virus. RS-788 inhibited HIV-1 containing the K65R discrimination mutation to a similar degree as WT virus. Viruses containing 3 to 6 TAMs showed decreased susceptibility to 3'-azido-2,6-DA-P and 3'-azido-ddG with fold-resistance values between 2.3-fold and 5.1-fold as compared to WT HIV-1 (**Table 6.3, Figure 6.3**). The same TAM-containing viruses were less resistant to inhibition by RS-788 with fold-resistance values between 1.6- and 2.3-fold relative to

WT HIV-1. Resistance to 3'-azido-2,6-DA-P, 3'-azido-ddG and RS-788 conferred by TAMs generally increased with increasing number of TAMs present in the virus.

Importantly, RS-788 was substantially more potent than 3'-azido-2,6-DA-P or 3'-azido-ddG against viruses harboring the Q151M complex or 69-insertion multi-NRTI resistance combinations **(Table 6.3, Figure 6.3)**. Against HIV-1 with the Q151M complex, the potency of RS-788 was decreased relative to that of WT virus only 2.3-fold (EC_{50} = 0.28 µM), whereas that of 3'-azido-2,6-DA-P (EC_{50} = 26.6 µM) and 3'-azido-ddG (EC_{50} = 27.3 µM) were decreased 23- and 26-fold, respectively. Similarly, the potency of RS-788 against HIV-1 with the 69-insertion mutations (EC_{50} = 0.44 µM) was decreased from that of WT virus 3.7-fold compared to 9.5- and 8.3-fold for 3'-azido-2,6-DA-P (EC_{50} = 11.2 µM) and 3'-azido-ddG (EC_{50} = 8.7 µM). Taken together, these data show that RS-788 has superior activity and a better cross-resistance profile than 3'-azido-2,6-DA-P or 3'-azido-ddG.

6.5.3 Inhibition of HIV-1 RT DNA synthesis by combinations of 3'-azido-2,6-DA-P-TP and 3'-azido-ddG-TP

As described in the previous chapter, the inhibition of WT and NRTI-resistant HIV-1 RT DNA synthesis by 3'-azido-2,6-DA-P-TP and 3'-azido-ddG-TP has been extensively characterized. These data however, do not fully explain the exceedingly superior activity of RS-788, compared to 3'-azido-2,6-DA- or 3'-azido-ddG, against multi-drug-resistant HIV-1 containing the Q151M complex or 69-insertion mutations. First, 3'-azido-2,6-DA-P-TP was significantly less potent than 3'-azido-ddG-TP against the Q151M complex RT with IC_{50} values of 4.2 µM and 0.3 µM, respectively (**Table 5.2**). Secondly, 3'-azido-2,6-DA-P-MP was a better substrate than 3'-azido-ddG-MP for excision by M41L/L210W/T215Y RT (data not shown). Therefore, the potent

inhibition of drug-resistant HIV-1 by RS-788 may be due to an alternate mechanism, such as incorporation and chain termination at both T and C positions by 3'-azido-2,6-DA-P-TP and 3'-azido-ddG-TP, respectively. To evaluate this hypothesis, we examined inhibition of WT, $Q151M_c$, and 69-insertion RT DNA synthesis by 3'-azido-2,6-DA-P and 3'-azido-ddG alone and in combination.

Steady-state RT DNA synthesis was evaluated in the presence of increasing concentrations of total NRTI-TP at three fixed-ratio combinations of 3'-azido-2,6-DA-P-TP:3'-azido-ddG-TP. The 3'-azido-2,6-DA-P-TP:3'-azido-ddG-TP ratios of 2.4:1 and 1.1:1 were chosen because these are the intracellular molar ratios of 3'-azido-2,6-DA-P-TP:3'-azido-ddG-TP detected in PBMC and P4/R5 cells, respectively. A third, experimental ratio, of 1:3 3'-azido-2,6-DA-P-TP:3'-azido-ddG-TP was also included for comparison. RT-mediated DNA synthesis was monitored by the incorporation of either [α-^{32}P]dATP or [α-^{32}P]dGTP radionucleotide, which compete with 3'-azido-2,6-DA-P-TP or 3'-azido-ddG-TP for RT incorporation, respectively. Consequently, one set of experiments used [α-^{32}P]dATP as the reporter nucleotide and a second set of experiments used [α-^{32}P]dGTP as the reporter nucleotide. Furthermore, experiments were performed in the absence and presence of 3 mM ATP to assess the effect of a functional excision mechanism on inhibition of DNA synthesis by 3'-azido-2,6-DA-P-TP and 3'-azido-ddG-TP alone and in combination.

The IC_{50} of single drug or total drug, calculated using Compusyn Software from median-effect plots (described in the Materials and Methods), are reported in **Table 6.4**. The IC_{50} values for inhibition of WT RT of 3'-azido-2,6-DA-P-TP and 3'-azido-ddG-TP were 0.86 μM and 1.2 μM, respectively when [α-^{32}P]dATP was used as the reporter, and 2.3 μM and 0.28 μM, respectively when [α-^{32}P]dGTP was used as the reporter.

Table 6.4 Inhibition of steady state WT, T69SSS, and Q151Mc RT DNA synthesis by 3'-azido-2,6-DA-P-TP, 3'-azido-ddG-TP, and their combinations.

	IC_{50} (μM) against HIV-1 RT DNA Synthesis [b]					
drug/ combination [a]	[α-^{32}P]dATP			[α-^{32}P]dGTP		
	WT	T69SSS	Q151M$_c$	WT	T69SSS	Q151M$_c$
3'-azido-2,6-DA-P -TP	0.86 ± 0.1	1.1 ± 0.2	3.0 ± 1.7	2.3 ± 0.8	3.7 ± 1.0	15 ± 2.8
3'-azido-ddG-TP	1.2 ± 0.8	3.4 ± 0.2	2.4 ± 0.9	0.28 ± 0.04	0.35 ± 0.02	1.2 ± 0.2
P4R5 (2.4:1)	0.55 ± 0.02	0.71 ± 0.03	2.4 ± 0.3	0.61 ± 0.1	0.71 ± 0.2	2.4 ± 0.6
PBM (1.1:1)	0.51 ± 0.1	0.70 ± 0.2	1.9 ± 0.7	0.41 ± 0.2	0.58 ± 0.2	1.6 ± 0.4
1:3	0.70 ± 0.1	0.90 ± 0.2	2.7 ± 0.4	0.27 ± 0.02	0.43 ± 0.1	0.96 ± 0.2
	IC_{50} (μM) against HIV-1 RT DNA Synthesis with Excision [c]					
drug/ combination	[α-^{32}P]dATP			[α-^{32}P]dGTP		
	WT	T69SSS	Q151M$_c$	WT	T69SSS	Q151M$_c$
3'-azido-2,6-DA-P -TP	1.6 ± 0.4	5.1 ± 1.0	11 ± 2.7	4.2 ± 0.7	48 ± 13.2	30 ± 8.5
3'-azido-ddG-TP	1.4 ± 0.4	53 ± 8.0	7.8 ± 0.4	0.33 ± 0.1	1.0 ± 0.1	1.7 ± 0.3
P4R5 (2.4:1)	0.71 ± 0.1	3.6 ± 1.3	3. 6 ± 1.0	0.64 ± 0.1	2.4 ± 0.5	2.9 ± 0.7
PBM (1.1:1)	0.73 ± 0.1	4.9 ± 0.3	3.3 ± 1.4	0.45 ± 0.1	1.6 ± 0.4	2.1 ± 0.5
1:3	0.71 ± 0.1	5.9 ± 0.7	2.8 ± 0.9	0.34 ± 0.02	1.4 ± 0.4	1.8 ± 0.2

[a] Drug combinations are displayed as the ratio 3'-azido-2,6-DA-P-TP:3'-azido-ddG-TP.
[b] Values are the mean 50% inhibitory concentration (IC_{50}) of single drugs or total drug for combinations ± standard deviations from at least 3 independent experiments. IC_{50} values were calculated from median-effect plots using CompuSyn Software.
[c] Experiments of DNA synthesis with a functional excision mechanism included 3 mM ATP.

6.5.4 Median-effect analysis indicates synergistic inhibition of RT DNA synthesis by 3'-azido-2,6-DA-P-TP+3'-azido-ddG-TP combinations

We first analyzed inhibition of RT DNA synthesis with a combination of 3'-azido-2,6-DA-P-TP and 3'-azido-ddG-TP, using the median-effect principal of Chou and Talalay (300). Median-effect analysis indicates the degrees of synergy or antagonism by a combination index (CI) value, where CI values < 1 indicate synergy, CI value = 1 indicate an additive effect, and CI values > 1 indicate antagonism. The average CI values determined from the 50%, 75%, 90%, and 95% inhibition levels are reported in **Table 6.5** and plots of the CI value versus fraction affected (*f*a, inhibition level) are shown in **Figure 6.4**.

Combinations of 3'-azido-2,6-DA-P-TP+3'-azido-ddG-TP demonstrated moderately synergistic inhibition of WT RT with the P4/R5 (2.4:1) and PBM cell (1.1:1) ratios, regardless of which reporter radionucleotide was used. Interestingly, the 1:3 experimental 3'-azido-2,6-DA-P-TP: 3'-azido-ddG-TP ratio (i.e. an arbitrary ratio not observed in cells) demonstrated slightly lower synergy for inhibition of WT RT when either reporter radionucleotide was used. Importantly against T69SSS RT, strong synergy was indicated by each of the three 3'-azido-2,6-DA-P-TP+3'-azido-ddG-TP combinations when [α-^{32}P]dATP was used (CI values = 0.72, 0.63, and 0.63 for the P4/R5 cell, PBM cell, and experimental ratios, respectively). Synergy was also indicated for the P4/R5 ratio 3'-azido-2,6-DA-P-TP+3'-azido-ddG-TP combination against T69SSS when [α-^{32}P]dGTP was used but weaker synergy was observed for the other two ratios. For inhibition of Q151M$_c$ RT, strong synergy was only indicated for combinations in the P4/R5 and PBM cell ratios with the [α-^{32}P]dGTP reporter. All other 3'-azido-2,6-DA-P-TP+3'-azido-ddG-TP combinations were additive for inhibition of Q151M$_c$ RT.

Table 6.5 Average combination index (CI) values for inhibition of WT, T69SSS, and Q151M$_c$ RT DNA synthesis by combinations of 3'-azido-2,6-DA-P-TP+3'-azido-ddG-TP.

	HIV-1 RT DNA Synthesis					
	[α-^{32}P]dATP			[α-^{32}P]dGTP		
RT	P4R5 (2.4:1) [a]	PBM (1.1:1)	1:3	P4R5 (2.4:1)	PBM (1.1:1)	1:3
WT	0.79 ± 0.2 [b]	0.73 ± 0.2	0.86 ± 1.0	0.69 ± 0.11	0.75 ± 0.02	0.92 ± 0.2
T69SSS	0.72 ± 0.1	0.63 ± 0.2	0.63 ± 0.1	0.65 ± 0.11	0.77 ± 0.08	0.93 ± 0.02
Q151M$_c$	1.1 ± 0.3	1.0 ± 0.1	1.2 ± 0.4	0.61 ± 0.04	0.73 ± 0.01	1.1 ± 0.4
	HIV-1 RT DNA Synthesis with Excision [c]					
	[α-^{32}P]dATP			[α-^{32}P]dGTP		
RT	P4R5 (2.4:1)	PBM (1.1:1)	1:3	P4R5 (2.4:1)	PBM (1.1:1)	1:3
WT	0.50 ± 0.1	0.51± 0.1	0.53 ± 0.1	0.59 ± 0.04	0.61 ± 0.04	0.68 ± 0.1
T69SSS	0.68 ± 0.2	0.74 ± 0.04	1.3 ± 0.4	0.51 ± 0.1	0.23 ± 0.02	0.09 ± 0.02
Q151M$_c$	0.48 ± 0.2	0.47 ± 0.2	0.55 ± 0.3	0.47 ± 0.1	0.52 ± 0.02	0.67 ± 0.1

[a] Drug combinations are displayed as the ratio of 3'-azido-ddG-TP-TP:3'-azido-ddG-TP.
[b] Data are the average CI values from the 50%, 75%, 90%, and 95% inhibition levels. Data are the means ± standard deviations from least 3 independent experiments.
[c] Experiments of DNA synthesis with a functional excision mechanism included 3 mM ATP.

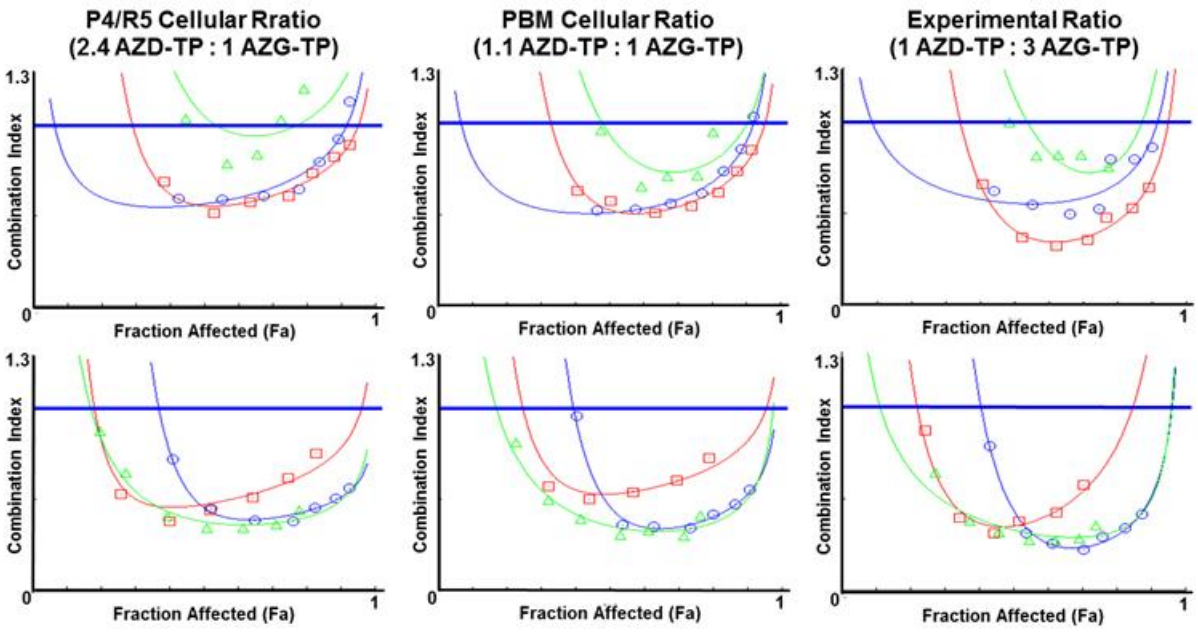

Figure 6.4 Fraction-affected versus combination index plots for 3'-azido-2,6-DA-P-TP+3'-azido-ddG-TP combinations.
The Fa-CI plots for inhibition of WT (blue circles), T69SSS (red squares), and Q151M$_c$ (green triangles) HIV-1 RT DNA synthesis in the absence (top panels) and presence (bottom panels) of nucleotide excision. The blue line at CI = 1 represents additive effect. Data are the means of 3 independent experiments using [α-^{32}P]dATP. The excision mechanism (bottom panels) was facilitated by the addition of 3 mM ATP.

For reactions in which ATP was included to facilitate NRTI-MP excision, every combination, regardless of which reporter radionucleotide was used, demonstrated strong or very strong synergy for inhibition of WT, T69SSS, and Q151M$_c$ RT (the one exception was the 1:3 3'-azido-2,6-DA-P-TP:3'-azido-ddG-TP combination with the [α-^{32}P]dATP reporter). The CI values for all 3'-azido-2,6-DA-P-TP+3'-azido-ddG-TP combinations from assays with a functional excision mechanism (i.e. ATP included) were almost always lower than those of the same combination for assays without ATP, although these were not statistically significant.

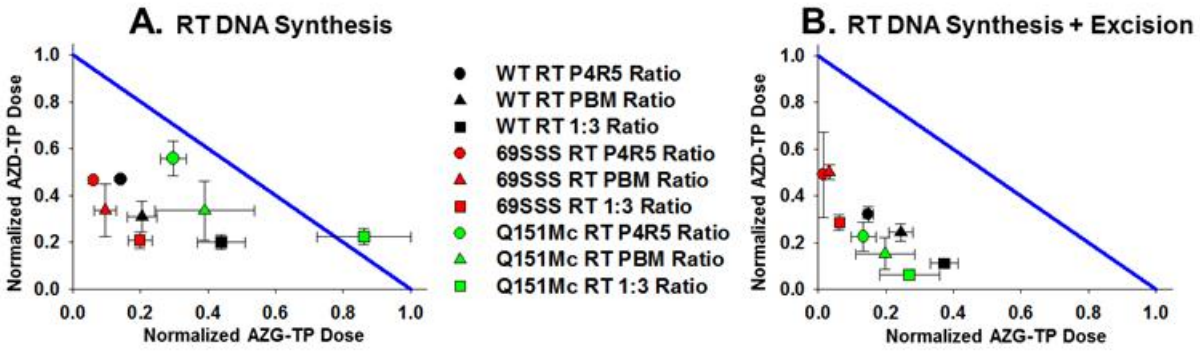

Figure 6.5 Normalized 50% effect isobolograms for of 3'-azido-ddG-TP-TP+3'-azido-ddG-TP combinations.
The plots show the ratios observed in P4R5 cells (2.4:1, circles), PBM cells (1.1:1, triangles), and a 1:3 ratio (squares) against WT (black symbols), 69SSS (red symbols), and $Q151M_c$ (green symbols) HIV-1 RT in the absence (A) and presence (B) of nucleotide excision. The diagonal blue line indicates additivity where data points below the line indicate synergy and data points above the line indicate antagonism. Data are the means ± standard deviations of three independent experiments obtained using [α-^{32}P]dATP.

6.5.5 Normalized isobologram plots indicate synergistic inhibition of RT DNA synthesis by 3'-azido-2,6-DA-P-TP+3'-azido-ddG-TP combinations

In order to eliminate bias based on the synergy analysis method, we also plotted normalized isobolograms from the same inhibition dataset. Isobologram analysis is a graphical approach to synergy determination that has been used since the eighteenth century as a time-tested and widely accepted method (301). Isobolograms are created by plotting the normalized doses of drug 1 and drug 2 on the x- and y-axes, respectively. A diagonal line connecting the points (0,1) and (1,0) is the line of additivity. Data points for combinations below the line are synergistic and those above the line are antagonistic. The isobolograms (**Figure 6.5**) showed that most combinations of 3'-azido-2,6-DA-P-TP+3'-azido-ddG-TP were synergistic for inhibition of WT, T69SSS, and $Q151M_c$ RT DNA synthesis, regardless of which reporter radionucleotide was used. The relative degree of synergy from isobolograms can be indicated as an average deviation

Table 6.6 Normalized 50% effect average deviation from additivity (ADA) values of 3'-azido-2,6-DA-P-TP+3'-azido-ddG-TP combinations against WT, 69SSS, and Q151M$_c$ RT DNA synthesis.

HIV-1 RT DNA Synthesis						
RT	[α-^{32}P]dATP			[α-^{32}P]dGTP		
	P4R5 (2.4:1) [a]	PBM (1.1:1)	1:3	P4R5 (2.4:1)	PBM (1.1:1)	1:3
WT	-0.39 [b,c]	-0.49	-0.36	-0.18*	-0.21*	-0.25*
T69SSS	-0.47	-0.57	-0.59	-0.26*	-0.13*	-0.04*
Q151M$_c$	-0.14*	-0.27	0.09*	-0.28*	-0.28*	-0.36*
HIV-1 RT DNA Synthesis With Excision [d]						
RT	[α-^{32}P]dATP			[α-^{32}P]dGTP		
	P4R5 (2.4:1)	PBM (1.1:1)	1:3	P4R5 (2.4:1)	PBM (1.1:1)	1:3
WT	-0.53	-0.51	-0.52	-0.32*	-0.28*	-0.2*
T69SSS	-0.49*	-0.46*	-0.65*	-0.28*	-0.23*	0.04*
Q151M$_c$	-0.64	-0.65	-0.67	-0.44*	-0.38*	-0.2*

[a] Drug combinations are displayed as the ratio of 3'-azido-ddG-TP-TP:3'-azido-ddG-TP.
[b] Data are the ADA values calculated as described in the Materials and Methods where $N \geq 3$ independent experiments.
[c] All values were statistically significant as determined by one-tailed homoscedastic T-tests.
[d] Assays of DNA synthesis with a functional excision mechanism included 3 mM ATP.
*Indicates $p < 0.05$, all other values $p < 0.01$.

from additivity (ADA) value, which is a calculation of the statistical distance of a combination data point from the additivity line (302). As long as the values are statistically significant (p-value < 0.05), negative ADA values indicate synergy and lower values indicate stronger synergy. The ADA values for 3'-azido-2,6-DA-P-TP+3'-azido-ddG-TP combinations are presented in **Table 6.6**. The ADA values for every 3'-azido-2,6-DA-P-TP+3'-azido-ddG-TP combination were statistically significant and most combinations displayed synergy for inhibition of DNA synthesis WT, T69SSS, and Q151M$_c$ RTs. Moreover, the degrees of synergy indicated by the isobologram ADA values and the median effect CI values are ostensibly identical, thus demonstrating good concordance between the two synergy analysis methods.

6.6 DISCUSSION

Our intracellular pharmacology studies show that RS-788, a novel phosphoramidate prodrug of 3'-azido-2,6-DA-P, is metabolized in P4/R5 cells to both 3'-azido-2,6-DA-P-TP and 3'-azido-ddG-TP, whereas 3'-azido-2,6-DA-P and 3'-azido-ddG are both converted to 3'-azido-ddG-TP as the major active metabolite. This pattern of intracellular metabolism in P4/R5 cells is consistent with RS-788 intracellular metabolism in PBM cells (254, 255). Of note, RS-788 incubation resulted in the intracellular delivery of the same amount of total nucleotide-TP (38 × 10^6 pmol/million cells 3'-azido-2,6-DA-P-TP/3'-azido-ddG-TP) to both P4/R5 cells and PBM cells. 3'-azido-2,6-DA-P, however, was metabolized 2.5-fold less efficiently to 3'-azido-ddG-TP/3'-azido-2,6-DA-P-TP in P4/R5 cells (23 × 10^6 pmol/million cells) compared to PBM cells (58 × 10^6 pmol/million cells). Additionally, the reduction of natural dATP and dGTP pools in cells treated with RS-788 would presumably decrease the competition for 3'-azido-2,6-DA-P-TP

and 3’-azido-ddG-TP incorporation by HIV-1 RT, which may be one mechanism responsible for the increased potency of RS-788. The prodrug RS-788 delivers two chemically distinct metabolites, 3’-azido-ddG-TP and 3’-azido-2,6-DA-P-TP, each of which are potent HIV-1 RT chain terminators that are incorporated opposite different complementary bases (cytosine for 3’-azido-ddG-TP and thymine for 3’-azido-2,6-DA-P-TP). The intracellular delivery of 2 different chain terminating nucleotides from one parent prodrug has not been previously achieved.

Next we characterized the antiviral activity and phenotypic cross-resistance profile of RS-788 against a broad panel of NRTI-resistant HIV-1. RS-788 exhibited 10-fold more potent activity against WT HIV-1 replication than its parent analogs 3’-azido-2,6-DA-P and 3’-azido-ddG. Furthermore, HIV-1 viruses carrying discrimination mutations were hypersusceptible or similarly susceptible as WT virus to RS-788 and HIV-1 containing multiple TAMs was only marginally decreased (2.3-fold) to RS-788 potency compared to WT HIV-1. RS-788 also had remarkable activity against multi-NRTI-resistant HIV-1compared to its parent analogs 3’-azido-2,6-DA-P and 3’-azido-ddG. Against HIV-1 with the Q151M complex, the potency of RS-788 was decreased relative to that of WT virus only 2.3-fold (EC_{50} = 0.28 μM), whereas that of 3’-azido-2,6-DA-P (EC_{50} = 26.6 μM) and 3’-azido-ddG (EC_{50} = 27.3 μM) were decreased 23- and 26-fold, respectively. Similarly, the potency of RS-788 against HIV-1 with the 69-insertion mutations (EC_{50} = 0.44 μM) was decreased from that of WT virus 3.7-fold compared to 9.5- and 8.3-fold for 3’-azido-2,6-DA-P (EC_{50} = 11.2 μM) and 3’-azido-ddG (EC_{50} = 8.7 μM). Taken together, these date show that RS-788 has a far superior activity and cross-resistance profile than 3’-azido-2,6-DA-P or 3’-azido-ddG.

The excellent activity of RS-788 against multi-NRTI-resistant HIV-1 could not be fully explained by structure-activity studies of purified RT described in the previous chapter because:

1) 3'-azido-2,6-DA-P-TP is less potent than 3'-azido-ddG-TP against the Q151M complex RT; and 2) 3'-azido-2,6-DA-P-MP is a better substrate than 3'-azido-ddG-MP for excision by M41L/L210W/T215Y RT. Consequently, we hypothesized that inhibition of drug resistant HIV-1 by RS-788 is due to an alternate mechanism, such as incorporation and chain termination at both T and C positions by 3'-azido-2,6-DA-P-TP and 3'-azido-ddG-TP, respectively. To evaluate this hypothesis, we performed DNA synthesis assays with WT and multi-NRTI-resistant RT in the presence of combinations of 3'-azido-2,6-DA-P-TP+3'-azido-ddG-TP. Drug synergy analyses by both the median-effect and normalized isobologram methods indicated synergistic inhibition of HIV-1 RT DNA synthesis by combinations of 3'-azido-2,6-DA-P-TP+3'-azido-ddG-TP at the intracellular molar ratios detected in P4/R5 and PBM cells. Moderate synergy was indicated for inhibition of WT and 69-insertion HIV-1 RT DNA synthesis, whereas weak synergistic or additive inhibition was seen against $Q151M_c$ RT. Furthermore, the excision mechanism conferred by TAMs does not diminish the observed synergy. Taken together our data demonstrate that the combined intracellular delivery of 3'-azido-2,6-DA-P-TP and 3'-azido-ddG-TP by RS-788 provides synergistic inhibition of reverse transcription by NRTI-resistant RT. These findings help explain the superior activity of RS-788, compared to its parent analogs 3'-azido-2,6-DA-P and 3'-azido-ddG, against highly NRTI-resistant HIV-1.

7.0 SUMMARY AND FINAL DISSCUSSION

Combination antiretroviral therapy, commonly containing two or more NRTI, suppresses HIV-1 replication and reduces patient morbidity and mortality (36). However, the effectiveness of the currently FDA approved NRTI is limited by the rapid selection of drug-resistant viral variants that are often cross-resistant to other NRTI (242). Therefore, there is a critical need to develop novel NRTI that show little or no cross-resistance with existing NRTI. To address this need, our research group adopted a rational drug design approach using mechanistic knowledge of how NRTI structural components affect activity against drug-resistant RT to direct the synthesis of novel analogs with improved activity against NRTI-resistant viral variants.

Shortly before this work began, Sluis-Cremer et al. and Parikh et al. described the initial structure-activity-resistance relationships that identified the 3'-azido-2',3'-dideoxypurines as lead class of novel NRTI that demonstrate excellent activity against NRTI-resistant HIV-1 (141, 212). Specifically, 3'-azido-ddG potently inhibited replication of HIV-1 containing the discrimination mutations K65R, L74V, and M184V, and against HIV-1 containing excision enhancing TAMs (172). Furthermore, 3'-azido-ddG had good specificity for inhibition of HIV-1 RT with minimal toxicity in multiple cell lines and showed a low potential for mitochondrial toxicity or bone marrow depletion.

The research presented in this dissertation sought to expand on this work by investigating the structure-activity-resistance relationships for: i) two novel *nucleotide* analogs, PMEO-DAPym and GS-9148; and ii) base-modified-3'-azido-2',3'-dideoxypurine *nucleoside* analogs.

i) PMEO-DApym and GS-9148 are both novel structural analogs of the NtRTI TFV. Preliminary studies showed that both PMEO-DAPym and GS-9148 had improved activity compared to TFV against clinical HIV-1 isolates containing discrimination mutations and those containing TAMs (262, 263). Additionally, cell culture selection experiments with GS-9148 yielded resistant variants with the novel combination of resistance mutations K70E/D123N/T165I that are not selected by other NRTI and are infrequently observed in treatment-naïve and treatment-experience patients (268). The encouraging activity and resistance phenotypes of each of these novel analogs warranted a detailed characterization of the molecular mechanisms of WT and NRTI-resistant RT inhibition.

ii) Given that natural base identity can influence NRTI activity towards drug-resistant RT, it is expected that base modification will also impact NRTI activity. However, the molecular interactions of base-modified analogs with WT or NRTI-resistant HIV-1 RT have not been extensively studied. Accordingly, we synthesized a series of novel base modified 3′-azido-2′,3′-dideoxypurine analogs (143). The specific molecular interactions of these analogs with HIV-1 RT were characterized in order to identify base modifications that may further improve 3′-azido-2′,3′-dideoxypurine activity against NRTI-resistant HIV-1.

The running hypothesis of the work in this dissertation was that acquiring specific knowledge of how NRTI structural components (such as base and sugar/pseudosugar) influence NRTI activity against WT and NRTI resistant RT, will inform the rational design and development of new analogs that demonstrate excellent activity and resistance properties. This

hypothesis was investigated in the context of the novel nucleotide and nucleoside reverse transcriptase inhibitors described above. The concluding chapter will summarize the important structure-activity-resistance findings from this research and highlight how they may influence future antiretroviral research and development.

7.1 PMEO-DAPym: A PURINE DISGUISED AS A PYRIMIDINE

The novel acyclic nucleoside phosphonate PMEO-DAPym differs structurally from the prototype analog TFV in both the pseudosugar and base components (261). With PMEO-DAPym a 2,6-diamino-pyrimidine base is linked to an ethoxy pseudosugar at the C6-ring position, whereas, with TFV the purine base (i.e. adenine) is linked to a propoxy pseudosugar at the traditional N-9 ring position. Using a combination of steady-state and transient kinetic RT DNA synthesis and molecular modeling analyses we characterized the molecular interactions between the active sites of WT and NRTI-resistant RT and PMEO-DAPym-DP.

We show that PMEO-DAPym-DP acts as a purine analog mimetic in that it is recognized by HIV-1 RT as an adenosine analog and specifically incorporated across from thymine in DNA templates or uracil in RNA templates. The 2,6-diamino-base substitutions and the novel linker position allow the PMEO-DAPym pyrimidine base to mimic an incomplete purine ring. Molecular modeling studies show that PMEO-DAPym-DP forms a similar base pairing interaction with thymine and assumes a similar conformation in the active site HIV-1 RT as TFV-DP. Our studies provide the first demonstration that a pyrimidine nucleotide analog can be selectively recognized as an adenine nucleotide derivative for binding and incorporation into the growing DNA chain by HIV-1 RT. It appears as though the molecular mimicry of an adenine

base by PMEO-DAPym is important for recognition by HIV-1 RT because the PME-pyrimidine derivatives (same ethoxy linker but the pyrimidine base linkage is at the traditional N-1 position) do not possess antiviral activity (274, 280). PMEO-DAPym-DP was also recognized as adenosine and incorporated across from thymine by human DNA polymerase α.

Although TFV and PMEO-DAPym are both recognized as adenosine, the efficiency with which PMEO-DAPym and TFV can be incorporated or excised across from thymine by WT and drug-resistant RT differs. HIV-1 RT containing the K65R mutation incorporated PMEO-DAPym-DP 3-fold more efficiently than TFV. Additionally, PMEO-DAPym-MP was a less efficient substrate than TFV-MP for ATP-mediated excision by RT containing TAMs. These divergent resistance characteristics may make it more difficult for the virus to escape drug pressure and may eventually exert lower phenotypic drug resistance levels. This is supported by lower phenotypic resistance of HIV-1 clinical isolates in cell culture for PMEO-DAPym compared to TFV (262). Additional studies, such as cell culture selection experiments and phenotypic cross-resistance analysis, should be performed for PMEO-DAPym to further elucidate the potential resistance advantages displayed by this nucleotide.

It is not known to what extent the differing pseudosugar linkers of PMEO-DAPym (i.e. ethoxy) and TFV (i.e. propoxy) affect the observed phenotypes. The PMPO-DAPym analog (i.e. identical DAPym base but with a propoxy linker like TFV) has slightly decreased activity against HIV-1 clinical isolates compared to PMEO-DAPym but its activity against NRTI-resistant HIV-1 or RT has not been thoroughly characterized (280). A direct structure-activity comparison of the incorporation and excision efficiencies of PMEO-DAPym and PMPO-DAPym could elucidate the specific role of the ethoxy and propoxy linkers.

The studies of PMEO-DAPym inhibition of HIV-1 RT and human DNA polymerases described here identify a novel substrate mimicry mechanism in which a base modified pyrimidine derivative can be recognized for incorporation by a polymerase as a purine analog. Using the PMEO-DAPym structure as a starting point, novel pyrimidine nucleotide analogs may be rationally designed to mimic incomplete purine ring systems. For example, PMEO-DAPym derivatives with 5-methyl, 5-bromo, and 5-Cl substitutions have been shown to inhibit HIV-1 replication but have not been thoroughly characterized (262). Ostensibly, these 5-position substitutions are compatible with adenine mimicry. Molecular comparisons of RT inhibition by the 5-modified derivatives and PMEO-DAPym, like those described in this work, would expand the structure-activity understanding of this nucleotide class. Other 2- and 4-position pyrimidine base substitutions (e.g. 2,4-dicarbonyl and combinations of amino-, carbonyl-, chloro-, bromo- modifications at each position) in the context of a C-6 sugar/pseudosugar may facilitate molecular mimicry of the guanine and hypoxanthine purine ring systems. In addition to base modifications, these DAPym derivatives can be linked at the C-6 position to other pseudosugar linker structures as well as natural and modified ribose and 2'-deoxyribose sugars in both the D and L conformations. These analogs should be evaluated for antiviral activity (against retroviruses and DNA viruses such as herpesviruses, poxviruses and hepatitis B virus), as potential antimetabolites in purine and pyrimidine nucleoside/nucleotide metabolism, and for activity toward other DNA and RNA polymerases.

7.2 GS-9148: SUGAR MODIFICATION LEADS TO DIVERGENT RESISTANCE MECHANISMS

Next, we used pre-steady state kinetic analyses to characterize the molecular mechanisms of discrimination resistance conferred by the previously unrecognized pattern of RT mutations, K70E/D123N/T165I which were selected by GS-9148, another investigational phosphonate NtRTI (268). GS-9148 and TFV both contain an adenine base and the same phosphonate structure but differ in their sugar/pseudosugar structure (263). TFV contains an acyclic propyl pseudosugar linker to the phosphonate, whereas GS-9148 contains a 2'-fluoro-3'-deoxy-2',3'-didehydroribose sugar linked to the phosphonate. Overall we observed low levels of resistance to GS-9148 by progressively increasing discrimination phenotypes towards GS-9148-DP by K70N, K70E, and K70E/D123N/T165I HIV-1 RT, respectively. The discrimination phenotype of K70E/D123N/T165I RT was driven by a 2.4-fold decrease in nucleotide binding affinity (K_d), compared to WT RT. This is contrary to the mechanism of resistance toward TFV-DP by RT containing the K65R or K70E mutations. Our studies and those in the literature showed that K65R and K70E resistance to TFV-DP is primarily due to decreased incorporation rate with little effect on nucleotide binding to the active site (160, 161). Furthermore, our results indicate that the K70E/D123N/T165I mutations confer resistance to GS-9148 and TFV by different mechanisms of discrimination between the natural nucleotide dATP and GS-9148 or TFV. Namely, GS-9148 showed deficits in both binding and incorporation rate compared to dATP, whereas TFV showed only a decreased incorporation rate in relation to dATP. The fact that GS-9148 and TFV, differing only in their sugar/pseudosugar structure, develop differing resistance mutations which confer resistance through different mechanisms reaffirms that nucleotide sugar is an important determinant for NtRTI resistance development.

The molecular mechanisms by which the K70E, D123N, and T165I mutations modulate the binding and rate of incorporation of GS-9148 are unknown. GS-9148 binding affinity is likely modulated through interactions of the RT active site residues with the GS-9148 modified sugar because decreased binding affinity was not observed for TFV or dATP, that contain the same base and phosphonate structures as GS-9148. The decreased rate of nucleotide incorporation for RT containing K70E has been attributed to destabilization of the nucleotide gamma phosphate modulated through the K65 residue (161, 211). A similar mechanism may be partially responsible in the case of GS-9148 incorporation rate deficits, however another mechanism must also be responsible since RT containing the D123N/T165I mutations alone also incorporated GS-9148 slower than dATP. Crystallization and/or molecular modeling studies could shed further light on the molecular basis of GS-9148 discrimination by this novel combination of mutations.

The K65R mutation, selected by TFV, and the K70E mutation are antagonistic to one another and are never found on the same genome (211). It would be interesting to examine whether significant phenotypic resistance could develop in the presence of both GS-9148 and TFV in cell culture selection studies. Additive or slightly synergistic anti-HIV-1 activity has already been demonstrated for the combinations of GS-9148 and TFV, and competition for activation by cellular enzymes was not observed for concentrations of TFV and GS-9148 combinations above those required for HIV-1 inhibition (290).

GS-9148 has a low potential for cross-resistance with existing NRTI due to its excellent activity against a broad panel of NRTI-resistant HIV-1 and the selection of a novel combination of infrequently observed resistance mutations (263, 268). Additionally, GS-9148 and its phosphonoamidate prodrug GS-9131 demonstrate favorable toxicity and pharmacokinetic

properties including a low potential for mitochondrial and renal toxicity, low possibility of pharmacokinetic interactions with other NRTI, and sufficient accumulation of active nucleotide triphosphate in lymphoid cells with a long intracellular half-life of 19 hours (263, 266, 290). These properties along with the novel mechanism of resistance described here suggest GS-9148 should be further evaluated as a clinical NRTI candidate.

7.3 BASE-MODIFIED ANALOGS OF 3'-AZIDO-2',3'-DIDEOXYGUANOSINE: SUBSTRATE MIMICRY

Applying the knowledge from Sluis-Cremer et al. that base identity, in the context of 3'-azido-2',3'-dideoxypurine NRTI, influences activity and resistance phenotypes we synthesized a series of novel 3'-azido-2',3'-dideoxypurine analogs with base modifications (141, 143). Five of these analogs, all with 6-position guanine base modifications, showed similar or greater anti-HIV-1 activity as 3'-azido-ddG in PBM cells. In the current work, we sought to expand the structure-activity-resistance profile of 3'-azido-2',3'-dideoxypurine NRTI through a mechanistic analysis of the activity of the 6-modified-3'-azido-2',3'-dideoxyguanosine analogs against WT and NRTI-resistant HIV-1 RT.

Steady state and transient kinetic RT DNA synthesis assays unexpectedly revealed that each of the 6-modified-3'-azido-ddG-TP analogs behaved as adenosine rather than guanosine mimetics for incorporation by HIV-1 RT across from thymine in DNA templates or uracil in RNA templates. The nature of the 6-modification, however, affected the efficiency of incorporation. In transient kinetic assays 3'-azido-2,6-DA-P-TP was incorporated by WT RT with similar efficiency as dATP (selectivity value versus dATP = 1.1). 3'-azido-6-CL-P-TP and

3’-azido-6-AA-P-TP were also efficiently incorporated into DNA by RT, however, were poor substrates for RT incorporation. Our molecular modeling analyses supported these results showing planer base pair interactions of the efficiently incorporated analogs with the template thymine. However, the poorly incorporated analogs, 3’-azido-6-DM-P-TP and 3’-azido-6-MX-P-TP, had altered base pair alignments, ostensibly due to steric clash of the branched 6-DM moiety and electronic incompatibility of the 6-MX group, respectively. The favorable base pair conformations seem to position the nucleotide α-phosphate for chemical reaction with the primer 3’-OH, whereas the α-phosphate is positioned further from the 3’-OH for analogs with misaligned bases. Furthermore, compared to the canonical A:T base pair (with two H-bonds), the additional hydrogen bond achieved by the 3’-azido-2,6-DA-P:thymine base pair may further stabilize the α-phosphate and explain the excellent catalytic efficiency observed in pre-steady-state assays.

The K65R, L74V and Q151M complex discrimination mutations conferred low levels of resistance to the 3’-azido-2’,3’-dideoxypurines, however, 6-position modification did not significantly affect the discrimination phenotype. The mutant HIV-1 RTs exhibited fold-resistance values to each of the 6-modified-3’-azido-ddGTP analogs that were similar (i.e. <2-fold) to the fold change in resistance values determined for 3’-azido-ddATP. The only statistically significant exceptions ($P<0.05$) included 3-azido-6-AA-P-TP and 3’-azido-2,6-DA-P-TP which exhibited better activity against K65R HIV-1 RT and M184V HIV-1 RT, respectively.

Assays of ATP-mediated excision revealed a different structure-activity relationship than that for 6-modified-3’-azido-ddG-TP incorporation. RT containing TAMs could unblock T/Ps chain-terminated with 3’-azido-ddAMP, 3’-azido-2,6-DA-P-MP, and 3’-azido-6- AA-P-MP. By

contrast, 3’-azido-6-Cl-P-MP, 3’-azido-6-MX-P-MP, and 3’-azido-6-DM-P-MP were poor substrates for ATP-mediated excision by RT containing TAMs. Consistent with the altered patterns of incorporation and excision observed in biochemical assays, our molecular models of the excision products of 6-modified-3’-azido-ddG analogs reveal different hydrogen bonding patterns than those observed in the models for nucleotide-TP incorporation. For example, 3’-azido-6-Cl-P-MP has lost a hydrogen bond in its excision model compared to the model for 3’-azido-6-Cl-P-TP incorporation. Together, these data suggest that the optimal conformation of the HIV-1 RT active site differs for the incorporation and excision reactions and further suggest that 6-position modifications differentially effect these two reactions. Therefore, our data support the hypothesis that it may be possible to rationally design new analogs that are efficiently incorporated by RT but poorly excised from blocked primers. For example, 3’-azido-6-Cl-P-TP is a relatively good substrate for incorporation, but it is not efficiently excised by either WT or TAM-containing HIV-1 RT. Analogs with these favorable but divergent qualities may exhibit more potent inhibition of drug-resistant HIV-1 replication, thus resulting in lower levels of phenotypic drug-resistance. Further optimization of these qualities might be achieved by structure-activity-resistance analyses of additional 3’-azido-2’-3’-dideoxypurine analogs modified at both the 2- and 6-positions of the purine ring system.

It remains to be seen whether the non-traditional base pair interactions observed with 6-position purine modifications would also facilitate efficient incorporation of NRTI with sugar structures other than 3’-azido-2’,3’-dideoxy-ribose. Synthesizing a series analogs containing the 6- modified-guanosine bases (especially the 2,6-DA-P base) with a diverse set of modified 2’,3’-didoxyribose sugars in order to more fully evaluate the antiviral benefits of this artificial base pair is tempting. Preliminary studies show that 3’-azido-2’-3’-dideoxypurine analogs are also

recognized as adenosine mimetics by human DNA polymerases suggesting the adenosine mimetic phenotype is not unique to incorporation by HIV-1 RT (unpublished, data not shown). Therefore, linking these modified bases to other sugars (such as ribose) may extend their activity to other polymerases (such as RNA polymerase).

7.4 RS-788: COMBINATION THERAPY FROM ONE PRODRUG?

Although, 3'-azido-2,6-DA-P-TP potently inhibited DNA synthesis by NRTI-resistant RT through incorporation and chain-termination as an adenosine analog in biochemical assays, it was extensively metabolized to 3'-azido-ddG in PBM and P4R5 cells (295, 296, CHAPTER FOUR). Therefore, the potent anti-HIV-1 activity of 3'-azido-2,6-DA-P is primarily attributed to RT inhibition by 3'-azido-ddG-TP and not due to incorporation of 3'-azido-2,6-DA-P-TP as an adenosine analog. In order to further improve 3'-azido-2,6-DA-P antiviral activity by increasing the intracellular delivery of its triphosphate form, we synthesized RS-788, a 5'-monophosphate prodrug of 3'-azido-2,6-DA-P-TP. Intracellular pharmacology studies in P4/R5 and PBM cells showed RS-788 is metabolized approximately 1:1 to both 3'-azido-2,6-DA-P-TP and 3'-azido-ddG-TP (295, 296, CHAPTER FOUR). Therefore, RS-788 delivers two structurally distinct active metabolites, each of which is a potent chain terminating inhibitor that is incorporated across from a different complementary base (thymine for 3'-azido-2,6-DA-P-TP and cytosine for 3'-azido-ddG-TP). The intracellular delivery of two different NRTI from a single prodrug has not been previously demonstrated.

In PBM cells, RS-788 was 60- and 17-fold more potent against WT HIV-1 replication than its parent analogs 3'-azido-ddG and 3'-azido-2,6-DA-P. RS-788 also demonstrated a far superior cross-resistance profile compared to 3'-azido-ddG and 3'-azido-2,6-DA-P against a broad panel of NRTI-resistant HIV-1 in P4/R5 cells. Importantly, RS-788 was substantially more potent than 3'-azido-2,6-DA-P or 3'-azido-ddG against viruses harboring the Q151M complex or 69-insertion multi-NRTI resistance mutations. For example, the potency of RS-788 against HIV-1 with the Q151M complex was decreased relative to that of WT virus only 2.3-fold, whereas that of 3'-azido-2,6-DA-P and 3'-azido-ddG were decreased 23- and 26-fold, respectively. Similarly, the potency of RS-788 against HIV-1 with the 69-insertion mutations was decreased from that of WT virus 3.7-fold compared to 9.5- and 8.3-fold for 3'-azido-2,6-DA-P and 3'-azido-ddG, respectively. The increased potency was not due to increased delivery of active metabolite because RS-788 delivered similar overall levels of 3'-azido-ddG-TP/3'-azido-2,6-DA-P-TP as 3'-azido-ddG and 3'-azido-2,6-DA-P.

To investigate whether the potent inhibition of drug-resistant HIV-1 by RS-788 may be due to additive or synergistic inhibition of RT resulting from incorporation and chain termination at both T and C positions by 3'-azido-2,6-DA-P-TP and 3'-azido-ddG-TP, respectively we performed RT DNA synthesis assays with combinations of 3'-azido-2,6-DA-P-TP+3'-azido-ddG-TP. Combinations of 3'-azido-2,6-DA-P-TP+3'-azido-ddG-TP at the molar ratios delivered in P4/R5 and PBM cells from RS-788 resulted in synergistic inhibition of RT DNA synthesis by incorporation of 3'-azido-2,6-DA-P-TP across from thymine and 3'-azido-ddG-TP across from cytosine. Synergy of 3'-azido-2,6-DA-P-TP+3'-azido-ddG-TP combinations was noted against WT as well as multi-NRTI resistant RT containing the Q151M complex or the T69SSS insertion mutations. Importantly, the excision mechanism did not impair drug synergy. These data suggest

that the low phenotypic levels resistance to RS-788 by multi-NRTI-resistant HIV-1 may be due to synergistic inhibition of RT DNA synthesis resulting from chain termination across from both thymine and cytosine template residues.

One reason for including two NRTI in combination antiretroviral therapy is increased antiretroviral potency through additive or synergistic inhibition of DNA synthesis (36, 39). We have shown that the combinations of 3'-azido-2,6-DA-P-TP+3'-azido-ddG-TP in the molar ratios delivered to cells by RS-788 synergistically inhibit HIV-1 RT DNA synthesis and that this results in increased potency against HIV-1 replication. A second rationale for including two NRTI in combination antiretroviral therapy is increased potency against drug-resistant HIV-1 variants or an increased barrier to resistance development by including NRTI with divergent resistance mechanisms (39, 242). In CHAPTER THREE we showed potent chain-termination of DNA synthesis by RT containing discrimination mutations and decreased chain-terminated primer unblocking by RT containing TAMs compared to AZT. In CHAPTER FOUR we showed that these favorable attributes translate to decreased phenotypic susceptibility in cells of drug-resistant HIV-1 variants to 3'-azido-2,6-DA-P, 3'-azido-ddG, and their combination delivered by the RS-788 prodrug. The inclusion of two NRTI in combination antiretroviral therapy can result in a higher barrier to resistance development because HIV-1 RT must simultaneously develop mutations that decrease the incorporation and/or increase the excision of two different NRTI while maintaining the ability to complete reverse transcription (242). Whether the combined delivery of 3'-azido-2,6-DA-P-TP and 3'-azido-ddG-TP from RS-788 also results in a higher barrier to resistance development was not examine in the current work. However, cell culture selection experiments were recently performed with 3'-azido-ddG and 3'-azido-ddA (142). Interestingly, 3'-azido-ddG selected for a complex pattern of mutations that only conferred low-

level resistance. Viruses resistant to 3'-azido-ddA could not be selected. By analogy, these results suggest that selection of resistance mutations in the presence of both 3'-azido-2,6-DA-P-TP and 3'-azido-ddG-TP may not readily occur. To evaluate this hypothesis cell culture selection experiments with RS-788, 3'-azido-2,6-DA-P, and 3'-azido-ddG should be performed.

Taken together, our data suggest that RS-788 may represent the first single prodrug that may achieve the same beneficial antiretroviral properties as two individual NRTI used in combination antiretroviral therapy. Such a prodrug would also improve patient adherence by decreasing patient pill burden as has been shown for fixed-dose NRTI combination pills. Consequently, RS-788 should undergo further pre-clinical evaluation. The kinetics of the intracellular accumulation, metabolism, and retention of the 3'-azido-2,6-DA-P-TP and 3'-azido-ddG-TP active metabolites should be examined in detail. Pharmacokinetic properties including absorption, tissue distribution, metabolism, and excretion should be evaluated in mice and non-human primates. Optimization of the unique metabolism and antiviral properties of RS-788 should also be pursued. These efforts should focus first on modification of the RS-788 phosphate moiety as this component has great influence on cellular accumulation and metabolism to the active triphosphate forms. Modification of the phosphate chemical shielding groups may alter the kinetics and ratios of the active 3'-azido-2,6-DA-P-TP and 3'-azido-ddG-TP metabolites produced in cells. Given that 3'-azido-2,6-DA-P-TP and 3'-azido-ddG-TP demonstrate different activities against WT and drug-resistant RT DNA synthesis, an altered intracellular ratio in favor of one triphosphate metabolite over the other may actually provide increased antiviral potency. Secondly, RS-788 analogs containing non-hydrolysable phosphate linkages should be considered. This could be a phosphonate linkage (C-P bond) like that of TFV and PMEO-DAPym or another non-hydrolysable linkage such as an imidophosphate (N-P bond) or

phosphothiol (S-P bond). Since the adenosine deaminase enzyme has substantially decreased activity toward the RS-788 nucleotide compared to the 3'-azido-2,6-DA-P-TP nucleoside, it is expected that an RS-788 analog containing a non-hydrolysable phosphate group would be metabolized in cells almost entirely to 3'-azido-2,6-DA-P-TP (296). Such an analog would allow examination of the anti-HIV-1 activity specifically due to incorporation of 3'-azido-2,6-DA-P-TP incorporation as an Adenosine analog. Finally, phosphate-containing prodrugs of 3'-azido-2',3'-dideoxypurine NRTI with bases other than 2,6-DA-P should be synthesized. These bases could include those described above that may alter the adenosine mimicry phenotype.

7.5 GENERAL PERSPECTIVES AND FUTURE DIRECTIONS

The structure-activity-resistance analyses presented in this dissertation unequivocally confirm that modifications to NRTI structural components (i.e. base and sugar/pseudosugar) affect activity against drug-resistant HIV-1. We have identified novel NRTI analogs (notably RS-788) that demonstrate improved activity against drug-resistant HIV-1 containing discrimination mutations or TAMs. These studies provide 'proof of concept' that a molecular understanding of how the structural components of NRTI affect RT enzyme sensitivity can direct the discovery novel NRTI analogs with potent activity against drug-resistant HIV-1.

Though beyond the scope of this dissertation, the rational design of novel NRTI using structure-activity relationships should be expanded to include considerations for other NRTI limitations such as cellular toxicity and pharmacology. For example, NRTI structure may potentially be optimized for decreased mitochondrial toxicity through structure-activity studies

of polymerase γ inhibition. Similarly, improved NRTI-TP cellular accumulation and retention (i.e. intracellular half-life) might be achieved through optimization of NRTI affinity for the cellular kinases.

PMEO-DAPym, GS-9148, 3'-azido-2,6-DA-P, and RS-788 all have improved activity compared to their parent analogs against the replication of HIV-1 containing discrimination mutations and TAMs. We have shown that these analogs also have improved incorporation activity and decreased excision activity with NRTI-resistant HIV-1 RT *in vitro*. Whether these favorable resistance characteristics against HIV-1 RT also provide a higher barrier to resistance development was not examined in this work. However, studies performed by others suggest that this is the case (142). Cell culture selection studies with 3'-azido-ddG and 3'-azido-ddA showed that resistance to these NRTI developed slowly and a complex combinations of mutations were required to develop low levels of phenotypic resistance (142).

The novel N(t)RTI analogs described in this dissertation (chiefly PMEO-DAPym, 3'-azido-2,6-DA-P, and RS-788) require further pre-clinical analysis. A more thorough examination of the cellular pharmacology should be performed including the kinetics of cellular accumulation and retention of the –MP, -DP, and –TP forms, identification of the kinases responsible, and kinetics of base metabolism (for 3'-azido-2,6-DA-P and RS-788). Given that any novel NRTI are likely to be used in combination with existing NRTI, the potential for synergy and antagonism for cellular phosphorylation and antiviral activity should be examined.

The studies described herein identify substrate mimicry mechanisms in which a pyrimidine (i.e. PMEO-DAPym) or a base-modified purine (i.e. the 6-position-modified-3'-azido-ddG analogs) are recognized by HIV-1 RT as adenosine analogs and are specifically incorporated across from thymine in DNA or uracil in RNA. This molecular mimicry phenotype

shows that HIV-1 RT and human DNA polymerases can recognize and incorporate nucleotide analogs with ambiguous base modifications. Our molecular modeling studies show these non-traditional bases can mimic conical Watson-Crick base pairing to allow efficient nucleotide incorporation. For example, 3'-azido-2,6-DA-P could be incorporated by HIV-1 RT with equal efficiency as the natural 2'-deoxynucleotide dATP. Other purine ring modifications at the 2- and 6-positions may facilitate incorporation across from cytosine thus mimicking a guanosine ring system. This molecular mimicry mechanism may represent a novel means of base-modified nucleotide analog design for the inhibition of microbial and human DNA and RNA polymerases that may have therapeutic use against viruses, bacteria, parasites, or cancer. For instance, linkage of such an ambiguous base to a ribose sugar may endow the analog with activity against RNA polymerases, such as the viral RNA polymerases required for HCV and dengue virus replication. Analogs with ambiguous bases should also be evaluated as anti-metabolites against the cellular nucleoside/nucleotide synthetic enzymes for potential therapeutic use in metabolic disorders.

The knowledge gained through this dissertation research has the potential to allow further optimization of lead analogs that may yield novel NRTI candidates for the treatment of highly drug-resistant HIV-1. Such analogs are crucial for the continued success of the NRTI drug class in combating the HIV-1 epidemic.

BIBLIOGRAPHY

1. Gallo, R.C., P.S. Sarin, E.P. Gelmann, M. Robert-Guroff, E. Richardson, V.S. Kalyanaraman, D. Mann, G.D. Sidhu, R.E. Stahl, S. Zolla-Pazner, J. Leibowitch, and M. Popovic. Isolation of human T-cell leukemia virus in acquired immune deficiency syndrome (AIDS). *Science*, 1983. **220**(4599): p. 865-7.

2. Barre-Sinoussi, F., J.C. Chermann, F. Rey, M.T. Nugeyre, S. Chamaret, J. Gruest, C. Dauguet, C. Axler-Blin, F. Vezinet-Brun, C. Rouzioux, W. Rozenbaum, and L. Montagnier. Isolation of a T-lymphotropic retrovirus from a patient at risk for acquired immune deficiency syndrome (AIDS). *Science*, 1983. **220**(4599): p. 868-71.

3. Mitsuya, H., K.J. Weinhold, P.A. Furman, M.H. St Clair, S.N. Lehrman, R.C. Gallo, D. Bolognesi, D.W. Barry, and S. Broder. 3'-Azido-3'-deoxythymidine (BW A509U): an antiviral agent that inhibits the infectivity and cytopathic effect of human T-lymphotropic virus type III/lymphadenopathy-associated virus in vitro. *Proc Natl Acad Sci U S A*, 1985. **82**(20): p. 7096-100.

4. Mitsuya, H. and S. Broder. Inhibition of the in vitro infectivity and cytopathic effect of human T-lymphotrophic virus type III/lymphadenopathy-associated virus (HTLV-III/LAV) by 2',3'-dideoxynucleosides. *Proc Natl Acad Sci U S A*, 1986. **83**(6): p. 1911-5.

5. Mitsuya, H., R.F. Jarrett, M. Matsukura, F. Di Marzo Veronese, A.L. Devico, M.G. Sarngadharan, D.G. Johns, M.S. Reitz, and S. Broder. Long-term inhibition of human T-lymphotropic virus type III/lymphadenopathy-associated virus (human immunodeficiency virus) DNA synthesis and RNA expression in T cells protected by 2',3'-dideoxynucleosides in vitro. *Proc Natl Acad Sci U S A*, 1987. **84**(7): p. 2033-7.

6. Salemi, M., K. Strimmer, W.W. Hall, M. Duffy, E. Delaporte, S. Mboup, M. Peeters, and A.M. Vandamme. Dating the common ancestor of SIVcpz and HIV-1 group M and the origin of HIV-1 subtypes using a new method to uncover clock-like molecular evolution. *FASEB J*, 2001. **15**(2): p. 276-8.

7. Korber, B., M. Muldoon, J. Theiler, F. Gao, R. Gupta, A. Lapedes, B.H. Hahn, S. Wolinsky, and T. Bhattacharya. Timing the ancestor of the HIV-1 pandemic strains. *Science*, 2000. **288**(5472): p. 1789-96.

8. Gao, F., E. Bailes, D.L. Robertson, Y. Chen, C.M. Rodenburg, S.F. Michael, L.B. Cummins, L.O. Arthur, M. Peeters, G.M. Shaw, P.M. Sharp, and B.H. Hahn. Origin of HIV-1 in the chimpanzee Pan troglodytes troglodytes. *Nature*, 1999. **397**(6718): p. 436-41.

9. Reeves, J.D. and R.W. Doms. Human immunodeficiency virus type 2. *J Gen Virol*, 2002. **83**(Pt 6): p. 1253-65.

10. Gao, F., L. Yue, A.T. White, P.G. Pappas, J. Barchue, A.P. Hanson, B.M. Greene, P.M. Sharp, G.M. Shaw, and B.H. Hahn. Human infection by genetically diverse SIVSM-related HIV-2 in west Africa. *Nature*, 1992. **358**(6386): p. 495-9.

11. UNAIDS, WHO Global Report. 2010 [cited 2012 May 25]; Available from: http://www.unaids.org/globalreport/global_report.htm.

12. Sharp, P.M., E. Bailes, R.R. Chaudhuri, C.M. Rodenburg, M.O. Santiago, and B.H. Hahn. The origins of acquired immune deficiency syndrome viruses: where and when? *Philos Trans R Soc Lond B Biol Sci*, 2001. **356**(1410): p. 867-76.

13. Taylor, B.S., M.E. Sobieszczyk, F.E. Mccutchan, and S.M. Hammer. The challenge of HIV-1 subtype diversity. *N Engl J Med*, 2008. **358**(15): p. 1590-602.

14. Levy, J.A. HIV and the Pathogenesis of AIDS. 2nd ed1998, Washington, D.C.: ASM Press.

15. Fauci, A.S. and R.C. Desrosiers. Pathogenesis of HIV and SIV, in *Retroviruses*, Coffin, J.M., S.H. Hughes, and H.E. Varmus, Editors. 1997, Cold Spring Harbor Laboratory Press: Cold Spring Harbor, NY.

16. Pantaleo, G., C. Graziosi, and A.S. Fauci. New concepts in the immunopathogenesis of human immunodeficiency virus infection. *N Engl J Med*, 1993. **328**(5): p. 327-35.

17. Abbas, W. and G. Herbein. Molecular Understanding of HIV-1 Latency. *Adv Virol*, 2012. **2012**: p. 574967.

18. National Institute of Health, US department of Health and Human Services. HIV Infection and AIDS: An Overview. 2005 [cited 2012 June 10]; Available from: http://www.niaid.nih.gov/factsheets/hivinf.htm.

19. Lucas, S. Causes of death in the HAART era. *Curr Opin Infect Dis*, 2012. **25**(1): p. 36-41.

20. Vogt, V.M. Retroviral Virions and Genomes, in *Retroviruses*, Coffin, J.M., S.H. Hughes, and H.E. Varmus, Editors. 1997, Cold Spring Harbor Laboratory Press: Cold Spring Harbor, NY.

21. Chertova, E., O. Chertov, L.V. Coren, J.D. Roser, C.M. Trubey, J.W. Bess, Jr., R.C. Sowder, 2nd, E. Barsov, B.L. Hood, R.J. Fisher, K. Nagashima, T.P. Conrads, T.D. Veenstra, J.D. Lifson, and D.E. Ott. Proteomic and biochemical analysis of purified human immunodeficiency virus type 1 produced from infected monocyte-derived macrophages. *J Virol*, 2006. **80**(18): p. 9039-52.

22. Dalgleish, A.G., P.C. Beverley, P.R. Clapham, D.H. Crawford, M.F. Greaves, and R.A. Weiss. The CD4 (T4) antigen is an essential component of the receptor for the AIDS retrovirus. *Nature*, 1984. **312**(5996): p. 763-7.

23. Klatzmann, D., E. Champagne, S. Chamaret, J. Gruest, D. Guetard, T. Hercend, J.C. Gluckman, and L. Montagnier. T-lymphocyte T4 molecule behaves as the receptor for human retrovirus LAV. *Nature*, 1984. **312**(5996): p. 767-8.

24. Chan, D.C. and P.S. Kim. HIV entry and its inhibition. *Cell*, 1998. **93**(5): p. 681-4.

25. Clapham, P.R., J.D. Reeves, G. Simmons, N. Dejucq, S. Hibbitts, and A. Mcknight. HIV coreceptors, cell tropism and inhibition by chemokine receptor ligands. *Mol Membr Biol*, 1999. **16**(1): p. 49-55.

26. Berger, E.A., P.M. Murphy, and J.M. Farber. Chemokine receptors as HIV-1 coreceptors: roles in viral entry, tropism, and disease. *Annu Rev Immunol*, 1999. **17**: p. 657-700.

27. Hunter, E. Viral Entry and Receptors, in *Retroviruses*, Coffin, J.M., S.H. Hughes, and H.E. Varmus, Editors. 1997, Cold Spring Harbor Laboratory Press: Cold Spring Harbor, NY.

28. Zhang, H., Y. Zhang, T.P. Spicer, L.Z. Abbott, M. Abbott, and B.J. Poiesz. Reverse transcription takes place within extracellular HIV-1 virions: potential biological significance. *AIDS Res Hum Retroviruses*, 1993. **9**(12): p. 1287-96.

29. Karageorgos, L., P. Li, and C. Burrell. Characterization of HIV replication complexes early after cell-to-cell infection. *AIDS Res Hum Retroviruses*, 1993. **9**(9): p. 817-23.

30. Skalka, A.M. and R.A. Katz. Retroviral DNA integration and the DNA damage response. *Cell Death Differ*, 2005. **12 Suppl 1**: p. 971-8.

31. Rabson, A.B. and B.J. Graves. Synthesis and Processing of Viral RNA, in *Retroviruses*, Coffin, J.M., S.H. Hughes, and H.E. Varmus, Editors. 1997, Cold Spring Harbor Laboratory Press: Cold Spring Harbor (NY).

32. Jacks, T. and H.E. Varmus. Expression of the Rous sarcoma virus pol gene by ribosomal frameshifting. *Science*, 1985. **230**(4731): p. 1237-42.

33. Swanstrom, R. and J.W. Wills. Synthesis, Assembly, and Processing of Viral Proteins, in *Retroviruses*, Coffin, J.M., S.H. Hughes, and H.E. Varmus, Editors. 1997, Cold Spring Harbor Laboratory Press: Cold Spring Harbor (NY).

34. Srinivasakumar, N., M.L. Hammarskjold, and D. Rekosh. Characterization of deletion mutations in the capsid region of human immunodeficiency virus type 1 that affect particle formation and Gag-Pol precursor incorporation. *J Virol*, 1995. **69**(10): p. 6106-14.

35. Ghosh, R.K., S.M. Ghosh, and S. Chawla. Recent advances in antiretroviral drugs. *Expert Opin Pharmacother*, 2011. **12**(1): p. 31-46.

36. Este, J.A. and T. Cihlar. Current status and challenges of antiretroviral research and therapy. *Antiviral Res*, 2010. **85**(1): p. 25-33.

37. Dorr, P., M. Westby, S. Dobbs, P. Griffin, B. Irvine, M. Macartney, J. Mori, G. Rickett, C. Smith-Burchnell, C. Napier, R. Webster, D. Armour, D. Price, B. Stammen, A. Wood, and M. Perros. Maraviroc (UK-427,857), a potent, orally bioavailable, and selective small-molecule inhibitor of chemokine receptor CCR5 with broad-spectrum anti-human immunodeficiency virus type 1 activity. *Antimicrob Agents Chemother*, 2005. **49**(11): p. 4721-32.

38. Matthews, T., M. Salgo, M. Greenberg, J. Chung, R. Demasi, and D. Bolognesi. Enfuvirtide: the first therapy to inhibit the entry of HIV-1 into host CD4 lymphocytes. *Nat Rev Drug Discov*, 2004. **3**(3): p. 215-25.

39. Cihlar, T. and A.S. Ray. Nucleoside and nucleotide HIV reverse transcriptase inhibitors: 25 years after zidovudine. *Antiviral Res*, 2010. **85**(1): p. 39-58.

40. Blas-Garcia, A., J.V. Esplugues, and N. Apostolova. Twenty years of HIV-1 non-nucleoside reverse transcriptase inhibitors: time to reevaluate their toxicity. *Curr Med Chem*, 2011. **18**(14): p. 2186-95.

41. Rittinger, K., G. Divita, and R.S. Goody. Human immunodeficiency virus reverse transcriptase substrate-induced conformational changes and the mechanism of inhibition by nonnucleoside inhibitors. *Proc Natl Acad Sci U S A*, 1995. **92**(17): p. 8046-9.

42. Nikolenko, G.N., A.T. Kotelkin, S.F. Oreshkova, and A.A. Il'ichev. [Mechanisms of HIV-1 drug resistance to nucleoside and non-nucleoside reverse transcriptase inhibitors]. *Mol Biol (Mosk)*, 2011. **45**(1): p. 108-26.

43. Sato, M., T. Motomura, H. Aramaki, T. Matsuda, M. Yamashita, Y. Ito, H. Kawakami, Y. Matsuzaki, W. Watanabe, K. Yamataka, S. Ikeda, E. Kodama, M. Matsuoka, and H. Shinkai. Novel HIV-1 integrase inhibitors derived from quinolone antibiotics. *J Med Chem*, 2006. **49**(5): p. 1506-8.

44. Qiu, X. and Z.P. Liu. Recent developments of peptidomimetic HIV-1 protease inhibitors. *Curr Med Chem*, 2011. **18**(29): p. 4513-37.

45. Zeldin, R.K. and R.A. Petruschke. Pharmacological and therapeutic properties of ritonavir-boosted protease inhibitor therapy in HIV-infected patients. *J Antimicrob Chemother*, 2004. **53**(1): p. 4-9.

46. Rooke, R., M.A. Parniak, M. Tremblay, H. Soudeyns, X.G. Li, Q. Gao, X.J. Yao, and M.A. Wainberg. Biological comparison of wild-type and zidovudine-resistant isolates of human immunodeficiency virus type 1 from the same subjects: susceptibility and resistance to other drugs. *Antimicrob Agents Chemother*, 1991. **35**(5): p. 988-91.

47. Larder, B.A. and S.D. Kemp. Multiple mutations in HIV-1 reverse transcriptase confer high-level resistance to zidovudine (AZT). *Science*, 1989. **246**(4934): p. 1155-8.

48. Gulick, R.M., J.W. Mellors, D. Havlir, J.J. Eron, C. Gonzalez, D. Mcmahon, D.D. Richman, F.T. Valentine, L. Jonas, A. Meibohm, E.A. Emini, and J.A. Chodakewitz. Treatment with indinavir, zidovudine, and lamivudine in adults with human immunodeficiency virus infection and prior antiretroviral therapy. *N Engl J Med*, 1997. **337**(11): p. 734-9.

49. Montaner, J.S., P. Reiss, D. Cooper, S. Vella, M. Harris, B. Conway, M.A. Wainberg, D. Smith, P. Robinson, D. Hall, M. Myers, and J.M. Lange. A randomized, double-blind trial comparing combinations of nevirapine, didanosine, and zidovudine for HIV-infected patients: the INCAS Trial. Italy, The Netherlands, Canada and Australia Study. *JAMA*, 1998. **279**(12): p. 930-7.

50. Marchand, C. The elvitegravir Quad pill: the first once-daily dual-target anti-HIV tablet. *Expert Opin Investig Drugs*, 2012. **21**(7): p. 901-4.

51. Telesnitsky, A. and S.P. Goff. Reverse Transcriptase and the Generation of Retroviral DNA, in *Retroviruses*, Coffin, J.M., S.H. Hughes, and H.E. Varmus, Editors. 1997, Cold Spring Harbor Laboratory Press: Cold Spring Harbor, NY.

52. Baltimore, D. RNA-dependent DNA polymerase in virions of RNA tumour viruses. *Nature*, 1970. **226**(5252): p. 1209-11.

53. Temin, H.M. and S. Mizutani. RNA-dependent DNA polymerase in virions of Rous sarcoma virus. *Nature*, 1970. **226**(5252): p. 1211-3.

54. Le Grice, S.F. "In the beginning": initiation of minus strand DNA synthesis in retroviruses and LTR-containing retrotransposons. *Biochemistry*, 2003. **42**(49): p. 14349-55.

55. Mak, J. and L. Kleiman. Primer tRNAs for reverse transcription. *J Virol*, 1997. **71**(11): p. 8087-95.

56. Peliska, J.A. and S.J. Benkovic. Mechanism of DNA strand transfer reactions catalyzed by HIV-1 reverse transcriptase. *Science*, 1992. **258**(5085): p. 1112-8.

57. Destefano, J.J., R.A. Bambara, and P.J. Fay. Parameters that influence the binding of human immunodeficiency virus reverse transcriptase to nucleic acid structures. *Biochemistry*, 1993. **32**(27): p. 6908-15.

58. Van Wamel, J.L. and B. Berkhout. The first strand transfer during HIV-1 reverse transcription can occur either intramolecularly or intermolecularly. *Virology*, 1998. **244**(2): p. 245-51.

59. Onafuwa-Nuga, A. and A. Telesnitsky. The remarkable frequency of human immunodeficiency virus type 1 genetic recombination. *Microbiol Mol Biol Rev*, 2009. **73**(3): p. 451-80, Table of Contents.

60. Fuentes, G.M., L. Rodriguez-Rodriguez, P.J. Fay, and R.A. Bambara. Use of an oligoribonucleotide containing the polypurine tract sequence as a primer by HIV reverse transcriptase. *J Biol Chem*, 1995. **270**(47): p. 28169-76.

61. Cirino, N.M., C.E. Cameron, J.S. Smith, J.W. Rausch, M.J. Roth, S.J. Benkovic, and S.F. Le Grice. Divalent cation modulation of the ribonuclease functions of human immunodeficiency virus reverse transcriptase. *Biochemistry*, 1995. **34**(31): p. 9936-43.

62. Ghosh, M., J. Williams, M.D. Powell, J.G. Levin, and S.F. Le Grice. Mutating a conserved motif of the HIV-1 reverse transcriptase palm subdomain alters primer utilization. *Biochemistry*, 1997. **36**(19): p. 5758-68.

63. Sarafianos, S.G., K. Das, C. Tantillo, A.D. Clark, Jr., J. Ding, J.M. Whitcomb, P.L. Boyer, S.H. Hughes, and E. Arnold. Crystal structure of HIV-1 reverse transcriptase in complex with a polypurine tract RNA:DNA. *EMBO J*, 2001. **20**(6): p. 1449-61.

64. Pullen, K.A., A.J. Rattray, and J.J. Champoux. The sequence features important for plus strand priming by human immunodeficiency virus type 1 reverse transcriptase. *J Biol Chem*, 1993. **268**(9): p. 6221-7.

65. Julias, J.G., M.J. Mcwilliams, S.G. Sarafianos, W.G. Alvord, E. Arnold, and S.H. Hughes. Effects of mutations in the G tract of the human immunodeficiency virus type 1 polypurine tract on virus replication and RNase H cleavage. *J Virol*, 2004. **78**(23): p. 13315-24.

66. Kvaratskhelia, M., S.R. Budihas, and S.F. Le Grice. Pre-existing distortions in nucleic acid structure aid polypurine tract selection by HIV-1 reverse transcriptase. *J Biol Chem*, 2002. **277**(19): p. 16689-96.

67. Gotte, M., M. Kameoka, N. Mclellan, L. Cellai, and M.A. Wainberg. Analysis of efficiency and fidelity of HIV-1 (+)-strand DNA synthesis reveals a novel rate-limiting step during retroviral reverse transcription. *J Biol Chem*, 2001. **276**(9): p. 6711-9.

68. Gotte, M., G. Maier, A.M. Onori, L. Cellai, M.A. Wainberg, and H. Heumann. Temporal coordination between initiation of HIV (+)-strand DNA synthesis and primer removal. *J Biol Chem*, 1999. **274**(16): p. 11159-69.

69. Ben-Artzi, H., J. Shemesh, E. Zeelon, B. Amit, L. Kleiman, M. Gorecki, and A. Panet. Molecular analysis of the second template switch during reverse transcription of the HIV RNA template. *Biochemistry*, 1996. **35**(32): p. 10549-57.

70. Smith, C.M., J.S. Smith, and M.J. Roth. RNase H requirements for the second strand transfer reaction of human immunodeficiency virus type 1 reverse transcription. *J Virol*, 1999. **73**(8): p. 6573-81.

71. Jacobo-Molina, A., J. Ding, R.G. Nanni, A.D. Clark, Jr., X. Lu, C. Tantillo, R.L. Williams, G. Kamer, A.L. Ferris, P. Clark, and Et Al. Crystal structure of human immunodeficiency virus type 1 reverse transcriptase complexed with double-stranded DNA at 3.0 A resolution shows bent DNA. *Proc Natl Acad Sci U S A*, 1993. **90**(13): p. 6320-4.

72. Farmerie, W.G., D.D. Loeb, N.C. Casavant, C.A. Hutchison, 3rd, M.H. Edgell, and R. Swanstrom. Expression and processing of the AIDS virus reverse transcriptase in Escherichia coli. *Science*, 1987. **236**(4799): p. 305-8.

73. Lightfoote, M.M., J.E. Coligan, T.M. Folks, A.S. Fauci, M.A. Martin, and S. Venkatesan. Structural characterization of reverse transcriptase and endonuclease polypeptides of the acquired immunodeficiency syndrome retrovirus. *J Virol*, 1986. **60**(2): p. 771-5.

74. Mous, J., E.P. Heimer, and S.F. Le Grice. Processing protease and reverse transcriptase from human immunodeficiency virus type I polyprotein in Escherichia coli. *J Virol*, 1988. **62**(4): p. 1433-6.

75. Lowe, D.M., A. Aitken, C. Bradley, G.K. Darby, B.A. Larder, K.L. Powell, D.J. Purifoy, M. Tisdale, and D.K. Stammers. HIV-1 reverse transcriptase: crystallization and analysis of domain structure by limited proteolysis. *Biochemistry*, 1988. **27**(25): p. 8884-9.

76. Kohlstaedt, L.A., J. Wang, J.M. Friedman, P.A. Rice, and T.A. Steitz. Crystal structure at 3.5 A resolution of HIV-1 reverse transcriptase complexed with an inhibitor. *Science*, 1992. **256**(5065): p. 1783-90.

77. Huang, H., R. Chopra, G.L. Verdine, and S.C. Harrison. Structure of a covalently trapped catalytic complex of HIV-1 reverse transcriptase: implications for drug resistance. *Science*, 1998. **282**(5394): p. 1669-75.

78. Rodgers, D.W., S.J. Gamblin, B.A. Harris, S. Ray, J.S. Culp, B. Hellmig, D.J. Woolf, C. Debouck, and S.C. Harrison. The structure of unliganded reverse transcriptase from the human immunodeficiency virus type 1. *Proc Natl Acad Sci U S A*, 1995. **92**(4): p. 1222-6.

79. Steitz, T.A., S.J. Smerdon, J. Jager, and C.M. Joyce. A unified polymerase mechanism for nonhomologous DNA and RNA polymerases. *Science*, 1994. **266**(5193): p. 2022-5.

80. Sarafianos, S.G., K. Das, A.D. Clark, Jr., J. Ding, P.L. Boyer, S.H. Hughes, and E. Arnold. Lamivudine (3TC) resistance in HIV-1 reverse transcriptase involves steric hindrance with beta-branched amino acids. *Proc Natl Acad Sci U S A*, 1999. **96**(18): p. 10027-32.

81. Das, K., R.P. Bandwar, K.L. White, J.Y. Feng, S.G. Sarafianos, S. Tuske, X. Tu, A.D. Clark, Jr., P.L. Boyer, X. Hou, B.L. Gaffney, R.A. Jones, M.D. Miller, S.H. Hughes, and E. Arnold. Structural basis for the role of the K65R mutation in HIV-1 reverse transcriptase polymerization, excision antagonism, and tenofovir resistance. *J Biol Chem*, 2009. **284**(50): p. 35092-100.

82. Tu, X., K. Das, Q. Han, J.D. Bauman, A.D. Clark, Jr., X. Hou, Y.V. Frenkel, B.L. Gaffney, R.A. Jones, P.L. Boyer, S.H. Hughes, S.G. Sarafianos, and E. Arnold. Structural basis of HIV-1 resistance to AZT by excision. *Nat Struct Mol Biol*, 2010. **17**(10): p. 1202-9.

83. Sarafianos, S.G., B. Marchand, K. Das, D.M. Himmel, M.A. Parniak, S.H. Hughes, and E. Arnold. Structure and function of HIV-1 reverse transcriptase: molecular mechanisms of polymerization and inhibition. *J Mol Biol*, 2009. **385**(3): p. 693-713.

84. Sarafianos, S.G., A.D. Clark, Jr., K. Das, S. Tuske, J.J. Birktoft, P. Ilankumaran, A.R. Ramesha, J.M. Sayer, D.M. Jerina, P.L. Boyer, S.H. Hughes, and E. Arnold. Structures of HIV-1 reverse transcriptase with pre- and post-translocation AZTMP-terminated DNA. *EMBO J*, 2002. **21**(23): p. 6614-24.

85. Tuske, S., S.G. Sarafianos, A.D. Clark, Jr., J. Ding, L.K. Naeger, K.L. White, M.D. Miller, C.S. Gibbs, P.L. Boyer, P. Clark, G. Wang, B.L. Gaffney, R.A. Jones, D.M. Jerina, S.H. Hughes, and E. Arnold. Structures of HIV-1 RT-DNA complexes before and after incorporation of the anti-AIDS drug tenofovir. *Nat Struct Mol Biol*, 2004. **11**(5): p. 469-74.

86. Ghosh, M., P.S. Jacques, D.W. Rodgers, M. Ottman, J.L. Darlix, and S.F. Le Grice. Alterations to the primer grip of p66 HIV-1 reverse transcriptase and their consequences for template-primer utilization. *Biochemistry*, 1996. **35**(26): p. 8553-62.

87. Julias, J.G., M.J. Mcwilliams, S.G. Sarafianos, E. Arnold, and S.H. Hughes. Mutations in the RNase H domain of HIV-1 reverse transcriptase affect the initiation of DNA synthesis and the specificity of RNase H cleavage in vivo. *Proc Natl Acad Sci U S A*, 2002. **99**(14): p. 9515-20.

88. Destefano, J.J. The orientation of binding of human immunodeficiency virus reverse transcriptase on nucleic acid hybrids. *Nucleic Acids Res*, 1995. **23**(19): p. 3901-8.

89. Gotte, M., G. Maier, H.J. Gross, and H. Heumann. Localization of the active site of HIV-1 reverse transcriptase-associated RNase H domain on a DNA template using site-specific generated hydroxyl radicals. *J Biol Chem*, 1998. **273**(17): p. 10139-46.

90. Gopalakrishnan, V., J.A. Peliska, and S.J. Benkovic. Human immunodeficiency virus type 1 reverse transcriptase: spatial and temporal relationship between the polymerase and RNase H activities. *Proc Natl Acad Sci U S A*, 1992. **89**(22): p. 10763-7.

91. Gotte, M., S. Fackler, T. Hermann, E. Perola, L. Cellai, H.J. Gross, S.F. Le Grice, and H. Heumann. HIV-1 reverse transcriptase-associated RNase H cleaves RNA/RNA in arrested complexes: implications for the mechanism by which RNase H discriminates between RNA/RNA and RNA/DNA. *EMBO J*, 1995. **14**(4): p. 833-41.

92. Schultz, S.J., M. Zhang, and J.J. Champoux. Recognition of internal cleavage sites by retroviral RNases H. *J Mol Biol*, 2004. **344**(3): p. 635-52.

93. Wohrl, B.M., R. Krebs, R.S. Goody, and T. Restle. Refined model for primer/template binding by HIV-1 reverse transcriptase: pre-steady-state kinetic analyses of primer/template binding and nucleotide incorporation events distinguish between different binding modes depending on the nature of the nucleic acid substrate. *J Mol Biol*, 1999. **292**(2): p. 333-44.

94. Vaccaro, J.A., H.A. Singh, and K.S. Anderson. Initiation of minus-strand DNA synthesis by human immunodeficiency virus type 1 reverse transcriptase. *Biochemistry*, 1999. **38**(48): p. 15978-85.

95. Boyer, P.L., S.G. Sarafianos, E. Arnold, and S.H. Hughes. Analysis of mutations at positions 115 and 116 in the dNTP binding site of HIV-1 reverse transcriptase. *Proc Natl Acad Sci U S A*, 2000. **97**(7): p. 3056-61.

96. Martin-Hernandez, A.M., E. Domingo, and L. Menendez-Arias. Human immunodeficiency virus type 1 reverse transcriptase: role of Tyr115 in deoxynucleotide binding and misinsertion fidelity of DNA synthesis. *EMBO J*, 1996. **15**(16): p. 4434-42.

97. Sawaya, M.R., R. Prasad, S.H. Wilson, J. Kraut, and H. Pelletier. Crystal structures of human DNA polymerase beta complexed with gapped and nicked DNA: evidence for an induced fit mechanism. *Biochemistry*, 1997. **36**(37): p. 11205-15.

98. Kati, W.M., K.A. Johnson, L.F. Jerva, and K.S. Anderson. Mechanism and fidelity of HIV reverse transcriptase. *J Biol Chem*, 1992. **267**(36): p. 25988-97.

99. Marchand, B. and M. Gotte. Site-specific footprinting reveals differences in the translocation status of HIV-1 reverse transcriptase. Implications for polymerase translocation and drug resistance. *J Biol Chem*, 2003. **278**(37): p. 35362-72.

100. Reardon, J.E. Human immunodeficiency virus reverse transcriptase: steady-state and pre-steady-state kinetics of nucleotide incorporation. *Biochemistry*, 1992. **31**(18): p. 4473-9.

101. Johansson, N.G. and S. Eriksson. Structure-activity relationships for phosphorylation of nucleoside analogs to monophosphates by nucleoside kinases. *Acta Biochim Pol*, 1996. **43**(1): p. 143-60.

102. Arner, E.S. and S. Eriksson. Mammalian deoxyribonucleoside kinases. *Pharmacol Ther*, 1995. **67**(2): p. 155-86.

103. Balzarini, J., D.A. Cooney, M. Dalal, G.J. Kang, J.E. Cupp, E. Declercq, S. Broder, and D.G. Johns. 2',3'-Dideoxycytidine: regulation of its metabolism and anti-retroviral potency by natural pyrimidine nucleosides and by inhibitors of pyrimidine nucleotide synthesis. *Mol Pharmacol*, 1987. **32**(6): p. 798-806.

104. Furman, P.A., J.A. Fyfe, M.H. St Clair, K. Weinhold, J.L. Rideout, G.A. Freeman, S.N. Lehrman, D.P. Bolognesi, S. Broder, H. Mitsuya, and Et Al. Phosphorylation of 3'-azido-3'-deoxythymidine and selective interaction of the 5'-triphosphate with human immunodeficiency virus reverse transcriptase. *Proc Natl Acad Sci U S A*, 1986. **83**(21): p. 8333-7.

105. Ho, H.T. and M.J. Hitchcock. Cellular pharmacology of 2',3'-dideoxy-2',3'-didehydrothymidine, a nucleoside analog active against human immunodeficiency virus. *Antimicrob Agents Chemother*, 1989. **33**(6): p. 844-9.

106. Shewach, D.S., D.C. Liotta, and R.F. Schinazi. Affinity of the antiviral enantiomers of oxathiolane cytosine nucleosides for human 2'-deoxycytidine kinase. *Biochem Pharmacol*, 1993. **45**(7): p. 1540-3.

107. Van Rompay, A.R., M. Johansson, and A. Karlsson. Phosphorylation of nucleosides and nucleoside analogs by mammalian nucleoside monophosphate kinases. *Pharmacol Ther*, 2000. **87**(2-3): p. 189-98.

108. Bourdais, J., R. Biondi, S. Sarfati, C. Guerreiro, I. Lascu, J. Janin, and M. Veron. Cellular phosphorylation of anti-HIV nucleosides. Role of nucleoside diphosphate kinase. *J Biol Chem*, 1996. **271**(14): p. 7887-90.

109. Krishnan, P., Q. Fu, W. Lam, J.Y. Liou, G. Dutschman, and Y.C. Cheng. Phosphorylation of pyrimidine deoxynucleoside analog diphosphates: selective phosphorylation of L-nucleoside analog diphosphates by 3-phosphoglycerate kinase. *J Biol Chem*, 2002. **277**(7): p. 5453-9.

110. Katz, R.A. and A.M. Skalka. Generation of diversity in retroviruses. *Annu Rev Genet*, 1990. **24**: p. 409-45.

111. Isel, C., C. Ehresmann, P. Walter, B. Ehresmann, and R. Marquet. The emergence of different resistance mechanisms toward nucleoside inhibitors is explained by the properties of the wild type HIV-1 reverse transcriptase. *J Biol Chem*, 2001. **276**(52): p. 48725-32.

112. Preston, B.D., B.J. Poiesz, and L.A. Loeb. Fidelity of HIV-1 reverse transcriptase. *Science*, 1988. **242**(4882): p. 1168-71.

113. Perelson, A.S., A.U. Neumann, M. Markowitz, J.M. Leonard, and D.D. Ho. HIV-1 dynamics in vivo: virion clearance rate, infected cell life-span, and viral generation time. *Science*, 1996. **271**(5255): p. 1582-6.

114. Gao, H.Q., P.L. Boyer, S.G. Sarafianos, E. Arnold, and S.H. Hughes. The role of steric hindrance in 3TC resistance of human immunodeficiency virus type-1 reverse transcriptase. *J Mol Biol*, 2000. **300**(2): p. 403-18.

115. Martin, J.L., J.E. Wilson, R.L. Haynes, and P.A. Furman. Mechanism of resistance of human immunodeficiency virus type 1 to 2',3'-dideoxyinosine. *Proc Natl Acad Sci U S A*, 1993. **90**(13): p. 6135-9.

116. Winters, M.A., R.W. Shafer, R.A. Jellinger, G. Mamtora, T. Gingeras, and T.C. Merigan. Human immunodeficiency virus type 1 reverse transcriptase genotype and drug susceptibility changes in infected individuals receiving dideoxyinosine monotherapy for 1 to 2 years. *Antimicrob Agents Chemother*, 1997. **41**(4): p. 757-62.

117. Harrigan, P.R., C. Stone, P. Griffin, I. Najera, S. Bloor, S. Kemp, M. Tisdale, and B. Larder. Resistance profile of the human immunodeficiency virus type 1 reverse transcriptase inhibitor abacavir (1592U89) after monotherapy and combination therapy. CNA2001 Investigative Group. *J Infect Dis*, 2000. **181**(3): p. 912-20.

118. Margot, N.A., B. Lu, A. Cheng, M.D. Miller, and T. Study. Resistance development over 144 weeks in treatment-naive patients receiving tenofovir disoproxil fumarate or stavudine with lamivudine and efavirenz in Study 903. *HIV Med*, 2006. **7**(7): p. 442-50.

119. Ueno, T., T. Shirasaka, and H. Mitsuya. Enzymatic characterization of human immunodeficiency virus type 1 reverse transcriptase resistant to multiple 2',3'-dideoxynucleoside 5'-triphosphates. *J Biol Chem*, 1995. **270**(40): p. 23605-11.

120. White, K.L., J.M. Chen, J.Y. Feng, N.A. Margot, J.K. Ly, A.S. Ray, H.L. Macarthur, M.J. Mcdermott, S. Swaminathan, and M.D. Miller. The K65R reverse transcriptase mutation in HIV-1 reverses the excision phenotype of zidovudine resistance mutations. *Antivir Ther*, 2006. **11**(2): p. 155-63.

121. Gu, Z., E.J. Arts, M.A. Parniak, and M.A. Wainberg. Mutated K65R recombinant reverse transcriptase of human immunodeficiency virus type 1 shows diminished chain termination in the presence of 2',3'-dideoxycytidine 5'-triphosphate and other drugs. *Proc Natl Acad Sci U S A*, 1995. **92**(7): p. 2760-4.

122. Parikh, U.M., S. Zelina, N. Sluis-Cremer, and J.W. Mellors. Molecular mechanisms of bidirectional antagonism between K65R and thymidine analog mutations in HIV-1 reverse transcriptase. *AIDS*, 2007. **21**(11): p. 1405-14.

123. White, K.L., N.A. Margot, J.K. Ly, J.M. Chen, A.S. Ray, M. Pavelko, R. Wang, M. Mcdermott, S. Swaminathan, and M.D. Miller. A combination of decreased NRTI incorporation and decreased excision determines the resistance profile of HIV-1 K65R RT. *AIDS*, 2005. **19**(16): p. 1751-60.

124. Deval, J., K.L. White, M.D. Miller, N.T. Parkin, J. Courcambeck, P. Halfon, B. Selmi, J. Boretto, and B. Canard. Mechanistic basis for reduced viral and enzymatic fitness of HIV-1 reverse transcriptase containing both K65R and M184V mutations. *J Biol Chem*, 2004. **279**(1): p. 509-16.

125. Feng, J.Y., F.T. Myrick, N.A. Margot, G.B. Mulamba, L. Rimsky, K. Borroto-Esoda, B. Selmi, and B. Canard. Virologic and enzymatic studies revealing the mechanism of K65R- and Q151M-associated HIV-1 drug resistance towards emtricitabine and lamivudine. *Nucleosides Nucleotides Nucleic Acids*, 2006. **25**(1): p. 89-107.

126. Deval, J., J.M. Navarro, B. Selmi, J. Courcambeck, J. Boretto, P. Halfon, S. Garrido-Urbani, J. Sire, and B. Canard. A loss of viral replicative capacity correlates with altered DNA polymerization kinetics by the human immunodeficiency virus reverse transcriptase bearing the K65R and L74V dideoxynucleoside resistance substitutions. *J Biol Chem*, 2004. **279**(24): p. 25489-96.

127. Selmi, B., J. Boretto, J.M. Navarro, J. Sire, S. Longhi, C. Guerreiro, L. Mulard, S. Sarfati, and B. Canard. The valine-to-threonine 75 substitution in human immunodeficiency virus type 1 reverse transcriptase and its relation with stavudine resistance. *J Biol Chem*, 2001. **276**(17): p. 13965-74.

128. Goldschmidt, V. and R. Marquet. Primer unblocking by HIV-1 reverse transcriptase and resistance to nucleoside RT inhibitors (NRTIs). *Int J Biochem Cell Biol*, 2004. **36**(9): p. 1687-705.

129. Arion, D., N. Kaushik, S. Mccormick, G. Borkow, and M.A. Parniak. Phenotypic mechanism of HIV-1 resistance to 3'-azido-3'-deoxythymidine (AZT): increased polymerization processivity and enhanced sensitivity to pyrophosphate of the mutant viral reverse transcriptase. *Biochemistry*, 1998. **37**(45): p. 15908-17.

130. Meyer, P.R., S.E. Matsuura, A.G. So, and W.A. Scott. Unblocking of chain-terminated primer by HIV-1 reverse transcriptase through a nucleotide-dependent mechanism. *Proc Natl Acad Sci U S A*, 1998. **95**(23): p. 13471-6.

131. Meyer, P.R., S.E. Matsuura, A.M. Mian, A.G. So, and W.A. Scott. A mechanism of AZT resistance: an increase in nucleotide-dependent primer unblocking by mutant HIV-1 reverse transcriptase. *Mol Cell*, 1999. **4**(1): p. 35-43.

132. Boyer, P.L., S.G. Sarafianos, E. Arnold, and S.H. Hughes. Selective excision of AZTMP by drug-resistant human immunodeficiency virus reverse transcriptase. *J Virol*, 2001. **75**(10): p. 4832-42.

133. Kellam, P., C.A. Boucher, and B.A. Larder. Fifth mutation in human immunodeficiency virus type 1 reverse transcriptase contributes to the development of high-level resistance to zidovudine. *Proc Natl Acad Sci U S A*, 1992. **89**(5): p. 1934-8.

134. Harrigan, P.R., I. Kinghorn, S. Bloor, S.D. Kemp, I. Najera, A. Kohli, and B.A. Larder. Significance of amino acid variation at human immunodeficiency virus type 1 reverse transcriptase residue 210 for zidovudine susceptibility. *J Virol*, 1996. **70**(9): p. 5930-4.

135. Dharmasena, S., Z. Pongracz, E. Arnold, S.G. Sarafianos, and M.A. Parniak. 3'-Azido-3'-deoxythymidine-(5')-tetraphospho-(5')-adenosine, the product of ATP-mediated excision of chain-terminating AZTMP, is a potent chain-terminating substrate for HIV-1 reverse transcriptase. *Biochemistry*, 2007. **46**(3): p. 828-36.

136. Kerr, S.G. and K.S. Anderson. Pre-steady-state kinetic characterization of wild type and 3'-azido-3'-deoxythymidine (AZT) resistant human immunodeficiency virus type 1 reverse transcriptase: implication of RNA directed DNA polymerization in the mechanism of AZT resistance. *Biochemistry*, 1997. **36**(46): p. 14064-70.

137. Meyer, P.R., S.E. Matsuura, R.F. Schinazi, A.G. So, and W.A. Scott. Differential removal of thymidine nucleotide analogues from blocked DNA chains by human immunodeficiency virus reverse transcriptase in the presence of physiological concentrations of 2'-deoxynucleoside triphosphates. *Antimicrob Agents Chemother*, 2000. **44**(12): p. 3465-72.

138. Mas, A., B.M. Vazquez-Alvarez, E. Domingo, and L. Menendez-Arias. Multidrug-resistant HIV-1 reverse transcriptase: involvement of ribonucleotide-dependent phosphorolysis in cross-resistance to nucleoside analogue inhibitors. *J Mol Biol*, 2002. **323**(2): p. 181-97.

139. Ray, A.S., E. Murakami, A. Basavapathruni, J.A. Vaccaro, D. Ulrich, C.K. Chu, R.F. Schinazi, and K.S. Anderson. Probing the molecular mechanisms of AZT drug resistance mediated by HIV-1 reverse transcriptase using a transient kinetic analysis. *Biochemistry*, 2003. **42**(29): p. 8831-41.

140. Marchand, B., K.L. White, J.K. Ly, N.A. Margot, R. Wang, M. Mcdermott, M.D. Miller, and M. Gotte. Effects of the translocation status of human immunodeficiency virus type 1 reverse transcriptase on the efficiency of excision of tenofovir. *Antimicrob Agents Chemother*, 2007. **51**(8): p. 2911-9.

141. Sluis-Cremer, N., D. Arion, U. Parikh, D. Koontz, R.F. Schinazi, J.W. Mellors, and M.A. Parniak. The 3'-azido group is not the primary determinant of 3'-azido-3'-deoxythymidine (AZT) responsible for the excision phenotype of AZT-resistant HIV-1. *J Biol Chem*, 2005. **280**(32): p. 29047-52.

142. Meteer, J.D., D. Koontz, G. Asif, H.W. Zhang, M. Detorio, S. Solomon, S.J. Coats, N. Sluis-Cremer, R.F. Schinazi, and J.W. Mellors. The base component of 3'-azido-2',3'-dideoxynucleosides influences resistance mutations selected in HIV-1 reverse transcriptase. *Antimicrob Agents Chemother*, 2011. **55**(8): p. 3758-64.

143. Zhang, H.W., S.J. Coats, L. Bondada, F. Amblard, M. Detorio, G. Asif, E. Fromentin, S. Solomon, A. Obikhod, T. Whitaker, N. Sluis-Cremer, J.W. Mellors, and R.F. Schinazi. Synthesis and evaluation of 3'-azido-2',3'-dideoxypurine nucleosides as inhibitors of human immunodeficiency virus. *Bioorg Med Chem Lett*, 2010. **20**(1): p. 60-4.

144. Meyer, P.R., J. Lennerstrand, S.E. Matsuura, B.A. Larder, and W.A. Scott. Effects of dipeptide insertions between codons 69 and 70 of human immunodeficiency virus type 1 reverse transcriptase on primer unblocking, deoxynucleoside triphosphate inhibition, and DNA chain elongation. *J Virol*, 2003. **77**(6): p. 3871-7.

145. Mas, A., M. Parera, C. Briones, V. Soriano, M.A. Martinez, E. Domingo, and L. Menendez-Arias. Role of a dipeptide insertion between codons 69 and 70 of HIV-1 reverse transcriptase in the mechanism of AZT resistance. *EMBO J*, 2000. **19**(21): p. 5752-61.

146. Rakik, A., M. Ait-Khaled, P. Griffin, T.A. Thomas, M. Tisdale, and J.P. Kleim. A novel genotype encoding a single amino acid insertion and five other substitutions between residues 64 and 74 of the HIV-1 reverse transcriptase confers high-level cross-resistance to nucleoside reverse transcriptase inhibitors. Abacavir CNA2007 International Study Group. *J Acquir Immune Defic Syndr*, 1999. **22**(2): p. 139-45.

147. Dornsife, R.E., M.H. St Clair, A.T. Huang, T.J. Panella, G.W. Koszalka, C.L. Burns, and D.R. Averett. Anti-human immunodeficiency virus synergism by zidovudine (3'-azidothymidine) and didanosine (dideoxyinosine) contrasts with their additive inhibition of normal human marrow progenitor cells. *Antimicrob Agents Chemother*, 1991. **35**(2): p. 322-8.

148. Yarchoan, R., J.A. Lietzau, B.Y. Nguyen, O.W. Brawley, J.M. Pluda, M.W. Saville, K.M. Wyvill, S.M. Steinberg, R. Agbaria, H. Mitsuya, and Et Al. A randomized pilot study of alternating or simultaneous zidovudine and didanosine therapy in patients with symptomatic human immunodeficiency virus infection. *J Infect Dis*, 1994. **169**(1): p. 9-17.

149. Bridges, E.G., G.E. Dutschman, E.A. Gullen, and Y.C. Cheng. Favorable interaction of beta-L(-) nucleoside analogues with clinically approved anti-HIV nucleoside analogues for the treatment of human immunodeficiency virus. *Biochem Pharmacol*, 1996. **51**(6): p. 731-6.

150. Villahermosa, M.L., J.J. Martinez-Irujo, F. Cabodevilla, and E. Santiago. Synergistic inhibition of HIV-1 reverse transcriptase by combinations of chain-terminating nucleotides. *Biochemistry*, 1997. **36**(43): p. 13223-31.

151. St Clair, M.H., J.L. Martin, G. Tudor-Williams, M.C. Bach, C.L. Vavro, D.M. King, P. Kellam, S.D. Kemp, and B.A. Larder. Resistance to ddI and sensitivity to AZT induced by a mutation in HIV-1 reverse transcriptase. *Science*, 1991. **253**(5027): p. 1557-9.

152. Nijhuis, M., R. Schuurman, D. De Jong, R. Van Leeuwen, J. Lange, S. Danner, W. Keulen, T. De Groot, and C.A. Boucher. Lamivudine-resistant human immunodeficiency virus type 1 variants (184V) require multiple amino acid changes to become co-resistant to zidovudine in vivo. *J Infect Dis*, 1997. **176**(2): p. 398-405.

153. Roche-Pharmaceuticals. M.D./Alert. [Letter] 2006 [cited 2012 June 10]; Available from: http://www.fda.gov/downloads/drugs/drug/safety/drugshortages/ucm086099.pdf.

154. Gotte, M., D. Arion, M.A. Parniak, and M.A. Wainberg. The M184V mutation in the reverse transcriptase of human immunodeficiency virus type 1 impairs rescue of chain-terminated DNA synthesis. *J Virol*, 2000. **74**(8): p. 3579-85.

155. Boyer, P.L., S.G. Sarafianos, E. Arnold, and S.H. Hughes. The M184V mutation reduces the selective excision of zidovudine 5'-monophosphate (AZTMP) by the reverse transcriptase of human immunodeficiency virus type 1. *J Virol*, 2002. **76**(7): p. 3248-56.

156. Naeger, L.K., N.A. Margot, and M.D. Miller. Increased drug susceptibility of HIV-1 reverse transcriptase mutants containing M184V and zidovudine-associated mutations: analysis of enzyme processivity, chain-terminator removal and viral replication. *Antivir Ther*, 2001. **6**(2): p. 115-26.

157. Miranda, L.R., M. Gotte, F. Liang, and D.R. Kuritzkes. The L74V mutation in human immunodeficiency virus type 1 reverse transcriptase counteracts enhanced excision of zidovudine monophosphate associated with thymidine analog resistance mutations. *Antimicrob Agents Chemother*, 2005. **49**(7): p. 2648-56.

158. Frankel, F.A., B. Marchand, D. Turner, M. Gotte, and M.A. Wainberg. Impaired rescue of chain-terminated DNA synthesis associated with the L74V mutation in human immunodeficiency virus type 1 reverse transcriptase. *Antimicrob Agents Chemother*, 2005. **49**(7): p. 2657-64.

159. Parikh, U.M., D.C. Barnas, H. Faruki, and J.W. Mellors. Antagonism between the HIV-1 reverse-transcriptase mutation K65R and thymidine-analogue mutations at the genomic level. *J Infect Dis*, 2006. **194**(5): p. 651-60.

160. Parikh, U.M., L. Bacheler, D. Koontz, and J.W. Mellors. The K65R mutation in human immunodeficiency virus type 1 reverse transcriptase exhibits bidirectional phenotypic antagonism with thymidine analog mutations. *J Virol*, 2006. **80**(10): p. 4971-7.

161. Sluis-Cremer, N., C.W. Sheen, S. Zelina, P.S. Torres, U.M. Parikh, and J.W. Mellors. Molecular mechanism by which the K70E mutation in human immunodeficiency virus type 1 reverse transcriptase confers resistance to nucleoside reverse transcriptase inhibitors. *Antimicrob Agents Chemother*, 2007. **51**(1): p. 48-53.

162. Romano, L., G. Venturi, S. Bloor, R. Harrigan, B.A. Larder, J.C. Major, and M. Zazzi. Broad nucleoside-analogue resistance implications for human immunodeficiency virus type 1 reverse-transcriptase mutations at codons 44 and 118. *J Infect Dis*, 2002. **185**(7): p. 898-904.

163. Kemp, S.D., C. Shi, S. Bloor, P.R. Harrigan, J.W. Mellors, and B.A. Larder. A novel polymorphism at codon 333 of human immunodeficiency virus type 1 reverse transcriptase can facilitate dual resistance to zidovudine and L-2',3'-dideoxy-3'-thiacytidine. *J Virol*, 1998. **72**(6): p. 5093-8.

164. Zelina, S., C.W. Sheen, J. Radzio, J.W. Mellors, and N. Sluis-Cremer. Mechanisms by which the G333D mutation in human immunodeficiency virus type 1 Reverse transcriptase facilitates dual resistance to zidovudine and lamivudine. *Antimicrob Agents Chemother*, 2008. **52**(1): p. 157-63.

165. Stoeckli, T.C., S. Mawhinney, J. Uy, C. Duan, J. Lu, D. Shugarts, and D.R. Kuritzkes. Phenotypic and genotypic analysis of biologically cloned human immunodeficiency virus type 1 isolates from patients treated with zidovudine and lamivudine. *Antimicrob Agents Chemother*, 2002. **46**(12): p. 4000-3.

166. Yap, S.H., C.W. Sheen, J. Fahey, M. Zanin, D. Tyssen, V.D. Lima, B. Wynhoven, M. Kuiper, N. Sluis-Cremer, P.R. Harrigan, and G. Tachedjian. N348I in the connection domain of HIV-1 reverse transcriptase confers zidovudine and nevirapine resistance. *PLoS Med*, 2007. **4**(12): p. e335.

167. Horwitz, J.R., J. Chua, M.A. Da Rooge, M. Noel, and I.L. Klundt. Nucleosides. IX. The formation of 2',2'-unsaturated pyrimidine nucleosides via a novel beta-elimination reaction. *J Org Chem*, 1966. **31**(1): p. 205-11.

168. Balzarini, J., P. Herdewijn, and E. De Clercq. Differential patterns of intracellular metabolism of 2',3'-didehydro-2',3'-dideoxythymidine and 3'-azido-2',3'-dideoxythymidine, two potent anti-human immunodeficiency virus compounds. *J Biol Chem*, 1989. **264**(11): p. 6127-33.

169. Barbier, O., D. Turgeon, C. Girard, M.D. Green, T.R. Tephly, D.W. Hum, and A. Belanger. 3'-azido-3'-deoxythimidine (AZT) is glucuronidated by human UDP-glucuronosyltransferase 2B7 (UGT2B7). *Drug Metab Dispos*, 2000. **28**(5): p. 497-502.

170. Weidner, D.A. and J.P. Sommadossi. 3'-Azido-3'-deoxythymidine inhibits globin gene transcription in butyric acid-induced K-562 human leukemia cells. *Mol Pharmacol*, 1990. **38**(6): p. 797-804.

171. Lee, H., J. Hanes, and K.A. Johnson. Toxicity of nucleoside analogues used to treat AIDS and the selectivity of the mitochondrial DNA polymerase. *Biochemistry*, 2003. **42**(50): p. 14711-9.

172. Sluis-Cremer, N., D. Koontz, L. Bassit, B.I. Hernandez-Santiago, M. Detorio, K.L. Rapp, F. Amblard, L. Bondada, J. Grier, S.J. Coats, R.F. Schinazi, and J.W. Mellors. Anti-human immunodeficiency virus activity, cross-resistance, cytotoxicity, and intracellular pharmacology of the 3'-azido-2',3'-dideoxypurine nucleosides. *Antimicrob Agents Chemother*, 2009. **53**(9): p. 3715-9.

173. Calvez, V., D. Costagliola, D. Descamps, A. Yvon, G. Collin, A. Cecile, C. Delaugerre, F. Damond, A.G. Marcelin, S. Matheron, A. Simon, M.A. Valantin, C. Katlama, and F. Brun-Vezinet. Impact of stavudine phenotype and thymidine analogues mutations on viral response to stavudine plus lamivudine in ALTIS 2 ANRS trial. *Antivir Ther*, 2002. **7**(3): p. 211-8.

174. Kuritzkes, D.R., R.L. Bassett, J.D. Hazelwood, H. Barrett, R.A. Rhodes, R.K. Young, V.A. Johnson, and A.P.T. Adult. Rate of thymidine analogue resistance mutation accumulation with zidovudine- or stavudine-based regimens. *J Acquir Immune Defic Syndr*, 2004. **36**(1): p. 600-3.

175. Sturmer, M., S. Staszewski, H.W. Doerr, B. Larder, S. Bloor, and K. Hertogs. Correlation of phenotypic zidovudine resistance with mutational patterns in the reverse transcriptase of human immunodeficiency virus type 1: interpretation of established mutations and characterization of new polymorphisms at codons 208, 211, and 214. *Antimicrob Agents Chemother*, 2003. **47**(1): p. 54-61.

176. Cooney, D.A., G. Ahluwalia, H. Mitsuya, A. Fridland, M. Johnson, Z. Hao, M. Dalal, J. Balzarini, S. Broder, and D.G. Johns. Initial studies on the cellular pharmacology of 2',3'-dideoxyadenosine, an inhibitor of HTLV-III infectivity. *Biochem Pharmacol*, 1987. **36**(11): p. 1765-8.

177. Masood, R., G.S. Ahluwalia, D.A. Cooney, A. Fridland, V.E. Marquez, J.S. Driscoll, Z. Hao, H. Mitsuya, C.F. Perno, S. Broder, and Et Al. 2'-Fluoro-2',3'-dideoxyarabinosyladenine: a metabolically stable analogue of the antiretroviral agent 2',3'-dideoxyadenosine. *Mol Pharmacol*, 1990. **37**(4): p. 590-6.

178. Ahluwalia, G., D.A. Cooney, H. Mitsuya, A. Fridland, K.P. Flora, Z. Hao, M. Dalal, S. Broder, and D.G. Johns. Initial studies on the cellular pharmacology of 2',3'-dideoxyinosine, an inhibitor of HIV infectivity. *Biochem Pharmacol*, 1987. **36**(22): p. 3797-800.

179. Johnson, M.A. and A. Fridland. Phosphorylation of 2',3'-dideoxyinosine by cytosolic 5'-nucleotidase of human lymphoid cells. *Mol Pharmacol*, 1989. **36**(2): p. 291-5.

180. Balzarini, J. Metabolism and mechanism of antiretroviral action of purine and pyrimidine derivatives. *Pharm World Sci*, 1994. **16**(2): p. 113-26.

181. Sharma, P.L. and C.S. Crumpacker. Attenuated replication of human immunodeficiency virus type 1 with a didanosine-selected reverse transcriptase mutation. *J Virol*, 1997. **71**(11): p. 8846-51.

182. Shirasaka, T., M.F. Kavlick, T. Ueno, W.Y. Gao, E. Kojima, M.L. Alcaide, S. Chokekijchai, B.M. Roy, E. Arnold, R. Yarchoan, and Et Al. Emergence of human immunodeficiency virus type 1 variants with resistance to multiple dideoxynucleosides in patients receiving therapy with dideoxynucleosides. *Proc Natl Acad Sci U S A*, 1995. **92**(6): p. 2398-402.

183. Deval, J., B. Selmi, J. Boretto, M.P. Egloff, C. Guerreiro, S. Sarfati, and B. Canard. The molecular mechanism of multidrug resistance by the Q151M human immunodeficiency virus type 1 reverse transcriptase and its suppression using alpha-boranophosphate nucleotide analogues. *J Biol Chem*, 2002. **277**(44): p. 42097-104.

184. Menendez-Arias, L. Mechanisms of resistance to nucleoside analogue inhibitors of HIV-1 reverse transcriptase. *Virus Res*, 2008. **134**(1-2): p. 124-46.

185. Daluge, S.M., S.S. Good, M.B. Faletto, W.H. Miller, M.H. St Clair, L.R. Boone, M. Tisdale, N.R. Parry, J.E. Reardon, R.E. Dornsife, D.R. Averett, and T.A. Krenitsky. 1592U89, a novel carbocyclic nucleoside analog with potent, selective anti-human immunodeficiency virus activity. *Antimicrob Agents Chemother*, 1997. **41**(5): p. 1082-93.

186. Faletto, M.B., W.H. Miller, E.P. Garvey, M.H. St Clair, S.M. Daluge, and S.S. Good. Unique intracellular activation of the potent anti-human immunodeficiency virus agent 1592U89. *Antimicrob Agents Chemother*, 1997. **41**(5): p. 1099-107.

187. Chittick, G.E., C. Gillotin, J.A. Mcdowell, Y. Lou, K.D. Edwards, W.T. Prince, and D.S. Stein. Abacavir: absolute bioavailability, bioequivalence of three oral formulations, and effect of food. *Pharmacotherapy*, 1999. **19**(8): p. 932-42.

188. Tisdale, M., T. Alnadaf, and D. Cousens. Combination of mutations in human immunodeficiency virus type 1 reverse transcriptase required for resistance to the carbocyclic nucleoside 1592U89. *Antimicrob Agents Chemother*, 1997. **41**(5): p. 1094-8.

189. Krebs, R., U. Immendorfer, S.H. Thrall, B.M. Wohrl, and R.S. Goody. Single-step kinetics of HIV-1 reverse transcriptase mutants responsible for virus resistance to nucleoside inhibitors zidovudine and 3-TC. *Biochemistry*, 1997. **36**(33): p. 10292-300.

190. Feng, J.Y. and K.S. Anderson. Mechanistic studies examining the efficiency and fidelity of DNA synthesis by the 3TC-resistant mutant (184V) of HIV-1 reverse transcriptase. *Biochemistry*, 1999. **38**(29): p. 9440-8.

191. Wilson, J.E., A. Aulabaugh, B. Caligan, S. Mcpherson, J.K. Wakefield, S. Jablonski, C.D. Morrow, J.E. Reardon, and P.A. Furman. Human immunodeficiency virus type-1 reverse transcriptase. Contribution of Met-184 to binding of nucleoside 5'-triphosphate. *J Biol Chem*, 1996. **271**(23): p. 13656-62.

192. De Clercq, E. Anti-HIV drugs: 25 compounds approved within 25 years after the discovery of HIV. *Int J Antimicrob Agents*, 2009. **33**(4): p. 307-20.

193. Yarchoan, R., C.F. Perno, R.V. Thomas, R.W. Klecker, J.P. Allain, R.J. Wills, N. Mcatee, M.A. Fischl, R. Dubinsky, M.C. Mcneely, and Et Al. Phase I studies of 2',3'-dideoxycytidine in severe human immunodeficiency virus infection as a single agent and alternating with zidovudine (AZT). *Lancet*, 1988. **1**(8577): p. 76-81.

194. Chen, C.H. and Y.C. Cheng. Delayed cytotoxicity and selective loss of mitochondrial DNA in cells treated with the anti-human immunodeficiency virus compound 2',3'-dideoxycytidine. *J Biol Chem*, 1989. **264**(20): p. 11934-7.

195. Chang, C.N., V. Skalski, J.H. Zhou, and Y.C. Cheng. Biochemical pharmacology of (+)- and (-)-2',3'-dideoxy-3'-thiacytidine as anti-hepatitis B virus agents. *J Biol Chem*, 1992. **267**(31): p. 22414-20.

196. Cammack, N., P. Rouse, C.L. Marr, P.J. Reid, R.E. Boehme, J.A. Coates, C.R. Penn, and J.M. Cameron. Cellular metabolism of (-) enantiomeric 2'-deoxy-3'-thiacytidine. *Biochem Pharmacol*, 1992. **43**(10): p. 2059-64.

197. Stein, D.S. and K.H. Moore. Phosphorylation of nucleoside analog antiretrovirals: a review for clinicians. *Pharmacotherapy*, 2001. **21**(1): p. 11-34.

198. Darque, A., G. Valette, F. Rousseau, L.H. Wang, J.P. Sommadossi, and X.J. Zhou. Quantitation of intracellular triphosphate of emtricitabine in peripheral blood mononuclear cells from human immunodeficiency virus-infected patients. *Antimicrob Agents Chemother*, 1999. **43**(9): p. 2245-50.

199. Schinazi, R.F., A. Mcmillan, D. Cannon, R. Mathis, R.M. Lloyd, A. Peck, J.P. Sommadossi, M. St Clair, J. Wilson, P.A. Furman, and Et Al. Selective inhibition of human immunodeficiency viruses by racemates and enantiomers of cis-5-fluoro-1-[2-(hydroxymethyl)-1,3-oxathiolan-5-yl]cytosine. *Antimicrob Agents Chemother*, 1992. **36**(11): p. 2423-31.

200. Hart, G.J., D.C. Orr, C.R. Penn, H.T. Figueiredo, N.M. Gray, R.E. Boehme, and J.M. Cameron. Effects of (-)-2'-deoxy-3'-thiacytidine (3TC) 5'-triphosphate on human immunodeficiency virus reverse transcriptase and mammalian DNA polymerases alpha, beta, and gamma. *Antimicrob Agents Chemother*, 1992. **36**(8): p. 1688-94.

201. Coates, J.A., N. Cammack, H.J. Jenkinson, I.M. Mutton, B.A. Pearson, R. Storer, J.M. Cameron, and C.R. Penn. The separated enantiomers of 2'-deoxy-3'-thiacytidine (BCH 189) both inhibit human immunodeficiency virus replication in vitro. *Antimicrob Agents Chemother*, 1992. **36**(1): p. 202-5.

202. Gao, Q., Z. Gu, M.A. Parniak, J. Cameron, N. Cammack, C. Boucher, and M.A. Wainberg. The same mutation that encodes low-level human immunodeficiency virus type 1 resistance to 2',3'-dideoxyinosine and 2',3'-dideoxycytidine confers high-level resistance to the (-) enantiomer of 2',3'-dideoxy-3'-thiacytidine. *Antimicrob Agents Chemother*, 1993. **37**(6): p. 1390-2.

203. Schinazi, R.F., R.M. Lloyd, Jr., M.H. Nguyen, D.L. Cannon, A. Mcmillan, N. Ilksoy, C.K. Chu, D.C. Liotta, H.Z. Bazmi, and J.W. Mellors. Characterization of human immunodeficiency viruses resistant to oxathiolane-cytosine nucleosides. *Antimicrob Agents Chemother*, 1993. **37**(4): p. 875-81.

204. Kavlick, M.F., T. Shirasaka, E. Kojima, J.M. Pluda, F. Hui, Jr., R. Yarchoan, and H. Mitsuya. Genotypic and phenotypic characterization of HIV-1 isolated from patients receiving (--)-2',3'-dideoxy-3'-thiacytidine. *Antiviral Res*, 1995. **28**(2): p. 133-46.

205. Svicher, V., C. Alteri, A. Artese, F. Forbici, M.M. Santoro, D. Schols, K. Van Laethem, S. Alcaro, G. Costa, C. Tommasi, M. Zaccarelli, P. Narciso, A. Antinori, F. Ceccherini-Silberstein, J. Balzarini, and C.F. Perno. Different evolution of genotypic resistance profiles to emtricitabine versus lamivudine in tenofovir-containing regimens. *J Acquir Immune Defic Syndr*, 2010. **55**(3): p. 336-44.

206. De Clercq, E. The acyclic nucleoside phosphonates from inception to clinical use: historical perspective. *Antiviral Res*, 2007. **75**(1): p. 1-13.

207. Naesens, L., N. Bischofberger, P. Augustijns, P. Annaert, G. Van Den Mooter, M.N. Arimilli, C.U. Kim, and E. De Clercq. Antiretroviral efficacy and pharmacokinetics of oral bis(isopropyloxycarbonyloxymethyl)-9-(2-phosphonylmethoxypropyl)adenine in mice. *Antimicrob Agents Chemother*, 1998. **42**(7): p. 1568-73.

208. Robbins, B.L., R.V. Srinivas, C. Kim, N. Bischofberger, and A. Fridland. Anti-human immunodeficiency virus activity and cellular metabolism of a potential prodrug of the acyclic nucleoside phosphonate 9-R-(2-phosphonomethoxypropyl)adenine (PMPA), Bis(isopropyloxymethylcarbonyl)PMPA. *Antimicrob Agents Chemother*, 1998. **42**(3): p. 612-7.

209. Wainberg, M.A., M.D. Miller, Y. Quan, H. Salomon, A.S. Mulato, P.D. Lamy, N.A. Margot, K.E. Anton, and J.M. Cherrington. In vitro selection and characterization of HIV-1 with reduced susceptibility to PMPA. *Antivir Ther*, 1999. **4**(2): p. 87-94.

210. Ross, L., P. Gerondelis, Q. Liao, B. Wine, M. Lim, M. Shaefer, A. Rodriguez, K. Limoli, W. Huang, N.T. Parkin, J. Gallant, and R. Lanier. Selection of the HIV-1 Reverse Transcriptase Mutation K70E in Antiretroviral-Naive Subjects Treated with Tenofovir/Abacavir/Lamivudine Therapy (abstract no. 92) in *14th International HIV Drug Resistance Workshop*. 2005. Québec City, Canada

211. Kagan, R.M., T.S. Lee, L. Ross, R.M. Lloyd, Jr., M.A. Lewinski, and S.J. Potts. Molecular basis of antagonism between K70E and K65R tenofovir-associated mutations in HIV-1 reverse transcriptase. *Antiviral Res,* 2007. **75**(3): p. 210-8.

212. Parikh, U.M., D.L. Koontz, C.K. Chu, R.F. Schinazi, and J.W. Mellors. In vitro activity of structurally diverse nucleoside analogs against human immunodeficiency virus type 1 with the K65R mutation in reverse transcriptase. *Antimicrob Agents Chemother*, 2005. **49**(3): p. 1139-44.

213. Sluis-Cremer, N., D. Arion, N. Kaushik, H. Lim, and M.A. Parniak. Mutational analysis of Lys65 of HIV-1 reverse transcriptase. *Biochem J*, 2000. **348 Pt 1**: p. 77-82.

214. Hawkins, T. Understanding and managing the adverse effects of antiretroviral therapy. *Antiviral Res*, 2010. **85**(1): p. 201-9.

215. Rauch, A., D. Nolan, C. Thurnheer, C.A. Fux, M. Cavassini, J.P. Chave, M. Opravil, E. Phillips, S. Mallal, and H. Furrer. Refining abacavir hypersensitivity diagnoses using a structured clinical assessment and genetic testing in the Swiss HIV Cohort Study. *Antivir Ther*, 2008. **13**(8): p. 1019-28.

216. Reisler, R.B., R.L. Murphy, R.R. Redfield, and R.A. Parker. Incidence of pancreatitis in HIV-1-infected individuals enrolled in 20 adult AIDS clinical trials group studies: lessons learned. *J Acquir Immune Defic Syndr*, 2005. **39**(2): p. 159-66.

217. Gerard, Y., L. Maulin, Y. Yazdanpanah, X. De La Tribonniere, C. Amiel, C.A. Maurage, S. Robin, B. Sablonniere, C. Dhennain, and Y. Mouton. Symptomatic hyperlactataemia: an emerging complication of antiretroviral therapy. *AIDS*, 2000. **14**(17): p. 2723-30.

218. Karras, A., M. Lafaurie, A. Furco, A. Bourgarit, D. Droz, D. Sereni, C. Legendre, F. Martinez, and J.M. Molina. Tenofovir-related nephrotoxicity in human immunodeficiency virus-infected patients: three cases of renal failure, Fanconi syndrome, and nephrogenic diabetes insipidus. *Clin Infect Dis*, 2003. **36**(8): p. 1070-3.

219. Sulkowski, M.S., D.L. Thomas, R.E. Chaisson, and R.D. Moore. Hepatotoxicity associated with antiretroviral therapy in adults infected with human immunodeficiency virus and the role of hepatitis C or B virus infection. *JAMA*, 2000. **283**(1): p. 74-80.

220. Geddes, R., S. Knight, M.Y. Moosa, A. Reddi, K. Uebel, and H. Sunpath. A high incidence of nucleoside reverse transcriptase inhibitor (NRTI)-induced lactic acidosis in HIV-infected patients in a South African context. *S Afr Med J*, 2006. **96**(8): p. 722-4.

221. Sabin, C.A., S.W. Worm, R. Weber, P. Reiss, W. El-Sadr, F. Dabis, S. De Wit, M. Law, A. D'arminio Monforte, N. Friis-Moller, O. Kirk, C. Pradier, I. Weller, A.N. Phillips, and J.D. Lundgren. Use of nucleoside reverse transcriptase inhibitors and risk of myocardial infarction in HIV-infected patients enrolled in the D:A:D study: a multi-cohort collaboration. *Lancet*, 2008. **371**(9622): p. 1417-26.

222. Cihlar, T., E.S. Ho, D.C. Lin, and A.S. Mulato. Human renal organic anion transporter 1 (hOAT1) and its role in the nephrotoxicity of antiviral nucleotide analogs. *Nucleosides Nucleotides Nucleic Acids*, 2001. **20**(4-7): p. 641-8.

223. Brinkman, K., H.J. Ter Hofstede, D.M. Burger, J.A. Smeitink, and P.P. Koopmans. Adverse effects of reverse transcriptase inhibitors: mitochondrial toxicity as common pathway. *AIDS*, 1998. **12**(14): p. 1735-44.

224. Dalakas, M.C., I. Illa, G.H. Pezeshkpour, J.P. Laukaitis, B. Cohen, and J.L. Griffin. Mitochondrial myopathy caused by long-term zidovudine therapy. *N Engl J Med*, 1990. **322**(16): p. 1098-105.

225. Lewis, W., T. Papoian, B. Gonzalez, H. Louie, D.P. Kelly, R.M. Payne, and W.W. Grody. Mitochondrial ultrastructural and molecular changes induced by zidovudine in rat hearts. *Lab Invest*, 1991. **65**(2): p. 228-36.

226. Johnson, A.A., A.S. Ray, J. Hanes, Z. Suo, J.M. Colacino, K.S. Anderson, and K.A. Johnson. Toxicity of antiviral nucleoside analogs and the human mitochondrial DNA polymerase. *J Biol Chem*, 2001. **276**(44): p. 40847-57.

227. Mckee, E.E., A.T. Bentley, M. Hatch, J. Gingerich, and D. Susan-Resiga. Phosphorylation of thymidine and AZT in heart mitochondria: elucidation of a novel mechanism of AZT cardiotoxicity. *Cardiovasc Toxicol*, 2004. **4**(2): p. 155-67.

228. Birkus, G., M.J. Hitchcock, and T. Cihlar. Assessment of mitochondrial toxicity in human cells treated with tenofovir: comparison with other nucleoside reverse transcriptase inhibitors. *Antimicrob Agents Chemother*, 2002. **46**(3): p. 716-23.

229. Piliero, P.J. Pharmacokinetic properties of nucleoside/nucleotide reverse transcriptase inhibitors. *Journal of acquired immune deficiency syndromes*, 2004. **37 Suppl 1**: p. S2-S12.

230. Rodriguez Orengo, J.F., J. Santana, I. Febo, C. Diaz, J.L. Rodriguez, R. Garcia, E. Font, and O. Rosario. Intracellular studies of the nucleoside reverse transcriptase inhibitor active metabolites: a review. *Puerto Rico health sciences journal*, 2000. **19**(1): p. 19-27.

231. Taburet, A.M., S. Paci-Bonaventure, G. Peytavin, and J.M. Molina. Once-daily administration of antiretrovirals: pharmacokinetics of emerging therapies. *Clinical pharmacokinetics*, 2003. **42**(14): p. 1179-91.

232. Solas, C., Y.F. Li, M.Y. Xie, J.P. Sommadossi, and X.J. Zhou. Intracellular nucleotides of (-)-2',3'-deoxy-3'-thiacytidine in peripheral blood mononuclear cells of a patient infected with human immunodeficiency virus. *Antimicrobial agents and chemotherapy*, 1998. **42**(11): p. 2989-95.

233. Ray, A.S. Intracellular interactions between nucleos(t)ide inhibitors of HIV reverse transcriptase. *AIDS reviews*, 2005. **7**(2): p. 113-25.

234. Gao, W.Y., R. Agbaria, J.S. Driscoll, and H. Mitsuya. Divergent anti-human immunodeficiency virus activity and anabolic phosphorylation of 2',3'-dideoxynucleoside analogs in resting and activated human cells. *The Journal of biological chemistry*, 1994. **269**(17): p. 12633-8.

235. Gao, W.Y., T. Shirasaka, D.G. Johns, S. Broder, and H. Mitsuya. Differential phosphorylation of azidothymidine, dideoxycytidine, and dideoxyinosine in resting and activated peripheral blood mononuclear cells. *The Journal of clinical investigation*, 1993. **91**(5): p. 2326-33.

236. Havlir, D.V., C. Tierney, G.H. Friedland, R.B. Pollard, L. Smeaton, J.P. Sommadossi, L. Fox, H. Kessler, K.H. Fife, and D.D. Richman. In vivo antagonism with zidovudine plus stavudine combination therapy. *J Infect Dis*, 2000. **182**(1): p. 321-5.

237. Veal, G.J., M.G. Barry, S.H. Khoo, and D.J. Back. In vitro screening of nucleoside analog combinations for potential use in anti-HIV therapy. *AIDS research and human retroviruses*, 1997. **13**(6): p. 481-4.

238. Ray, A.S., L. Olson, and A. Fridland. Role of purine nucleoside phosphorylase in interactions between 2',3'-dideoxyinosine and allopurinol, ganciclovir, or tenofovir. *Antimicrob Agents Chemother*, 2004. **48**(4): p. 1089-95.

239. Waters, L.J., G. Moyle, S. Bonora, A. D'avolio, L. Else, S. Mandalia, A. Pozniak, M. Nelson, B. Gazzard, D. Back, and M. Boffito. Abacavir plasma pharmacokinetics in the absence and presence of atazanavir/ritonavir or lopinavir/ritonavir and vice versa in HIV-infected patients. *Antiviral therapy*, 2007. **12**(5): p. 825-30.

240. Yuen, G.J., S. Weller, and G.E. Pakes. A review of the pharmacokinetics of abacavir. *Clinical pharmacokinetics*, 2008. **47**(6): p. 351-71.

241. Luber, A.D., D.V. Condoluci, P.D. Slowinski, M. Andrews, K. Olson, C.A. Peloquin, K.A. Pappa, and G.E. Pakes. Steady-state amprenavir and tenofovir pharmacokinetics after coadministration of unboosted or ritonavir-boosted fosamprenavir with tenofovir disoproxil fumarate in healthy volunteers. *HIV medicine*, 2010. **11**(3): p. 193-9.

242. Menendez-Arias, L. Molecular basis of human immunodeficiency virus drug resistance: an update. *Antiviral Res*, 2010. **85**(1): p. 210-31.

243. Sigaloff, K.C., J.C. Calis, S.P. Geelen, M. Van Vugt, and T.F. De Wit. HIV-1-resistance-associated mutations after failure of first-line antiretroviral treatment among children in resource-poor regions: a systematic review. *The Lancet infectious diseases*, 2011. **11**(10): p. 769-79.

244. Hamkar, R., M. Mohraz, S. Lorestani, A. Aghakhani, H.M. Truong, W. Mcfarland, M. Banifazl, A. Eslamifar, M. Foroughi, A. Pakfetrat, and A. Ramezani. Assessing subtype and drug-resistance-associated mutations among antiretroviral-treated HIV-infected patients. *AIDS*, 2010. **24 Suppl 2**: p. S85-91.

245. Dvali, N., M.M. Parker, N. Chkhartishvili, L. Sharvadze, N. Gochitashvili, A. Abutidze, M. Karchava, J.A. Dehovitz, and T. Tsertsvadze. Characterization of HIV-1 subtypes and drug resistance mutations among individuals infected with HIV in Georgia. *Journal of medical virology*, 2012. **84**(7): p. 1002-8.

246. Jain, V., T. Liegler, E. Vittinghoff, W. Hartogensis, P. Bacchetti, L. Poole, L. Loeb, C.D. Pilcher, R.M. Grant, S.G. Deeks, and F.M. Hecht. Transmitted drug resistance in persons with acute/early HIV-1 in San Francisco, 2002-2009. *PLoS One*, 2010. **5**(12): p. e15510.

247. Little, S.J., S. Holte, J.P. Routy, E.S. Daar, M. Markowitz, A.C. Collier, R.A. Koup, J.W. Mellors, E. Connick, B. Conway, M. Kilby, L. Wang, J.M. Whitcomb, N.S. Hellmann, and D.D. Richman. Antiretroviral-drug resistance among patients recently infected with HIV. *The New England journal of medicine*, 2002. **347**(6): p. 385-94.

248. Weinstock, H.S., I. Zaidi, W. Heneine, D. Bennett, J.G. Garcia-Lerma, J.M. Douglas, Jr., M. Lalota, G. Dickinson, S. Schwarcz, L. Torian, D. Wendell, S. Paul, G.A. Goza, J. Ruiz, B. Boyett, and J.E. Kaplan. The epidemiology of antiretroviral drug resistance among drug-naive HIV-1-infected persons in 10 US cities. *The Journal of infectious diseases*, 2004. **189**(12): p. 2174-80.

249. Wensing, A.M., D.A. Van De Vijver, G. Angarano, B. Asjo, C. Balotta, E. Boeri, R. Camacho, M.L. Chaix, D. Costagliola, A. De Luca, I. Derdelinckx, Z. Grossman, O. Hamouda, A. Hatzakis, R. Hemmer, A. Hoepelman, A. Horban, K. Korn, C. Kucherer, T. Leitner, C. Loveday, E. Macrae, I. Maljkovic, C. De Mendoza, L. Meyer, C. Nielsen, E.L. Op De Coul, V. Ormaasen, D. Paraskevis, L. Perrin, E. Puchhammer-Stockl, L. Ruiz, M. Salminen, J.C. Schmit, F. Schneider, R. Schuurman, V. Soriano, G. Stanczak, M. Stanojevic, A.M. Vandamme, K. Van Laethem, M. Violin, K. Wilbe, S. Yerly, M. Zazzi, and C.A. Boucher. Prevalence of drug-resistant HIV-1 variants in untreated individuals in Europe: implications for clinical management. *The Journal of infectious diseases*, 2005. **192**(6): p. 958-66.

250. Broder, S. The development of antiretroviral therapy and its impact on the HIV-1/AIDS pandemic. *Antiviral Res*, 2010. **85**(1): p. 1-18.

251. Ammaranond, P. and S. Sanguansittianan. Mechanism of HIV antiretroviral drugs progress toward drug resistance. *Fundamental & clinical pharmacology*, 2012. **26**(1): p. 146-61.

252. Brenner, B., M.A. Wainberg, H. Salomon, D. Rouleau, A. Dascal, B. Spira, R.P. Sekaly, B. Conway, and J.P. Routy. Resistance to antiretroviral drugs in patients with primary HIV-1 infection. Investigators of the Quebec Primary Infection Study. *International journal of antimicrobial agents*, 2000. **16**(4): p. 429-34.

253. Munier, C.M., C.R. Andersen, and A.D. Kelleher. HIV vaccines: progress to date. *Drugs*, 2011. **71**(4): p. 387-414.

254. Van De Vijver, D.A. and C.A. Boucher. The risk of HIV drug resistance following implementation of pre-exposure prophylaxis. *Curr Opin Infect Dis*, 2010. **23**(6): p. 621-7.

255. Deeks, S.G., B. Autran, B. Berkhout, M. Benkirane, S. Cairns, N. Chomont, T.W. Chun, M. Churchill, M.D. Mascio, C. Katlama, A. Lafeuillade, A. Landay, M. Lederman, S.R. Lewin, F. Maldarelli, D. Margolis, M. Markowitz, J. Martinez-Picado, J.I. Mullins, J. Mellors, S. Moreno, U. O'doherty, S. Palmer, M.C. Penicaud, M. Peterlin, G. Poli, J.P. Routy, C. Rouzioux, G. Silvestri, M. Stevenson, A. Telenti, C.V. Lint, E. Verdin, A. Woolfrey, J. Zaia, and F. Barre-Sinoussi. Towards an HIV cure: a global scientific strategy. *Nat Rev Immunol*, 2012. **12**(8): p. 607-614.

256. Donnell, D., J.M. Baeten, J. Kiarie, K.K. Thomas, W. Stevens, C.R. Cohen, J. Mcintyre, J.R. Lingappa, and C. Celum. Heterosexual HIV-1 transmission after initiation of antiretroviral therapy: a prospective cohort analysis. *Lancet*, 2010. **375**(9731): p. 2092-8.

257. Huggins, D.J., W. Sherman, and B. Tidor. Rational approaches to improving selectivity in drug design. *Journal of medicinal chemistry*, 2012. **55**(4): p. 1424-44.

258. Mandal, S., M. Moudgil, and S.K. Mandal. Rational drug design. *European journal of pharmacology*, 2009. **625**(1-3): p. 90-100.

259. Blum, A., J. Bottcher, A. Heine, G. Klebe, and W.E. Diederich. Structure-guided design of C2-symmetric HIV-1 protease inhibitors based on a pyrrolidine scaffold. *Journal of medicinal chemistry*, 2008. **51**(7): p. 2078-87.

260. Drag, M. and G.S. Salvesen. Emerging principles in protease-based drug discovery. *Nature reviews. Drug discovery*, 2010. **9**(9): p. 690-701.

261. De Clercq, E., G. Andrei, J. Balzarini, P. Leyssen, L. Naesens, J. Neyts, C. Pannecouque, R. Snoeck, C. Ying, D. Hockova, and A. Holy. Antiviral potential of a new generation of acyclic nucleoside phosphonates, the 6-[2-(phosphonomethoxy)alkoxy]-2,4-diaminopyrimidines. *Nucleosides Nucleotides Nucleic Acids*, 2005. **24**(5-7): p. 331-41.

262. Balzarini, J., D. Schols, K. Van Laethem, E. De Clercq, D. Hockova, M. Masojidkova, and A. Holy. Pronounced in vitro and in vivo antiretroviral activity of 5-substituted 2,4-diamino-6-[2-(phosphonomethoxy)ethoxy] pyrimidines. *J Antimicrob Chemother*, 2007. **59**(1): p. 80-6.

263. Cihlar, T., A.S. Ray, C.G. Boojamra, L. Zhang, H. Hui, G. Laflamme, J.E. Vela, D. Grant, J. Chen, F. Myrick, K.L. White, Y. Gao, K.Y. Lin, J.L. Douglas, N.T. Parkin, A. Carey, R. Pakdaman, and R.L. Mackman. Design and profiling of GS-9148, a novel nucleotide analog active against nucleoside-resistant variants of human immunodeficiency virus type 1, and its orally bioavailable phosphonoamidate prodrug, GS-9131. *Antimicrob Agents Chemother*, 2008. **52**(2): p. 655-65.

264. Cihlar, T., G. Laflamme, R. Fisher, A.C. Carey, J.E. Vela, R. Mackman, and A.S. Ray. Novel nucleotide human immunodeficiency virus reverse transcriptase inhibitor GS-9148 with a low nephrotoxic potential: characterization of renal transport and accumulation. *Antimicrob Agents Chemother*, 2009. **53**(1): p. 150-6.

265. Birkus, G., R. Wang, X. Liu, N. Kutty, H. Macarthur, T. Cihlar, C. Gibbs, S. Swaminathan, W. Lee, and M. Mcdermott. Cathepsin A is the major hydrolase catalyzing the intracellular hydrolysis of the antiretroviral nucleotide phosphonoamidate prodrugs GS-7340 and GS-9131. *Antimicrob Agents Chemother*, 2007. **51**(2): p. 543-50.

266. Mackman, R.L., A.S. Ray, H.C. Hui, L. Zhang, G. Birkus, C.G. Boojamra, M.C. Desai, J.L. Douglas, Y. Gao, D. Grant, G. Laflamme, K.Y. Lin, D.Y. Markevitch, R. Mishra, M. Mcdermott, R. Pakdaman, O.V. Petrakovsky, J.E. Vela, and T. Cihlar. Discovery of GS-9131: Design, synthesis and optimization of amidate prodrugs of the novel nucleoside phosphonate HIV reverse transcriptase (RT) inhibitor GS-9148. *Bioorg Med Chem*, 2010. **18**(10): p. 3606-17.

267. White, K., J. Ly, K. Eastoak-Siletz, G. Laflamme, N. Kutty, A. Ray, T. Cihlar, and M. Miller. Resistance Mechanisms of the K70E HIV-1 Reverse Transcriptase Mutant to GS-9148 and Other NRTIs. Abstract H-1039. in *47th Interscience Conference on Antimicrobial Agents and Chemotherapy*. 2007. Chicago, IL.

268. Laflamme, G., D. Grant, K. White, K. Stray, C. Boojamra, L. Zhang, R. Mackman, A. Ray, M. Miller, and T. Cihlar. Novel Nucleotide Inhibitor GS-9148 Selects for a K70E Mutation in HIV-1 Reverse Transcriptase and Low-Level Resistance In Vitro. Abstract H-1037. in *47th Interscience Conference on Antimicrobial Agents and Chemotherapy*. 2007. Chicago, IL.

269. De Clercq, E., A. Holy, I. Rosenberg, T. Sakuma, J. Balzarini, and P.C. Maudgal. A novel selective broad-spectrum anti-DNA virus agent. *Nature*, 1986. **323**(6087): p. 464-7.

270. Balzarini, J., A. Holy, J. Jindrich, H. Dvorakova, Z. Hao, R. Snoeck, P. Herdewijn, D.G. Johns, and E. De Clercq. 9-[(2RS)-3-fluoro-2-phosphonylmethoxypropyl] derivatives of purines: a class of highly selective antiretroviral agents in vitro and in vivo. *Proc Natl Acad Sci U S A*, 1991. **88**(11): p. 4961-5.

271. De Clercq, E., T. Sakuma, M. Baba, R. Pauwels, J. Balzarini, I. Rosenberg, and A. Holy. Antiviral activity of phosphonylmethoxyalkyl derivatives of purine and pyrimidines. *Antiviral Res*, 1987. **8**(5-6): p. 261-72.

272. Pauwels, R., J. Balzarini, D. Schols, M. Baba, J. Desmyter, I. Rosenberg, A. Holy, and E. De Clercq. Phosphonylmethoxyethyl purine derivatives, a new class of anti-human immunodeficiency virus agents. *Antimicrob Agents Chemother*, 1988. **32**(7): p. 1025-30.

273. Balzarini, J., A. Holy, J. Jindrich, L. Naesens, R. Snoeck, D. Schols, and E. De Clercq. Differential antiherpesvirus and antiretrovirus effects of the (S) and (R) enantiomers of acyclic nucleoside phosphonates: potent and selective in vitro and in vivo antiretrovirus activities of (R)-9-(2-phosphonomethoxypropyl)-2,6-diaminopurine. *Antimicrob Agents Chemother*, 1993. **37**(2): p. 332-8.

274. De Clercq, E. Acyclic nucleoside phosphonates: past, present and future. Bridging chemistry to HIV, HBV, HCV, HPV, adeno-, herpes-, and poxvirus infections: the phosphonate bridge. *Biochem Pharmacol*, 2007. **73**(7): p. 911-22.

275. Mul, Y.M., R.T. Van Miltenburg, E. De Clercq, and P.C. Van Der Vliet. Mechanism of inhibition of adenovirus DNA replication by the acyclic nucleoside triphosphate analogue (S)-HPMPApp: influence of the adenovirus DNA binding protein. *Nucleic Acids Res*, 1989. **17**(22): p. 8917-29.

276. Holy, A., I. Votruba, A. Merta, J. Cerny, J. Vesely, J. Vlach, K. Sediva, I. Rosenberg, M. Otmar, H. Hrebabecky, and Et Al. Acyclic nucleotide analogues: synthesis, antiviral activity and inhibitory effects on some cellular and virus-encoded enzymes in vitro. *Antiviral Res*, 1990. **13**(6): p. 295-311.

277. Xiong, X., J.L. Smith, C. Kim, E.S. Huang, and M.S. Chen. Kinetic analysis of the interaction of cidofovir diphosphate with human cytomegalovirus DNA polymerase. *Biochem Pharmacol*, 1996. **51**(11): p. 1563-7.

278. Magee, W.C., K.A. Aldern, K.Y. Hostetler, and D.H. Evans. Cidofovir and (S)-9-[3-hydroxy-(2-phosphonomethoxy)propyl]adenine are highly effective inhibitors of vaccinia virus DNA polymerase when incorporated into the template strand. *Antimicrob Agents Chemother*, 2008. **52**(2): p. 586-97.

279. Xiong, X., J.L. Smith, and M.S. Chen. Effect of incorporation of cidofovir into DNA by human cytomegalovirus DNA polymerase on DNA elongation. *Antimicrob Agents Chemother*, 1997. **41**(3): p. 594-9.

280. Balzarini, J., C. Pannecouque, E. De Clercq, S. Aquaro, C.F. Perno, H. Egberink, and A. Holy. Antiretrovirus activity of a novel class of acyclic pyrimidine nucleoside phosphonates. *Antimicrob Agents Chemother*, 2002. **46**(7): p. 2185-93.

281. Holy, A., I. Votruba, M. Masojidkova, G. Andrei, R. Snoeck, L. Naesens, E. De Clercq, and J. Balzarini. 6-[2-(Phosphonomethoxy)alkoxy]pyrimidines with antiviral activity. *J Med Chem*, 2002. **45**(9): p. 1918-29.

282. Hockova, D., A. Holy, M. Masojidkova, G. Andrei, R. Snoeck, E. De Clercq, and J. Balzarini. 5-Substituted-2,4-diamino-6-[2-(phosphonomethoxy)ethoxy]pyrimidines-acyclic nucleoside phosphonate analogues with antiviral activity. *J Med Chem*, 2003. **46**(23): p. 5064-73.

283. Ying, C., A. Holy, D. Hockova, Z. Havlas, E. De Clercq, and J. Neyts. Novel acyclic nucleoside phosphonate analogues with potent anti-hepatitis B virus activities. *Antimicrob Agents Chemother*, 2005. **49**(3): p. 1177-80.

284. Le Grice, S.F. and F. Gruninger-Leitch. Rapid purification of homodimer and heterodimer HIV-1 reverse transcriptase by metal chelate affinity chromatography. *Eur J Biochem*, 1990. **187**(2): p. 307-14.

285. Le Grice, S.F., C.E. Cameron, and S.J. Benkovic. Purification and characterization of human immunodeficiency virus type 1 reverse transcriptase. *Methods Enzymol*, 1995. **262**: p. 130-44.

286. Johnson, K.A. Rapid quench kinetic analysis of polymerases, adenosinetriphosphatases, and enzyme intermediates. *Methods Enzymol*, 1995. **249**: p. 38-61.

287. Zinnen, S., J.C. Hsieh, and P. Modrich. Misincorporation and mispaired primer extension by human immunodeficiency virus reverse transcriptase. *J Biol Chem*, 1994. **269**(39): p. 24195-202.

288. Gu, Z., H. Salomon, J.M. Cherrington, A.S. Mulato, M.S. Chen, R. Yarchoan, A. Foli, K.M. Sogocio, and M.A. Wainberg. K65R mutation of human immunodeficiency virus type 1 reverse transcriptase encodes cross-resistance to 9-(2-phosphonylmethoxyethyl)adenine. *Antimicrob Agents Chemother*, 1995. **39**(8): p. 1888-91.

289. Cherrington, J.M., A.S. Mulato, M.D. Fuller, and M.S. Chen. Novel mutation (K70E) in human immunodeficiency virus type 1 reverse transcriptase confers decreased susceptibility to 9-[2-(phosphonomethoxy)ethyl]adenine in vitro. *Antimicrob Agents Chemother*, 1996. **40**(9): p. 2212-6.

290. Ray, A.S., J.E. Vela, C.G. Boojamra, L. Zhang, H. Hui, C. Callebaut, K. Stray, K.Y. Lin, Y. Gao, R.L. Mackman, and T. Cihlar. Intracellular metabolism of the nucleotide prodrug GS-9131, a potent anti-human immunodeficiency virus agent. *Antimicrob Agents Chemother*, 2008. **52**(2): p. 648-54.

291. Scarth, B.J., K.L. White, J.M. Chen, E.B. Lansdon, S. Swaminathan, M.D. Miller, and M. Gotte. Mechanism of resistance to GS-9148 conferred by the Q151L mutation in HIV-1 reverse transcriptase. *Antimicrob Agents Chemother*, 2011. **55**(6): p. 2662-9.

292. Goody, R.S., B. Muller, and T. Restle. Factors contributing to the inhibition of HIV reverse transcriptase by chain-terminating nucleotides in vitro and in vivo. *FEBS Lett*, 1991. **291**(1): p. 1-5.

293. Labute, P. Protonate3D: assignment of ionization states and hydrogen coordinates to macromolecular structures. *Proteins*, 2009. **75**(1): p. 187-205.

294. Cheong, C., I. Tinoco, Jr., and A. Chollet. Thermodynamic studies of base pairing involving 2,6-diaminopurine. *Nucleic Acids Res*, 1988. **16**(11): p. 5115-22.

295. Schinazi, R.F., S.J. Coats, H.-H. Zhang, M. Detorio, A. Obikhod, G. Asif, B.D. Herman, J.H. Nettles, N. Sluis-Cremer, and J.W. Mellors. β-D-3'-Azido-2,6-diamino-2',3'-dideoxypurine AZD) is a Potent Inhibitor of HIV-1 and is Bioconverted Intracellularly to both AZD-TP and its Guanosine-5'-triphosphate Form. Poster # 557. in *16th Conference on Retroviruses and Opportunistic Infections.* 2009. Montreal, Canada.

296. Schinazi, R.F., Unpublished data. Personal communication from Schinazi et al. (Emory University) to Herman, B.D. and Sluis-Cremer, N., 2010-2012.

297. Brehm, J.H., D. Koontz, J.D. Meteer, V. Pathak, N. Sluis-Cremer, and J.W. Mellors. Selection of mutations in the connection and RNase H domains of human immunodeficiency virus type 1 reverse transcriptase that increase resistance to 3'-azido-3'-dideoxythymidine. *J Virol*, 2007. **81**(15): p. 7852-9.

298. Reed, L.J. and H. Muench. A simple method of estimating fifty percent endpoints. *Am. J. Hyg. (Lond.)*, 1938. **27**: p. 439-497.

299. Ludwig, J. and F. Eckstein. Rapid and efficient synthesis of nucleoside 5'-O-(1-thiotriphosphates), 5'-triphosphates and 2',3'-cyclophosphorothioates using 2-chloro-4H-1,3,2-benzodioxaphosphorin-4-one. . *J. Org. Chem.*, 1989. **54**: p. 631-635.

300. Chou, T.C. and P. Talalay. Quantitative analysis of dose-effect relationships: the combined effects of multiple drugs or enzyme inhibitors. *Adv Enzyme Regul*, 1984. **22**: p. 27-55.

301. Greco, W.R., G. Bravo, and J.C. Parsons. The search for synergy: a critical review from a response surface perspective. *Pharmacol Rev*, 1995. **47**(2): p. 331-85.

302. Selleseth, D.W., C.L. Talarico, T. Miller, M.W. Lutz, K.K. Biron, and R.J. Harvey. Interactions of 1263W94 with other antiviral agents in inhibition of human cytomegalovirus replication. *Antimicrob Agents Chemother*, 2003. **47**(4): p. 1468-71.